Innovation Center Iceland

F I B
F.A. Finger-Institut für Baustoffkunde

Interaction of cement and admixtures and its effect on rheological properties

Stefan Kubens

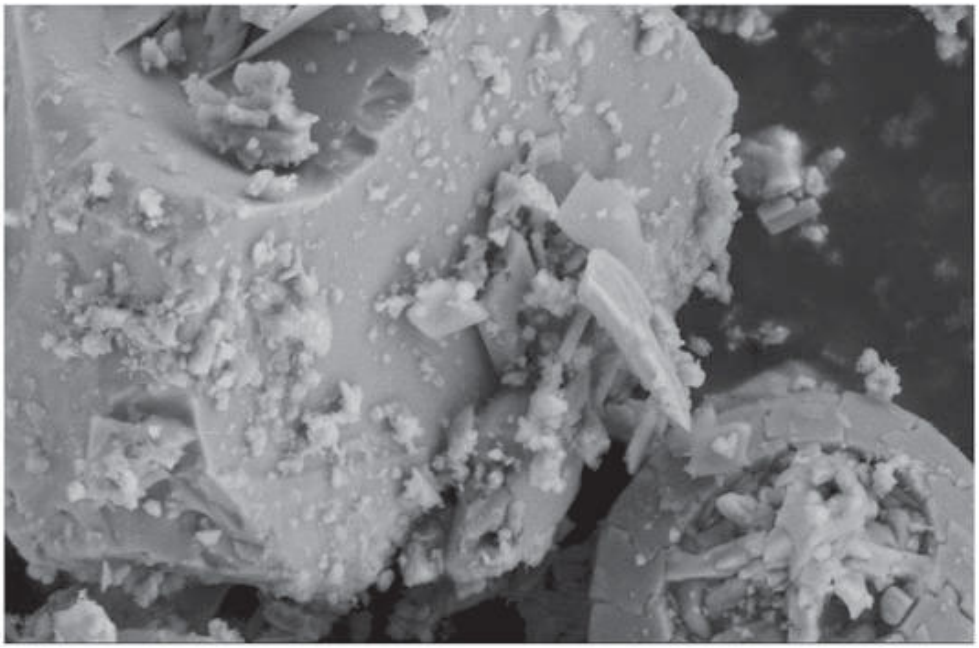

Cuvillier Verlag Göttingen
Internationaler wissenschaftlicher Fachverlag

Interaction of cement and admixtures and its influence on rheological properties

Dissertation zur Erlangung des akademischen Grades
Doktor-Ingenieur (Dr.-Ing.)
erstellt von

Stefan Kubens

am F.A. Finger Institut für Baustoffkunde
(Fakultät Bauingenieurwesen, Bauhaus-Universität Weimar)

Gutachter:

Prof. Dr.-Ing. habil. J. Stark (Weimar)
Prof. Dr.-Ing. O.H. Wallevik (Reykjavik)
Prof. Dr.-Ing. A. Bentur (Haifa)

Die öffentliche Disputation der Arbeit fand am 08.04.2010 in Weimar statt.

Bibliografische Information der Deutschen Nationalbibliothek
Die Deutsche Nationalbibliothek verzeichnet diese Publikation in der Deutschen Nationalbibliografie; detaillierte bibliografische Daten sind im Internet über http://dnb.d-nb.de abrufbar.
1. Aufl. - Göttingen : Cuvillier, 2010
Zugl.: Weimar, Univ., Diss., 2010

978-3-86955-350-4

Nonnenstieg 8, 37075 Göttingen
Telefon: 0551-54724-0
Telefax: 0551-54724-21
www.cuvillier.de

1. Auflage, 2010
Gedruckt auf säurefreiem Papier

978-3-86955-350-4

This thesis is dedicated to my mother, Christine Kubens and to the memory of my father, Christian Kubens for their love, patience and support.

Acknowledgements

This thesis was written as an external doctorate at ICI Rheocenter Reykjavik from 2005 to 2009. Without the cooperation of Bauhaus University Weimar, Innovation Center Iceland and Reykjavik University this work would not have been possible.

I would like to thank the chief of the Concrete Division and local supervisor Prof. Olafur H. Wallevik from Reykjavik University for his guidance and support during the last four years. Whenever it was possible, our research group was sent out to conferences to improve presentation skills and discuss our findings with other scientists to get another perspective. I greatly value this opportunity.

Equal thanks go to Prof. Jochen Stark from F.A. Finger Institute at Bauhaus University Weimar for the freedom he provided and the trust he had in this work. I would like to thank Prof. Jochen Stark also for his strong support in economical difficult times for Iceland. During several trips to Weimar I enjoyed the scientific exchange with Christiane Rössler, Frank Bellmann, Thomas Sowoidnich, Kathy Löhmer, Bernd Möser and Bernd Gathemann. In particular, Bernd Möser contributed considerably with his knowledge in electron microscopy. Special thanks go to Ursula Stark, Stefan Erfurt and Prof. Anette Müller from the Chair of Processing of Building Materials and Reuse at Bauhaus University Weimar for the dynamic particle size measurements.

Many thanks go to my colleagues Sonja Oesterheld, Florian Müller and Björn Hjartarsson for their assistance in the lab. A big thank you goes to geologist Erla María Hauksdóttir from the Innovation Center Iceland and her “nerdy network” for helping to identify the micro-fossils in cement.

A vital thing for the academic exchange were the international and Icelandic students who helped in one way or another during the pre tests and brought a new perspective in the project. Thanks go to Julia Schmitt from Stanford University, Petr Hajicek from Prague University, Sif Grétarsdóttir from University of Iceland and Michael Kraus from Bauhaus University Weimar.

Thanks go to Moshe Puterman from the Technion Haifa for his valuable input in the project and his great humour about life and science. Also, I like to thank Prof. Arnon Bentur from the Technion for his editorial remarks and critical comments on the half time report.

I want to thank Birgir Jóhannesson and Jón Matthíasson for their patience and endurance during the many hours in front of the SEM. Because of these two guys the Leo Supra 25 microscope at the Innovation Center Iceland is an excellent device. Furthermore, I owe thanks to Jón Baldvinsson and Björn Ásgeir Ásgeirsson for the standard tests on cement during the last four years.

Very special thanks go to Dr. Jón Elvar Wallevik from ICI Rheocenter for his help and comments during the rheological part of this study. Also, I would like to thank Nikolai Mikanovic and Jeff Sharman from Sherbrooke University for the interesting discussions we had on conferences and via mail. Thanks go also to Rögnvaldur S. Gíslason from Innovation Center Iceland for the critical view and valuable comments he contributed to the final report. Many thanks go to Paul Sandberg from W.R. Grace and Knut O. Kjellsen from Norcem for the fruitful discussions and the encouraging words.

Many thanks go to Rannveig Guicharnaud, Tryggvi Eiríksson and Britta Berglund from the Agricultural University of Iceland for their help during the TOC measurements.

The work reported here is part of a comprehensive research program at ICI Rheocenter in which cement deliveries from 6 countries have been investigated. Many thanks go to the project partners. The project was supported by Aalborg Portland (DK), Cementa (S), Consolis Technology Oy Ab (FIN), ConTec (IS), EKA Chemicals (S), ELKEM Materials (N), Norcem (N), Norstone AS (N), Rannís (Icelandic Centre for Research), Samey (IS), Steinsteypunefnd (IS), Steypustödin/MEST (IS), TBG Hungaria (H), TBR Centre of Technology (D), Vegagerðin (IS) and W.R. Grace (USA).

Living abroad in a different culture with a nice but difficult language can sometimes mean a challenge. Therefore, a big thank you goes to all the friends and people I met during my stay in Iceland and helped to make it the great adventure it was. Thanks go to the speedy Gonzales running team for the many kilometres through snow and sun, to the hiking team and to Elisa for the support and editing help.

Reykjavik, October 2009 Stefan Kubens

Nomenclature and abbreviations

τ	Yield value (Pa)
μ	Plastic viscosity (Pa·s)
γ	Shear rate (1/s)
v	Velocity (m/s)
v_x	Velocity component in direction of the x-axis in a Cartesian coordinate system
ω	Angular velocity (rad/s)
F	Force (N)
r	Radius (m)
T	Torque (Nm)
ρ	Density (kg/dm³)
σ	Stress (N/mm²)
mA	Milliampere
mAs	Milliampere second
G	G-yield (mA) is equal to yield value
H	H-viscosity (mA·s) is equal to plastic viscosity
t	Time (s)
h	Height (m)
w	Width (m)
rps	Revolution per second (1/s)
R_o	Radius of outer cylinder (m)
R_i	Radius of inner cylinder (m)
A	Area (m²)
w/c	Water to cement ratio (by weight)
s/c	Sand to cement ratio (by weight)
N	Newton
Nm	Newton meter
ppm	Parts per million
n/a	not analysed

(E)SEM	(Environmental) Scanning Electron Microscope
TOC	Total Organic Carbon
PC	Polycarboxylate
Mel	Sulphonated melamine condensate
SCC	Self Compacting Concrete
Eco-SCC	Economical and ecological Self Compacting Concrete
(Q)XRD	(Quantitative) X-Ray Diffraction

Tricalcium aluminate (aluminate/C_3A)	$3\ CaO \cdot Al_2O_3$
Tricalcium silicate (alite/C_3S)	$3\ CaO \cdot SiO_2$
Dicalcium silicate (belite/C_2S)	$2\ CaO \cdot SiO_2$
Calcium aluminate ferrite (ferrite/$C_2(A,F)$)	$4\ CaO \cdot Al_2O_3 \cdot Fe_2O_3$
Dihydrate (gypsum)	$CaSO_4 \cdot 2H_2O$
Hemi hydrate (bassanite)	$CaSO_4 \cdot ½H_2O$
Ettringite (AFt)	$3\ CaO \cdot Al_2O_3 \cdot 3CaSO_4 \cdot 32H_2O$
Portlandite (CH)	$Ca\ (OH)_2$
Calcium silicate hydrate (C-S-H)	$x\ CaO \cdot SiO_2 \cdot yH_2O$
Mono sulphate (AFm)	$3\ CaO \cdot Al_2O_3 \cdot CaSO_4 \cdot 12H_2O$

Relevant standards

EN 12350	Testing Fresh Concrete, Part 1: Sampling, Part 2: Slump test, Part 5: Flow table test
EN 196	Methods of testing cement, Part 1: Determination of strength, Part 2: Chemical analysis of cement, Part 3: Determination of setting times and soundness
EN 197-1	Cement, Part 1 Composition, specifications and conformity criteria for common cements
EN 933-1	Tests for geometrical properties of aggregates, Part 1: Determination of particle size distribution - Sieving method
EN 206-1	Concrete, Part 1: Specification, performance, production and conformity
EN 934-2	Admixtures for concrete, mortar and grout - Part 2: Concrete admixtures; Definitions, requirements, conformity, marking and labelling
EN 1008	Mixing water for concrete. Specification for sampling, testing and assessing the suitability of water, including water recovered from processes in the concrete industry, as mixing water for concrete
ASTM C40	Standard Test Method for organic impurities in fine aggregates for concrete
ASTM D1544	Standard Test Method for color of transparent liquids (Gardner ColorScale)
ASTM C143	Standard Test Method for Slump of Hydraulic-Cement Concrete
ASTM C20	Standard Test Methods for Fineness of Hydraulic Cement by Air-Permeability Apparatus
SR90/1:1990	CEB Bulletin of Information 197. State of the art report: High Performance Concrete

1 Introduction

1.1 The Innovation Center Iceland (ICI) and ICI Rheocenter

The Innovation Center Iceland (ICI) was established August 1, 2007 with the merger of the Technical Institute of Iceland (IceTec) and the Icelandic Building Research Institute (IBRI). It operates under the Ministry of Industry and receives revenue from both the public and private sectors. Projects are usually carried out in cooperation with engineering consultancies, contractors and building material producers. The Department of Concrete Research is a member of RILEM, ACI, Eurolab, ENBRI, NORDTEST, NBS, ASTM und CIB /ICI 1/. ICI Rheocenter is a partner for the building industry when it comes to research effort in the field of rheology of cementitious systems like mortar and concrete. ICI Rheocenter is a cooperation between Reykjavik University and Innovation Center Iceland. ICI Rheocenter was established as a center of excellence in cement based materials, focusing on rheology, cement admixture interactions, and special concrete like SCC. The laboratory is equipped with a wide range of viscometers and rheometers. The head of the department is Prof. Olafur H. Wallevik.

1.2 The project

This thesis is based on work within the project “Innovation in concrete production by use of rheology”. The project was divided into four major parts: (1) activation time of admixtures, (2) development of Rheometer4SCC/Rheomixer, (3) interaction of cement and admixtures, and (4) evaluation of a form pressure releasing agent. This report is mainly covering the third part (interaction of cement and admixtures).
With the start of mass application of concrete toward the end of the 19th and beginning of the 20th century, concrete was modified by the help of admixtures. The first concrete admixtures were accelerators (1873), retarders (1885) and densifiers (1900) /Sta 1/. In the 1930´s plasticizers were used for the first time in concrete technology. By using admixtures, the properties of fresh and hardened concrete were improved significantly. In the early days of concrete technology, the main reason for using plasticizers was the reduction of w/c-ratio in order to achieve a higher strength level and thereby also to reduce the water permeability. Adding plasticizers in the concrete resulted in a better workability, or in rheological terms, the yield value and plastic viscosity of the concrete were lowered to a more concrete worker friendly state. Basically, concrete admixtures can be distinguished by the five groups listed below:

- accelerators
- retarders
- water proofing agents/densifiers
- plasticizers
- air-entraining agents

The most important group for today´s concrete engineers are the plasticizers. Only by using plasticizers is it possible to meet the quality demands for fresh and hardened concrete described in the relevant standards. Standard plasticizers are normally based on sulfonated Lignine, sulfonated Melamine, sulfonated Naphthalene or a combination of these. Despite the fact that some of these products are more than 50 years old, they are still used for normally vibrated concrete and semi-flowable concrete.

With the development of Self Compacting Concrete (SCC), a more effective type of dispersing admixture was needed. Pioneer work in this field was mainly done by Japanese scientists. During the 80´s they succeeded in developing a new type of superplasticizer on the

basis of polycarboxylate ether (PCE). These new plasticizers are more effective than the older products using lignine, melamine or naphthalene as a base. The water reducing effect of the PCEs is reached by a higher dispersion of the cement particles. Two factors are responsible for the higher dispersing effect of the PCEs compared to the old products. The first factor is the electrostatic repulsion between cement particles due to the negative charge of the polycarboxylate ether molecules. Electrostatic repulsion occurs with other older chemicals like melamine. The second factor is based on the steric hindrance between cement particles due to the stretching of side and main chains of the polymers. The combination of both factors makes the PCEs much more powerful than the older products.

Both admixtures of the old generation (melamine and naphtalene) and admixtures of the new generation (polycarboxylate ether) have challenged engineers in science and concrete industry with various problems. In some cases it has been observed that certain cement/superplasticizer combinations showed a rather quick workability loss (incompatible combination), whereas the same cement with a different superplasticizer maintained a sufficient workability over a long periode of time (compatible combination). This effect is most likely related to the interaction between the cement and the dispersing admixture used.

The practical background of this study is the influence of production date of cement on rheology of concrete. During prolonged concrete jobs, the rheological parameters of fresh concrete are sometimes known to fluctuate significantly with cement batches, even if delivered from same plant and production line. This effect can be considerably more prominent if dispersing admixtures are present in the concrete mix. The two important questions from perspective of cement producer are:

(1) How big are the fluctuations in rheology when a new cement delivery is used?

(2) What are the main influencing factors for these fluctuations?

Therefore, cement samples from several producers, randomly picked during routine cement production (representing up to 3 year production period) were tested in order to achieve information about the major influencing factors on rheology. Another approach was to investigate the effect of significant changes in chemical composition (e.g. aluminates, sulphates) on rheological properties.

This thesis has the character of a research report. It was written as an external doctoral thesis for F.A. Finger-Institute for Building Material Science, Bauhaus University Weimar at ICI Rheocenter, Reykjavik, Iceland between 2005 and 2009.

1.3 Introduction to rheology

1.3.1 Background and basic terms

Rheology is the science of deformation and flow of matter. The term rheology was invented in 1920 by Professor Eugen C. Bingham at Lafayette College in Indiana. Bingham, who was a professor of chemistry, studied new materials with strange flow behaviour, in particular paints /IR 1/. The syllable “Rheo” is from the Greek words “panta rhei…” /Me 1/, meaning everything is in flow/motion, so the name rheology was taken to mean the theory of deformation and flow of matter.

In rheological science, fluids are distinguishable by their physical properties. Newtonian fluids are fluids that obey Newton´s linear law of friction. Fluids that do not follow the linear law are called non-Newtonian. These fluids are usually highly viscous fluids and their elastic properties are also of importance /IR 1/. The theory of non-Newtonian fluid is a part of rheology. Typical non-Newtonian fluids are polymer solutions, thermoplastics, drilling fluids, mortar and fresh concrete /IR 1/.

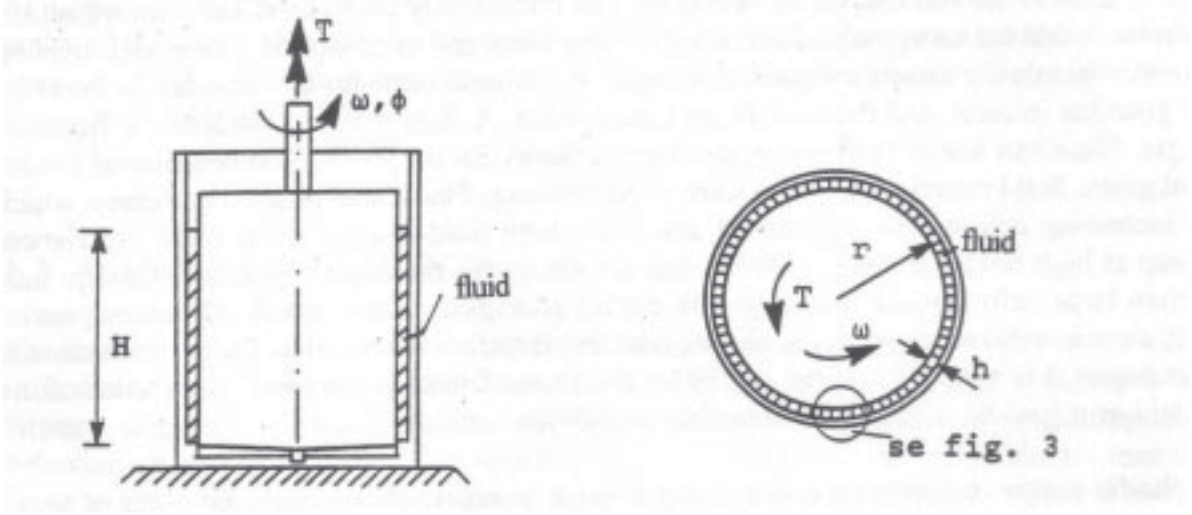

Figure 1.3.1.1: Cylinder viscometer /IR 1/

Figure 1.3.1.1 shows a cylinder viscometer. A cylinder can rotate in a cylindrical container about a vertical axis. The annular space between the two concentric cylindrical surfaces is filled with a liquid. The cylinder is subjected to a torque T and comes in rotation with a constant angular velocity ω [rad/s]. The distance h between the two cylindrical surfaces is so small compared to the radius r of the cylinder that the motion of the liquid may be considered to be like the flow between two parallel plane surfaces (see Figure 1.3.1.2, left side) /IR 1/.

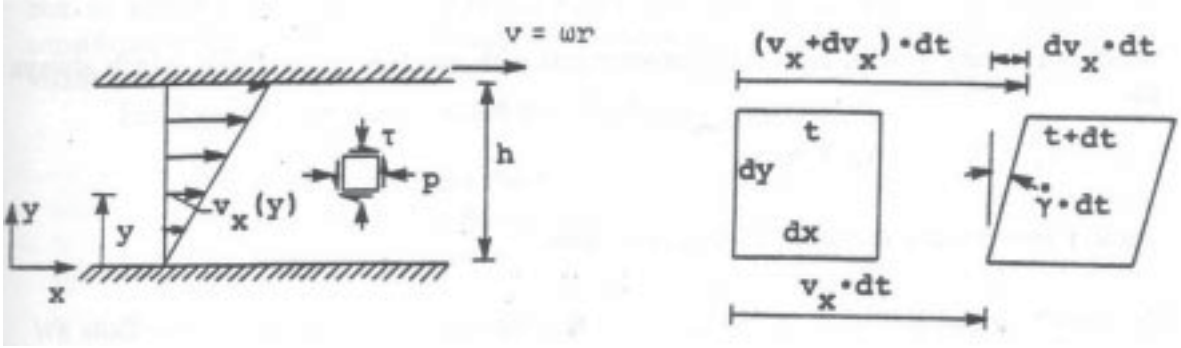

Figure 1.3.1.2: Simple shear flow (left side) and fluid element (right side)

For moderate ω-values the velocity field is given by

$v_x = (v/h)y$, $v_y = v_z = 0$
Where v_x, v_y, and v_z are velocity components in the directions of the axes in a Cartesian coordinate system O_{xyz} /IR 1/.

The term

$v = \omega r$

is the velocity of the fluid particle at the wall of the rotating cylinder /IR 1/.

The quantity

$\gamma = v/h$

is called the rate of shear strain, or for short the shear rate. The flow described by the velocity field and shown in Figure 1.3.1.2 (right side), is called simple shear flow. The unit of shear rate is 1/s. The fluid element in Figure 1.3.1.2 (left side) is subjected to normal stresses on all sides and a shear stress τ on four sides. The shear stress may be determined from the balance law of angular momentum applied to the rotating cylinder. For the case of steady flow at constant angular velocity ω the torque T is balanced by the shear stresses τ on the cylindrical wall /IR 1/. The unit of shear stress is Pascal [Pa], 1 Pa = 1 N/m² = 1 kg/ms².

Thus

$[\tau\, r]\, [2\, \pi\, r\, H] = T \Rightarrow \tau = T / (2\, \pi\, r^2\, H)$

The viscometer records the relationship between the torque T and the angular velocity ω. A relationship is obtained between the shear stress τ and the shear rate γ. A Newtonian fluid (see Figure 1.3.2.1) is a purely viscous fluid with a linear constitutive equation /IR 1/.

$\tau = \mu\, \gamma$

The coefficient μ is called the viscosity of the fluid. The unit of the viscosity is Pascal seconds [Pa s], 1 Pa·s = 1 Ns/m² = 1 kg/sm.

1.3.2 Fluid types

Basically, fluids can be classified into four main groups, depending upon their flow properties /Wa 1/:

- Newtonian fluids
- Non-Newtonian fluids, time independent
- Non-Newtonian fluids, time dependent
- Visco-elastic fluids

For Newtonian fluids the viscosity remains constant for all rate of shear. The viscosity function is constant, and therefore the simplest one that can occur /Wa 1/. Figure 1.3.2.1 shows the flow curve, where the shear stress is plotted against the rate of shear for a Newtonian fluid. Liquids which show Newtonian flow behaviour are often simple, single

phase liquids and solutions of liquids with low molecular weights, for example: water, glycerol, petrol and oil /Wa 1/.

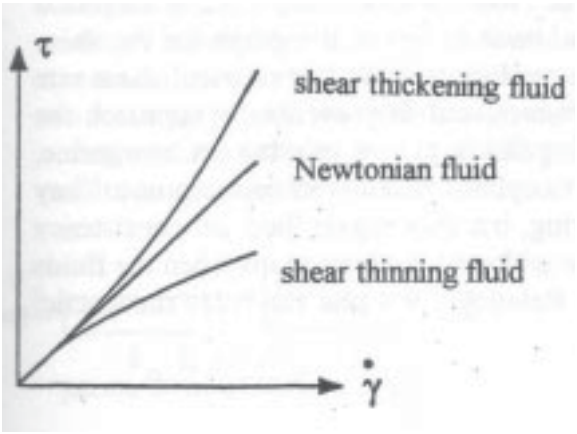

Figure 1.3.2.1: Flow behaviour of Newtonian fluid, shear thickening fluid and shear thinning fluid /Wa1/

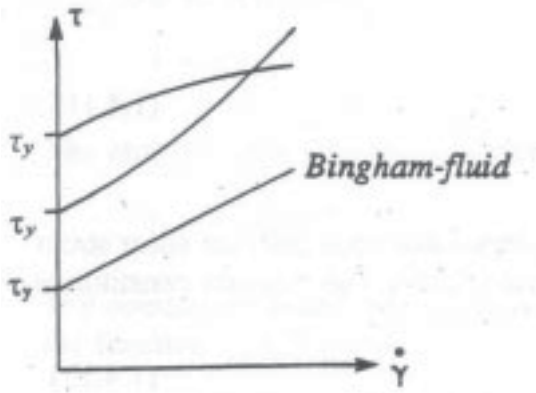

Figure 1.3.2.2: Flow behaviour of shear thinning fluid (upper curve), shear thickening fluid (medium curve) and fluid with a yield value (Bingham fluid) /Wa1/

Non-Newtonian, time independent fluids show a viscosity which is dependend on the shear rate applied to the sample. These fluids do not have a constant viscosity. The apparent viscosity of the sample is changing with a change in shear rate (see Figure 1.3.2.2) /Wa 1/.

The flow behaviour of non-Newtonian, time independent fluids are shown in Figure 1.3.2.2 and can further be classified into:

- Shear thinning fluids
- Shear thickening fluids
- Fluids with a yield value

Examples of fluids exhibiting a yield value are: drilling fluids, sand in water, margarine, mortar and fresh concrete.

1.3.3 Rheology of fresh concrete and mortar

Fresh concrete and mortar requires the application of force in order to flow. In other words, it has a certain resistance to flow. The force required to initiate flow is called the yield value (τ), as can be seen in Figure 1.3.3.1 a). There are two types of yield values, namely the static yield value and the dynamic yield value /Wa 6/. The static yield value is related to the amount of shear necessary to make the test material start flowing, meaning the transformation from a solid state to a viscoplastic state /Wa 6/. The dynamic yield value is equal to the shear stress at which a flowing test material stops flowing, meaning the transformation from a viscoplastic state to the solid state /Wa 6/. In this thesis, the yield value of interest is the dynamic yield value. Due to mechanical entanglements and coagulation of cement particles at rest, the static yield value is usually higher than the dynamic yield value.
Note that below the yield value, no flow occurs. Increasing the rate of flow (rate of shear) causes the resistance (shear stress) to increase, as shown in Figure 1.3.3.1 b). The slope of the line is an expression of the plastic viscosity of the mass /Wa 1/. The yield value and plastic viscosity of fresh concrete or mortar can be measured with the help of a viscometer. Such a viscometer records the shear resistance (stresses) at different flow rates /Wa 1/.

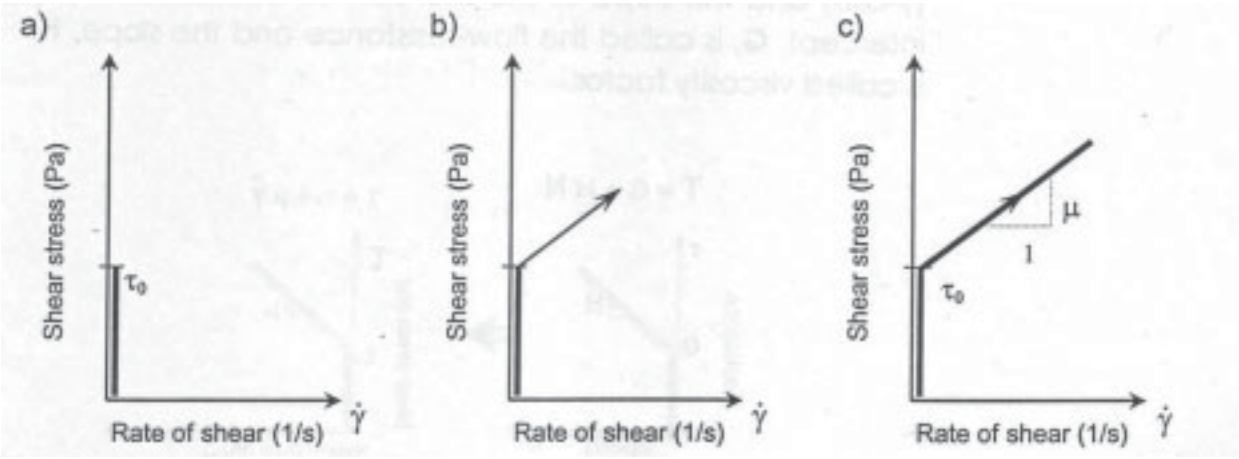

Fig. 1.3.3.1: Evolution of resistance or shear stresses when starting a movement in the fresh concrete or mortar. A simple flow-curve of fresh concrete or mortar /Wa 1/

According to the Bingham model, the flow properties are characterized by two parameters, yield value (τ_0) and the plastic viscosity (μ).

$$\tau = \tau_0 + \mu \times D$$

where: τ = shear stress [Pa]

D = rate of shear [1/s]

The yield value (see Figure 1.3.3.1 a) can also be described as a property of the fluid close to shear rate zero (i.e. the material is nearly at rest). Hence, it is mainly affected by (1) attractive forces between cement particles and (2) mechanical entanglements between aggregate particles and also cement particles. A relatively good correlation exists between the yield value measured with a rheometer and results from standardized methods like the slump flow test /Ab 1/ or the German flow table test /DIN 1/. However, both standardized tests are relatively primitive and are only a rough approximation.

Another phrase for yield value used in this thesis is the expression G-yield. The G-yield is a rheological parameter obtained by use of ConTec Rheomixer and is equal to the yield value.

On the other hand, the plastic viscosity (see Figure 1.3.3.1 c) is a property of the fluid already in motion. It is therefore mainly determined by parameters like dynamic friction between the moving elements, such as aggregate particles and cement particles.

A further phrase for plastic viscosity used in this thesis is the expression H-viscosity. The H-viscosity is a rheological parameter obtained by use of ConTec Rheomixer and is equal to the plastic viscosity.

Liquids such as fresh concrete or mortar belong to the group of Non-Newtonian liquids (time independent). They are also called Bingham fluids. A Bingham fluid shows a plastic (such as a rigid body) behaviour below the yield stress and the behaviour of a Newtonian fluid above the yield stress, as can be seen in Figure 1.3.3.1 c).

1.4 Prerequisites and limitations of study

The reference cement for this study represents a three year production period of a normal Portland cement (CEM I 52,5N). Initially it was planned to use only cement from 25 kg bags for the study. This was not possible because the ships to Iceland did not always carry 25 kg bags, so bulk/silo cement was incorporated in the study. After testing many cement deliveries it turned out that the reference cement is a relatively stable and reliable product. In other words, the rheology fluctuations of the reference cement were less than those encountered for most other cements.
One project sponsor stopped sending his cement samples during the first year of the project. This was a loss from a scientific point of view because the cement provided by this supporter showed relatively high fluctuations in rheology. A few results with this cement are available. Cement samples were tested as soon as possible after they arrived at ICI. Thereafter, the samples were stored in sealed containers or multi-layer plastic bags. In preliminary investigations it was shown that if cement is stored correctly under laboratory conditions, changes in cement properties during storage periods of up to one year are negligible.
The chemical and mineralogical composition of the cement was determined by use of x-ray fluorescence (XRF), modified Bogue and Rietveld refinement. The alkali content discussed here is the total amount of alkalies. It should be noted that the soluble amount of alkalies would be more accurate, as only the alkalies present in the liquid phase can influence the effectiveness of the admixture. To investigate the cement-admixture interaction, four polycarboxylate based and one melamine based admixtures were used in the study. The polycarboxylates used represent steric hindrance. The melamine used represents electrostatic stabilisation.
Rheological tests were done on mortar mixes produced with standardized sand (standard sand according to EN 196-1) and not on paste mixes. In our opinion mortar mixes are more realistic than paste mixes for this kind of study since the paste volume of mortar is more in line with paste volume of concrete than that of pure cement paste. A certain cement-admixture incompatibility observed in paste might be difficult to observe to the same extent in concrete. On the other hand a cement-admixture incompatibility observed in mortar can be clearly seen in concrete.
The yield stress of mortar mixes without admixtures was in the range of 300 to 400 Pascal (Pa). This relatively stiff consistency is characteristic of normally vibrated concrete. The yield stress of mortar mixes with admixtures was in the range of 50 to 200 Pa. This relatively fluid consistency is characteristic of self compacting concrete and flowable concrete (F5 to F6 classes according to EN 206). Microstructural investigations were made on cement pastes in order to correlate rheological behaviour to microstructure. Conclusions based on the Scanning Electron Microscope (SEM) and Environmental Scanning Electron Microscope (ESEM) pictures have to be taken with reservation as these methods give only qualitative results and no quantitative results. The mixing energy (shear history) has an effect on the rheological results. All results discussed here were obtained under the same mixing regime, as described in chapter 3.3.1.

1.5 Report structure

The report is organized as follow: chapter 1.3 serves as a basic introduction to rheology. Chapter 2 gives an overview of the literature in the field of cement hydration, the dispersing mechanisms in cementitious systems and cites references regarding cement-admixture interaction. Chapter 3 describes the objective of the project and the methods and materials used for the investigation. Chapter 4 presents the characteristic values, the rheological results and the mineralogical composition of all cements used for the main series. Chapter 5

discusses the results obtained by the experiments. Finally, chapter 6 includes conclusions and suggestions for future work.

2. Literature survey

2.1 Purpose of literature survey

The purpose of the literature survey is to analyse and evaluate publications dealing with cement hydration, hydration models and the interaction of cement and admixtures.

2.2 Portland cement

2.2.1 Composition of Portland cement

Portland cement is produced by heating a mixture of limestone and clay, or other materials of similar bulk composition and sufficient reactivity, ultimately to a temperature of about 1450°C. Partial fusion occurs, and nodules of clinker are produced. The clinker is mixed with a few per cent of calcium sulphate and finely ground, to make the cement /Tay 1/. Calcium sulphate is added to control the setting behaviour of the hydrating cement, in particular of the aluminate phase (C_3A). The clinker typically has a composition in the region of 67% CaO, 22% SiO_2, 5% Al_2O_3, 3% Fe_2O_3 and 3% other components /Tay 1/. These oxids form the major phases, called alite (C_3S), belite (C_2S), aluminate (C_3A) and ferrite ($C_2(A,F)$). Several other phases, such as alkali sulphates and calcium oxide, are normally present in minor amounts /Tay 1/.

Tricalcium silicate (alite)

Alite is the most important constituent of Portland cement clinker, of which it constitutes 50-70%. Pure tri calcium silicate contains 73,7% of CaO and 26,3% of SiO_2. Alites in clinkers typically contain 3-4% of substituent oxides. It is the most important of the constituent phases for strength development /Tay 1/. Tricalcium silicate can be present in different crystal structures, monoclinic and triclinic depending upon the incorporation of substituent ions. Incorporated substituents can be Mg^{2+}, Al^{3+} and Fe^{3+}. The differences in crystal formations have a relatively small influence on its hydraulic reactivity /Sta 3/. Several hypothesis describing the hydration of tricalcium silicate exist. In the initial reaction, C_3S dissolves and a material is deposited. This reaction product forms an overlying surface layer about 1 nanometre in average thickness. Within 30 s the C_3S is almost isolated from the solution. During the early part of the induction period, C-S-H nucleates and begins to grow. This implies dissolution of the surface layer and increased access of solution to the C_3S, which thus dissolves more rapidly. The rate of reaction in this stage is controlled by the growth of C-S-H, the rate of which increases with the amount already formed /Tay 1/. Tricalcium silicate reacts relatively fast with water. However, the amount of tricalcium silicate consumed for hydration in the first three hours after water addition is relatively low. According to /Tay 1/ it is in the range of 3-5% of the total amount of tricalcium silicate.

Dicalcium silicate (belite)

Belite constitutes 15-30% of normal Portland cement clinkers. Pure dicalcium silicate contains 34,9% of SiO_2 and 65,1% of CaO. Belites in clinker typically contain 4-6% of substituent oxides. Dicalcium silicate can be present in three different crystal structures, depending upon cooling rate and incorporation of substituent ions /Sta 3/. Belite is predominantly of β–C_2S structure and rarely of α and α' forms. Dicalcium silicate reacts slowly with water, thus contributing little to the strength during the first 28 days, but substantially to the further increase in strength that occurs at later stages. According to /Tay 1/, the kinetics and mechanism of β–C_2S hydration are similar to those for C_3S, apart from the much lower rate of reaction.

Tricalcium aluminate (aluminate)

Aluminate constitutes 5-10% of most normal Portland cement clinkers. Pure tricalcium aluminate contains 62,3% CaO and 37,7% Al_2O_3. Production clinkers have been found to

contain cubic or orthorhombic forms of aluminate, alone or in combination /Tay 1/. The orthorhombic aluminate is considered to be more reactive than the cubic. The orthorhombic modification can arise only if sufficient alkali is available, but its formation appears to be favoured also by rapid cooling and by bulk compositions potentially able to yield a relatively high proportion of aluminate /Tay 1/. Aluminate reacts rapidly with water, and can cause undesirably rapid setting unless a set-controlling agent, usually gypsum, is added /Tay 1/. Together with water, the added gypsum forms ettringite on the surface of the aluminate phase, so that the reaction of the aluminate phase is slowed down. Without the addition of gypsum, the hydrating cement would set immediately and not be workable.

Calcium aluminate ferrite (ferrite)
Ferrite makes up to 5-15% of normal Portland cement clinkers. The theoretical composition of C_4AF is 46,1% CaO, 21,0% Al_2O_3 and 32,9% Fe_2O_3. The composition of the ferrite phase differs markedly from the pure phase. It contains about 10% substituent ions and is much lower in Fe_2O_3. The rate at which it reacts with water appears to be somewhat variable, perhaps due to differences in composition or other characteristics, but in general is high initially and low or very low at later ages /Tay 1/.

2.2.2 Hydration reaction of Portland cement

The hydration reaction of Portland cement is comparable to the hydration of its pure clinker phases. In the early stage of hydration, ettringite is formed by the aluminate phase and the calcium sulphates. At later stage (during the main phase of hydration), C-S-H-phases are formed by the alite phase. The amount of calcium sulphate (for setting control) is limited to 3,5 to 4% due to its expansive behaviour. Therefore, not all aluminates will be transformed into ettringite. /Sta 2/

Early phase of hydration /Sta 2/
The hydration reaction of Portland cement can be distinguished in several periods depending upon their heat release. After a short and intense reaction in the first minutes after water addition (see Figure 2.2.2.1) the dormant period begins. The reactivity is very low during this period.

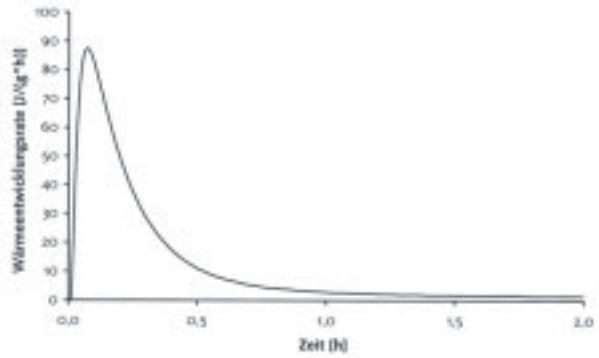

Figure 2.2.2.1: Hydration curve of Portland cement in the early phase of hydration /Sta 2/

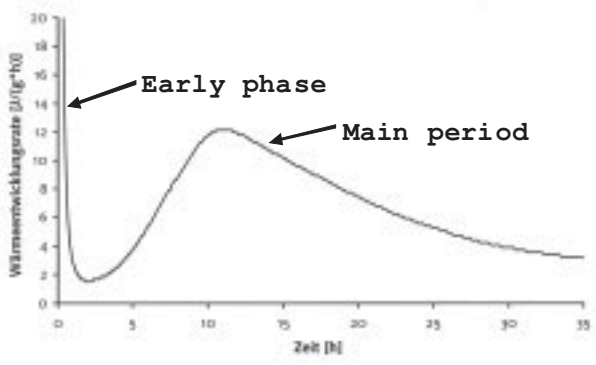

Figure 2.2.2.2: Hydration curve of Portland cement in the main phase /Sta 2/

The dormant period lasts for several hours and is followed by the main hydration reaction, namely the acceleration and decelleration periods. Thereafter, the heat of hydration measured is very small, meaning the intensity of the cement hydration is still occuring but on a low level /Sta 2/.

If cement and water come in contact with each other, a peak in the hydration curve occurs in the first few minutes. This peak lasts only for one or two minutes. The reactions taking place during first minutes and hours after water addition are as following /Sta 2/:

- Free lime from clinker reacts directly with water to calcium hydroxide (see Figure 2.2.2.5). This exotherm reaction is relatively quick as the free lime is not incorporated in the cement clinker. The free lime is present in grains with a diameter of 10 to 20 µm (see Figures 2.2.2.3 and 2.2.2.4). Other possible reactions of the free lime are (1) the formation of gypsum from free lime and alkali sulphates and (2) the formation of ettringite from aluminates and alkali sulphates /Sta 2/.
- During the cooling process of clinker, alkali sulphates are crystalizing on the clinker surface. Hence, alkali sulphates are easily accessible for water and their solubility in water is relatively high. Depending upon their composition, alkali sulphates can be present as arcanite, thenardite, aphtitalite and calcium langbeinite /Sta 2/.
- High concentration of potassium and sulphate ions can occur when arcanite dissolves, leading to syngenite formation (see Figure 2.2.2.6). The formation of syngenite is also promoted by a high calcium ion concentration in the pore solution. Syngenite occurs as thin bar and needle shaped crystals with a length of up to 10 µm. These crystals can have a significant effect on the rheological properties of cement paste. If too much syngenite is present, early stiffening can occur /Be 3/. However, if the paste is stirred intensively after stiffening, the syngenite crystals are broken resulting in better rheology.

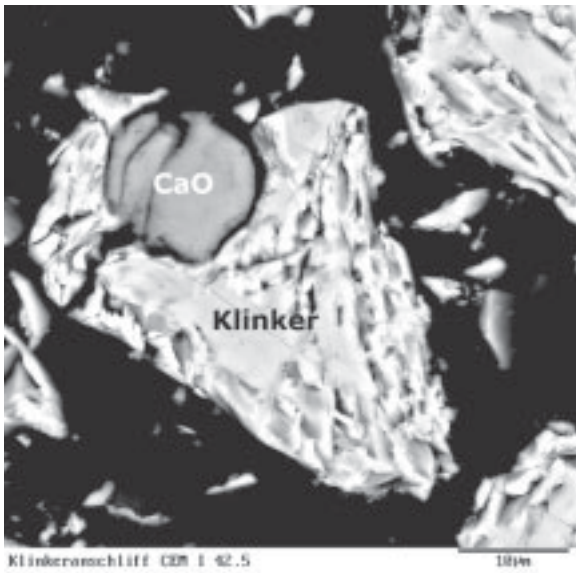

Figure 2.2.2.3: Free lime particle in the thin section of cement clinker /Sta 2/

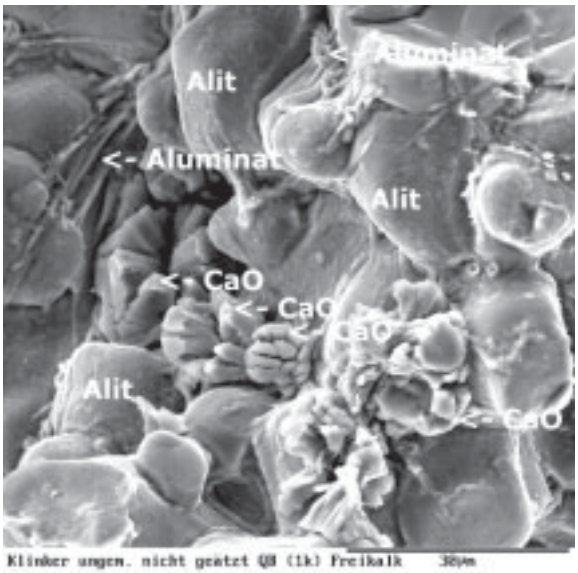

Figure 2.2.2.4: Free lime particles in the fractured surface of cement clinker /Sta 2/

- A very important reaction in the early phase of hydration is the formation of ettringite (see Figure 2.2.2.7). As mentioned already, the aluminates react fastest with water. If no sulphates are present, thin and platy calcium aluminate hydrate crystals are formed, bridging the free space between the cement particles. The mix stiffens immediately (flash set). To prevent the formation of calcium aluminate hydrate crystals (2 x 2 x 0,05 µm), calcium sulphate is added. When calcium sulphate is present, ettringite with a length of 100 to 400 nm and a thickness of 50 to 100 nm forms on the surface of the aluminate phase. Microstructural investigations by use of an ESEM-FEG showed that ettringite is not solely present on the aluminate phase. Ettringite was also found on other clinker phases (though in smaller amounts).

Sulphate ions originating from alkali sulphates and calcium ions originating from free lime can also promote the formation of ettringite. The reactivity and amount of calcium sulphates has to be tailor made for each clinker. If the calcium sulphate is not sufficiently able to transform the aluminates into ettringite, the saturation index for ettringite in the pore solution decreases. This can result in the formation of long prismatic ettringite or calcium aluminate hydrate /Sta 2/.

- During cement milling, calcium sulphates are added as a mixture of gypsum ($CaSO_4 \cdot 2H_2O$) and anhydrite ($CaSO_4$). Due to the high temperatures in the cement mill, the gypsum dehydrates fully or partly to hemihydrate ($CaSO_4 \cdot 0{,}5H_2O$). If the cement gets in contact with water, hemihydrate (and later the anhydrite) can react to secondary formed gypsum resulting in poor rheology (see Figure 2.2.2.8). However, the formation of secondary formed gypsum is rarely observed /Sta 2/.
- A reaction occurs on the surface of alite and belite which is not fully understood. This reaction causes the dormant period during cement hydration, meaning alite and belite are rather inactive for several hours. After the dormant period, the reaction proceeds relatively fast (particularly with alite).
- The high specific surface area of cement causes a slight exothermic effect during the wettening process of cement /Sta 2/.

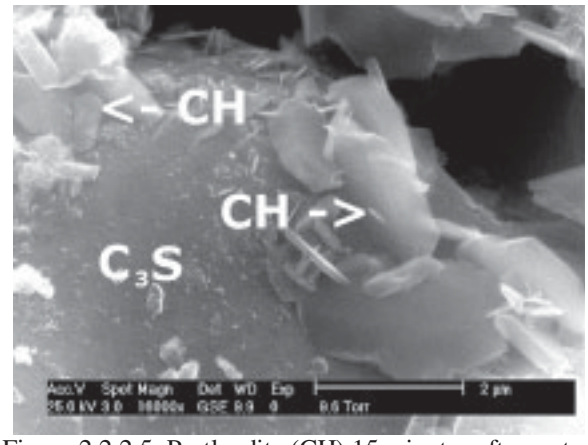

Figure 2.2.2.5: Portlandite (CH) 15 minutes after water addition (specimen C_3S) /Sta 2/

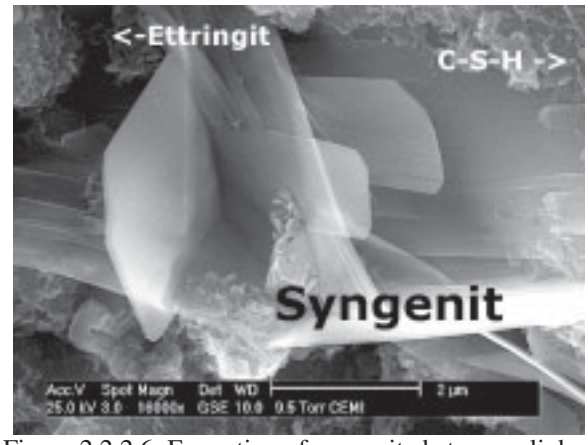

Figure 2.2.2.6: Formation of syngenite between clinker particles (4 hours hydration) /Sta 2/

The following processes occur during the early phase of cement hydration /Sta 2/:

- Wettening of the cement surface
- Free lime reacts with water
- Alkali sulphates are dissolving in water
- The primary hydration products ettringite and syngenite are formed, depending upon cement composition gypsum and portlandite can also occur
- A reaction occurs on alite and belite

The above mentioned processes were observed by use of an Environmental Scanning Electron Microscope (ESEM) /Mö 1, Mö 2/, pore solution analysis and quantitative X-ray diffraction (Rietveld) /Sta 2/.

<u>Pore solution composition during early hydration phase /Sta 2/</u>

The reaction of free lime (if available in sufficient amounts) with water results in the formation of portlandite. Thereby, the ionic balance to form portlandite are reached (calcium 20 mmol, hydroxide 40 mmol). This is corresponding to a pH level of 12,45 at 25°C.

When alkali sulphate dissolve, the concentration of alkali ions (particularly potassium) and sulphate ions increases. The actual concentration depends upon the amount of water soluble

alkali sulphates. Hence, the ionic concentration can vary widely. The following values were measured on an alkali rich and (low alkali) cement CEM I 42,5 after one hour of hydration: potassium= 453 (141) mmol/l, sodium= 52 (15) mmol/l and sulphate= 206 (49) mmol/l. Although alkali ions are originating from alkali sulphates, the sulphate ions are not balancing the alkali ions in solution. A deficite of sulphate ions occurs when sulphates are consumed during ettringite formation (and also secondary formed gypsum). The precipitation of the sulphate containing minerals ettringite and gypsum reduces the amount of free sulphate ions in solution without changing the amount of free alkali ions in solution. The positively charged alkali ions are then also balanced by hydroxide ions. Hence, the formation of ettringite causes the replacement of sulphate ions by hydroxide ions. And an increase in hydroxide ion concentration results in an increase in pH value. At the same time, the concentration of calcium ions is decreasing due to the fact that calcium ion concentration has to be lower at higher pH values /Sta 2/.
The temporarily formation of syngenite results in a temporarily reduction of sulphate and potassium ions.
The concentration of silicium is very low during the complete hydration process. Only during first minutes of hydration a slightly higher level could be detected.

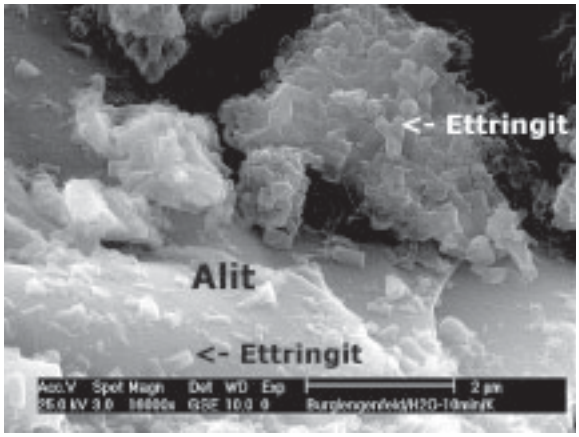

Figure 2.2.2.7: Ettringite forms primarily on aluminates, other phases are less covered /Sta 2/

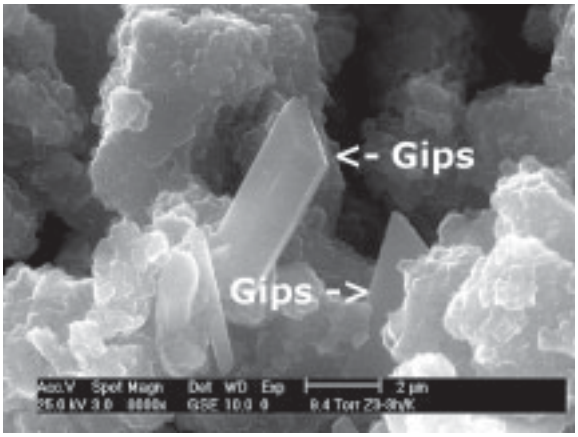

Figure 2.2.2.8: Formation of secondary formed gypsum between clinker particles /Sta 2/

Main hydration phase /Sta 2/
After the first intense reaction of cement with water, the hydration process comes nearly to a halt for several hours. This due to the formation of ettringite shells around the aluminates. Thereby, the hydration proceeds at a low intensity level, whereas the main reaction of the alite has not started yet. This state is characteristic for the dormant period. /Sta 2/
The hydration of alite starts two to three hours after water addition. This phase is named acceleration period. During acceleration phase, C-S-H-phases occur locally on the clinker surface. At the same time, cavities and holes develop on the clinker surface (see Figure 2.2.2.9). C-S-H-phases are growing to a length of one to two µm with a thickness of 50 nm. However, C-S-H-phases consist of even smaller structures in the range of few nanometers. The small size of the single C-S-H-phases results in the very high specific surface area of hydrating cement (50 to 200 m2/g). The C-S-H-phases are forming a dense layer of needle shaped formations around the clinker grain. Usually, C-S-H-phases are growing perpendicular into the free pore space, resulting in a interconnected and stable network of C-S-H-phases (see Figure 2.2.2.10). If the water to cement ratio is low, the particle distance is low too whereas the packing density is relatively high. Therefore, the increase in compressive strength of concrete with a low water to cement ratio is presumably due to a lower porosity (due to lower particle to particle distance) and more mechanical entanglements between cement particles than in high water concrete. /Sta 2/

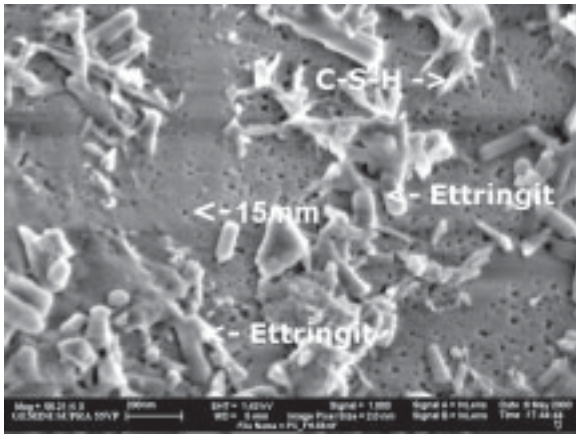

Figure 2.2.2.9: Cavities occur on the clinker surface during C-S-H phase formation /Sta 2/

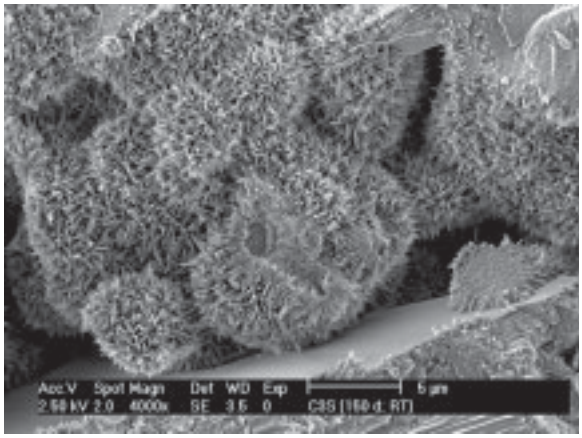

Figure 2.2.2.10: Orientated growth of C-S-H phases on the clinker results in an interconnected matrix /Sta 2/

The growth of C-S-H-phases leaves sometimes a gap between the growing hydration product and unhydrated clinker surface (see Figure 2.2.2.11). This gap might be filled with other hydration products. C-S-H-phases do not solely occur on alite. They can also be observed on the slower hydrating belite and ferrite. C-S-H-phases were also reported on fine mineral additions, such as lime stone filler (see Figure 2.2.2.12). The major part of the hydration layer consists of C-S-H-phases. Ettringite can be found in between (see Figure 2.2.2.13). It is assumed that this ettringite contains aluminium originating from impurities in the pure alite phase. On the contrary, aluminate phases are densly covered with ettringite (see Figure 2.2.2.14). /Sta 2/

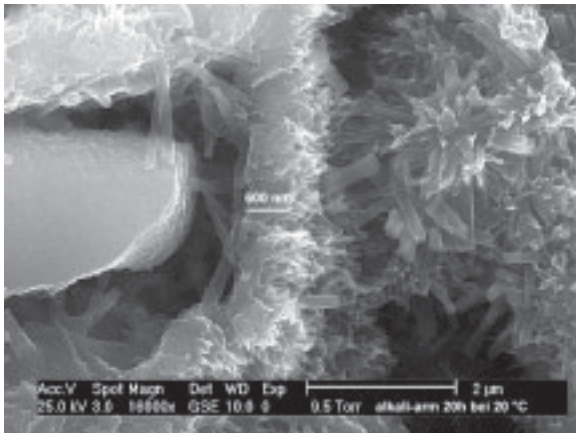

Figure 2.2.2.11: Ettringite crystals in the gap between unreacted cement clinker and C-S-H phases /Sta 2/

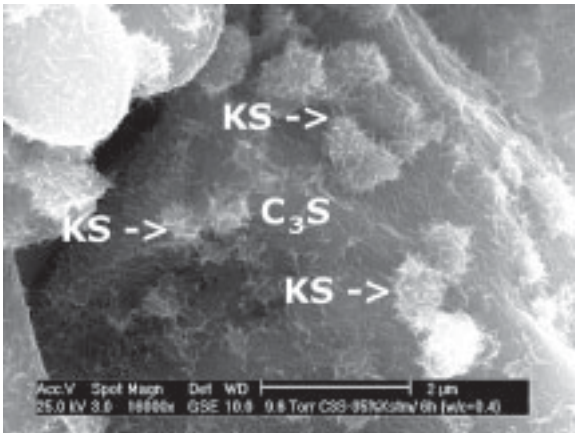

Figure 2.2.2.12: C-S-H phases on the surface of lime stone powder /Sta 2/

C-S-H-phases are needle shaped hydration products originating from the main cement clinker phases alite and belite. The dashes indicate a variable chemical composition. The Ca/Si ratio is reported with 1,6 to 1,9 (atomic ratio). The water content of C-S-H-phases is between 20 and 40 weight-% /Tay 1/. The exact mineralogical composition of the C-S-H- phases is still unknown. IMR-analysis indicates that C-S-H-phases contain tetraeders of silicium connected by three single chains (see Figure 2.2.2.15). Due to incompletly connected chains and impurities in their structure, C-S-H-phases are nearly undetectable by use of X-ray diffraction. This led to the false assumption that C-S-H-phases might be a gel. /Sta 2/

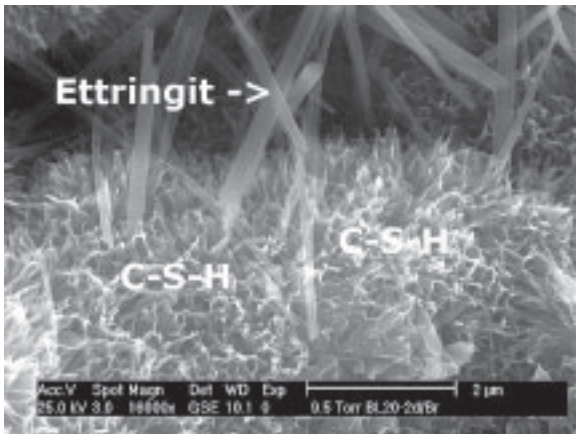

Figure 2.2.2.13: Ettringite crystals between C-S-H phases /Sta 2/

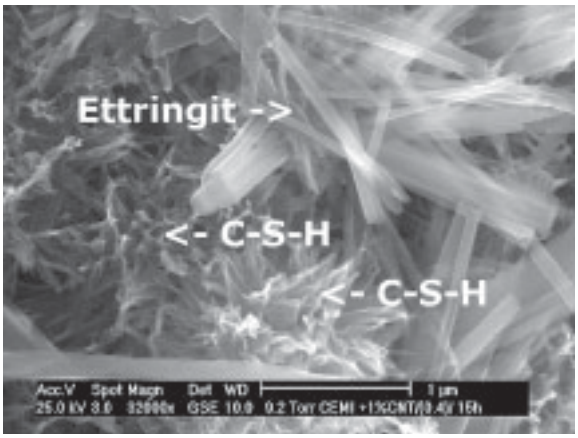

Figure 2.2.2.14: Local ettringite formation /Sta 2/

During the acceleration phase, alite is the major hydrating phase. However, the hydration reaction is slowing down when dense layers made of C-S-H-phases are covering the alite phase (deceleration phase). While small particles hydrate completely, the bigger particles remain unhydrated in their core. The core contains primarily more slowly reacting phases such as beliet and ferrite (see Figure 2.2.2.16). After the deceleration period and at later ages, cement hydration occurs at a very low level. The major contributing phases after the deceleration period are presumably belite and ferrite. Though, all the processes occurring at later ages (1 to 2 days after water addition) are of big importance for the final strength and permeability of the matrix. When the early hydration is stopped premature, the microstructure of the paste will become rather porous. This is particularly important for slowly hydrating cement, such as slag cement. /Sta 2/

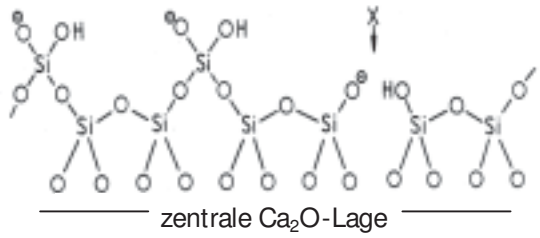

Figure 2.2.2.15: Assumed structure of silicate tetraeder within the C-S-H phases /Sta 2/

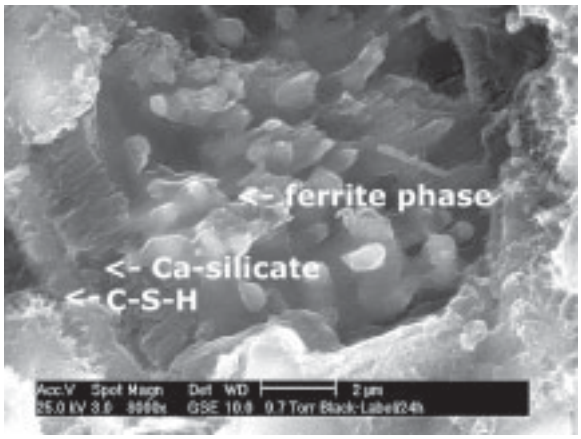

Figure 2.2.2.16: Less active phases in unhydrated cement grain /Sta 2/

Not all the calcium oxide from alite is bound during C-S-H formation. The excess calcium is present in the paste as calcium hydroxide (also named portlandite). Portlandite occurs as hexagonal shaped plates which form agglomerates between cement particles (see Figure 2.2.2.17). /Sta 2/

C-S-H-phases do not only form on alite and belite, they can also be found on other surfaces. If additional surface area is available (i.e. by adding lime stone filler to cement), the hydration products cover the cement grains less densely, as they can be found both on cement grains and on mineral additions. This is one reason why mineral additions accelerate the hydration process during the acceleration period. By adding very fine lime stone powder, the C-S-H-phases can precipitate on the fine mineral powder (see Figure 2.2.2.12). The layers of C-S-H-

phases surrounding the cement grains are less dense and therefore more C_3S can be transformed into C-S-H-phases and portlandite. /Sta 2/

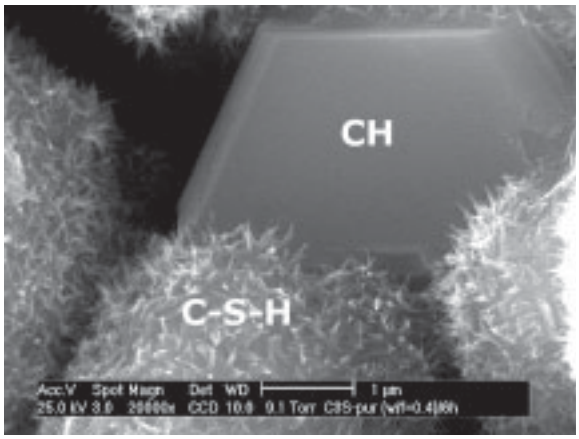

Figure 2.2.2.17: Portlandite crystal /Sta 2/

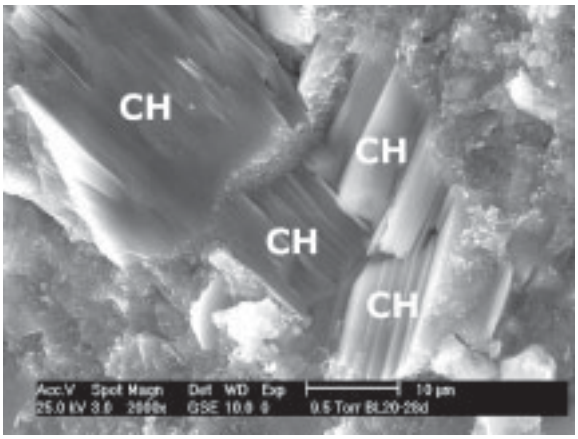

Figure 2.2.2.18: Agglomerated portlandite /Sta2/

The degree of hydration and the compressive strength can be increased by (1) adding fine mineral additions and (2) increasing the milling time. An increased milling time results in finer cements with less big particles. Finer clinker particles are able to hydrate completely, while an unhydrated core remains only with the bigger particles. Hence, the degree of hydration is higher with finer cement. /Sta 2/

As already mentioned, C-S-H-phases are formed during a very intense reaction of water and alite (acceleration phase). During this reaction aluminium is also made available for further hydration with calcium sulphate and water. Aluminates are also released during the hydration of alite and belite. Both phases contain aluminium, sodium, magnesium, potassium and other elements as impurities. When the main phase reacts, impurities are released in the pore solution. /Sta 2/

The freshly released aluminium is presumably bound in ettringite. This leads to the consumption of all available calcium sulphate within one day. In absence of calcium sulphate, aluminium reacts to AFm-phases. Equations 5 to 7 depict the possible reactions.

Eq. 5: C3A + Ca(OH)2 + 18 H2O -> C4AH19
Eq. 6: C3A + 3CaSO4 32H2O + 2C3A + 4H2O -> 3 C3A CaSO4 12H2O
Eq. 7: C3A + CaCO3 + 11H2O -> C3A CaCO3 11H2O

These phases are of hexagonal shape. Their centre comprises of calcium and aluminium ions interconnected by OH ions. These Ca-Al-OH layers can also incorporate water molecules and further anions. Hydroxide ions, sulphate ions, carbonate ions or other ions can be built-in. /Gl 1, Sta 2/

Various AFm-phases can be formed when all calcium sulphate is consumed. This depends upon several conditions:

- Calcium aluminate hydrate (Eq. 5) is formed at low temperatures, while mono sulphate (Eq. 6) occurs presumably at higher temperatures.
- More water is needed for the formation of calcium aluminate hydrate than for the formation of mono sulphate because the water from ettringite is also available to form mono sulphate. Hence, less water has to migrate through the ettringite layer, which surrounds the hydrating aluminate.
- If lime stone filler is present, mono carbonate can be formed (Eq. 7)

If mono sulphate is formed according to Eq. 6, the amount of primary ettringite is reduced. However, mono sulphate is unstable at room temperature resulting in the formation of ettringite and calcium aluminate hydrate. /Sta 2/

Eq. 8: 3 C3A CaSO4 12H2O + 8H2O -> C3A 3CaSO4 32H2O + 2 C3AH6

Secondary ettringite is formed very slowly. Due to its volume increase, secondary formed ettringite can damage the hardened cement paste.

Pore solution during cement hydration /Sta 2/

The hydration of cement is a constant dissolving and precipitation process /Gl 2/. This means that at contact with water the easily soluble clinker phases dissolve into their ions. Thereby, the ion concentration within the pore solution increases to a level equal to the solubility product of the precipitating mineral. If the pore solution is oversaturated with respect to the less soluble hydrate phases, the hydrate phases crystallize from solution. It is possible to follow the dissolving and precipitation processes occurring during cement hydration by means of pore solution analysis. /Sta 2/

Enough pore solution is found and obtained in the early phase of hydration. With increasing hydration time, cement pores are getting drier as water is incorporated in the hydration products (self-desiccation). Obtaining the pore solution from cement pastes having a very low water to cement ratio can therefore become difficult. One possibility is, to squeeze out the pore solution from cement paste by applying a high pressure (~320 MPa) to it. At early ages, the pore solution is obtained by vacuum extraction or by use of a centrifuge. The pore solution is then investigated on its ionic composition. /Sta 2/

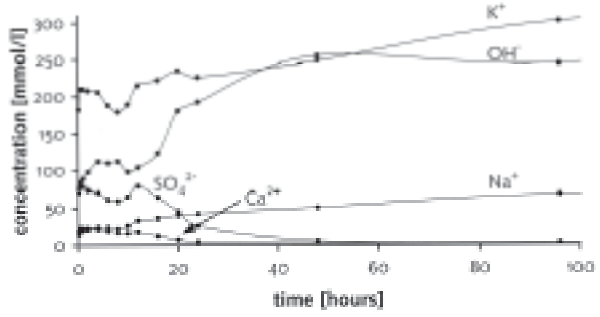

Figure 2.2.2.19: Ion concentration as a function of time for a sulphate resistant cement /Sta 2/

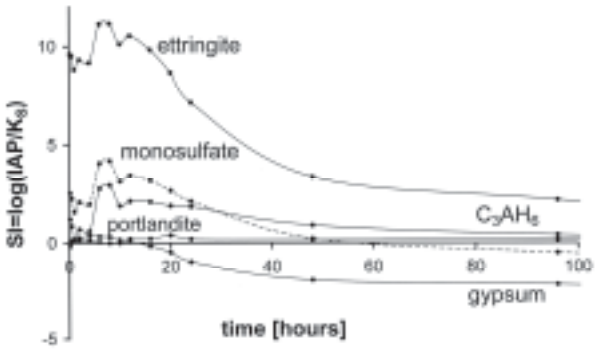

Figure 2.2.2.20: Oversaturation index for several mineral phases /Sta 2/

Based on the results of pore solution analysis, oversaturation or undersaturation of mineral phases can be calculated. The saturation level is calculated by comparing the ion activity product (IAP) to the equilibrium value Ksp. If the saturation index is above zero (oversaturated), the phase is forming rapidly or may form soon. If the saturation index is around zero (equilibrium), the phase is present and stable. In case the saturation index is below zero (undersaturated), the phase is not present or is rapidly dissolving. /Th 1/

During the early phase of hydration, free lime reacts, alkali sulphates dissolve, and primary hydration products such as ettringite, syngenite and gypsum form. This goes together with a fast increase in alkali and sulphate ion concentration. When sulphate ions are consumed during ettringite formation, OH ions replace the sulphate ions leading to a higher pH-value. After the first intense reactions, the ion concentration remains stable for few hours. Then, two to three hours after water addition, the alite reacts and releases aluminates. Together with sulphates these aluminates form ettringite. The sulphate ion concentration is kept relatively high as long as readily available anhydrite, hemihydrates and gypsum are available in

sufficient amounts. The sulphate ion concentration drops rapidly when all calcium sulphate is consumed. Figure 2.2.2.20 shows an oversaturation for gypsum until 12 hours after water addition. After 16 hours of hydration gypsum is undersaturated. Presumably, all calcium sulphate sources were consumed at that time (see Figure 2.2.2.19). A sharp drop in sulphate ion concentration can be seen in the pore solution data. /Sta 2/

In the early phase of hydration, the pore solution is also dominated by water soluble alkali ions. Alkali sulphates tend to crystallize during the cooling process of the clinker on the clinker surface. Due to the composition of clinker raw materials, it is mainly potassium sulphate which is present at the clinker surface. During cement hydration, the alkali ion concentration is constantly increasing. Impurities (such as sodium and potassium) in the main clinker phases dissolve constantly during the hydration process. Additionally, the self-desiccation phenomenon of cement paste reduces the free water and thereby increases the ion concentration. It is reported that if alkali concentration is high, alkali ions can partly adsorb on C-S-H-phases /Ho 3/. The potassium ion concentration can be influenced by local formed syngenite. However, sodium containing mineral phase (equivalent to potassium containing syngenite) does not exist.

With an increase in alkali ions and a reduction in sulphate ions, the pH-value and the OH ion concentration increase. The raise in OH ion concentration forces the calcium ions out of the solution, meaning that the calcium ion concentration is decreasing with increasing OH ion concentration. Figure 2.2.2.21 depicts the effect of pH-value on the calcium ion concentration (Portlandite balance). /Sta 2/

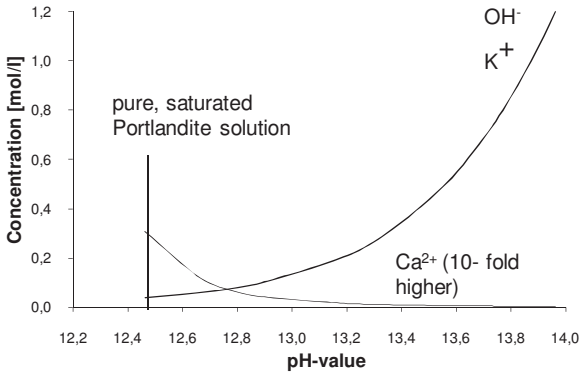

Figure 2.2.2.21: Effect of pH value (addition of KOH to a saturated portlandite solution) on calcium ion concentration /Sta 2/

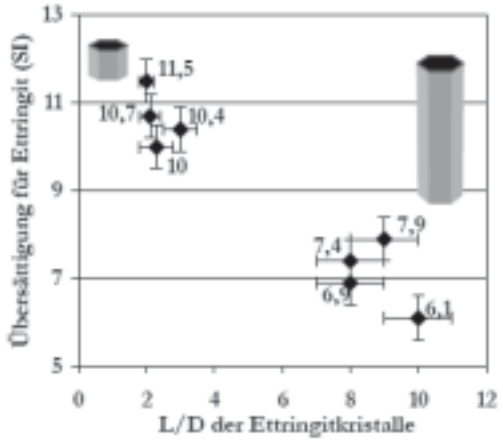

Figure 2.2.2.22: Effect of ettringite supersaturation on crystal morphology (Rößler & Stark) /Rö 3/

The concentration of aluminium and silicium ions is very low. Exact quantitative measurements are relatively difficult. However, the aluminium concentration is needed to calculate the supersaturation for mono sulphate, ettringite and other aluminate containing minerals. Figure 2.2.2.20 depicts a relatively high supersaturation for ettringite during the early phase of hydration. Similar results were obtained by Rothstein et al. /Ro 1/. If the saturation index is around 10 for ettringite, the ettringite occurs as short prismatic type. Lower saturation indices result only in a length increase of the existing ettringite. Rößler & Stark /Rö3/ investigated the relationship between the saturation index and ettringite morphology (see Figure 2.2.2.22).

Structure of cement paste after hydration

After the major hydration processes, the structure of cement paste consists of hydrated phases, unhydrated clinker particles, pores and a high alkaline pore solution. The phases formed

during the hydration process of normal Portland cement are: C-S-H, portlandite, ettringite, and AFm. Instead of AFm, hydrogranate (C_3AH_6) can also be formed.
The degree of hydration of clinker minerals is differing greatly. Alite and aluminates reach a relatively high hydration degree, whereas belite and ferrites are less reactive. Figure 2.2.2.24 depicts the phases formed during cement hydration as a function of time.

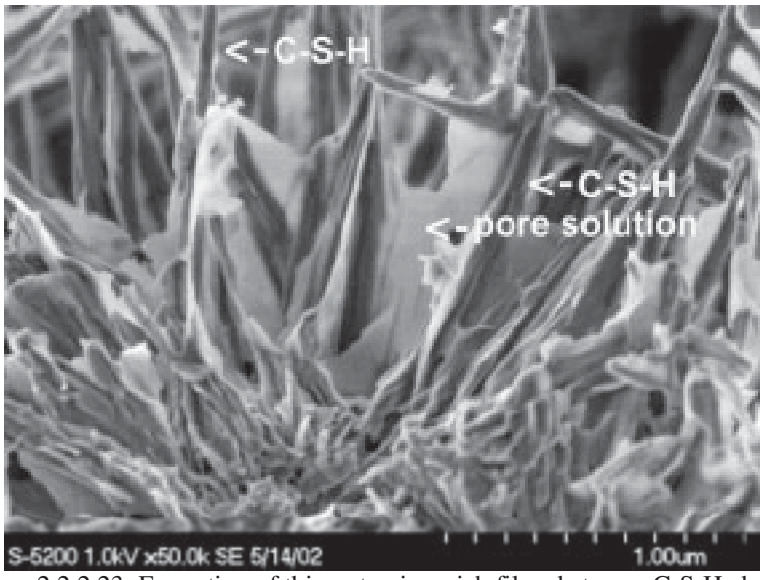

Figure 2.2.2.23: Formation of thin potassium rich films between C-S-H phases during the drying of pore solution /Sta 2/

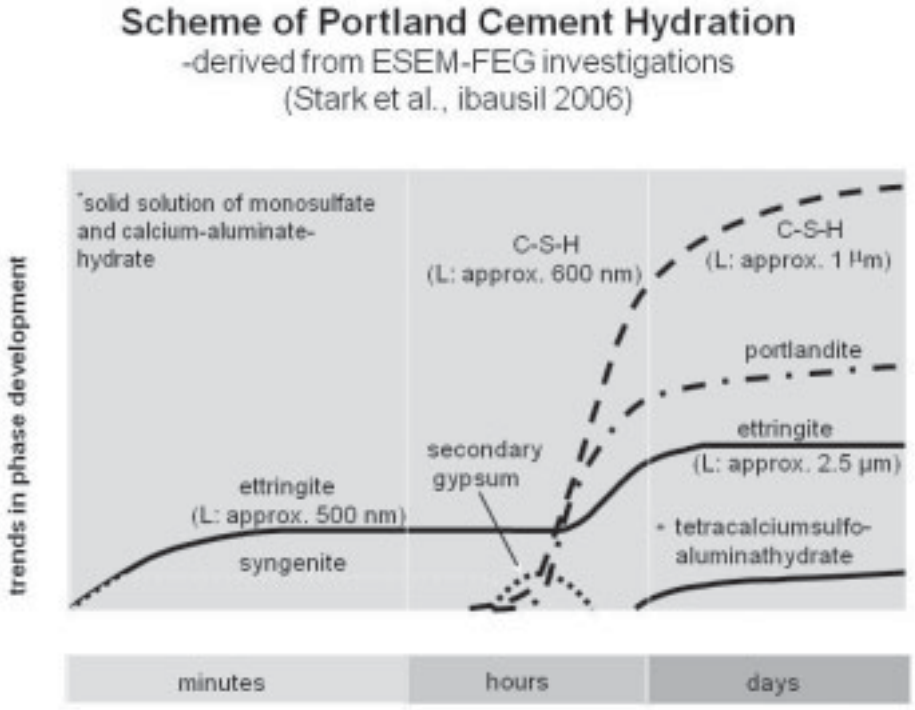

Figure 2.2.2.24: Phases formed during cement hydration (Möser & Stark)

2.2.3 Role of sulfates in cement

As mentioned before, the early stage of hydration (phase I) is dominated by the reaction between the aluminate phase and the sulfates. The first peak in Figure 2.2.2.1 depicts this strongly exothermic reaction. Hydration means the process of formation of hydrates under

water consumption. One good example for hydration under excessive water cosumption is the hydration process of the aluminates (C_3A). If no calcium sulfates are present, the C_3A hydrates immediately under formation of calcium aluminate hydrate. These hydrates grow straightaway when water is added, forming a structure between the cement particles. The material gets stiff immediately (flash set). /Sta3/

$$2C_3A + 21H \rightarrow C_4AH_{13} + C_2AH_8$$

C_4AH_{13} and C_2AH_8 are not stable. Both form the more stable hydrate C_3AH_6. /Sta3/

$$C_4AH_{13} + C_2AH_8 \rightarrow 2(C_3AH_6) + 9H$$

Due to early stiffening, the material is not workable. /Sta3/

If calcium sulfates are present, the hydration process is slowed down. On the surface of the C_3A grains, ettringite is formed. /Sta3/

$$2C_3A + 3CSH_2 + 26H \rightarrow 2C_3A \cdot 3CS \cdot H_{32}$$

The cover layer formed of ettringite prevents the transport of H_2O and SO_4^{2-}. The further reaction is then controlled by diffusion /Sta3/. According to Chartschenko et al. /Ch 1/ the OH concentration (and thus the pH-value) is the major influencing factor on the formation of ettringite. The morphology of ettringite and the ratio between length and thickness of ettringite crystals is strongly dependent upon the OH ion concentration /Ch 1/.

Gypsum plays a crucial role in cement hydration, particularly with setting. Most of the calcium sulfate introduced into cement is present in one or more forms, gypsum ($CaSO_4$ x H_2O), hemihydrate ($CaSO_4$ x 0,5 H_2O), soluble anhydrite, or natural anhydrite ($CaSO_4$) /Be 1/. It is important that the calcium sulfate be sufficiently soluble in the cement/water aqueous phase to provide calcium and sulfate ions for the formation of the initial hydrates and to prevent flash set /Be 1/.

Cement mills typically operate at 90-130°C. Finished cement typically contains a range of calcium sulphate hydrates, ranging from gypsum to hemihydrate and often also chemical/soluble anhydrite. False set occurs if the aluminate phase is not reactive enough to consume the dissolved calcium sulphate originating from fast-dissolving dehydrated gypsum. The dissolved calcium then precipitates back to large interlocking crystals of gypsum. This phenomenon is called false set, since stiffening is not due to proper cement hydration. The precipitated gypsum can be broken up upon mixing /Sa 4/.

Figure 2.2.3.1 illustrates the balance between calcium sulphate type (e.g. rate of dissolution) and reactivity of aluminate phases. A lack of soluble sulphate causes partially uncontrolled aluminate hydration, which may result in accelerated slump loss and possibly retardation of strength development. The amount of soluble sulphate required to control the hydration of the aluminate phase depends on the reactivity of the aluminate phase /Sa 4/.

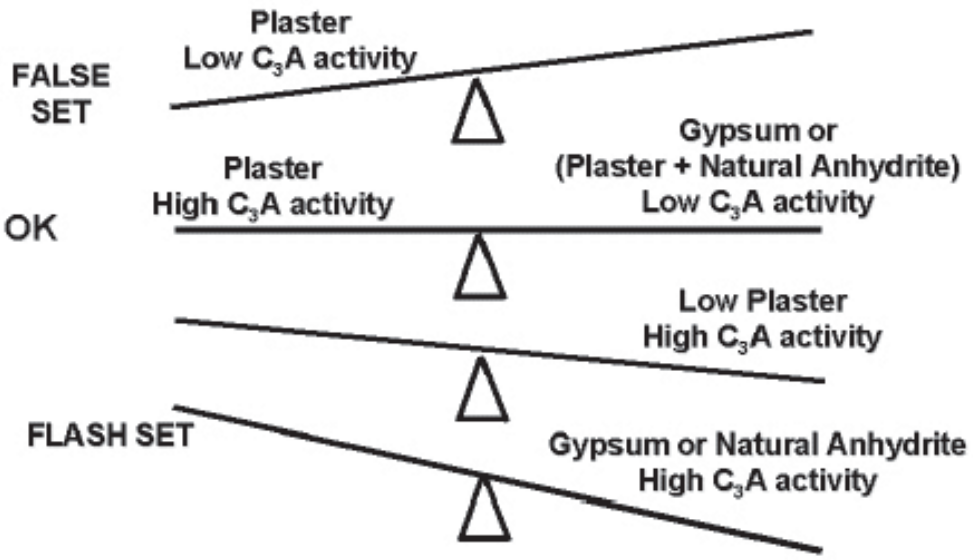

Figure 2.2.3.1: Balance between calcium sulphate type and reactivity of aluminate phase /Sa 4/

Table 2.2.3.1 gives an overview of the solubility of the different types of sulphates which are found in cements. The sulphates are added to the cement during the grinding process. Due to the high process temperatures during grinding, gypsum can dehydrate completely or partly to hemi hydrate ($CaSO_4 \cdot H_2O$). Hemi hydrate and anhydrite differ in solubility. The reactivity of the sulphates (available to form ettringite) is basically influenced by its solubility in water. From table 2.2.3.1 it can be seen that hemi hydrate has a three times higher solubility than anhydrite /Sta 3/.

Table 2.2.3.1: Solubility of different sulphates at 25°C /Sta 3/

Calcium sulphate	Formula	Solubility (g/l)
Gypsum	$CaSO_4 \cdot 2H_2O$	2,4
Hemi hydrate	$CaSO_4 \cdot 0{,}5H_2O$	6
Soluble anhydrite III	$CaSO_4$	6
Natural anhydrite	$CaSO_4$	2,1

2.2.4 Role of alkalies in cement

Alkalies in clinker originate from the raw materials used for the manufacture of Portland cement (clay, limestone, chalk and shale). Jawed et al. /Ja 1, Ja 2/ report that alkalies can also come from coal ash if coal is used as the primary fuel. Most of alkalies in clinker (Na_2O and K_2O) exist in some combination with sulfur. The alkali sulphates most commonly formed are potassium sulphate (arcanite, K_2SO_4), sodium potassium sulphate (aphthitalite, $Na_2SO_4 \cdot 3K_2SO_4$) and calcium potassium sulphate (calcium langbeinite, $2CaSO_4 \cdot K_2SO_4$) /Ja 1/. The remaining alkalies are distributed between the silicates (C_3S, C_2S), aluminates (C_3A) and aluminoferrites (C_4 A,F). Aluminates and ferrites accommodate about half or more of the available alkalies. Alkali sulphates dissolve faster than the alkalies bound in the solid clinker phases.
According to Pollit and Brown /Po 1/, the introduction of alkalies into C_3A modifies its normal cubic form to orthorhombic. The hydraulic reactivity of the C_3A is thereby increased. Potassium seems to have a higher effect on the reactivity than sodium. The effect of alkalines on hydration of the aluminate phase is described differently in literature. According to /Sp 1/ a solution of NaOH retards the hydration process of C_3A. The contrary was observed by /Os 1/. In this reference, alkalies are found to accelerate the hydration of C_3A. Alkalies also alter the hydration conditions, thus influencing the formation of the primary hydration product ettringite. According to Brown et al. /Br 1/, a higher NaOH concentration retard the formation of ettringite.
Spiratos et al. /Sp 3/ summarized the influence of alkalies in cement on rheology of pastes. They found that in the absence of dispersing admixtures the cements containing high alkali levels often exhibit poor early rheological behaviour or higher water demand. This is related to the rapid solubilization of alkali sulfates in the very early hydration process, altering the C_3A/SO_4 balance and the early formation of ettringite and gypsum. Another explanation for poor rheological behaviour are the higher levels of electrolytes in the solution due to alkali sulfates (higher ionic strength) promoting the coagulation of mineral particles in a slurry /Sp 3/.
Jiang et al. /Ji 1/ evaluated the importance of adequate soluble alkali content to ensure cement/superplasticizer compatibility. The study focused on the impact that soluble alkalies have on the compatibility of cement and polynaphthalene sulfonate superplasticizer during the first few minutes of hydration. The authors found that the amount of soluble alkalis that go into solution during the first few minutes is a key parameter in controlling fluidity and fluidity loss of a cement paste made with superplasticizer. The optimum soluble alkali content for increasing initial fluidity and decreasing fluidity loss with time was found to be on the order of 0,4%-0,5% Na_2O equivalent in the six cements under study. The authors highlight that the optimum alkali content is independent of the superplasticizer dosage and cement type /Ji 1/.
Rößler et al. /Rö 2, Ku 2/ investigated the effect of admixtures and calcium sulphate carrier composition on hydration, flowability and strength development of Portland cement. Among others, the formation of syngenite was observed, which was attributed to a reduction in flowability.
Odler et al. /Od 1/ found that the strengths at any hydration time were lowered significantly in the presence of either Na_2SO_4 or K_2SO_4 in the system. It was assumed that the observed decline of strength is related to changes of the structures and intrinsic properties of the hydrates formed in the presence of alkalies /Od 1/.

2.2.5 Organic compounds used during cement production

One of the obstacles during cement production is the grinding process of the freshly burned cement clinker. The world cement production currently amounts to 2,8 billion ton per year and the grinding process consumes nearly 2% of the electricity produced in the whole world /Ts 1/. The grinding process of clinker consumes about one third of the power to produce one ton of cement, resulting in an average specific power consumption of 57 kWh/t /Se 1/. Grinding aids are added to the mill for several reasons: (1) to prevent the cement particles from coating the grinding media and the armour plating in the mill, (2) to prevent re-agglomeration of freshly broken cement particles, (3) to increase the mill capacity and thereby increase efficiency.
Grinding aids used in cement production are organic chemical compounds /Je 1/ based on:

- Aliphatic amines, such as triethylenetetramine (TETA) and tetraethylenepentamine (TEPA)
- Aminealcohols, such as diethanolamine (DEA), triethanolamine (TEA) and tri-isopropanolamine (TIPA)
- Glycols, such as ethyleneglycol (EG) and diethyleneglycol (DEG)
- Phenol and phenol-derivates

The most commonly used grinding aids in cement industry and their chemical compounds are given in table 2.2.5.1.

Table 2.2.5.1 Grinding aids used in cement industry and their molecular formula

Grinding aid	Molecular formula
Triethylenetetramine (TETA)	$C_6 H_{18} N_4$
Tetraethylenepentamine (TEPA)	$C_8 H_{23} N_2$
Diethanolamine (DEA)	$C_4 H_{11} NO_2$
Triethanolamine (TEA)	$C_6 H_{15} NO_3$
Triisopropanolamine (TIPA)	$C_9 H_{21} NO_3$
Ethylene glycol (EG)	$C_2 H_4 (OH)_2$
Diethylene glycol (DEG)	$C_4 H_{10} O_3$
Phenol and its derivates	$C_6 H_5 OH$

Grinding aids are added before milling, and should prevent agglomeration of newly crushed cement particles. The agglomeration phenomenon during cement milling is one of the most important priorities for the cement manufacturer /Ts 1/ as it greatly influences efficiency. Due to their highly polar nature, grinding aids adsorb on surfaces formed by the fracture of electrovalent bonds (i.e. Ca-O and Si-O) /Je 1/. The adsorbed molecules reduce surface energy forces which cause the agglomeration of fresh cement grains /Je 1/. Usually, grinding aids are added at dosages between 0,01 and 0,1% of cement weight. After the grinding process, grinding aids may no longer be present in their original chemical form, since mill temperatures can reach as high as 115°C /Je 1/. This relatively high temperature in the cement mill could possibly change the chemical structure of the grinding aid. During cement hydration, the amines are incorporated in the cement matrix and thereby do not harm the environment. Triethanolamine (TEA) is one of the most frequently used grinding aids in cement industry. The reference cement used within this study was ground by use of TEA. However, its action in the hydration process is not fully understood. It is not even clear if TEA acts like an accelerator or a retarder. At an addition of 0,02% to Portland cement, TEA acts as a set accelerator, at 0,25% it acts as a mild set retarder, at 0,5% TEA acts as a severe retarder, and at 1% its is a very strong accelerator /Do 1/. The effect of TEA on C_3A hydration was investigated by Ramachandran et al. /Ra 2/ and he found that TEA accelerated the hydration of C_3A to the hexagonal aluminate hydrate and its conversion to the cubic aluminate hydrate during first hour of hydration. The rate of hydration increased with increased amounts of TEA /Ra 2/.

2.2.6 Effect of chemical admixture on hydration

By addition of admixtures, the hydration of Portland cement in the first hours is retarded depending upon the type and dosage of admixtures. Figure 2.2.6.1 depicts the delay in hydration of cement C due to the addition of a polycarboxylate based admixture. The peak in blank mix (no admixture) is reached after approx. 7 hours, whereas the peak in the PC mix is reached after approx. 9 hours.

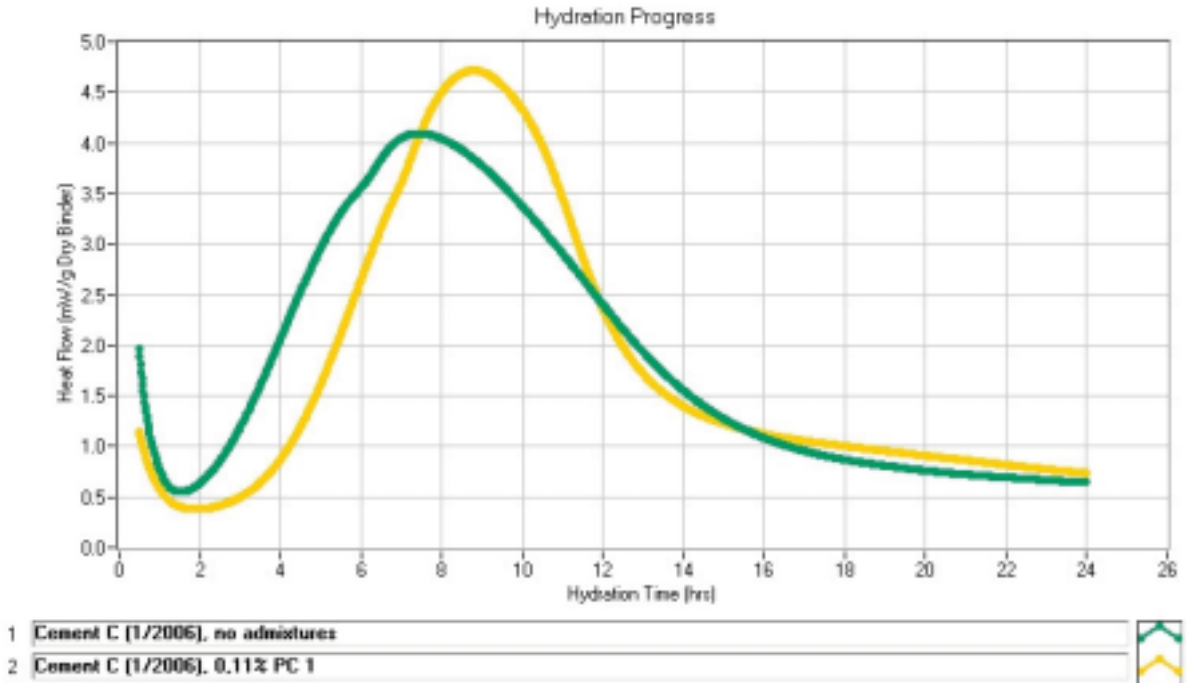

Figure 2.2.6.1: Hydration curve of cement C (blank and PC mix)

Uchikawa et al. /Uc 1/ have investigated the effect of different kind of admixture on cement hydration. The admixtures used were polycarboxylic acid-based, lignin sulfonic acid-based and other products. The heat evolution curves showed that the hydration was delayed by any admixture. Depending upon the timing of addition (simultaneous or later addition of admixtures) the retardation of hydration process was between 1 and 12 hours. Later addition resulted in a clearly longer retardation. The polycarboxylic based admixture caused the strongest retardation of all four admixtures used in the study. The retarding effect of all admixtures was indirectly related to the higher adsorption rates of the polymers on the aluminate phase than on the alite phase /Uc 1/.
Cerulli et al. have reported about a new type of polycarboxylate superplasticizer, developed for utilization in cold climates. The authors saw a need for this type of superplasticizer due to the sometimes strong retarding effect of polycarboxylate polymers on cement hydration. /Ce 1/ This disadvantage of polycarboxylate polymers can limit the use of these superplasticizers in cold climates (e.g. Iceland), particularly in the cases where early strength development is required /Ce 1/. The new polycarboxylate superplasticizer, characterized by a completely different molecular structure in comparison with the traditional ones, gave sufficient strength development in cold climates. The authors believe that the characteristics of the new superplasticizer seem to be ascribed to its capacity to modify the morphological structure of ettringite formed in the first period of hydration /Ce 1/.

2.3 Dispersing mechanisms in cementitious systems

Plasticizers and superplasticizers for concrete act by adsorption at the solid-liquid interface between the particles and the aqueous phase. After adsorption, repulsive forces between the superplasticizer polymers lead to the dispersion of the cement grains. For sufficient workability of a cementitious system (i.e. concrete), the repulsive forces have to be stronger than the adhesion forces (van der Waals or electrostatic forces) between the colloidal particles. Without superplasticizer, the colloidal cement grains would flocculate and reduce the workability of the mix /Tay1/.

2.3.1 Colloidal particles

The particle size distribution of cement is varying from micrometres (10^{-6} m) to nanometres (10^{-9} m). Therefore, cement is, at least partly, a colloidal system. Although the amount of particles smaller than 1 µm is only in a range of 8 to 10 % (by weight), these particles are very important from rheological point of view. The small particles, responsible for the high specific surface, are the place where the polymers act as dispersing admixtures. Shaw et al. /Sh 1/ summarized the factors which contribute most to the overall nature of a colloidal system like cement as following:

- Particle size
- Particle shape and flexibility
- Surface properties (including electrical ones)
- Particle-particle interactions
- Particle-solvent interactions

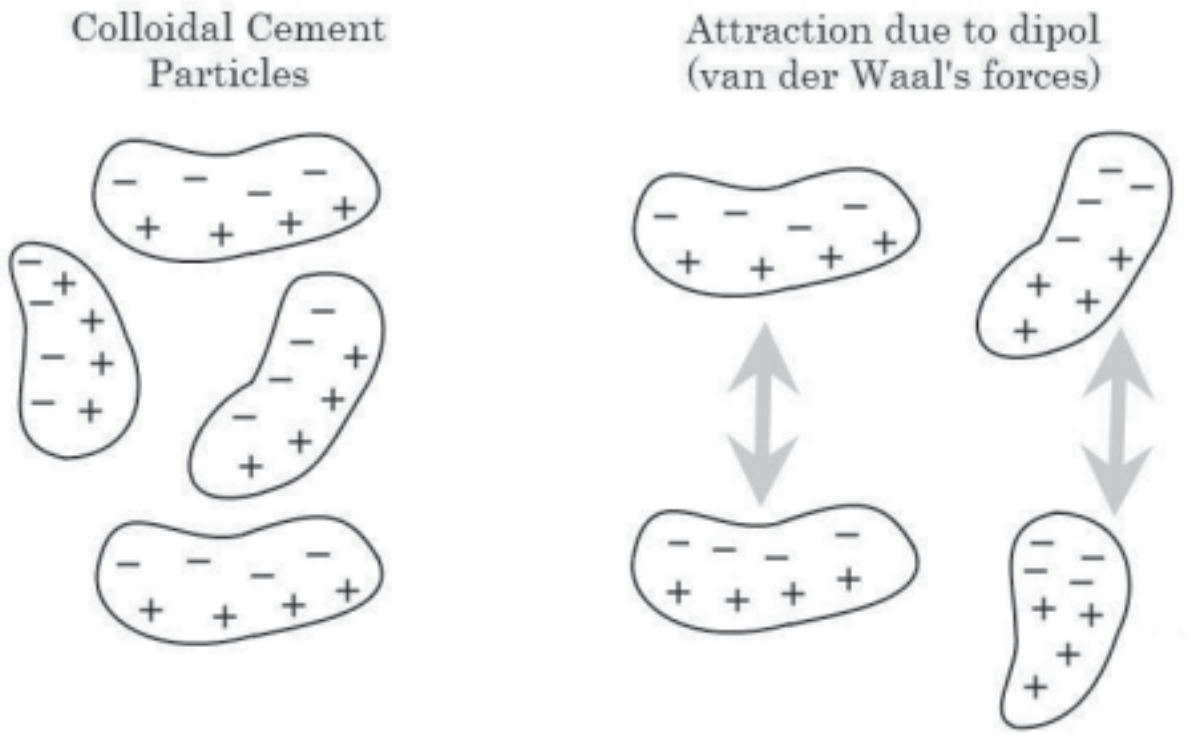

Figure 2.3.1.1: Schematic draft of attractive forces between colloidal particles

The prominent force in a cementitious system which leads to flocculation of particles and therefore increasing the yield stress of the system are van der Waals forces (see Figure

2.3.1.1). These are forces of attraction due to the particles having dipoles. Particles with dipoles have a distribution of electrons such that the electron density is higher at one end than the other. These forces are only active in the immediate vicinity of the particles and are of great importance particularly for small particles. In other words, the distribution of electrons on the surface has a greater influence on the particle-particle interaction than e.g. the g-force on the particle. To control the interactions between colloidal particles, polymeric stabilization has been widely used, especially when the dispersions are subject to harsh processing conditions where the temperature and ionic strength are not constant. Cementitious systems show a rapid increase in ionic strength as ions are released from the cement particle surfaces and a rise in temperature as the hydration reaction progresses between cement particles /Ko 1/.

2.3.2 Electrostatic stabilisation

The more traditional products like lignosulfonate, naphthalene and melamine based superplasticizers disperse the cement particles through a mechanism of electrostatic repulsion. The polymers are adsorbed on the surface of the cement particles, giving them a negative charge so that they repel each other (see Figure 2.3.2.1). This charge is the so-called zeta potential. It describes the cement particles ability to affect other charged cement particles in the suspension. Observations indicate that the absolute zeta potential of ordinary Portland cement particles with naphthalene- or melamine-type superplasticizers must be more than 20 mV /Li 1/. Thereby, yield stress and viscosity is reduced. After a certain time fluidity is lost again, primarily due to the increase in the ionic strength of the cementitious system, which leads to re-flocculation driven by van der Waals attraction. Since the strong polyelectrolytes (i.e. melamine) do not provide significant steric repulsion (see 2.3.3) to prevent this re-flocculation, copolymers such as weak or grafted polyelectrolytes have been developed to provide both electrostatic and steric stabilization in a single molecular species /Ko 1/.

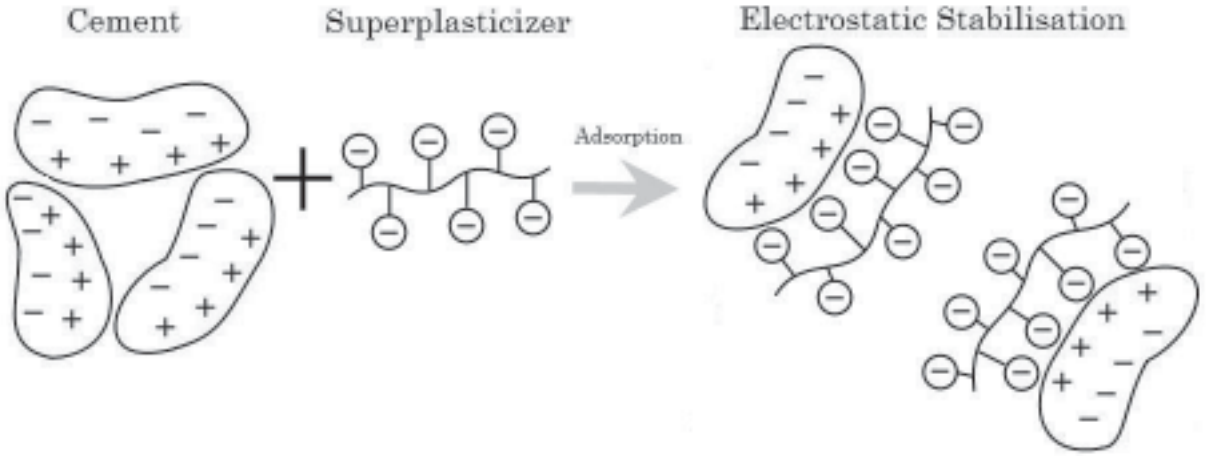

Figure 2.3.2.1: Schematic draft showing electrostatic stabilisation of cement

The primary factor influencing the dispersing effect of admixtures working on the basis of electrostatic stabilisation seems to be the ionic strength of the pore solution. During the hydration process, numerous ions are dissolved and then the so-called pore solution becomes far from an ideal electrolyte. The interparticle interaction forces are strongly influenced by the ionic composition of the pore solution /Ho 1/. In practice, admixtures based on electrostatic stabilisation can provide sufficient workability of concrete for a period of 30 to 60 minutes. The relatively fast workability loss in presence of lignosulfonate, naphthalene and melamine

based admixtures can be related to the increase of the ionic strength of the suspending medium, which compresses the adsorbed polyelectrolyte layers and weakens the electrostatic repulsion. As a result, van der Waals attraction leads to re-flocculation of the cement particles /Ho 1/.

2.3.3 Steric hindrance

The dispersing effect of plasticizers from the newer generation like polycarboxylate ether is based on a combination of steric hindrance and electrostatic stabilisation /Ho 1/. Comb type polymers have carboxylic groups in the main chain and comb-type superplasticizers are adsorbed on to cement particles /Ta 2 and Sa 1/. Carboxylic groups of comb-type superplasticizers are coupled with Ca^{2+} ions on the surface of cement particles or hydrated products /Sa 3/. The side chains prevent the particles from coming closer to each other, so that no van der Waals forces can act (see Figure 2.3.3.1). Hence the effect can be seen as a combination of steric and electrostatic repulsion.
According to /Yo 1/, /Uc 1/ and /Uc 3/, the absolute zeta potential (negative charge induced by admixtures) of ordinary Portland cement particles with polycarboxylate based superplasticizers is less than -10 mV. Sakai et al. /Sa 3/ report values between -0,3 and -5 mV for comb type admixtures. This is significantly less than with electrostatic stabilisation. Hence, most of the dispersing effect with comb-type polymers is due to the steric separation provided by the side chains.

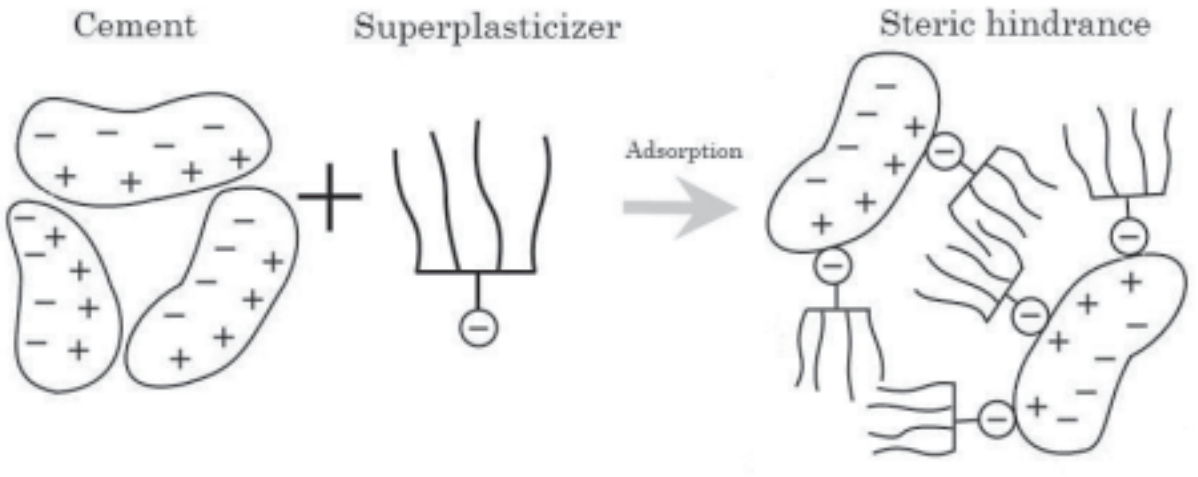

Figure 2.3.3.1: Schematic draft showing stablisation by steric hindrance

The key parameters, which govern the steric repulsion, are the adsorption layer thickness and its conformation at the solid liquid interface /Ho 1/. The effects of the chemical structure on the properties of polycarboxylate-type superplasticizer have been investigated by Yamada et al. /Ya 1/. The parameters evaluated were the polyoxyethylene (PEO) side chain length, the degree of backbone polymerization, the composition of functional groups such as carboxylic and sulfonic groups, and the purity of polymers. Rheological measurements were done on mixes with several w/c-ratios. Among others, the authors found that with decreasing w/c-ratio the chemical structure of the polymers becomes significant. Polymers with longer PEO side chains, lower degrees of backbone polymerization, and higher contents of sulfonic groups showed higher dispersing power /Ya 1/.

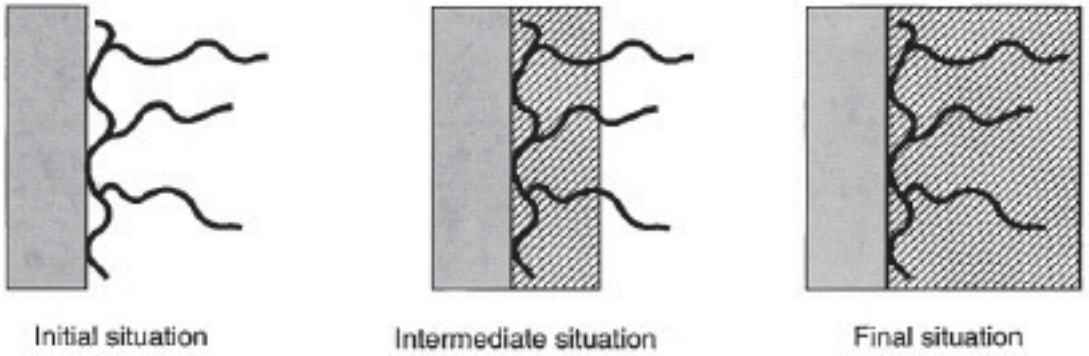

Figure 2.3.3.2: Schematic draft which shows how comb polymers with polyethylene side chains are incorporated by growing hydration layers /Fl 1 and Sa 1/

In practice, admixtures based on steric hindrance can provide sufficient workability for a concrete mix over a period of 60 to 90 minutes. The increase in workability is due to steric hindrance provided by the side chains. According to Sakai et al. /Sa 1/ workability is lost when the hydration layers growing from the surface have incorporated the polymers (see also Figure 2.3.3.2).

2.3.4 Adsorption of polymers on cement surface

Plank et al. /Pl 1/ investigated the zeta potential of early hydration products and found it to be a key factor for superplasticizer adsorption. The authors conclude that the adsorbed amount of superplasticizer strongly depends on the existence of a positive zeta potential of the hydration phase /Pl 1/. (1) Therefore, ettringite (due to its positive charge) is able to adsorb high quantities of negatively charged superplasticizers. Mineral phases with a zeta potential around zero or even a negative zeta potential do not adsorb significant amounts of superplasticizers. (2) High surface area by itself does not lead to adsorption if the zeta potential is negative or only slightly positive. Thus, a positive zeta potential is a key factor for adsorption /Pl 1/. (3) At comparable specific surface area, ettringite shows 2-4 times more polymer adsorbed per surface area than monosulfate. (4) Another finding was that the adsorbed amount of polycondensates (in mg/g or mg/m²) is much higher than for polycarboxylates (approx. 20 vs. 3-5 mg/m² on ettringite) /Pl 1/. (5) The adsorption ratio of polycarboxylates also depends on their anionic charge density: the higher this charge density, the stronger the adsorption /Pl 1/. Plank et al. conclude that a hydrating grain is best represented by a mosaic structure (see Figure 2.3.4.1), with superplasticizer molecules mainly adsorbed on ettringite (see Figure 2.3.4.1) and some on monosulfate and C-S-H nucleated at surface /Pl 1/.

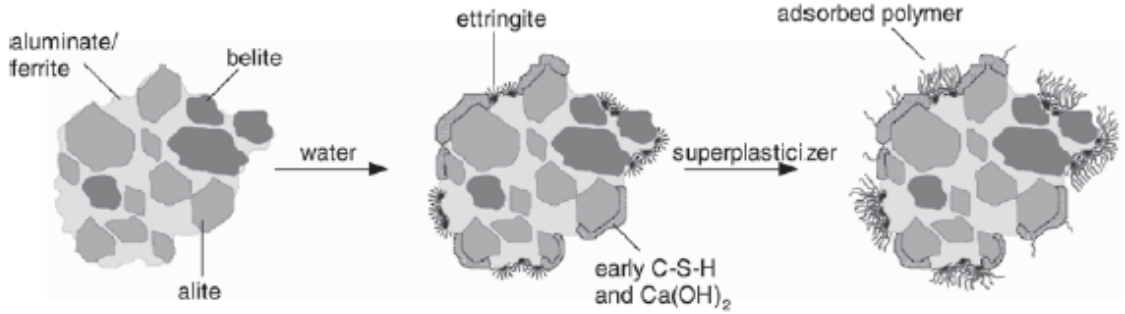

Figure 2.3.4.1: Schematic representation of the cross section of a hydrating cement grain showing uneven polymer distribution on its surface /Pl 1/

Yoshioka et al. /Yo 2/ investigated the adsorption characteristics of various superplasticizers on Portland cement component minerals. Adsorption isotherms of various types of superplasticizers and zeta potentials of cement component materials at the maximum adsorption of the superplasticizers were measured /Yo 2/. The authors found that for all types of superplasticizers, a larger amount of superplasticizer was adsorbed on C_3A and C_4AF than C_3S and C_2S. Without superplasticizer, C_3S and C_2S had negative zeta potential (around -5 mV). On the contrary, C_3A and C_4AF had positive zeta potential (in the range of +5 to +10 mV). Figure 2.3.4.2 depicts the zeta potential of each mineralogical composition of cement in a solution with and without superplasticizer. Yoshioka et al. concluded that accelerated coagulation of cement particles in a paste with no admixtures might occur due to this opposite charge in particles /Yo 2/. Another finding was that all mineralogical components of cement showed negative zeta potential when they are dispersed in a solution with superplasticizer.

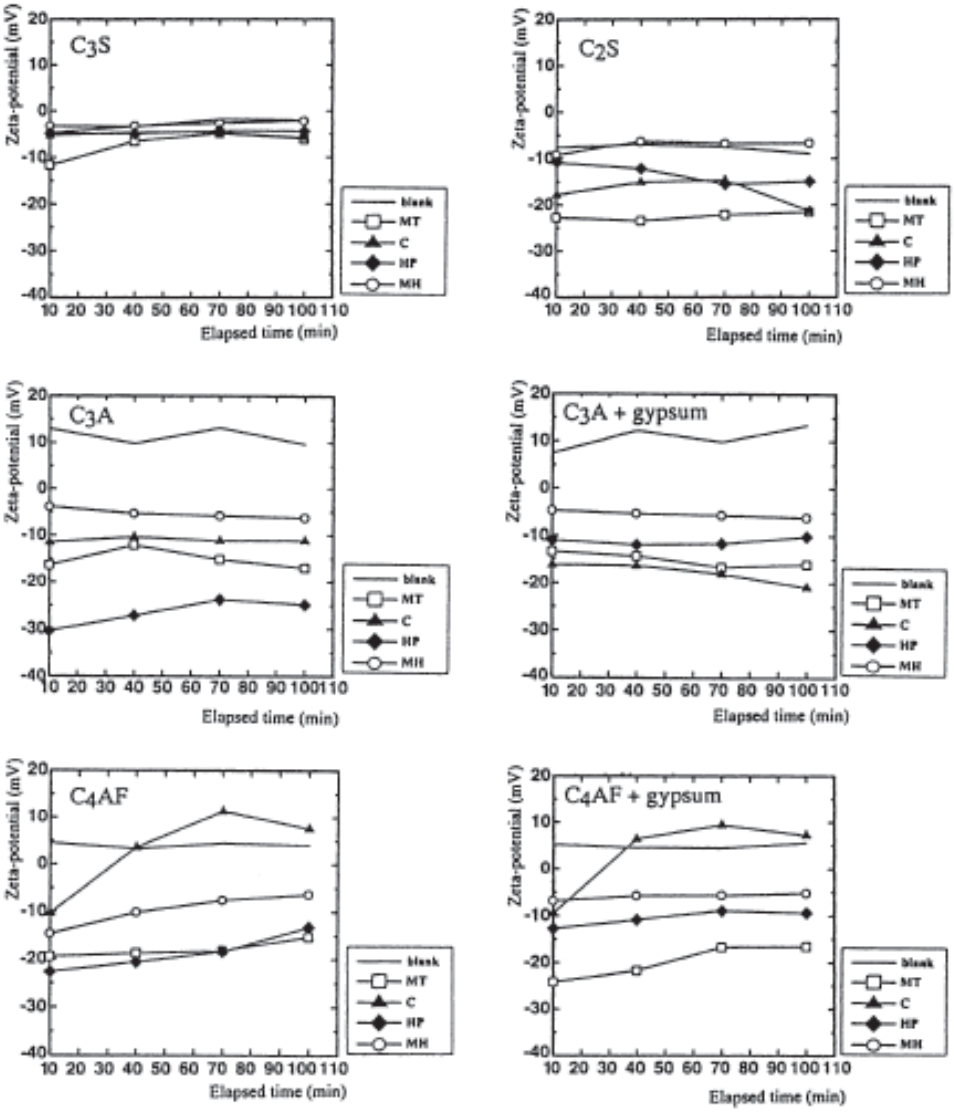

Figure 2.3.4.2: The zeta potentials of each mineralogical composition of cement in a solution with and without superplasticizer /Yo 2/

2.4 Interaction between cement and admixture

Flatt et al. /Fl 1/ have given a simplified view on the chemical effects perturbing the action of superplasticizers. The authors proposed three categories which describe the interactions and

state of superplasticizers with the cement suspensions. According to their model, the first part of polymers is consumed by intercalation, coprecipitation or micellization, i.e., by formation of an organo-mineral phase (OMP). A second part of the polymer is adsorbed onto the surface of particles and helps disperse cement agglomerates. The third part consists of the excess superplasticizer neither consumed nor adsorbed and which remains dissolved in the aqueous phase /Fl 1/. In the conclusion the authors state that, at equal dosage, a cement with a larger degree of consumption (due to formation of OMP) can have a lower surface coverage and consequently poorer workability. The authors specifically highlight the difference between the consumption of polymers and the adsorption of polymers on the clinker surface /Fl 1/. The intercalation of polycarboxylates into C_3A phases was also reported by Plank et al. /Pl 2/.

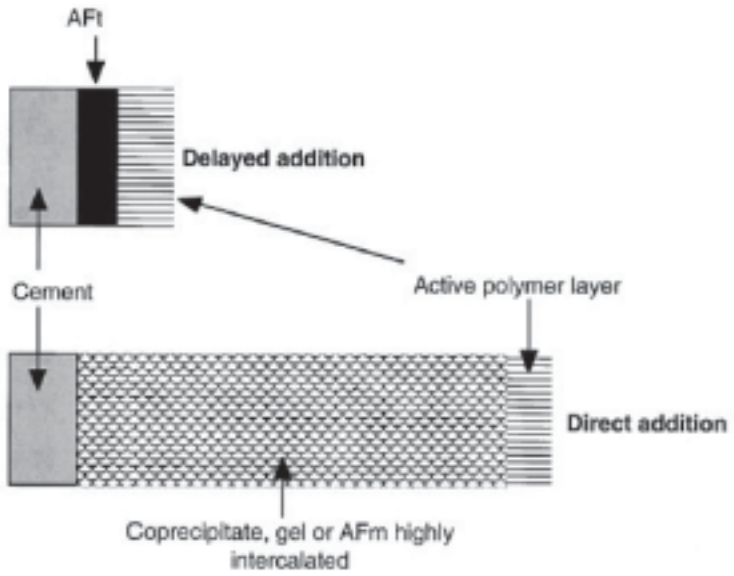

Figure 2.4.1: Schematic illustration of OMP precipitation /Fl 1/

Figure 2.4.1 shows the chemical sink effect of OMP precipitation. In the case of direct addition, many polymers are consumed uselessly. The plane of action for the van der Waals force would be shifted from the surface towards the base of the polymer /Fl 1/.
An important factor with regards to cement-admixture interaction is the timing of addition of the dispersing admixture. Uchikawa et al. /Uc 1/ have shown the effect of simultaneous (with water) and delayed (after water) addition for four kinds of organic admixtures on composition, structure and property of fresh cement paste. It was found that the flowability of cement paste produced by later addition of any admixture was higher than that of cement paste produced by simultaneous addition /Uc 1/. It was also found that any admixture is more adsorbed on the aluminate phase than on the alite phase. By later addition, the adsorption of admixtures on the clinker surface (in particular on C_3A) is reduced, leading to an improvement of fluidity /Uc 1/.
Cement admixture interaction problems, which are well-known by concrete producers, were investigated by Hanehara et al. /Ha 1/. The problems reported from practice range from variation of initial slump to large slump loss during concrete production and placement /Ha 1/. Normal Portland cements coming from four different plants were tested with different types of admixtures. The chemical admixtures were based on lignin sulfonate, naphthalene sulfonate, melamine sulfonate, amino sulfonate and polycarboxylate ether. Several interaction problems were observed during this research, which were classified in two groups. (1) Problems caused by the effect of the admixture´s addition on the hydration reaction of cement, and (2) problems caused by the adsorption of the admixture on the cement particles /Ha 1/. The authors state that the rheology (flow values) of the four types of cement paste prepared without admixtures is almost identical, while those prepared with admixtures

fluctuated highly. The authors also observed an important influence of addition time on fluidity of paste. In case of polycarboxylic acid-based admixture, the major influencing factor on fluidity was found to be the amount of alkaline sulphates in cement /Ha 1/.
In /Ze 1/ the development, trial tests and production of a nuclear shielding concrete is described. The task here was to develop a concrete with a high slag content cement (CEM III/A 32,5) and high density materials. The concrete should show sufficient workability for 60 minutes and segregate not too much. During the trial tests many admixtures of traditional and co-polymer type were tested. Finally, only one polycarboxylate based admixture met the requirements, although the polycarboxylate based admixtures were added at the same dosage or even higher. According to the authors, fluctuations in workability due to type of admixture are considerable.
Bedard et al. give a brief overview of admixture-cement incompatibilities. The authors highlight cases of early stiffening and undesirable retardation of the setting time caused by admixtures /Be 1/. Early stiffening has been found to be caused by changes in the rate of reaction between C_3A and sulphate of the cement. Retardation is found to result from an overdose of admixtures which leads to delayed calcium silicate hydration /Be 1/. With regards to rheology, the authors give examples of cement-superplasticizer incompatibilities in high-performance concrete. The incompatibilities mentioned are: low fluidification effect, rapid slump loss, severe segregation, loss of entrained air and extended set retardation. It was found that the cement superplasticizer (SP) incompatibility problems are magnified in high-performance concrete because of the much reduced water/cement ratios and the higher superplasticizer doses. The authors state that the principal cement and admixture factors influencing rheological behaviour in HPC-SP systems are related to the cement´s C_3A content, Blaine fineness, solubility of the gypsum, and composition of the cement /Be 1/.
Further, it is shown how a low fluidification effect can finally lead to severe segregation of the mix. This can happen when larger dosages of the admixture are added to offset the lack of initial fluidizing of the concrete or to reinstate workability (e.g. after rapid slump loss). Thereby, the saturation point for the admixture can be exceeded easily. At this point one can use the well-known trick from practice to save a segregating concrete. The authors recommend addition of extra quantities of cement to the mix to consume the excess admixture. Extended retardation of mixes containing SP is found to be closely related to Blaine surface, chemical composition (mainly C_3A content) of the cement, SP dosage and concrete temperatures. With equal dosage of SP, cements with lower C_3A content are retarded considerably more than cements with higher C_3A content /Be 1/.
Zingg et al. /Zi 1/ investigated the micro structural development of fresh cement pastes without and with polycarboxylate-type (PCE) of superplasticizers by use of cryo-FIB and cryo-SEM techniques. During the investigations, the natural structure of fresh cement pastes was preserved by high pressure freezing. The authors found that in absence of PCE, early hydrates (ettringite) tend to precipitate on clinker surfaces and tend to form agglomerates, which will lead to interlocking bridges and thus, to higher yield stresses at later hydration times /Zi 1/. The interstitial pore space in cement pastes without PCE is almost free of smallest hydrate particles. In contrast, in presence of PCE, the hydrates (mainly ettringite) are well dispersed in the interstitial pore space and only minor amounts are attached on the clinker surfaces. With PCE, almost no agglomerates are formed during the first minutes of hydration /Zi 1/.
Tagnit-Hamou and Aitcin /Tag 1/ summarize some cases of cement-superplasticizer incompatibility which were reported in the literature. Most cases could be explained by variations in sulphate solubility and fluctuations in the sulphate carrier composition /Tag 1/.

2.5 Cement and admixture characteristics influencing rheology

Chandra et al. /Ch 2, Ch 3/ investigated the influence of cement and superplasticizer type and dosage on the slump loss of Portland cement mortars. Cements varying in aluminate content, alkali content and SO_3 content were used in mortar. The work focused on studying the influence of lignosulfonic acid- and melamine sulfonic acid-based superplasticizers on the fluidity of mortars made with ordinary Portland cement, low alkali cement and white cement at different water to cement ratios. It was shown that the ligno sulphonate was more effective than the melamine sulphonate in providing better fluidity. The highest fluidity came from the white cement, which was attributed to its lower aluminate content and alkali content, and higher SO_3 content. The authors found that many factors influence the fluidity and hydration process of the cement paste. In their opinion, a theory based on only one parameter is irrelevant /Ch 2/.

Vikan et al. /Vi 1/ investigated the influence of cement characteristics such as cement fineness and clinker composition on the flow resistance of cement paste (here measured as the area under the shear stress – shear rate flow curve). Plasticizers based on naphthalene sulphonate-formaldehyde condensate, polyether grafted polyacrylate and lignosulphonate have been tested on six different cements. The flow resistance of the pastes correlated well with a modified cement fineness, considering the relative reactivity of cubic C_3A and C_3S. It was found to be either a linear or exponential function of the combined cement characteristic depending on plasticizer type and dosage /Vi 1/. An earlier study by Bonen et al. /Bo 1/ gave similar results.

Sakai et al. /Sa 3/ evaluated the relation between the molecular structure and the dispersion-adsorption mechanisms of three types of comb-type superplasticizers used in Japan. The authors found that the copolymer components and the grafted chain lengths of polyethylene oxide influenced the dispersibility and workability of comb-type superplasticizers. The adsorbing behaviour of comb-type superplasticizers was primarily affected by the sulphate ion concentration /Sa 3/.

Ohta et al. /Oh 1/ report (among others) about the influence of sulphate ion concentration on the dispersing effect when polycarboxylates are present. One important finding of the authors was that polycarboxylate polymers could shrink by 50% when the sulphate ion concentration increased /Oh 1/.

Kauppi et al. /Ka 1/ reported about results from a European Research Programme known as the Superplast project /Ho 2/. The authors studied the mechanisms involved in the adsorption of polymers in concrete. The adsorption of a modified polycarboxylate polymer and a lignosulfonate polymer on dead burnt magnesium oxide powder (MgO) was investigated. The ionic concentration of the dispersing media both for model MgO powders and cement suspensions was found to be of high importance during rheological measurements, adsorption studies and AFM-colloidal probe measurements /Ka 1/. The ionic medium composition (with or without Ca) influences in particular the polycarboxylate polymers. The authors concluded that the ionic strength seems to control the relative effect of the steric and electrostatic contributions to the repulsive interparticle forces /Ka 1/.

Flatt et al. /Fl 2/ investigated the model powders used in the above mentioned study /Ka 1/. The authors choose model powders made of dead burnt MgO because their isoelectric points are around pH 12,4, in the same range as that of Portland cement. However, the authors point out that calcium carbonate powder ($CaCO_3$), with its isoelectric point around pH 10, should have a surface behaviour similar to cement /Fl 2/. It was found that the MgO model powders make it possible to study the adsorption of superplasticizers, the evolution of zeta potential as a function of adsorbed superplasticizer and rheology of suspensions /Fl 2/. Different MgO powders have been investigated. Despite the fact that MgO was dead or hard burnt, it was found that it reacts in contact with an aqueous solution. Between 30 and 120 minutes the

surface properties were reasonably stable and the powder was considered inert during this period of time /Fl 2/.

2.6 Brief summary of literature survey

The task of the literature survey was to obtain basic information about the hydration process of cement, the basic models for dispersing mechanisms in cementitious systems and reported cases of cement admixture interaction problems.

Hydration process

Several hydration models for Portland cement can be found in the literature /Sta 4, Sta 5/. The model by Stark et al. is strongly based on:

- microstructural investigations by use of ESEM-FEG
- pore solution analysis and
- results of quantitative X-ray diffraction (Rietveld).

Among others, this model gives an quantitative and qualitative overview about the primary hydration products. An interesting observation made by Stark et al. is the formation of syngenite at early stage of hydration and its influence on rheology. The formation of syngenite was even observed in cements having a relatively low alkali content. Furthermore, the role of sulphates, the importance of the gypsum/hemi hydrate ratio and the influence of alkalies is highlighted.

Dispersing mechanisms in cementitious systems

It is widely accepted that polymers adsorb on the clinker and therefore lead to dispersion of the small cement grains. The survey distinguished between two dispersing mechanisms (1) electrostatic stabilization and (2) steric hindrance. For the traditional products which are based on lignosulfonate, naphthalene and melamine, the dispersing effect is provided by electrostatic stabilization. The cement particles are charged by the polymers so that they repel each other. After a certain time (approx. 60 min) this effect is for instance reduced by increasing ionic strength in the pore solution, in practice known as workability loss. The newer products based on polycarboxylate disperse the cement particles mainly by steric hindrance and a minor part of electrostatic repulsion. The charge induced by the polycarboxylates is much lower. The so-called steric hindrance is provided by the side chains of the polymers stretching into the liquid phase, preventing the cement particles from agglomerating again. The dispersing effect lasts up to 90 min and longer at a lower dosage than with i.e. melamine. For polycarboxylates, workability is lost when the side chains are submerged by growing hydration layers from cement surface. The dispersing effect is highly influenced by the soluble alkalies in the mix.

Cement-admixtures interaction

In the overview given by Flatt /Fl 1/, the authors arrange the interaction of cement and admixtures into three categories. A first part of polymers is consumed by formation of an organo-mineral phase (OMP), which is lost for dispersion. A second part is adsorbed on clinker surface and leads to the dispersion of the cement particles. A third part remains dissolved in the aqueous phase (neither consumed by OMP nor adsorbed). In some literature sources compatibility problems were reported. Same types of cement coming from different plants were investigated. It was observed that the fluidity of mixes without admixtures were almost identical, while those prepared with admixtures fluctuated clearly. Several authors highlighted the importance of inert model systems such as dead burnt MgO powder or $CaCO_3$ powder if one wants to study the mechanisms involved in the adsorption of polymers.

3. Experimental

3.1 Objective and scope of research

The objective and scope of this research cover three issues. The primary task was to evaluate the effect of cement delivery on rheological properties. Several cement producers sent cement samples to ICI over a long period of time, in one case representing a 3 year production period. The cement was tested in mortar with all parameters held constant except the production date of the cement. The secondary task was to identify the constituents in the cements which cause the fluctuations in rheology. Properties with a clear influence on rheology were then further investigated. In the third part of the study the cement deliveries which had already been tested in mortar, were now used for production of SCC. In mortar mixes, one melamine based admixture was used, representing electrostatic stabilisation as dispersing mechanism. One polycarboxylate based admixture was used, representing steric hindrance as dispersing mechanism. In concrete mixes, two polycarboxylates were used as dispersing admixtures.

3.2 Research program

The cements used for this research were supplied by seven cement producers from six different countries located on three continents (Europe, Middle East and Asia). From this group one Portland composite cement and four pure Portland cements were incorporated in the advanced testing program (see Fig. 3.2.1). The cements have been examined on their rheology in blank, polycarboxylate and melamine mortar mixes. The testing methods applied were:

- specific surface according to Blaine, measurement of density, water demand and norm consistency
- measurement of particle size distribution and specific surface by laser diffractometry
- chemical analysis using XRF and calculation of clinker phase composition according to modified Bogue and Rietveld refinement
- rheological measurements in ConTec Rheomixer and ConTec Viscometer 6
- measurement of hydration energy under semi-adiabatic and isothermal conditions

Rheologic and calorimetric measurements were done on more than 1000 mortar and 30 concrete mixes. Around 100 cement pastes were prepared for adsorption measurements and pore solution analysis.

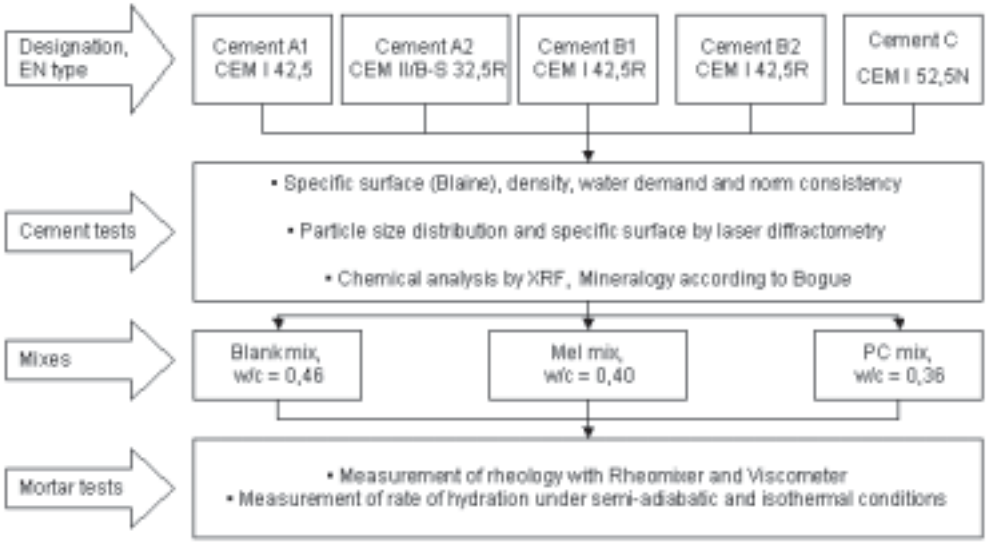

Figure 3.2.1: Schematic overview of testing program

3.3 Test methods

3.3.1 ConTec Rheomixer

3.3.1.1 Generals about Rheomixer

The Rheomixer (see Figure 3.3.1.1.1) is a device that can mix paste/mortar and measures its rheology in one continuous operation in a closed container. The device measures the current needed (mA) at a certain rotation speed. The parameters obtained by the measurement are the G-yield (mA) and the H-viscosity (mA s), corresponding to yield stress (Pa) and plastic viscosity (Pa s). Measurements with same mix in a coaxial cylinder viscometer showed a good correlation between both devices (see Appendix C). Results obtained by ConTec Rheomixer are based on the Bingham model. For both mixing and measuring, the same impeller is used. The impeller during this study is equipped with two types of blades (see Figure 3.3.1.1.2), (1) mixing blades and (2) measuring blades. The mixing blades are attached directly to the axis of the impeller. These blades are optimized for agitating the mortar/paste during the mixing process. The measuring blades are connected to the axis of the impeller by steel rods. These measuring blades have a triangle shaped cross section optimized for the measurement of the mortar/paste. Due to the shape of the measuring blades, the generation of liquid to the shearing zone is reduced to a minimum.

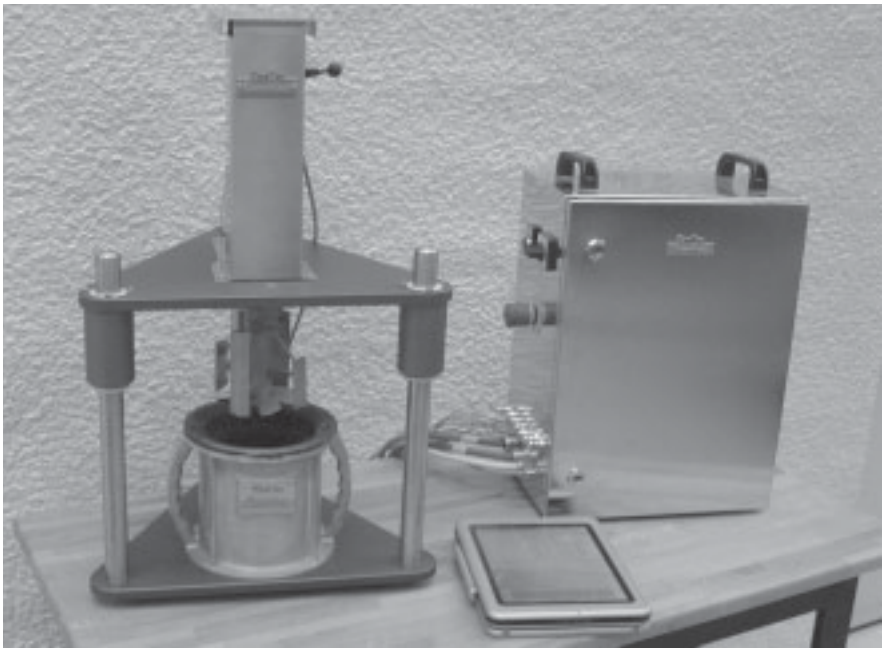

Figure 3.3.1.1.1: Rheomixer (stativ version) with control box and Touchpad computer using Bluetooth connection

Rheomixer is mainly designed for laboratory use, although it has already given valuable results (for means of quality control) when pastes and slurries were tested under site conditions. With Rheomixer, the measuring zone is the gap between the outer diameter of the impeller and the inner diameter of the bucket. The control box of Rheomixer is measuring the current (mA) needed by the motor to rotate the impeller (see Figure 3.3.1.1.2) at certain speed levels in the mortar/paste. The measuring blades of the impeller cut through the mortar/paste like a wing of an airplane through the air. Hence, the measuring blades have a triangle shaped cross section (see Figure 3.3.1.1.2). The shear forces are generated partly by the measuring blades and the mixing blades. The impeller could also be seen as a “semi-inner cylinder”. Hence, the measuring zone is the space between the semi-inner cylinder and the bucket.

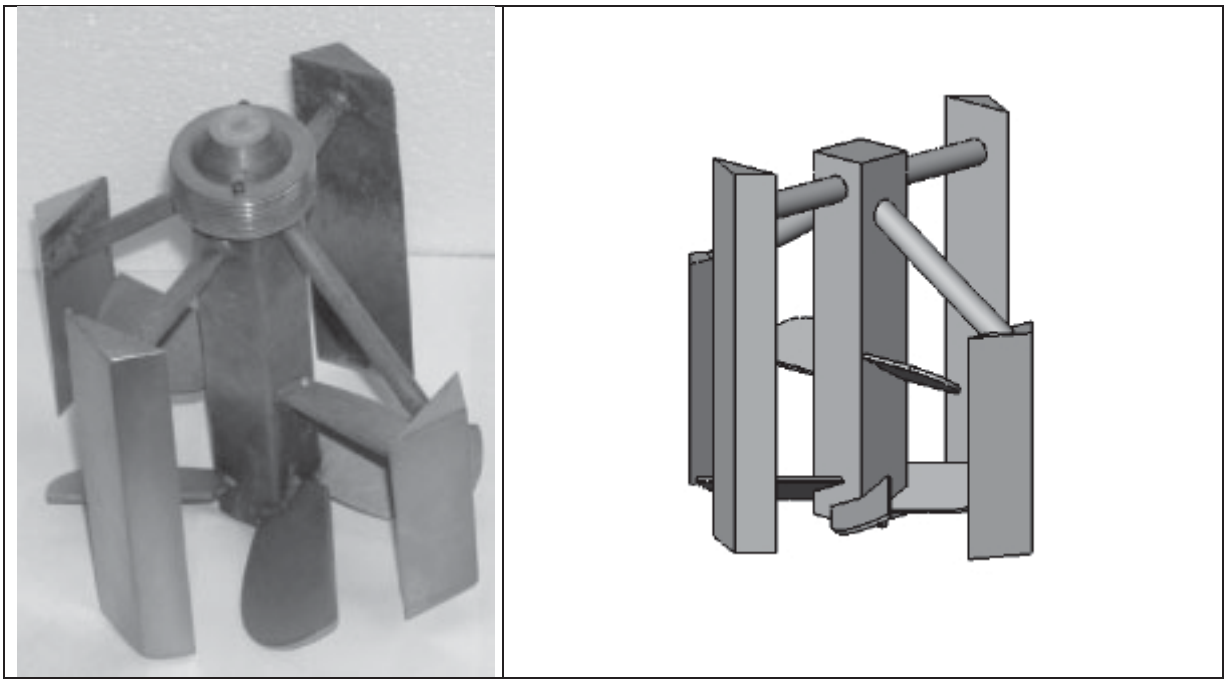

Figure 3.3.1.1.2: Impeller for mixing and measuring mortar and paste

A profile of the mixing- and measuring process of Rheomixer is given in Figure 3.3.1.1.3. At the end of the mixing procedure the rheological test is conducted. Measurements at three fixed times (after 6, 13 and 15 min) are performed. The profile can be divided into three mixing regimes and three measuring regimes. During first 30 s the mixing profile consists of three 10s cycles of forward and reverse rotations of the impeller at a speed of +/- 1,5 rps. In the following 120 s the amplitude of the cycles are increased to 5 rps and the cycles time is decreased to 2 s. Thereafter a constant speed of 1,5 rps is maintained over the next 55 seconds. After the mixing, the mortar is at rest (from 205 to 355 s) followed by the rheological measurements at 6, 13 and 15 minutes. /IB 2/ Characteristic value is the mean of the 13 and 15 minute measurement.

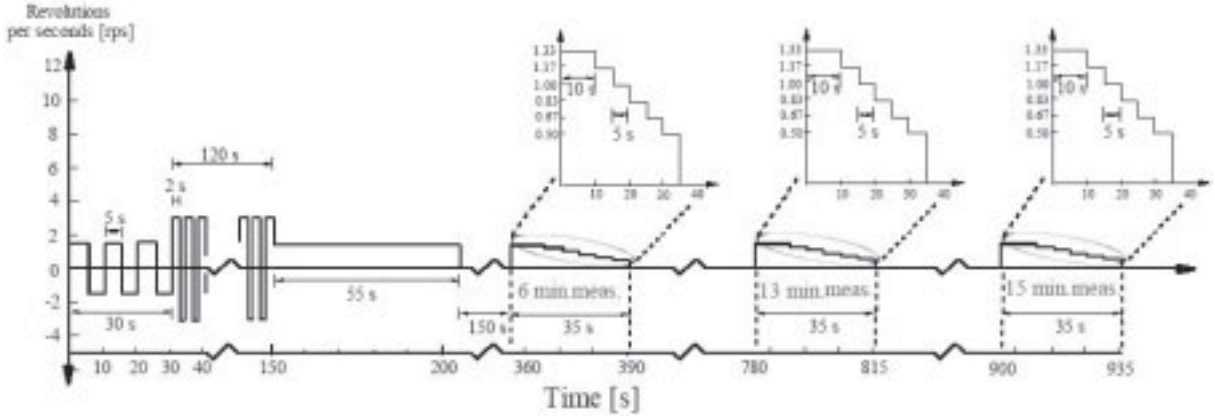

Figure 3.3.1.1.3: Mixing and measuring profile of Rheomixer /IB 2/

The confident measuring range of the Rheomixer is between 0 and 500 Pa for yield stress and 0 to 20 Pa s for plastic viscosity. The Rheomixer is equipped with an 8 channel calorimeter, measuring the rate of hydration under semi-adiabatic conditions. The Windows software for controlling the Rheomixer is also used for temperature logging /IB 2/. The device is operated with 220V/50Hz. Maximum aggregate size for Rheomixer in standard setup is 4 mm. Special modified versions might be capable of mixing and measuring bigger aggregate size (such as present in microcrete). Repeatability tests were made on several mortar mixes, which were

mixed and tested in the Rheomixer. The mortar was prepared with cement from the same bag and EN-sand. After tests in Rheomixer, the mortar was tested in ConTec Viscometer 6. Note that the tests in ConTec Viscometer 6 were done several minutes after the tests in Rheomixer. As can be seen in Figure 3.3.1.1.4, the repeatability seems to be very good in general and also relative to the results from the ConTec Viscometer 6. /IB 2/

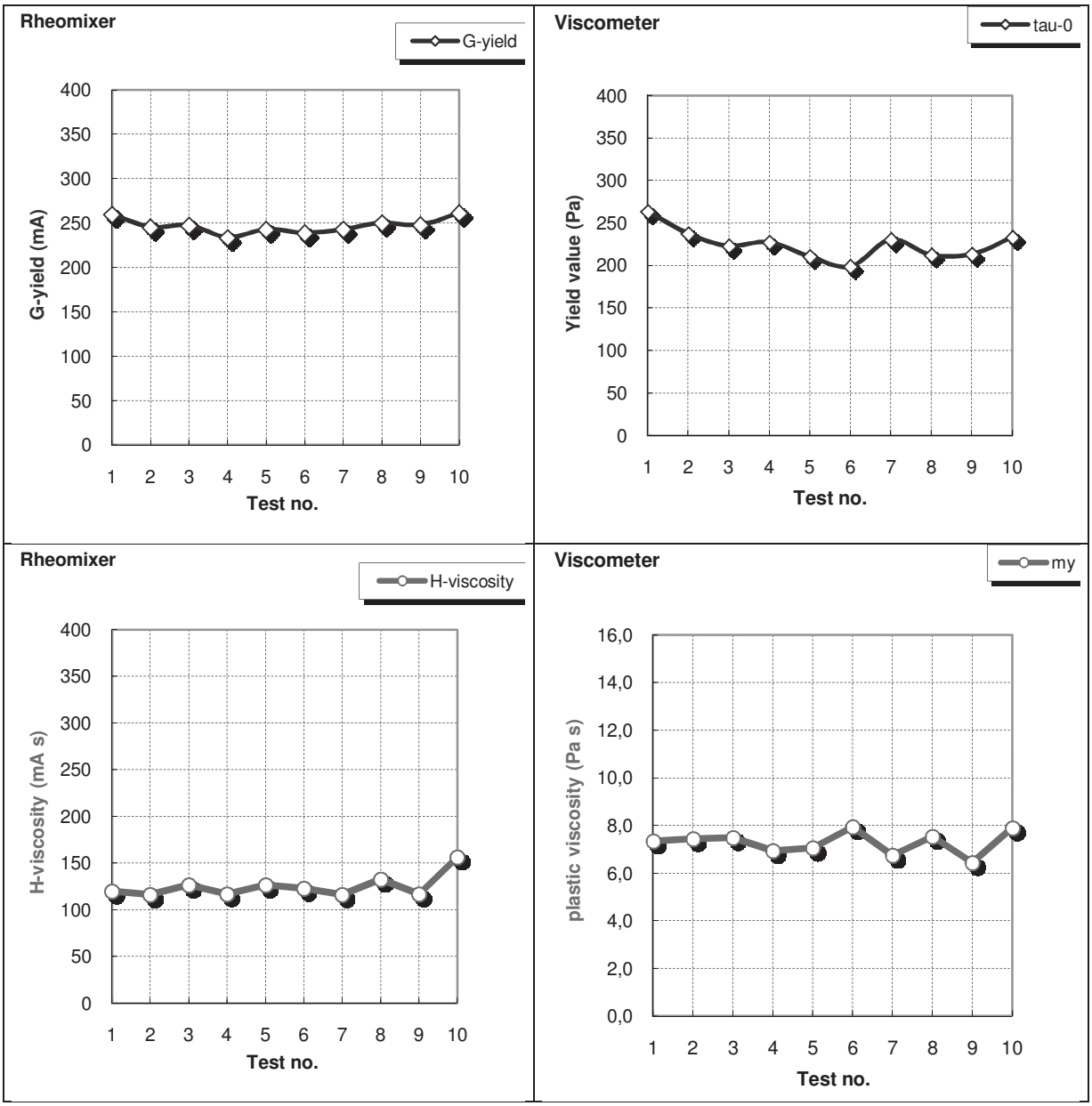

Figure 3.3.1.1.4: Results of repeatability tests on 10 mortar mixes

3.3.1.2 Signal logging of Rheomixer

The data logging during measurement is performed by the variable speed drive. The computer software sends a query to the drive every 0,25 second /Hj 1/. The query contains information to the drive about how fast to rotate the motor and once the drive receives the query it sends back information about the measured torque and the feedback speed. The reason for the selection of the logging time, i.e. 4 logs per second was made due to the speed of the communication between the drive and the computer /Hj 1/. The drive's processor logs the signal every 250 microseconds which means 4000 logs per second. The drive processes the signal in a vector which contains 500 signals. When a new signal is added to the vector the oldest signal is discarded. The average value of the 500 signals is calculated and when the computer sends a query to the drive and asks about the value for the drive´s torque /Hj 1/.

Table 3.3.1.2.1: Measurement setup for rheological measurement of mortar with ConTec Rheomixer

Step no.	Speed (rps)	Duration (sec)	Measurement (sec)
1	1,33	10	4
2	1,17	5	4
3	1,00	5	4
4	0,83	5	4
5	0,67	5	4
6	0,50	5	4
	Total	**35**	**24**

The speed is varied stepwise from 1,33 rps to 0,50 rps. The characteristic value of each step is the median of the collected data, i.e. the median of 16 data points. The total running time is 35 seconds and thereof 24 seconds as actual logging signal.

3.3.2 Flow calculation for the ConTec Rheomixer

3.3.2.1 Background

The geometry of the ConTec Rheomixer is rather complex, something that represents a challenge for analytical analysis. Of course, a numerical simulation of the flow inside the Rheomixer is possible, but such a process would be too complex, and is beyond the scope of the current work. A comprehensive description of Rheomixer can be found in chapter 3.3.1.

3.3.2.2 The geometry of the ConTec Rheomixer

The Rheomixer consists of a bucket, which constitutes the outer cylinder of radius R_o, and a impeller. As will be clear later, the impeller will constitute a "semi – inner cylinder" of radius R_i. A picture of the impeller and the bucket is shown in Figures 3.3.1.1.1 and 3.3.1.1.2. As shown in these illustrations, the impeller consists of four measuring blades, which are connected to a central axis. Figure 3.3.2.2.1 shows a schematic top view of the impeller and the bucket. There, it is shown how the rod connects the central axis (i.e. the center) to the middle position of each blade. Each rod has a different radii designated as R_1, R_2, R_3 and R_4. Thus, the average radius of the impeller system is presented with $R_i = (R_1 + R_2 + R_3 + R_4)/4$.

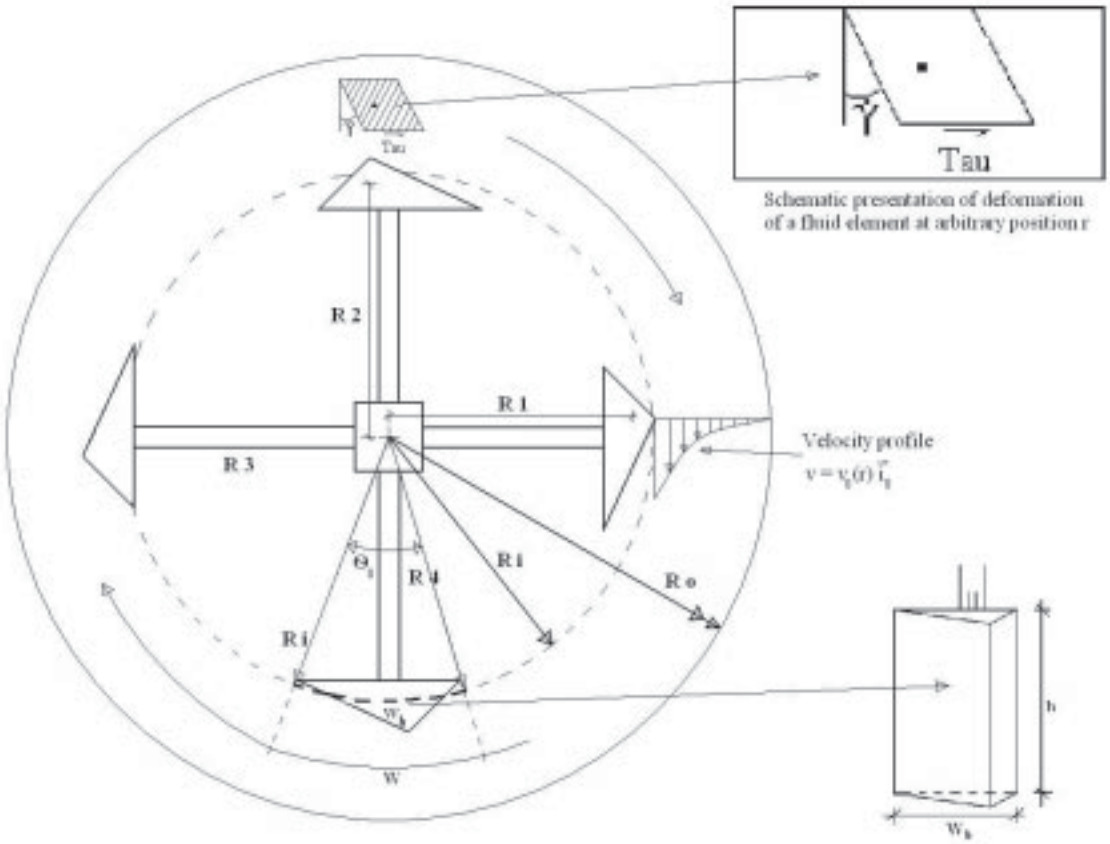

Figure 3.3.2.2.1: Schematic draft of Rheomixer impeller rotating in the testing bucket (top view)

Shown to the right of Figure 3.3.2.2.1 is a schematic illustration of a single blade. The four blades are identical in all aspects, except for the height h. The height of blade number 1 to 4 will be designated as h_1, h_2, h_3 and h_4, respectively. Thus, the average height of the blades is presented with $h = (h_1 + h_2 + h_3 + h_4)/4$. During a rheological measurement, all blades are immersed in the test sample. The width of each blade is the same, and is designated with w_b (see Figure 2). During a single rheological test, the impeller (which constitutes the central axis, blades and the connecting rods) rotates at predetermined angular velocity, while the bucket is stationary. During that time, the impeller registers the applied torque T_{tot} from the test material.

3.3.2.3 Velocity profile

The calculations made here apply in the region between the blades and the bucket. That is, the flow is not calculated between the blades and the central axis, shown in Figure 3.3.2.2.1. The fundamental assumption about the flow between the blades and the bucket is that it is circular. That means, each fluid element that resides there will (roughly) go in a circular path. In terms of cylindrical coordinates, this means the following velocity profile

$$\mathbf{v} = v_\theta(r)\, \mathbf{i}_\theta \qquad (1)$$

where r and θ are the radial coordinates. The term $\mathbf{i}_\theta$ is the unit vector in the θ-direction and v_θ is the speed in the same direction (see Equation (3.8) in /Wa 6/). There is no question that this assumption could be considered somewhat crude, meaning that most likely a fluid element will also travel in radial directions as well as in vertical directions. But if we assume that such movements are overshadowed by a circular motion, as a consequence of the circular rotation of the impeller (during a measurement), the assumption shown in the above equation could be

considered to be correct at least as a first approximation. The use of a more complicated flow behaviour than Equation (1) above, will result in a set of equations that can only be solved by numerical simulation, something that is outside of the scope of the current work.

3.3.2.4 Torque and shear stress

With the velocity profile presented with Equation (1) above, the test material (between the blades and the bucket) can be considered as cylindrical shells, each with the thickness δR. For such cases, it has been shown in /Wa 6/ (Section 3.3.2) that the torque applied on each such shell is constant. This applies at the arbitrary distance r, anywhere inside the test material (but still in between the blades and the bucket). This means:

$$T = \text{constant}, \quad \text{for } r \in [R_i, R_o] \tag{2}$$

Since T is a constant, its value is also equal to the torque applied on the outer sides of the four blades. As mentioned in previous section, the term T_{tot} represents the torque applied from the test material on the impeller as a whole. Since we are only calculating the flow between the blades (i.e. the semi-inner cylinder) and the bucket (i.e. the outer cylinder), the torque calculated here will be the one applied on the outer sides of the four blades. This torque will be designated with T and represents the sum of torques applied on the four blades at the outside area.

The torque applied on a cylindrical shell from its outer material can be calculated as

$$T = r \cdot F \sin 90° = T \cdot A \tag{3}$$

Where under normal circumstances, the area A of the cylindrical shell would be the whole circumference multiplied with the height h, meaning A = 2 π r h. However, since the area in which the shear stress (and thus torque) is measured, is only A = 4 h w (the number 4 is from four blades, in which each has the area of h w_b), then a similar rule must apply for the cylindrical shell, namely w h = r θ_0 h. Note that the width of each blade is $w_b = R_i$ θ_0 = constant, while the corresponding width of shell area is $w = r$ θ_0. This is because the torque applied on the blades is the same as on each cylindrical shell, c.f. Equation (2) above. With Equations (2) and (3), the following is attained,

$$T = r \times \tau \cdot 4 \cdot (h \cdot w) = r \times \tau \cdot 4 \cdot (h \cdot r \cdot \theta_0) \tag{4}$$

Solving for shear stress in the above, gives the following,

$$\tau = \frac{T}{4 \cdot r^2 \cdot h \cdot \theta_0} \tag{5}$$

Combining the above result with Equation 3.18 in /Wa 6/, gives the governing equation for a fluid element between the blades and the outer cylinder.

$$\eta \cdot (\frac{dv}{dr} - \frac{v}{r}) = \tau = \frac{T}{4 \cdot r^2 \cdot h \cdot \theta_0} \quad \text{for } r \in [R_i, R_o] \tag{6}$$

Now, using the Bingham model in the above, gives the following:

$$(\mu + \frac{\tau_0}{\dot{\gamma}}) \cdot (\frac{dv}{dr} - \frac{v}{r}) = \frac{T}{4 \cdot r^2 \cdot h \cdot \theta_0} \tag{7}$$

With the velocity profile shown in Equation (1) above, the shear rate can be presented with Equation (8) below /Wa 6/:

$$\dot{\gamma} = \left| \frac{dv}{dr} - \frac{v}{r} \right| = -\left(\frac{dv}{dr} - \frac{v}{r} \right) \tag{8}$$

By definition in theoretical rheology/continuum mechanics (see Equation (2.24) in /Wa 6/), the shear rate is always a positive number. Due to how the velocity profile will change as a function of radius *r*, the term *dv/dr – v/r* will always be negative. Because of this, a negative sign is used in Equation (8) above. Combining Equations (8) and (9) gives,

$$\mu \cdot (\frac{dv}{dr} - \frac{v}{r}) - \tau_0 = \frac{T}{4 \cdot r^2 \cdot h \cdot \theta_0} \tag{9}$$

after few mathematical steps, the above equation can be rewritten to

$$d(\frac{v}{r}) = \left\{ \frac{T}{4 \cdot r^3 \cdot h \cdot \theta_0 \cdot \mu} + \frac{\tau_0}{\mu \cdot r} \right\} dr \tag{10}$$

Solving the above differential equation gives

$$\frac{v}{r} = \frac{-T}{8 \cdot r^2 \cdot h \cdot \theta_0 \cdot \mu} + \frac{\tau_0}{\mu} \ln(r) + C \tag{11}$$

where C is the constant of integration. With the no slip boundary conditions at the bucket, meaning $v(R_o) = 0$, one can solve for C in the above equation.

$$v(R_o) = 0 = -\frac{T}{8 \cdot R_o \cdot h \cdot \theta_0 \cdot \mu} + \frac{\tau_0 \cdot R_o}{\mu} \ln(R_o) + C \cdot R_o$$

giving

$$C = \frac{T}{8 \cdot R_o^2 \cdot h \cdot \theta_o \cdot \mu} - \frac{\tau_0}{\mu} \ln(R_o) \tag{12}$$

Combining Equations (11) and (12), give after few mathematical steps, the velocity profile between the blade and the outer cylinder.

$$v = -\frac{T \cdot r}{8 \cdot h \cdot \theta_0 \cdot \mu} \cdot (\frac{1}{r^2} - \frac{1}{R_o^2}) + \frac{\tau_0 \cdot r}{\mu} \cdot \ln(\frac{r}{R_o}) \quad \text{for } r \in [R_i, R_o] \tag{13}$$

Assuming partial slip conditions at the blades

$$v(R_i) = R_i \cdot \omega_i - \delta \cdot R_i \cdot \omega_i = R_i \cdot \omega_i \cdot (1 - \delta) \tag{14}$$

Where δ is a slip parameter, with $0 \le \delta < 1$, where $\delta = 0$ represents no slippage and $\delta = 1$ complete and full slippage. The last-mentioned condition is assumed to be non-physical and thus never occurring. Using the boundary condition represented with Equation (14) in Equation (13) gives after few mathematical steps the following,…

$$-T = \frac{8 \cdot h \cdot \theta_0 \cdot \mu \cdot \omega_i \cdot (1 - \delta)}{(\frac{1}{R_i^2} - \frac{1}{R_o^2})} + \frac{8 \cdot h \cdot \theta_0 \cdot \tau_0}{(\frac{1}{R_i^2} - \frac{1}{R_o^2})} \cdot \ln(\frac{R_o}{R_i}) \tag{15}$$

The minus sign in front of the torque symbol *T*, in Equation (15), is just a consequence of that the blades are rotating and not the outer cylinder (i.e. not the bucket). Thus, the minus sign is a purely mathematical consequence (see Equations 3.12 and 3.16, pp. 57 – 58, in /Wa. 6/).

Since the torque is measured positive, the negative sign can be omitted from here on, and Equation (15) can be rewritten to

$$T_1 = \frac{8 \cdot h \cdot \theta_0 \cdot \mu \cdot \omega_i \cdot (1-\delta)}{(\frac{1}{R_i^2} - \frac{1}{R_o^2})} + \frac{8 \cdot h \cdot \theta_0 \cdot \tau_0}{(\frac{1}{R_i^2} - \frac{1}{R_o^2})} \cdot \ln(\frac{R_o}{R_i}) \qquad (16)$$

To summarize, we have put $-T = T_1$ in the above equation, where T_1 represents positive torque (i.e. equal to or greater than zero) applied on the outer sides on the rotating blades as shown in Figure 3.3.2.2.1 (also as T1, as shown in Figure 3.3.2.4.1).

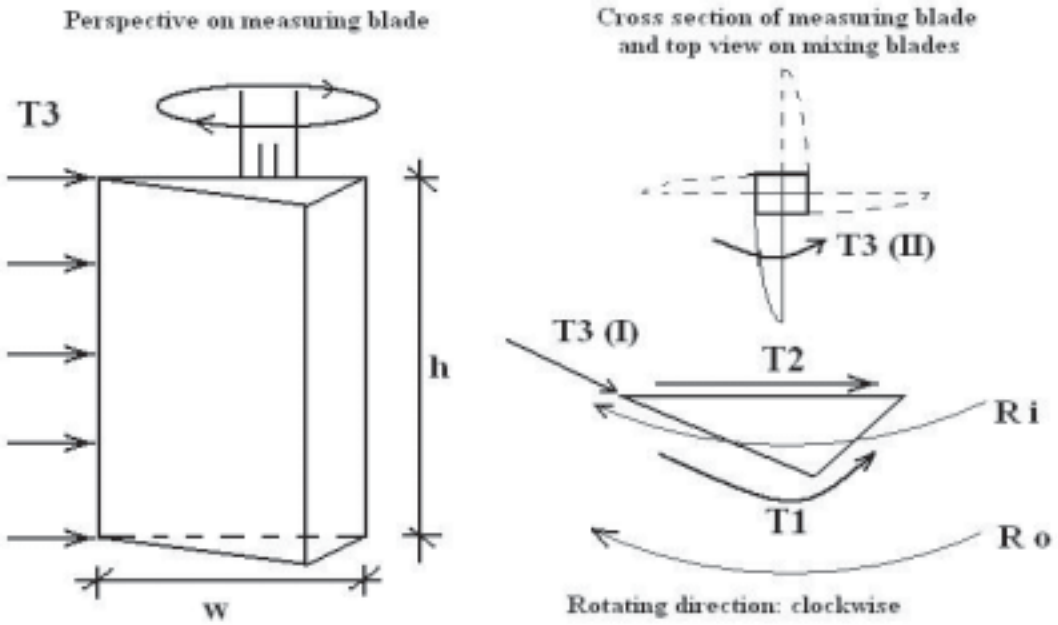

Figure 3.3.2.4.1: Perspective and cross section of measuring blade

3.3.2.5 Necessary simplifications and assumptions

What now follows are presentation of some series of simplifications and assumptions, which are most necessary to be able to make analytical calculations for the Rheomixer possible. Unfortunately, the only alternative to these steps is to make a numerical simulation of the flow inside the Rheomixer. But such a step would be too extensive and well beyond the scope of the current work.

Now, both terms T_2 and T2 designates the torque generated by the shear stress applied on the inner side of the measuring blade (see Figures 3.3.2.2.1 and 3.3.2.4.1). For simplicity, it will be assumed that torque applied on the inner and outer side of the blade is equal, meaning

$$T_1 = T_2 \qquad (17)$$

The term $T_{3(I)}$ (as well as T3 (I)) will here represent the sums of torque generated by the aggregate collision onto the front edge of the blades. This is shown with the right illustration of Figure 3.3.2.4.1. Likewise, the term $T_{3(II)}$ (or equally T3 (II)) will represent the torque generated by the test sample on the mixing blades also shown in the same figure. As shown with Equation (18), then the sum of these two contributions are represented with the term T_3.

It is not unlikely that all the terms T_1, $T_{3(I)}$ and $T_{3(II)}$ are linearly dependent on the angular velocity of the blade system ω_1 (see Equation (16)). If so, T_3 will be linear proportional to T_1. The constant of proportionality will be designated with the term ψ.

$$T_3 = T3(I) + T3(II) = \psi \cdot T_1 \tag{18}$$

3.3.2.6 The total torque

The total torque applied on the total blade system from the test material is designated with T_{Nm} and given by (see also Figures 3.3.2.2.1 and 3.3.2.4.1)

$$T_{\mathrm{Nm}} = T_1 + T_2 + T_3 \tag{19}$$

The subscript Nm in the above equation is used to stress out that the total torque is in Newton-meters. Shortly, the total torque will also be presented in Am (i.e. Ampere-meter) and will be designated with T_{Am}. Although both terms T_{Am} and T_{Nm} represent the same thing, their absolute value will differ as a consequence of different units used (i.e. Ampere-meter vs. Newton-meter). Now, combining Equations (17), (18) and (19), the following is attained

$$T_{\mathrm{Nm}} = (2 + \psi) \cdot T_1 \tag{20}$$

Thereafter we put Equation (16) in Equation (20), and the following is attained,

$$T_{\mathrm{Nm}} = \underbrace{\left[\frac{(2+\psi) \cdot 8 \cdot h \cdot \theta_0 \cdot \mu \cdot (1-\delta)}{\left(\frac{1}{R_i^2} - \frac{1}{R_o^2}\right)} \cdot 2\pi \right]}_{H_{\mathrm{Nm}}} \cdot f_i + \underbrace{\left[\frac{(2+\psi) \cdot 8 \cdot h \cdot \theta_0 \cdot \tau_0}{\left(\frac{1}{R_i^2} - \frac{1}{R_o^2}\right)} \cdot \ln\left(\frac{R_o}{R_i}\right) \right]}_{G_{\mathrm{Nm}}} \tag{21}$$

3.3.2.7 Torque as measured by the Rheomixer

The calibration of Rheomixer is done by use of a mechanical brake, which is connected to a load cell and an amplifier displaying the measured torque in Nm /Hj 1/. The torque measured by the load cell is compared to the torque measured by the drive of the device. The mechanical brake, consisting of a brake bracket, teflon ring and brake pads, is mounted on the motor axle. If an adjustment screw is tightened, the brake pads are pushed to the surface of the motor axle mounting. This setup is similar to a brake system of a car. Once the brake pedal is pressed the brake pads push to the surface of the brake disks and slow the car down. Here the adjustment screw has the function of a brake pedal. The accuracy of the brake force is estimated to be ± 0,2 Nm. The brake force is increased from 0 to 10 Nm in 4 steps, where the first step is at 2,5 Nm. After that the brake force is increased in 4 steps to 30 Nm /Hj 1/. The calibration curve of the motor used during this study is given in Figure 3.3.2.4.2 (see also Appendix I).

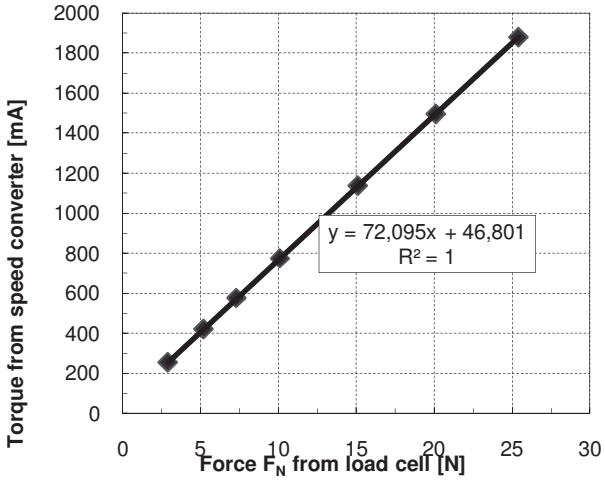

Figure 3.3.2.4.2: Calibration measurements for ConTec Rheomixer (Force from load cell [N] vs. torque from speed converter [mA])

The arm of force connected to the load cell, used for the force measurements in Figure 3.3.2.4.2, had a length of 0,116 m. Equation 22 describes the relationship between the torque given by the speed converter and the force F_N measured by the load cell.

$$T_{mA} = 72,095 \cdot F_N + 46,801 \tag{22}$$

Considering the arm of length from the load cell, F_N can be written as.

$$T_{Nm} = F_N \cdot 0,116 \Rightarrow F_N = \frac{T_{Nm}}{0,116} \tag{23}$$

Then we put F_N from Equation (23) in Equation (22) and we get.

$$T_{mA} = \frac{72,905 \cdot T_{Nm}}{0,116} + 46,801 \Rightarrow \underbrace{621,51}_{\alpha} \cdot T_{Nm} + \underbrace{46,801}_{\beta} \Rightarrow T_{Nm} = \left[\frac{T_{mA} - \beta}{\alpha}\right] \tag{24}$$

Where $\alpha = 621,51 \ \frac{mA}{Nm}$ $\beta = 46,801$ mA

3.3.2.8 Retrieving the fundamental physical quantities

By combining Equations (21) and (24), the following is attained.

$$\left[\frac{T_{mA} - \beta}{\alpha}\right] = \underbrace{\left[\frac{(2+\psi) \cdot 8 \cdot h \cdot \theta_0 \cdot \mu \cdot (1-\delta)}{(\frac{1}{R_i^2} - \frac{1}{R_o^2})} \cdot 2\pi\right]}_{H_{Nm}} \cdot f_i + \underbrace{\left[\frac{(2+\psi) \cdot 8 \cdot h \cdot \theta_0 \cdot \tau_0}{(\frac{1}{R_i^2} - \frac{1}{R_o^2})} \cdot \ln(\frac{R_o}{R_i})\right]}_{G_{Nm}} \tag{25}$$

Solving the above for T_{mA}, gives after several steps,

$$T_{\mathrm{mA}} = \frac{\alpha \cdot (2+\psi) \cdot 8 \cdot h \cdot \theta_0 \cdot \mu \cdot 2 \cdot \pi \cdot (1-\delta)}{(\frac{1}{R_i^2} - \frac{1}{R_o^2})} \cdot f_i + \frac{\alpha \cdot (2+\psi) \cdot 8 \cdot h \cdot \theta_0 \cdot \tau_0}{(\frac{1}{R_i^2} - \frac{1}{R_o^2})} \cdot \ln(\frac{R_o}{R_i}) + \beta \quad (26)$$

The above can be rewritten to,

$$T_{\mathrm{mA}} = H_{\mathrm{mA}} f_{\mathrm{i}} + G_{\mathrm{mA}} \quad (27)$$

where

$$H_{\mathrm{mA}} = \frac{\alpha \cdot (2+\psi) \cdot 8 \cdot h \cdot \theta_0 \cdot \mu \cdot 2 \cdot \pi \cdot (1-\delta)}{(\frac{1}{R_i^2} - \frac{1}{R_o^2})} \quad (28)$$

$$G_{\mathrm{mA}} = \frac{\alpha \cdot (2+\psi) \cdot 8 \cdot h \cdot \theta_0 \cdot \tau_0}{(\frac{1}{R_i^2} - \frac{1}{R_o^2})} \cdot \ln(\frac{R_o}{R_i}) + \beta \quad (29)$$

Solving for the plastic viscosity in Equation (28) gives,

$$\mu = \frac{(\frac{1}{R_i^2} - \frac{1}{R_o^2})}{\alpha \cdot (2+\psi) \cdot 8 \cdot h \cdot \theta_0 \cdot 2 \cdot \pi \cdot (1-\delta)} \cdot H_{\mathrm{mA}} \quad (30)$$

Likewise, solving for Equation (29) gives,

$$\tau_0 = \frac{(\frac{1}{R_i^2} - \frac{1}{R_o^2}) \cdot (G_{\mathrm{mA}} - \beta)}{\alpha \cdot (2+\psi) \cdot 8 \cdot h \cdot \theta_0 \cdot \ln(\frac{R_o}{R_i})} \quad (31)$$

By comparing the G_{mA} from the Rheomixer with the measured yield stress τ_0 from the ConTec Viscometer 6 for quite many mixes, the empirical value ψ has shown to be approximately equal to 0,70. This means that the torque from aggregate collision and mixing blades is approximately 70% of the torque generated on one side of the measuring blade. Results obtained by Equation (31) are as accurate as ±10 Pa when compared to measured values, and results from Equation (30) are as accurate as ±2 Pa·s when compared to measured values. The scatter in the calculated values is due to different testing ages, as G_{mA} and H_{mA} used in the Equations (30) and (31), were measured 15 minutes after water addition, whereas the comparison values were measured 22 minutes after water addition.

3.3.3 ConTec Viscometer 6

The ConTec Viscometer 6 (see Figure 3.3.3.1) is a coaxial cylinder system, capable of measuring the rheological parameters yield stress (Pa) and plastic viscosity (Pa s) in mortar and paste /Wa 6/. It has a stationary inner cylinder connected to a load cell measuring the torque T, and a rotating outer cylinder. For this study, the ConTec Viscometer 6 was used with the measuring system M-100. The M stands for mortar and the 100 represents the diameter of the inner cylinder in millimetres. The Viscometer 6 is working according to the principle of a Couette system. The rotation speed of the outer cylinder is varied while the torque is measured on the inner cylinder. The ConTec Viscometers are controlled by a computer software named FreshWin. Relevant parameters for each measuring system (such as height of cylinder, inner and outer radius) are incorporated as standard set-up in the software. Results obtained by ConTec Viscometer 6 are based on the Bingham model /Co 1/.

According to the Bingham model, the flow properties are characterized by two parameters, yield value (τ_0) and the plastic viscosity (μ).

$$\tau = \tau_0 + \mu \cdot \gamma$$

where:		
	τ = shear stress	[Pa]
	γ = rate of shear	[1/s]
	μ=plastic viscosity	[Pa·s]

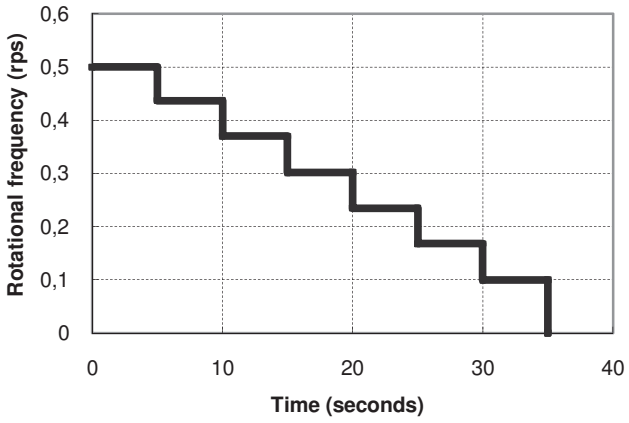

Figure 3.3.3.1: ConTec Viscometer 6 and testing regime used

Maximum aggregate size for ConTec Viscometer 6 in standard setup is 5 mm. The measuring gap width is 10 mm with the M100 system. Normally, the mortar was tested on its rheological properties after 18 and 22 minutes. During these two measurements in Viscometer 6, the test cylinder was released from the mortar and the mortar was briefly handmixed to prevent any segregation or generation of liquid to the shearing zone. Characteristic value is the mean of both measurements. The test setup used for mortar is given in table 3.3.3.1.

Table 3.3.3.1: Test setup

Minimum rotation speed [rps]	Maximum rotation speed [rps]	Measured points [-]	Interval between measurements [sec]	Interval for measurement [sec]	Data points [-]
0,09	0,48	7	2	3	50

3.3.4 ConTec Viscometer 5

The ConTec Viscometer 5 (see Figure 3.3.4.1) is the newest device in the ConTec BML family. It was developed by Wallevik et al. /Wa 2/ in the end of the eighties and the use of it was first published in 1990. Its first version was built after intense research with the Tattersall two-point test apparatus. Limitations of the two-point test apparatus were reduced with the BML /Wa 2/. In 1992 the device was made commercially available. The ConTec Viscometer 5 is a coaxial cylinders system. Its outer cylinder has a volume of 17 liters (volume of concrete tested). The rotation speed of the outer cylinder is varied while the torque is measured on the inner cylinder. Results are interpreted by using the Bingham model. The device measures the yield value and plastic viscosity of fresh concrete, where the yield value is a measure of the force required to initiate flow while the plastic viscosity is a measure of the resistance to increase in the rate of flow. The rheological properties are displayed in fundamental units. For measurement of yield stress and plastic viscosity, the outer cylinder starts at a speed level of 0,5 rps. The speed level is then decreased stepwise to 0,07 rps. The ConTec Viscometer 5 fulfills the following criteria:

Figure 3.3.4.1: ConTec Viscometer5

- The ratio between outer and inner cylinder radius should not be much higher than 1. According to references /Wa 2, Ta 1, Wa 1/ a ratio of ≤1,2 is still acceptable. The distance between inner and outer cylinder should be three times the maximum aggregate size /Wa 1/.
- The power of the motor should be high enough to perform tests on relatively stiff concrete.
- The shearing rate should not result in segregation of concrete. Therefore, the shearing rate should be as close as possible to the mixing speed of a truck mixer /Ta 1/.
- The difference between the highest and the lowest speed level should be relatively small, so that the Bingham model can be applied.

By using the measuring unit C-200 with the Viscometer 5 the maximum aggregate size which can be tested is 22 mm /Wa 1/. The measured torque can be between 0 and 60 Nm and the rotation speed can be altered from 0,0022 to 0,85 1/s /Wa 1/. The device can be calibrated by using a calibration oil and a calibrated load cell. Based on the Reiner-Rivlin equation /Wa 1/ results are reported as viscosity and yield stress.

$$\Omega = 2\pi N = \frac{T}{4\pi\mu h}\cdot\left(\frac{1}{r_i^2}-\frac{1}{r_o^2}\right)-\frac{\tau_0}{\mu}\cdot\ln\left(\frac{r_o}{r_i}\right)$$

Ω= angular velocity of outer cylinder (1/s)
T= torque, measured on inner cylinder (Nm)
N= rotation speed of outer cylinder (1/s)
h= penetration depth (into the concrete) of inner cylinder (m)
r_i= radius of inner cylinder (m)
r_a= radius of outer cylinder (m)

BML and ConTec viscometers are used in several laboratories worldwide /Wa 1/, and comparison tests with other devices have shown a good correlation between devices /Fe 1, Pa 1/. The default test setup used for concrete is given in table 3.3.4.1.

Table 3.3.4.1: Test setup

Minimum rotation speed [rps]	Maximum rotation speed [rps]	Measured points [-]	Interval between measurements [sec]	Interval for measurement [sec]	Data points [-]
0,07	0,50	8	2	3	50

3.3.5 ConTec Rheometer-4SCC

The Rheometer-4SCC (see Figure 3.3.5.1) was developed from 2004 to 2006 /Wa 7/. ConTec Rheometer-4SCC was officially introduced at the 4th International RILEM Symposium on Self-Compacting Concrete (SCC 2005 USA). The following points were the main design goals during the design process for the ConTec Rheometer-4SCC:

- The device has to be as accurate as similar devices currently available on the market.
- The device must be simple to operate.
- The device must be operable at construction sites.
- The device must be light and easily manageable for one person.
- No single component which the user has to lift or carry may exceed 25 kg.

Figure 3.3.5.1: ConTec Rheometer-4SCC

The ConTec Rheometer-4SCC /Wa 7/ is a so-called rotating index system. The impeller is completely immersed in the concrete and the current needed (mA) to rotate the impeller at a certain speed level (1/s) is measured. The volume of the sample bucket is only seven liters, making the handling much easier than with the Viscometer 5. Rheometer-4SCC measures the G-value (A) and H-value (A s) while ConTec Viscometer 5 measures the corresponding yield stress (Pa) and plastic viscosity (Pa s). The stiffer the mix, the higher is the measured value

for G-yield (A) in Rheometer-4SCC or the yield stress (Pa) in Viscometer 5. With multiplying the apparent unit (A) by a correlation factor it is possible to obtain fundamental values. The Rheometer-4SCC was developed for Self Compacting Concrete (SCC). According to Wallevik et al. /Wa 3/ SCC is defined by certain rheological boundary conditions (see Figure 3.3.5.2).

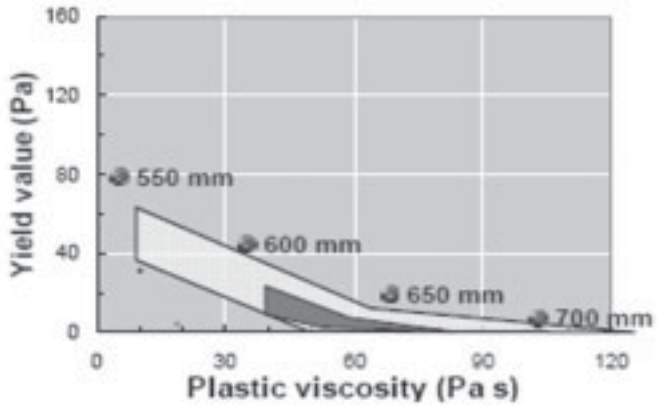

Figure 3.3.5.2: Target area (yellow) for SCC according to Wallevik et al. /Wa 3/

The measuring procedure starts with the highest rotation speed and decreases stepwise to the lowest rotation speed. Figure 3.3.5.3 shows the software interface to operate the Rheometer-4SCC. The setup used for concrete is given in table 3.3.5.1.

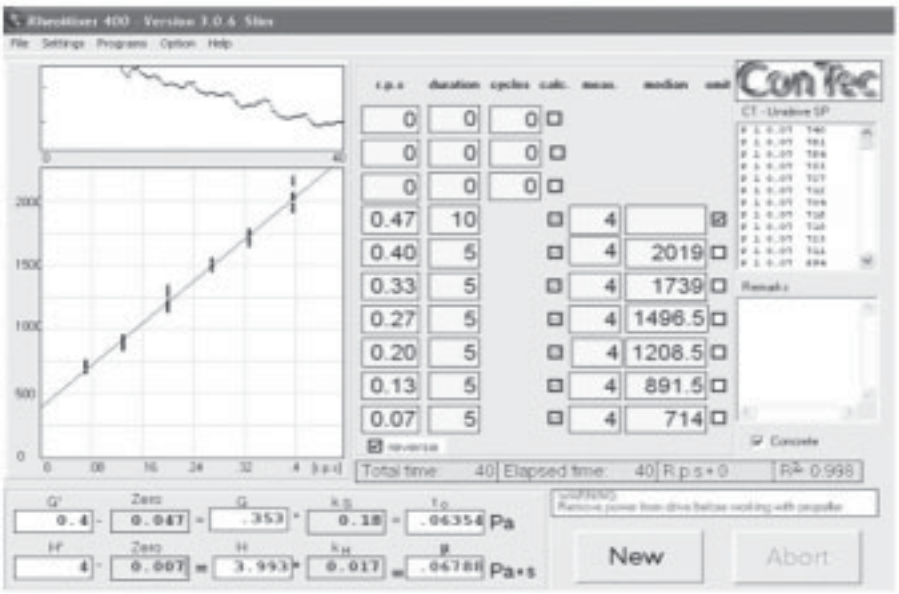

Figure 3.3.5.3: User interface of the Rheometer-4SCC software

Table 3.3.5.1: Test setup

Minimum rotation speed [rps]	Maximum rotation speed [rps]	Measured points [-]	Interval between measurements [sec]	Interval for measurement [sec]	Data points [-]
0,07	0,47	7	1	4	16

3.3.6 Semi-adiabatic calorimeter

The Rheomixer is equipped with a 8-channel semi-adiabatic calorimeter. It measures the heat evolution under semi adiabatic conditions over a certain period of time. The mortar sample is given in a coffee cup shaped sample container and thereafter placed in an insulated measuring cell (see Figure 3.3.6.1). Before the measurement can be started, a heat sensitive wire is put into the mortar and the measuring cell is closed with a lid, since the Rheomixer software is also used for temperature logging. Although the measuring cell is made of high insulating material (styrene plastic), a certain loss of hydration energy to the environment can not be prevented. Due to the incomplete adiabatic conditions, it is named semi-adiabatic calorimeter. However, the data obtained with this method gives a good indication of the hydration progress of the cement (see Figure 3.3.6.2). All measuring cells and lids have the same dimensions and therefore the same loss of energy during hydration process. The calorimeter is logging both the environmental temperature in the laboratory and the temperature increase in the sample with a measuring interval of one minute.

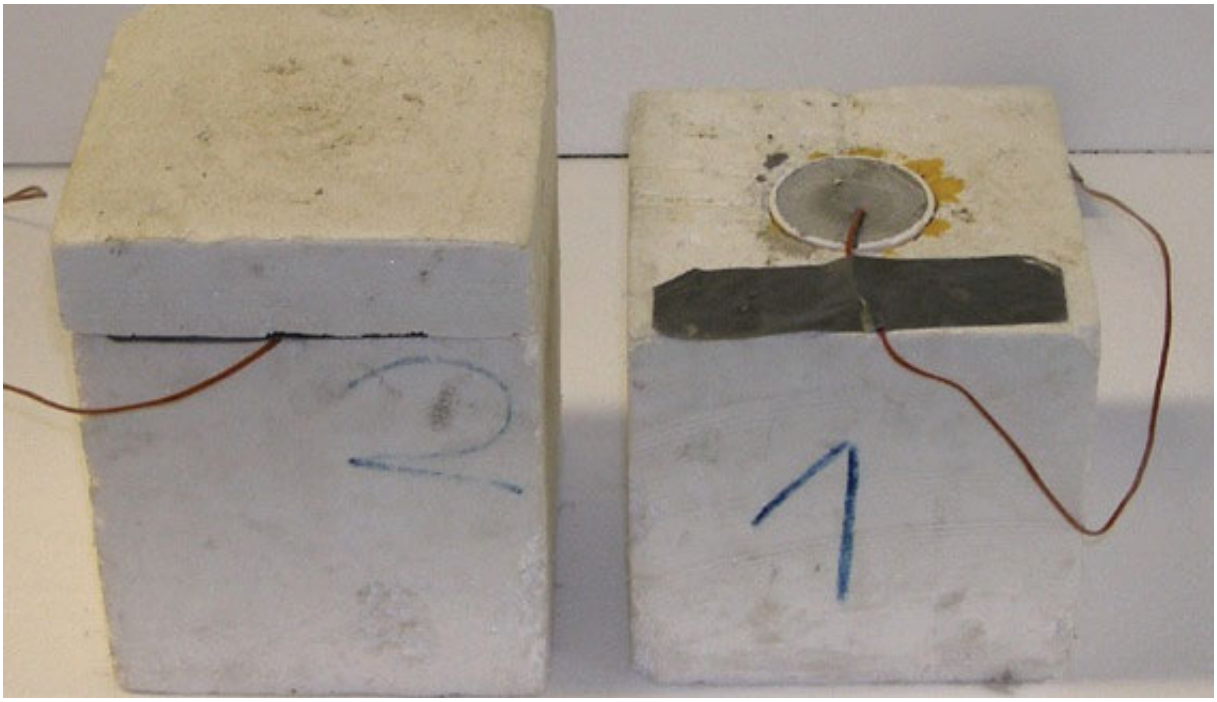

Figure 3.3.6.1: Measuring cells (left closed, right open) of calorimeter, used for hydration measurements

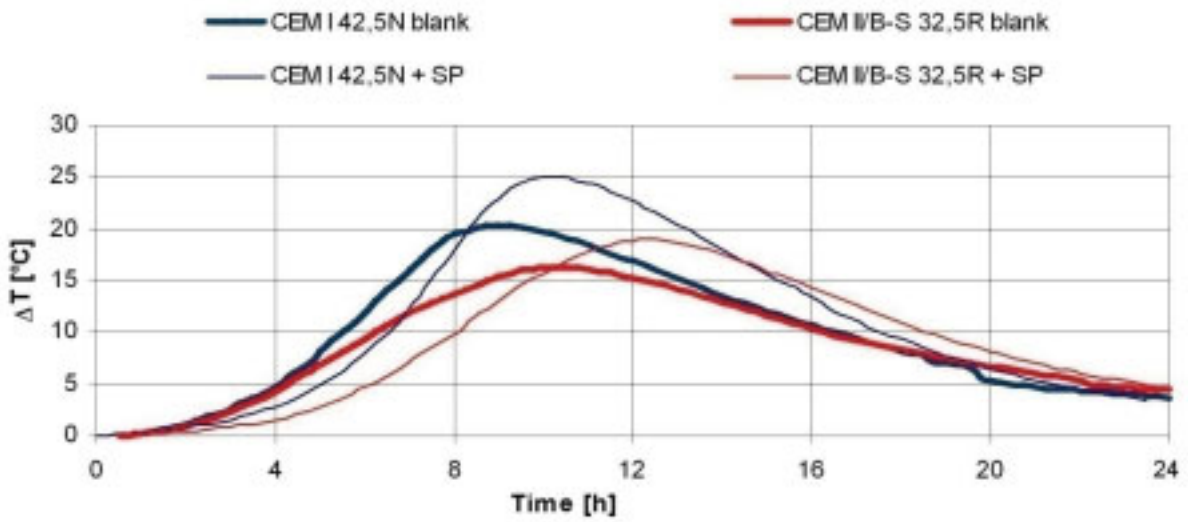

Figure 3.3.6.2: Hydration curves obtained by semi-adiabatic calorimetry

3.3.7 Isothermal calorimeter

The isothermal calorimeter used was a TAM Air Calorimeter (see Figure 3.3.7.1) operated with a Solidus software. It measures the heat flow from the sample over time compared with an inert reference. The heat flow curve provides a fingerprint of the chemical reactions in the sample /Sa 2/. After the last measurement in Viscometer 6 (at 22 minutes) a small amount of mortar is transferred to a sample container and placed into the calorimeter. The difference between the isothermal and the semi-adiabatic calorimeter is that the isothermal measures heat flow from the sample to a heat sensor at close to constant temperatures, whereas the semi-adiabatic measures a temperature rise in partially insulated mortar or concrete /Gr 1/. Table 3.3.7.1 gives an overview about the sample size needed to conduct a test in both calorimeters. For all tests reported here, the time between addition of water to cement and loading into the calorimeter was 26 minutes. A software logs the data. Graphs given out by the software are already normalized, meaning the results are showing the heat evolution per gram of cement. Before start of measurement, the correct percentage of cementitious materials has to be entered. The high accuracy of the device and the possibility to compare all data made this calorimeter a real contribution to the study. One limitation observed during the study was related to the initital hydration (during first 30 minutes). This curve is highly dependent upon the initial reaction of the cement (initial peak) and the temperature of the constituents used. Small changes can significantly influence the curve during the first 30 minutes. A case study was carried out to evaluate the effect of aggregate temperature on hydration curves (see Appendix B). When a less reactive and cold mortar sample is placed into the calorimeter, the hydration curve which is displayed in real time can run below the x-axis (see Appendix B1). In this case, the cold mortar generates a heat flow from the calorimeter/measuring cell into the sample, which is displayed as an endothermic reaction. After a certain time, the mortar has reached the temperature of the calorimeter and the heat curve depicts an exothermic reaction. From then on, the data is reliable. The same effect can be observed with a hot mortar sample. If a “hot mortar” is placed into the calorimeter, the hydration curve shows a very intense exothermic reaction during the first minutes (see Appendix B1). But note that this reaction might be a “fake reaction”, because it is caused by the cooling effect of the calorimeter on the sample. An important observation is that the peak at the end of the acceleration period (see Appendix B2) and the total energy release (see Appendix B3) were not affected by the differences in aggregate temperature.

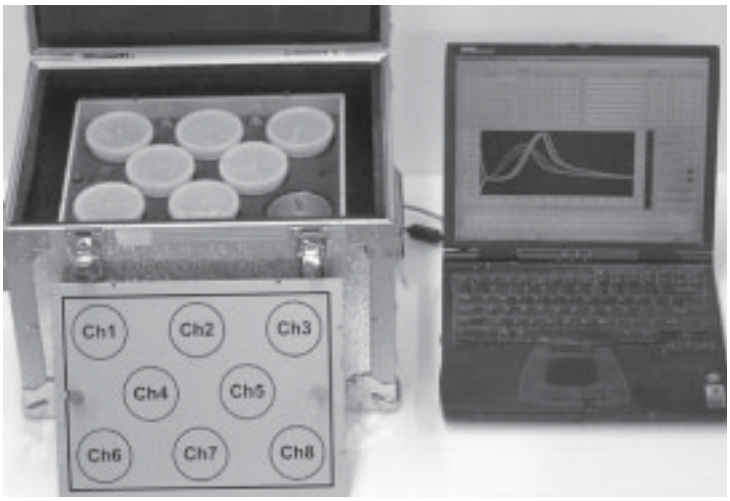

Figure 3.3.7.1: TAM Air isothermal calorimeter (8-channel) with control software

Table 3.3.7.1: Sample size in isothermal and semi-adiabatic calorimeter /Gr 1/

Type of sample	Isothermal	Semi-adiabatic
Paste	10-20 g	200-500 g
Mortar	40-130 g	500-1000 g
Concrete	300-400 g	4000 g

3.3.8 Sympatec HELOS-system for particle size analysis

For the detemination of particle size and particle size distribution a Sympatec HELOS-system (see Figure 3.3.8.1) was used. It is based on laser diffraction. The device is designed on a modular basis and the setup used for tests on cements included the following components. The laser diffraction sensor is the central unit of the measuring device, and consists of three functional parts. First part is the laser-light source including the focusing lense. The second part is the measuring zone, where the laser light and the particles interact. The third part is an optical system that converts the diffraction of the laser light into an image detectable by the photo detector. The intensity of the light is converted into electrical signals. A software converts the data into the particle size distribution (PSD). Laser diffractometry allows the particle size analysis of dispersed matter in gas or liquid regardless if the particles are solid, gaseous (bubbles) or liquid (droplets) /Sy 1/. For this study, the dispersed cements were investigated in an air stream (gaseous). The measuring range used is named R4, ranging from 1,8 µm to 350 µm. The device was used over a period of 3 years. Hence, some control measurements on a defined material (silicium powder) were carried out. This inert material consists of grains in a certain particle size range with defined particle size distribution. The results of the control measurements showed a very good correlation with the values given by Sympatec. It is very important for the measurement that the sample is free of agglomerates, because laser diffractometry analyses the dimensions of a agglomerate as one particle. The dispersion device is taking care of this step. The cements of this study were dispersed by aerodispersion in the RODOS dispersing system. Agglomerates are dispersed in single particles between the velocity gradient of a vacuum and a propulsion jet. After the dispersed aerosol stream has passed the measuring beam (laser-light) of the laser diffraction sensor, it is collected and sucked into the vacuum unit /Sy 1/. Results are given in graphs and text file. For the calculation of the specific surface (by the Sympatec Helos Sensor), it is assumed that all counted particles are spheres.

Figure 3.3.8.1: Work station for particle size analysis

3.4 Materials

3.4.1 Standardized sand according to EN 196-1

The sand used meets the requirements of EN 196, part 1. This sand is produced by Normensand GmbH in Beckum/Germany. EN-sand from this producer is a mixture of four sands. The sand consists of two types of sands in the small grading fraction, a third type of sand in the medium grading fraction and a fourth type of sand in the large grading fraction. All sands are coming from different quarries, the exact origin of the sands kept confidential by the producer. The four sands are natural, round shaped and quartz-rich. The sand production seems to be very accurate according to the results of quality control measurements over a period of five years, evaluated by MPA Stuttgart (Otto-Graf-Institut). In this report /MP 1/, the sieve residues of quality control measurements (n=2102) are evaluated by statistical calculation. Although the data looks very good on the paper, one has to bear in mind that EN-sand is mainly used for standard strength tests with mortar prisms. EN-sand is not specifically produced for rheological tests. Hence, one has to be aware of possible parameters originating from sand which might influence rheology. Influences from sand on rheology can come from two sources. First, the particle size distribution in the small grading fraction can change from bag to bag. As can be seen in Figure 3.4.1.1, the requirements with regards to production stability assumed in EN are not too strict. Particularly, in the small grading fraction (0 – 0,16 mm), the upper and lower limit leave enough play for the producer which can influence the rheology. Second, organic impurities could be present and influence rheological data. Hence, (1) the effect of variations in fineness of EN-sand was evaluated in a study (see chapter 5.1.1) and (2) single bags from various sand deliveries were tested on organic impurities in accordance to ASTM C40 and ASTM D1544. Throughout the test series standardized sand was free of organic impurities. The intention for using this relatively stable product was to minimize the effects from sand on rheology. The sand/cement ratio in the mixes was around 2 and kept constant throughout the test series.

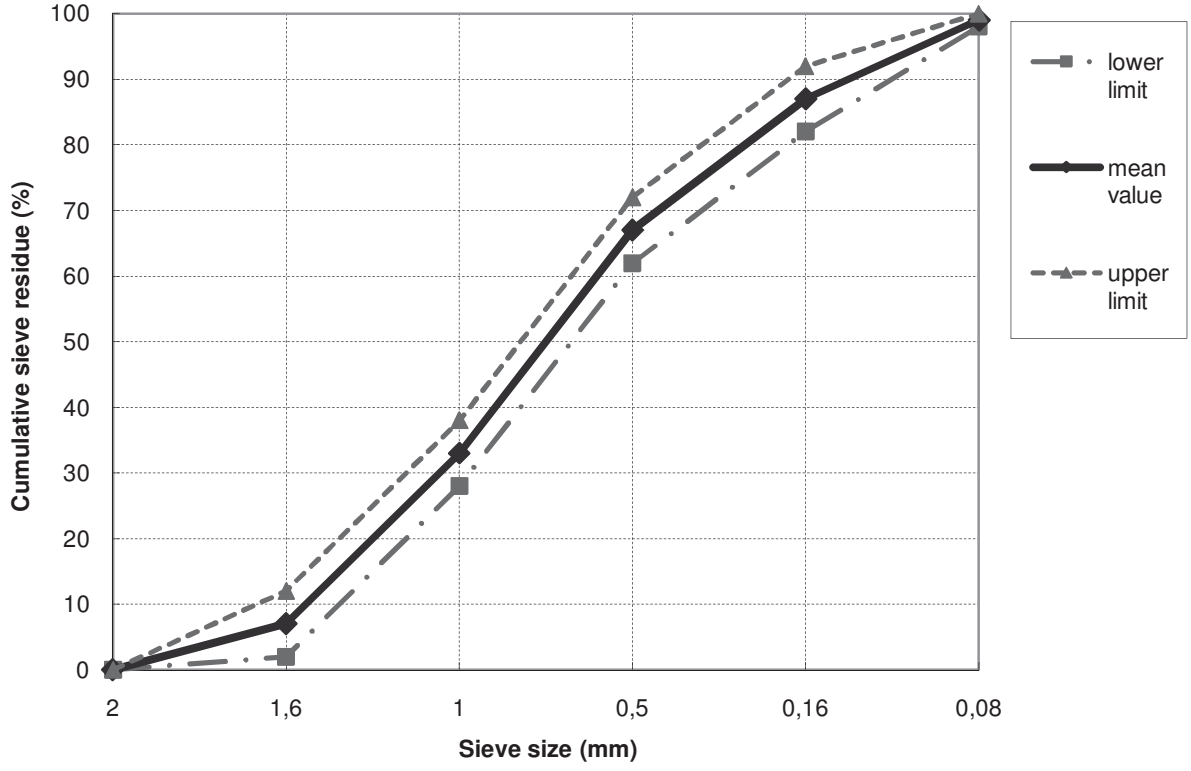

Figure 3.4.1.1: Permissible variations for EN-sand (according to EN 196, part 1)

3.4.2 Cement

The cements used for the in deep study were supplied by several cement producers. Four pure Portland cements and a Portland composite cement were investigated on their rheology in mortar mixes. During the project it turned out that some sponsors supplied the project with fewer cement samples and others with more cement samples. Therefore, the cement from which the most deliveries (production dates) were available was chosen as the reference cement. In this case it was cement C, representing a CEM I 52,5N. Table 3.4.2.1 gives an overview of the tested cements and their characteristic properties. The cements A-1, A-2 and B-1 were taken directly from the production line and sent to ICI in sealed containers. Cements B-2 and C were received in regular 25 kg cement bags and stored in plastic bags and sealed containers throughout the test series. The chemical composition was measured with the XRF-device from Sementsverksmidjan hf. in Akranes, Iceland and by use of Rietveld refinement at F.A. Finger Institute in Weimar, Germany. Hence, the mineralogical composition was obtained by use of (1) modified Taylor-Bogue equations and (2) Rietveld refinement. One has to be aware, that modified Taylor-Bogue is not the most precise way to determine the mineralogy of cement. However, modified Taylor-Bogue is still sufficient to distinguish between single cement production dates.
Rheological tests were carried out right after arrival of cement samples. Check samples of each batch were stored in sealed containers.

Table 3.4.2.1: Characteristic properties of cements used (modified Bogue calculation)

Type of cement	Cement A-1 CEM I 42,5N	Cement A-2 CEM II/B-S 32,5R	Cement B-1 CEM I 42,5R	Cement B-2 CEM I 42,5R	Cement C CEM I 52,5N
Country	A	A	B	B	C
Delivery displayed	7/2004	3/2004	12/2004	10/2005	10/2005-1
Density (g/cm³)	2,99	2,96	2,98	2,98	3,15
Blaine (cm²/g)	3000	3300	3800	3610	4240
Setting time start (h:min)	3:17	3:25	3:10	3:05	2:25
Setting time end (h:min)	4:12	4:18	3:50	4:52	3:35
Water demand (%)	27%	29%	29%	28,5%	27%
C_3S (%)	61	-)	52	56	60
C_2S (%)	12	-)	18	18	13
C_3A (%)	7	-)	8	7	5
$C_2(A,F)$ (%)	9	-)	7	7	12

-) modified Taylor Bogue cannot be used to calculate the mineralogical composition of CEM II/B-S cement

3.4.3 Water

The water used for this study was normal Icelandic tap water. Before being added to mixes, the water was stored for two days in a closed bucket under laboratory conditions.

3.4.4 Admixtures

The two types of admixtures used were sulfonated melamine polymer and modified polycarboxylate ether. Some characteristic properties of these admixtures are given in table 3.4.4.1. Through the complete test series only one batch of each admixture was used.
The sulfonated melamine used (Mel) disperses the cement particles by means of electrostatic repulsion. At a water/cement ratio of 0,40, the melamine provided a sufficient workability for 15-20 minutes after water addition. Thereafter, mixes stiffened quickly.

Table 3.4.4.1: Characteristic values of admixtures used

Designation	Mel	PC1	PC2	PC3	PC4
Based on	Sulfonated melamine polymer	Polycarboxylate ether	Polycarboxylate ether	Polycarboxylate ether	Polycarboxylate ether
Chloride content	<0,1%	<0,1%	<0,1%	<0,1%	<0,1%
Density	1,21 kg/dm³	1,10 kg/dm³	1,07 kg/dm³	1,05 kg/dm³	1,05 kg/dm³
Polymer content	39,5%	36,9%	30,2%	23,5%	20,3%
Recommended dosage by the producer (dry polymer)	0,15 – 0,8%	0,1 – 0,7%	0,1 – 0,9%	0,1 – 0,7%	0,1 – 0,6%
Workability	<30 minutes	30-60 minutes	>60 minutes	>60 minutes	>60 minutes

PC1 consists of a polymer type which adsorbs rather quickly and aggressively on the cement surface and disperses the cement particles by means of steric repulsion /Ba 1/. PC1 is a pure water reducer and is mainly used in the pre cast industry. PC2, PC3 and PC4 polymers are slump retainers, meaning their adsorption is clearly slower than PC1. PC2, PC3 and PC4 polymers represent the opposite of PC1 within the group of polycarboxylates. An overview of the characteristics and performance of the admixtures is given in chapter 5.1.7. Figure 3.4.4.1 schematically depicts the dispersing effect of PC1. At a water/cement ratio of 0,36, PC1 provided a good workability for 25-30 minutes. Thereafter, mixes stiffened quickly.

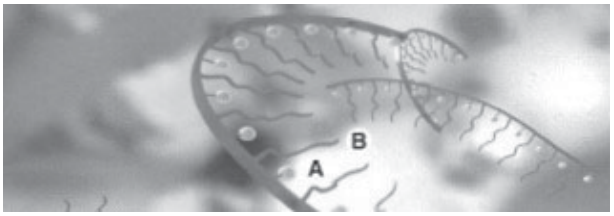

The polycarboxylate molecule in solution, comprising of functional groups of chains of different lengths. The backbone is slightly negatively charged (A), whereas the side chains (B) stretch out in the aqueous phase /MB 1/.

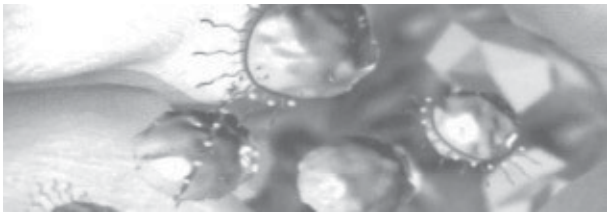

The polycarboxylate molecules are attracted by the positively charged cement particles and wrap themselves around the cement during mixing /MB 1/.

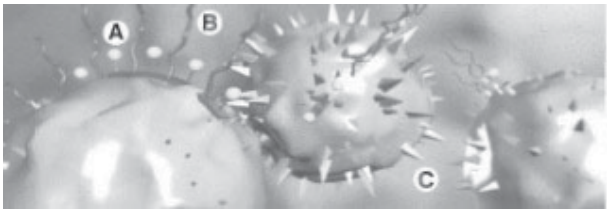

This increases the negative charge of the surface of the cement particles and causes electrostatic repulsion. The long side chains (B) build a steric hindrance which keeps the cement particles separate from each other (C) /MB 1/.

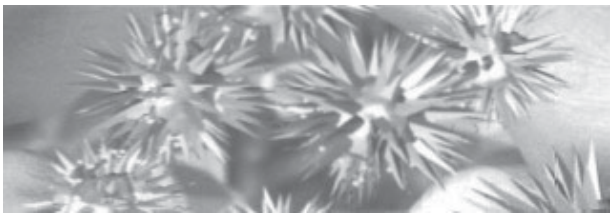

When the first hydration products grow further they incorporate the polymers leading to workability loss and stiffening of the system.

Figure 3.4.4.1: Schematic draft describing the dispersing effect of PC1 /MB 1/

3.5 Mix design of mortar mixes

The mortar was mixed under laboratory conditions at a temperature of 20°C in the Rheomixer. First, sand and cement were dry mixed in the Rheomixer for 20 seconds. Second, the water was added through a funnel followed by the admixture. The delay in admixture addition was approximately 5 seconds. The mix design for blank, polycarboxylate and melamine mixes are given in table 3.5.1. Figure 3.5.1 depicts the volumetric composition of the different mortar mixes. Further information how the reference system was determined is described in chapter 5.1.5.

Table 3.5.1: Mix design of mortars

Constituents	Density (kg/dm³)	Blank mixes	Melamine mixes	PC1 mixes	PC2 mixes	PC3 mixes	PC4 mixes
EN sand	2,62	1350,0 g	1350,0 g	1350,0 g	1350,0 g	1350,0 g	1350,0 g
Water at 20°C	1,00	286,8 g	267,5 g	257,0 g	255,3 g	255,2 g	255,5 g
Cement	3,15	623,5 g	684,4 g	717,5 g	722,7 g	723,2 g	722,2 g
Admixtures	Mel = 1,21	-	10,40 g				
	PC1 = 1,10	-	(0,60%)	2,14 g			
	PC2 = 1,07	-		(0,11%)	6,94 g		
	PC3 = 1,05	-			(0,29%)	6,77 g	
	PC4 = 1,05	-				(0,22%)	5,69 g (0,16%)
w/c-ratio	-	0,46	0,40	0,36	0,36	0,36	0,36
sand/cement ($M_{aggr.}$ / $M_{cem.}$)		2,17	1,97	1,88	1,87	1,87	1,87

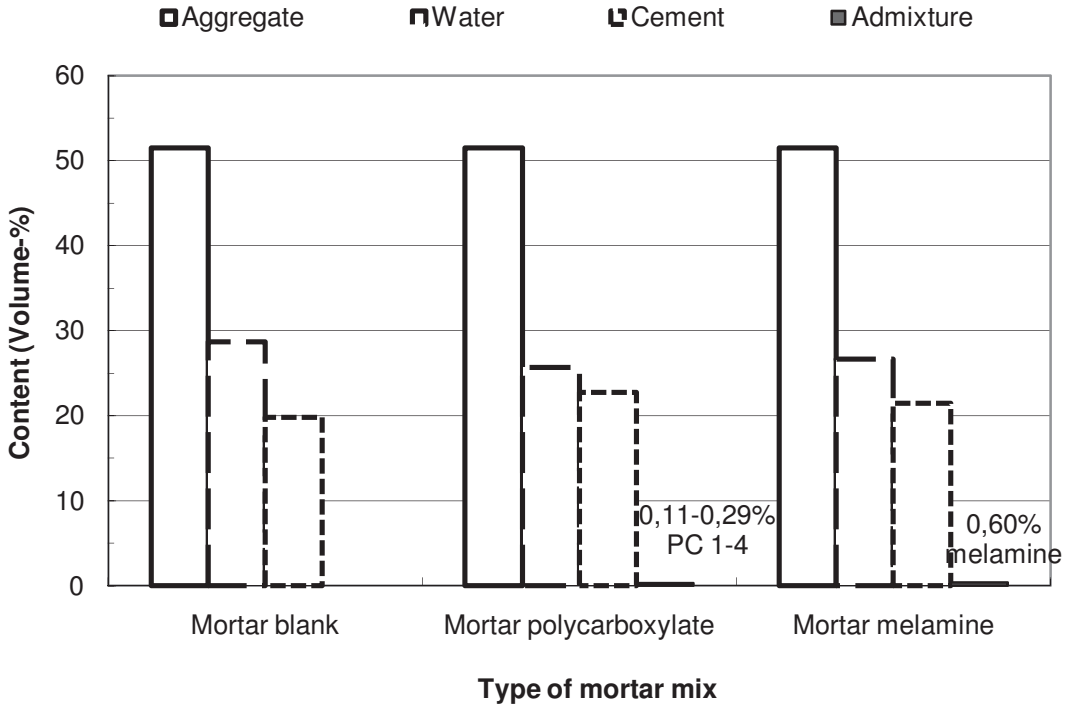

Figure 3.5.1: Volumetric composition of mortar mixes

3.6 Mix design of concrete mixes

Two types of SCC were investigated. The concrete used for this evaluation is (1) standard SCC and (2) so-called Eco-SCC. Standard SCC is normally used for robustness tests at ICI-Rheocenter. The mix design is given in table 3.6.1. Eco-SCC is a self compacting concrete

with a relatively low binder content. The amount of cementitious materials in this concrete is 300 ±15 kg/m³. The mix design is given in table 3.6.1. The sand used was natural sand from Norway, size 0-8 mm. The stone used was crushed granite from Norway, size 8-16 mm. The grading curve of the aggregates, the water content and the amount of admixtures were kept constant in all mixes. The only parameter changing was the cement delivery/production date. /Wa 4/

Table 3.6.1: Mix design for standard SCC and Eco-SCC

Type of SCC	-	Standard SCC	Eco-SCC
Strength class	N/mm²	C45/55	C25/30
Target slump flow (low yield cement)	mm	640±20	640±20
Target yield stress (Viscometer 5 @12 min)	Pa	30±10	50±10
Target plastic viscosity (Viscometer 5 @12 min)	Pa·s	40±10	30±10
Type of cement		CEM I 52,5N	CEM I 52,5N
Cement content, c	kg/m³	460	315
Water content, w	kg/m³	188	195
w/c		0,41	0,62
Aggregates			
0-8mm	kg/m³	1295	1390
8-16mm	kg/m³	435	460
Admixtures			
Superplasticizer based on polycarboxylate (PC1)	%	0,30	0,28
Stabilizer based on polysaccharide	%	-	0,05
$M_{aggr.} / M_{cem.}$	-	3,8	5,9

The mixing regime was the same for both SCC types. Stone, cement and sand were loaded into a 50 liter pan mixer (Gustav Eirich) and dry mixed for four minutes. The batch size of each mix was 40 liters. The water was added four minutes after start of mixing. Stabilizer and superplasticizer were added seven minutes after start of mixing, then the concrete was mixed for another three minutes. Slump flow was measured at 13 and 30 minutes after start of mixing. Rheological measurements by ConTec Rheometer-4SCC and ConTec Viscometer 5 were done at 12 and 16 minutes and at 28 and 32 minutes. Rheological data obtained with both machines is based on the Bingham model /Wa 4/.

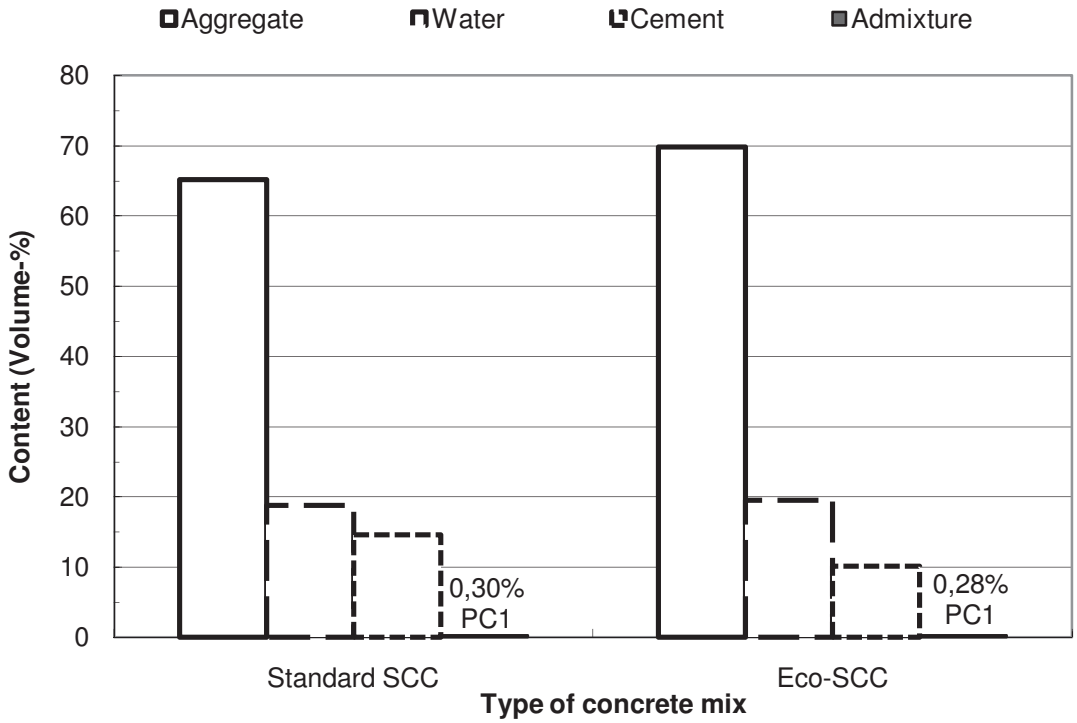

Figure 3.6.1: Volumetric composition of concrete mixes

4. Results

4.1 Country A

Two cements were tested from country A, one Portland composite cement (CEM II/B-S 32,5R) and one pure Portland cement (CEM I 42,5). Both cements were produced between 2/2004 and 7/2004. Apparently, the supply stopped after 7/2004, although it would have been very interesting to follow the fluctuations with the CEM II. The available free lime was estimated with 1,0% for cements from country A. The mineralogical composition shown in table 4.1.2 was obtained by use of modified Taylor-Bogue equation. The term "specific surface" relates to a surface which is calculated by the Sympatec Helos Sensor. It is assuming that all counted particles are spheres.

Table 4.1.1: Characteristic values and rheological results of cement from country A

Cement sample		Laser diffractometry (Helos)						G-yield (mA)		
Name	Type of cement	Blaine (cm^2/g)	Specific surface [cm^2/g]	<1,8 µm [%]	<10 µm [%]	<60 µm [%]	<86 µm [%]	Blank	PC1	Mel
A1#2	CEM I 42,5	3420	3700	11	40,7	93,7	98,2	314	116	52
A1#3	CEM I 42,5	3320	3730	11,1	40,9	94,5	98,2	308	204	175
A1#6	CEM I 42,5	3000	3790	11,1	42,4	95,9	98,5	378	298	504
A2#1	CEM II/B-S 32,5R	3340	3880	11,2	43,2	96,6	99,2	319	124	28
A2#4	CEM II/B-S 32,5R	3300	4000	11,8	45,2	98,4	100	297	60	47
A2#5	CEM II/B-S 32,5R	3660	4260	13	47,9	97,7	100	323	263	316

Table 4.1.2: Mineralogical composition of cement from country A

Cement sample		Mineralogical composition (%)								
Name	Type of cement	C_3S	C_2S	C_3A	$C_2(A,F)$	K_2O	Na_2O	Na_2O_{eq}	SO_3	CaO free *)
A1#2	CEM I 42,5	54,1	18,1	7,2	8,4	0,87	0	0,57	3,41	1,00
A1#3	CEM I 42,5	42,2	29,8	7,0	8,5	0,88	0,05	0,63	3,36	1,00
A1#6	CEM I 42,5	61,3	11,8	7,1	8,9	0,7	0	0,46	3,28	1,00
A2#1	CEM II/B-S 32,5R	-	-	-	-	-	-	-	-	
A2#4	CEM II/B-S 32,5R	-	-	-	-	-	-	-	-	
A2#5	CEM II/B-S 32,5R	-	-	-	-	-	-	-	-	

*) assumed with 1% as available free lime of these samples was not measured
-) modified Taylor Bogue cannot be used to calculate the mineralogical composition of CEM II/B-S cement

4.2 Country B

Two cements were tested from country B. Both cements were pure Portland cements (CEM I 42,5R), produced between 10/2004 and 2/2006. The mineralogical composition in table 4.2.2 was obtained by use of modified Taylor-Bogue equation. It is assumed that the cement factory is adding 5,0% lime stone filler to cements B1 and B2.

Table 4.2.1: Characteristic values and rheological results of cement from country B

Cement sample		Laser diffractometry (Helos)						G-yield (mA)		
Name	Type of cement	Blaine (cm^2/g)	Specific surface [cm^2/g]	<1,8 µm [%]	<10 µm [%]	<60 µm [%]	<86 µm [%]	Blank	PC1	Mel
B1#13	CEM I 42,5R	3750	4190	11,9	48,4	99,7	100	312	516	N/a
B1#14	CEM I 42,5R	3800	4250	12,2	48,6	99,4	100	309	621	N/a
B2#1	CEM I 42,5R	3570	4150	12,6	44,5	96,9	99,5	412	535	218
B2#2	CEM I 42,5R	3550	4200	12,8	45,5	97	99,6	404	368	153
B2#3	CEM I 42,5R	3610	4080	12,3	44,5	96,6	99,6	394	491	172
B2#4	CEM I 42,5R	3620	4130	12,5	45,4	96,3	99,2	383	470	302
B2#5	CEM I 42,5R	3550	4100	12,3	44,6	96,4	99,3	371	321	128

Table 4.2.2: Mineralogical composition of cement from country B

Cement sample		Mineralogical composition (%)								
Name	Type of cement	C_3S	C_2S	C_3A	$C_2(A,F)$	K_2O	Na_2O	Na_2O_{eq}	SO_3	CaO free
B1#13	CEM I 42,5R	56,7	13,2	8,2	6,4	1,23	0,04	0,85	3,38	1,48
B1#14	CEM I 42,5R	52,2	18,2	7,7	6,8	1,41	0,04	0,97	3,33	1,37
B2#1	CEM I 42,5R	57,5	16,2	6,8	7,8	1,04	0	0,68	3,34	1,10
B2#2	CEM I 42,5R	55,7	17,4	6,8	8,3	0,99	0	0,65	3,3	1,69
B2#3	CEM I 42,5R	55,8	18,0	7,4	7,3	0,88	0	0,58	3,18	1,79
B2#4	CEM I 42,5R	53,5	19,6	6,4	8,4	0,95	0	0,63	3,19	2,18
B2#5	CEM I 42,5R	58,9	14,2	6,7	8,9	0,86	0	0,57	3,18	1,53

Table 4.2.3: Results of standard tests on cement B

Name	Type of cement	Blaine (cm^2/g)	Setting time start (min)	Setting time end (min)	Water demand (%)	Ratio Blaine/LD
B2#1	CEM I 42,5R	3570	182	232	29	0,86
B2#2	CEM I 42,5R	3550	173	221	30	0,85
B2#3	CEM I 42,5R	3610	185	292	28,5	0,88
B2#4	CEM I 42,5R	3620	198	243	29,5	0,88
B2#5	CEM I 42,5R	3550	197	248	29	0,87

4.3 Country C

Cement C, corresponding to a CEM I 52,5N, was produced between 8/2004 and 8/2007. According to information from the cement factory, the CEM I 52,5N is blended with 4% limestone filler. This cement is produced with 100% dihydrate ($CaSO_4 \cdot 2H_2O$), which dehydrates in the mill depending on the mill temperature. The mineralogical composition shown in table 4.3.2 was obtained by use of modified Taylor-Bogue equation.

Table 4.3.1: Characteristic values and rheological results of cement from country C

Cement sample		Laser diffractometry (Helos)						G-yield (mA)		
Name	Type of cement	Blaine (cm^2/g)	Specific surface [cm^2/g]	<1,8 µm [%]	<10 µm [%]	<60 µm [%]	<86 µm [%]	Blank	PC1	Mel
C#6	CEM I 52,5N	4070	4330	13,8	45,9	96,7	99,2	274	222	384
C#6.2	CEM I 52,5N	4130	4420	13,9	46,0	96,7	99,0	272	135	177
C#7	CEM I 52,5N	4470	4750	15,4	49,0	96,7	98,7	384	86	244
C#8	CEM I 52,5N	4310	4840	15,7	50,2	96,8	98,7	364	289	262
C#9	CEM I 52,5N	4240	4840	15,8	49,9	97,1	98,9	368	149	113
C#10	CEM I 52,5N	4350	4730	15,1	49,3	97,5	99,2	402	193	174
C#11	CEM I 52,5N	4250	4650	14,5	49,0	99,4	100	322	306	328
C#12	CEM I 52,5N	4320	4660	15,0	49,3	98,7	100	316	156	167
C#13	CEM I 52,5N	4280	4520	14,3	47,6	98,0	99,4	328	166	66
C#14	CEM I 52,5N	4190	4430	14,0	47,6	98,0	99,2	319	146	49
C#15	CEM I 52,5N	4310	4570	14,9	48,3	97,4	98,9	368	200	159
C#16	CEM I 52,5N	4280	4480	13,5	48,7	97,4	99,3	297	260	391
C#17	CEM I 52,5N	4050	4453	13,7	48	97	99,2	397	259	167
C#18	CEM I 52,5N	4170	4547	13,9	48,7	97,9	99,5	346	234	326
C#19	CEM I 52,5N	4140	4500	13,7	48,3	97,9	99,5	345	233	348
C#20	CEM I 52,5N	4130	4687	14,7	49,6	96,8	99,3	304	217	291
C#21	CEM I 52,5N	4130	4397	13,3	47,6	97,8	99,7	429	220	241
C#22	CEM I 52,5N	4160	4447	13,6	47,9	97,8	99,7	424	293	368
C#23	CEM I 52,5N	4150	4490	13,7	48,1	97,9	99,7	399	268	314
C#24	CEM I 52,5N	4150	4523	13,8	48,3	98	99,7	420	279	342
C#25	CEM I 52,5N	4160	4510	13,8	48,1	98	99,8	433	258	271
C#26	CEM I 52,5N	4130	4530	13,8	48,5	98,2	99,8	442	315	273
C#27	CEM I 52,5N	4120	4417	13,4	47,6	98,4	99,9	419	204	161
C#28	CEM I 52,5N		4560	14,4	49,4	97,9	99,6	270	247	490
C#29	CEM I 52,5N		4630	14,8	47,7	98,8	99,9	249	177	297
C#30	CEM I 52,5N		4670	15,0	50,1	97,9	99,2	252	181	345
C#31	CEM I 52,5N		4730	15,3	50,6	97,2	98,9	369	209	122
C#32	CEM I 52,5N		4740	15,2	51,0	99,3	100,0	311	173	326
C#33	CEM I 52,5N		4830	15,6	52,1	99,0	99,9	365	190	271

Table 4.3.2: Mineralogical composition of cement from country C

Cement sample		Mineralogical composition (%)								
Name	Type of cement	C_3S	C_2S	C_3A	$C_2(A,F)$	K_2O	Na_2O	Na_2O_{eq}	SO_3	CaO free
C#6	CEM I 52,5N	61,8	10,8	4,9	11,8	0,45	0,06	0,36	3,39	1,28
C#6.2	CEM I 52,5N	61,4	12,2	4,7	11,8	0,38	0,04	0,29	3,29	1,17
C#7	CEM I 52,5N	59,6	13,3	4,3	12,4	0,44	0,07	0,36	3,34	1,17
C#8	CEM I 52,5N	58,6	13,8	4,6	12,4	0,45	0,09	0,39	3,29	1,53
C#9	CEM I 52,5N	60,2	12,8	4,6	12,2	0,41	0,1	0,37	3,33	1,42
C#10	CEM I 52,5N	62,3	10,9	4,7	12,3	0,42	0,1	0,38	3,34	1,25
C#11	CEM I 52,5N	59,8	12,6	4,4	12,8	0,49	0,14	0,46	3,37	0,85
C#12	CEM I 52,5N	61,9	10,8	4,7	12,6	0,5	0,1	0,43	3,32	0,69
C#13	CEM I 52,5N	62,3	11,2	4,8	12,0	0,41	0,15	0,42	3,34	0,76
C#14	CEM I 52,5N	61,4	12,0	4,6	12,5	0,44	0,12	0,41	3,33	0,60
C#15	CEM I 52,5N	62,1	10,6	4,6	12,7	0,45	0,13	0,43	3,35	0,62
C#16	CEM I 52,5N	56,3	16,3	4,5	12,5	0,49	0,12	0,44	3,36	0,88
C#17	CEM I 52,5N	54,7	17,4	4,9	12,4	0,48	0,12	0,44	3,43	1,04
C#18	CEM I 52,5N	59,1	13,1	4,9	12,2	0,47	0,11	0,42	3,37	0,87
C#19	CEM I 52,5N	55,6	16,8	4,8	12,1	0,51	0,1	0,44	3,32	0,98
C#20	CEM I 52,5N	68,6	4,8	5,5	11,9	0,54	0,11	0,47	3,41	0,97
C#21	CEM I 52,5N	64,9	8,9	5,1	12,5	0,52	0,1	0,44	3,43	1,02
C#22	CEM I 52,5N	66,2	7,7	5,3	12,4	0,5	0,09	0,42	3,34	0,96
C#23	CEM I 52,5N	66,5	7,5	5,2	12,3	0,51	0,09	0,43	3,35	0,95
C#24	CEM I 52,5N	59,8	13,0	4,8	12,4	0,5	0,11	0,44	3,35	1,01
C#25	CEM I 52,5N	60,6	12,2	4,8	12,4	0,5	0,1	0,43	3,35	0,99
C#26	CEM I 52,5N	61,4	11,3	4,8	12,3	0,52	0,09	0,43	3,37	1,03
C#27	CEM I 52,5N	59	14	4,7	12,6	0,49	0,11	0,43	3,39	0,81
C#28	CEM I 52,5N	60,5	12,2	5,1	11,9	0,47	0,05	0,36	3,28	0,70
C#29	CEM I 52,5N	56,1	17,1	4,6	12,1	0,51	0,06	0,40	3,35	0,74
C#30	CEM I 52,5N	52,9	19,2	4,3	12,5	0,5	0,07	0,40	3,34	0,78
C#31	CEM I 52,5N	58,7	14,1	4,7	11,8	0,47	0,05	0,36	3,35	0,77
C#32	CEM I 52,5N	51,7	22,0	4,4	11,4	0,47	0,05	0,36	3,19	0,98
C#33	CEM I 52,5N	52,9	20,5	4,5	11,5	0,47	0,06	0,37	3,16	0,87

Table 4.3.3: Results of standard tests on cement C

Cement sample		Standard tests on cement				
Name	Type of cement	Blaine (cm^2/g)	Setting time start (min)	Setting time end (min)	Water demand (%)	Ratio Blaine/LD
C#6	CEM I 52,5N	4070	197	265	28,5	0,94
C#6.2	CEM I 52,5N	4130	205	230	28	0,93
C#7	CEM I 52,5N	4470	188	243	27,5	0,94
C#8	CEM I 52,5N	4310	185	232	28	0,89
C#9	CEM I 52,5N	4240	145	215	27	0,88
C#10	CEM I 52,5N	4350	145	205	28	0,92
C#11	CEM I 52,5N	4250	152	198	28	0,91
C#12	CEM I 52,5N	4320	141	208	27,5	0,93
C#13	CEM I 52,5N	4280	177	247	28	0,95
C#14	CEM I 52,5N	4190	190	240	27,5	0,95
C#15	CEM I 52,5N	4310	173	245	28,5	0,94
C#16	CEM I 52,5N	4280	207	252	27,5	0,96
C#17	CEM I 52,5N	4050	182	220	27,5	0,91
C#18	CEM I 52,5N	4170	170	217	27	0,92
C#19	CEM I 52,5N	4140	178	215	27,5	0,92
C#20	CEM I 52,5N	4130	216	266	27,5	0,88
C#21	CEM I 52,5N	4130	127	171	28	0,94
C#22	CEM I 52,5N	4160	142	205	29	0,94
C#23	CEM I 52,5N	4150	135	170	28	0,92
C#24	CEM I 52,5N	4150	139	169	28,5	0,92
C#25	CEM I 52,5N	4160	143	197	28,5	0,92
C#26	CEM I 52,5N	4130	153	195	29	0,91
C#27	CEM I 52,5N	4120	121	184	28	0,93

Tables 4.3.4 to 4.3.6 give results of cements with differing rheology (cement C) in mortar and concrete. The results reported for G-yield and yield stress in mortar are the mean of tests on 3 mixes.

Table 4.3.4: Rheology of mortar in blank and PC1 mixes (based on /Ku 1/)

Cement sample		G-yield (mA)		Yield stress (Pa)	
Production date	Type of cement	blank	PC	blank	PC
01.11.2006	CEM I 52,5N	397	259	359	251
28.11.2006	CEM I 52,5N	399	268	399	255
24.02.2005	CEM I 52,5N	272	135	257	141
23.05.2005	CEM I 52,5N	384	86	371	77
04.12.2006	CEM I 52,5N	419	204	376	193

Table 4.3.5: Results of standard tests on high yield and low yield cement /Wa 4/

Production date	Blaine (cm²/g)	Setting. start (min)	Setting, end min)	Water demand (%)
01.11.2006	4050	182	220	27,5
28.11.2006	4150	135	170	28
24.02.2005	4130	205	230	28
23.05.2005	4470	188	243	27,5
04.12.2006	4120	121	184	28

Table 4.3.6: Rheology of Eco-SCC produced with high yield and low yield cement /Wa 4/

Cement sample		Rheometer-4SCC		Viscometer 5		Standard tests	
Production date	used in SCC mix no.	G-value (A)	H-value (A·s)	Yield stress (Pa)	Plastic viscosity (Pa·s)	Slump flow 13 minutes	Slump flow 30 minutes
01.11.2006	Eco115ME	n/a	n/a	80	55	580	550
28.11.2006	Eco122ME	0,64	5,7	88	47	550	550
24.02.2005	Eco117ME	n/a	n/a	57	50	610	600
23.05.2005	Eco121ME	0,42	5,3	50	43	650	620
04.12.2006	Eco130ME	0,55	4,8	70	54	600	590

4.4 Country D

One cement was tested from country D. Cement D, corresponding to a CEM II/A-M 42,5R, was produced between 10/2007 and 2/2008. The mineralogical composition was obtained by use of modified QXRD/Rietveld.

Table 4.4.1: Characteristic values and rheological data of cement from country D

Cement sample			Laser diffractometry (Helos sensor)				G-yield (mA)		
Name	Type of cement	Blaine (cm²/g)	Specific surface [cm²/g]	<1,8 µm [%]	<10 µm [%]	<60 µm [%]	<86 µm [%]	Blank	PC1	Mel
10/2006 (1)	CEM II/A-M 42,5R		3870	10,9	42,3	95,4	98,9	327	127	n/a
01/2007 (1)	CEM II/A-M 42,5R		3900	11,2	42,1	94,4	98,5	381	640	n/a
10/2007 (1)	CEM II/A-M 42,5R		3750	10,8	40,2	92,2	97,4	414	239	n/a
10/2007 (2)	CEM II/A-M 42,5R		3790	10,8	40,4	95,2	98,5	375	246	n/a
10/2007 (3)	CEM II/A-M 42,5R		3880	10,9	42,2	96,0	99,4	320	128	n/a
11/2007 (1)	CEM II/A-M 42,5R		3860	11,0	41,7	95,4	98,9	331	126	n/a
11/2007 (2)	CEM II/A-M 42,5R		3730	10,5	40,1	95,1	98,7	340	124	n/a
11/2007 (3)	CEM II/A-M 42,5R									
01/2008 (1)	CEM II/A-M 42,5R									
01/2008 (2)	CEM II/A-M 42,5R									
02/2008 (1)	CEM II/A-M 42,5R									

5. Discussion

5.1 Preliminary investigations

5.1.1 Effect of fluctuations in sieve curve of EN sand on rheology

As can be seen in Figure 3.4.1.1, the permissible variations for standard sand according to EN 196-1 are quite high, and the content of fines passed through the 0,16 mm sieve can range from 8% to 18% (by weight). Due to higher specific surface, particles of the size of 0 to 0,16 mm claim more water than the larger grading fractions. Hence, the variations in fineness could influence the rheology of mortars. A study was carried out to investigate the effect of variations of the fine grading fraction on rheology. The fines were substituted from a regular EN sand bag in exchange for the large/small grading fraction. Rheological measurements were done in Rheomixer and Viscometer 6 on blank mixes with a w/c of 0,50. The addition of 5% fines (0-0,16 mm) in exchange for the large grading fraction represents the lower limit according to EN 196-1. The substitution of 5% fines (0-0,16 mm) with the large grading fraction represents the upper limit of EN sand. Results are given in table 5.1.1.1.

Table 5.1.1.1: Rheological results for variations in fines

	Rheomixer		Viscometer	
	G-yield	H-viscosity	Yield stress	Plastic viscosity
Mix	(mA)	(mA·s)	(Pa)	(Pa·s)
+5% fines	279	60	242	4
+2,5% fines	262	64	235	4
+1% fines	258	72	232	4
reference	255	77	221	4
-1% fines	255	74	221	4
-2,5% fines	246	73	200	4
-5% fines	247	68	198	4

By adding 5% fines to one bag of EN sand (in exchange for the large grading fraction), the G-yield increased by ~10%, from 255 mA to 279 mA. On the contrary, when 5% fines were substituted by the large grading fraction, the G-yield decreased by 3% from 255 mA to 247 mA. Results from Viscometer 6 showed a similar trend. According to quality control measurements of Normensand GmbH /MP 1/, the standard deviation of fines (0-0,16 mm) for EN sand production in Beckum is around 1%. From Figure 5.1.1.1 it can be seen that a fluctuation of ±1% in fines had hardly any influence on rheology. The differences measured for a fluctuation of ±1% are also in the tolerance range of both devices. From these results it can be concluded that fluctuations in the range of ±1% in fines are negligible for the study.

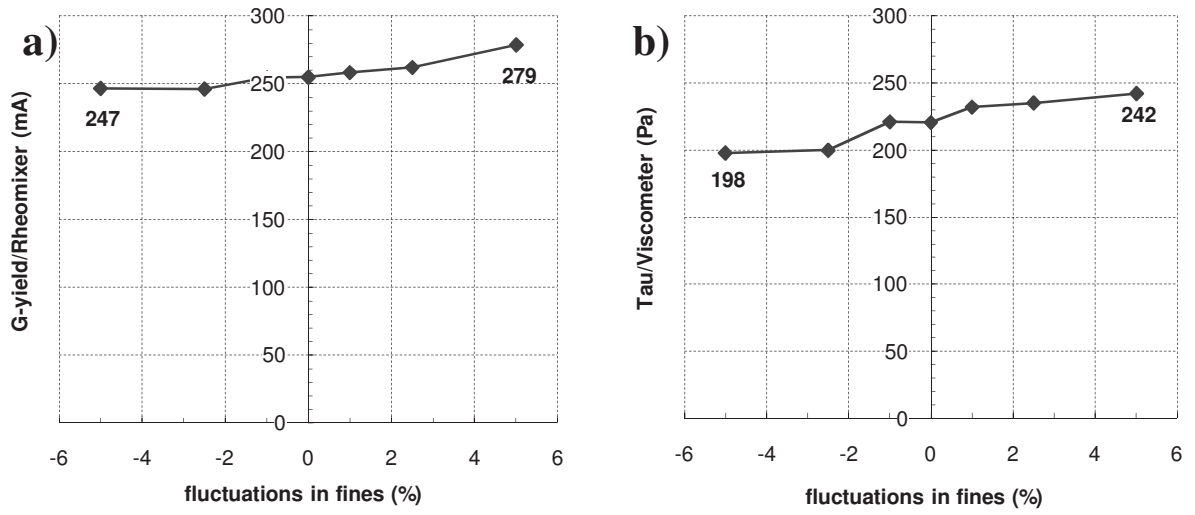

Figure 5.1.1.1: Effect of fluctuations in fines of EN sand on rheology

5.1.2 Effect of aging of cement samples on rheology

Cement samples in this study were normally tested right after arrival at ICI, corresponding to a testing age of ~4 weeks after cement production. Due to time schedule and longer transportation period it sometimes could happen that cement samples were stored in sealed containers for up to 1 month after arrival at ICI until the cement was tested. For that reason the effect of prolonged storage periods on rheological properties of stored cement samples was investigated. A similar study has already been carried out with Norcem /Wa 5/. The effect of cement aging on rheology is shown in Figure 5.1.2.1 for two different production dates. Cement C, the reference cement, was used for this investigation. Figure 5.1.2.1 C#19 shows the effect of testing age on G-yield of cement C#19. Figure 5.1.2.1 C#26 shows the effect of testing age on G-yield of cement C#26. In mixes without admixtures, the G-yield was decreasing with testing age. This was observed for both tested production dates of cement C. The G-yield decreased approximately by 20% during the one year storage period. In the mixes with admixtures (0,11% PC1), the G-yield was less influenced by the testing age. The G-yield of cement C#19 increased slightly, whereas the G-yield of cement C#26 decreased slightly. The variations in G-yield due to testing age were around 10% compared to the initial values. These relatively small variations due to testing are most likely not visible in concrete mixes. Research at ICI Rheocenter indicates that the fluctuations observed in mortar mixes are reduced by about half in concrete mixes due to the lower volume of cementitious materials in concrete /Wa 4/.

Table 5.1.2.1: Effect of testing age on rheology of cement C#19 (15.11.2006) and C#26 (01.12.2006)

Cement sample	Mix design	Testing age (days)	G-yield (mA)	H-viscosity (mA s)	Yield stress (Pa)	Plastic viscosity (Pa s)
C#19 from 15.11.06	Without admixtures	49	345	96	304	5,4
		247	327	91	292	5,9
		395	288	87	260	5,1
	With 0,11% PC1	49	233	183	226	7,1
		247	221	197	208	6,8
		395	250	185	211	7,4
C#26 from 01.12.06	Without admixtures	34	442	98	433	6,8
		231	425	92	397	7,2
		379	378	77	367	5,3
	With 0,11% PC1	34	315	197	322	7,8
		231	292	185	309	6,5
		379	282	162	300	6,6

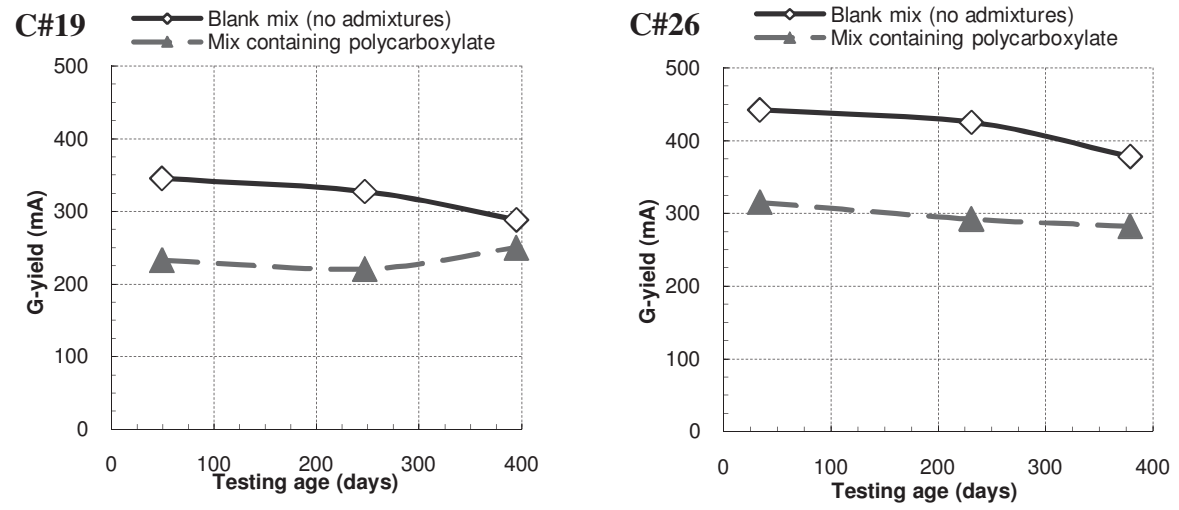

Figure 5.1.2.1: Effect of aging of cement on G-yield

Figure 5.1.2.2 depicts the effect of testing age on H-viscosity. It can be seen that the H-viscosity of the cement C#19 was stable over the whole testing period. Cement C#26 showed a slight decrease in H-viscosity over the testing period of one year. A similar tendency was also observed in ConTec Viscometer 6.

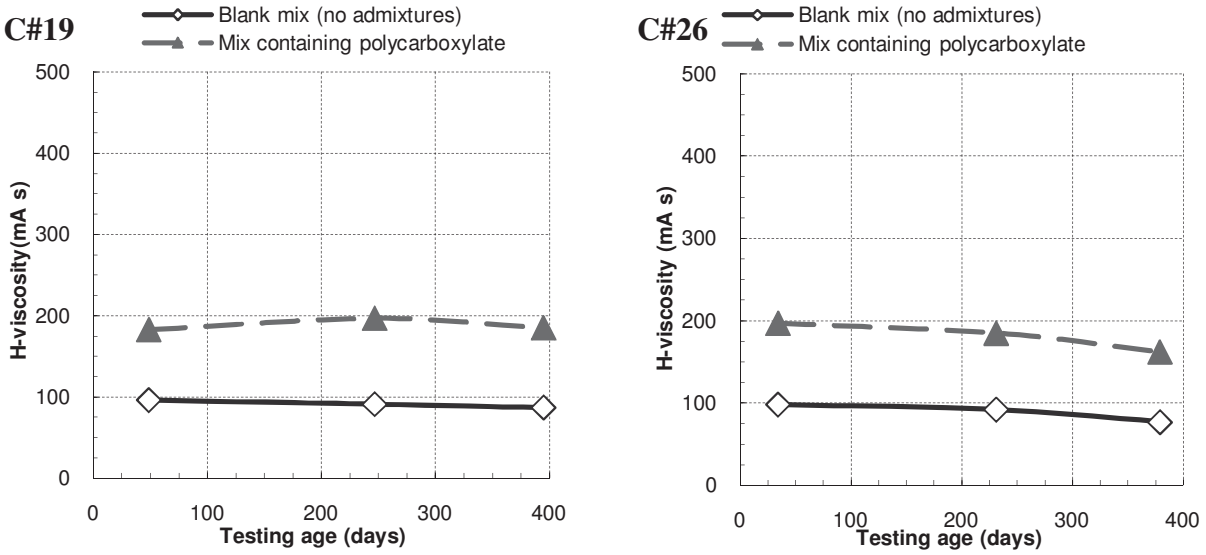

Figure 5.1.2.2: Effect of aging of cement on plastic viscosity

The results obtained here on cement C are partly in line with the results reported in /Wa 5/. However, the variations in G-yield and H-viscosity due to testing age were considerably higher in /Wa 5/. Based on these results the following can be concluded:
A storage period of <200 days has only minor influence on the rheological properties of a cement sample if it is stored properly. Proper storage condition means that the cement bag is put into multi layer plastic bags, and then stored in sealed containers.
A storage period of ~400 days mostly results in a decrease of G-yield and H-viscosity. In mixes without admixtures, the decrease in G-yield can be around 20% compared to the initial values. In mixes with admixtures (0,11% PC1), the change in G-yield is less, only around 10%. These trends were observed in both devices, ConTec Rheomixer and ConTec Viscometer 6.
These changes in rheology with increased storage time are most likely due to some initital hydration on the surface of cement caused by humidity. Thus, the surface properties of the cement particles are changed.

5.1.3 Standard tests versus Rheomixer

In a cement plant, the properties of cement are mainly tested by use of simple standard tests. These tests determine the specific surface according to the Blaine method, the water demand, the start of setting time and the end of setting time. Standard tests were carried out on cement C in order to see if the results from standard tests can be correlated with rheological data obtained by use of ConTec Rheomixer. Note that standard tests are carried out on mixes without admixtures. The fact that admixtures do not have to be incorporated in the tests is one limitation of the standard procedures. The probably most known standard test is the measurement of specific surface according to Blaine method. The standard deviation for the Blaine method can be relatively high, and the results are highly dependent upon the operator. Figure 5.1.3.1 a) depicts the relation between the specific surface according to Blaine and the G-yield in blank mixes. The first 14 deliveries of cement C gave a relatively clear picture. With an increase in specific surface the G-yield increased. However, the latest tested cements did not fit to this data. In the mixes containing polycarboxylate and melamine, no relation between G-yield and specific surface was found.

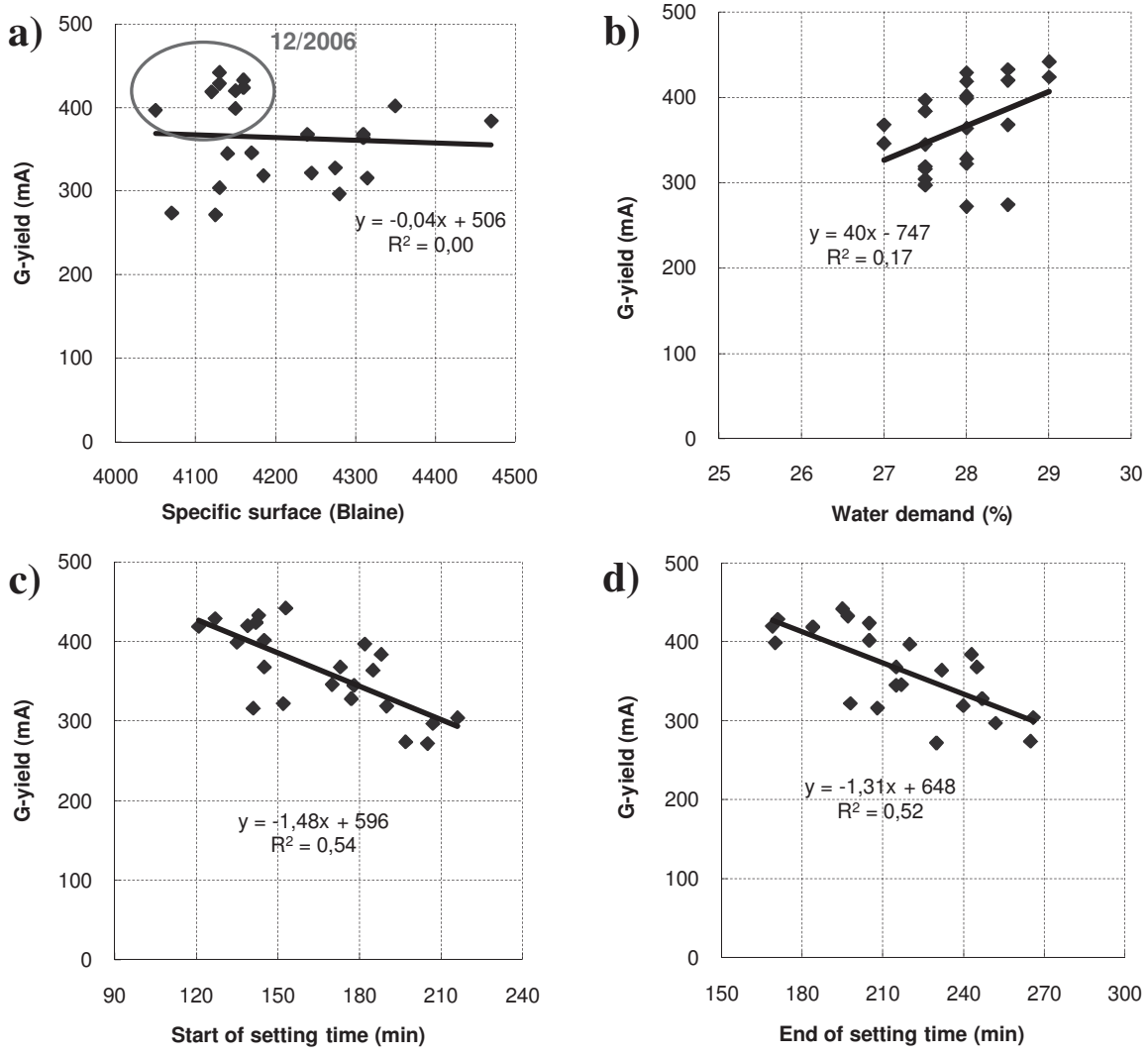

Figure 5.1.3.1: Correlation between standard test results and rheological data (G-yield) in blank mixes

The specific surface was also measured by use of laser diffraction. The correlation between surface measurements according to Blaine method and surface measurements by use of laser diffraction was very good.

Another parameter obtained by use of standard tests is the water demand. This parameter tells how much water (in weight %) is necessary to reach the norm consistency of a cement paste. Figure 5.1.3.1 b) depicts the relation between G-yield and water demand of cement C in blank mixes (no admixtures). Half of the data points show a good correlation between the measured water demand and the G-yield. Some outlying data points caused the relatively low correlation. Even so, the results indicate a relation between water demand and G-yield. An explanation for the outlying data points might be the low fluctuation of water demand within the test series. The water demand of cement C was ranging from 27% to 29% for a production period of nearly three years. However, a small inaccuracy (during preparation of pastes) resulting in a failure of ±0,5% in water demand has a big influence on such a data set. Or in other words, the lower the variation in water demand during routine cement production, the higher is the influence of a measuring failure on the data set.
Figure 5.1.3.1 c) depicts the relation between start of setting time and G-yield in mixes without admixtures. Cements which started to set early, at around ~120 minutes, showed a high initial G-yield (~400 mA equivalent to ~370 Pa). Cements which started to set relatively late, at around ~210 minutes, showed a low initial G-yield (~300 mA equivalent to 270 Pa). The G-yield of mixes without admixtures correlated also with the end of setting time (see Figure 5.1.3.1 d). Both trends are most likely affected by the reactivity of the aluminate phase and the calcium sulphate carrier composition. The first structural build up in the paste volume is due to the hydration of the aluminate phase. Hence, the higher the reactivity of the aluminate phase and the more fast dissolving sulphates are available in the aqueous phase, the more water is consumed for ettringite, the primary hydration product.

5.1.4 Isothermal calorimeter versus semi-adiabatic calorimeter

Both devices were briefly introduced in chapter 3.3.5 and 3.3.6. Most hydration curves displayed in this report were obtained with the isothermal calorimeter. To compare both devices several tests were carried out. The tests were done with mortar from same mix. After rheological tests in ConTec Rheomixer and ConTec Viscometer (26 minutes after water addition), one sample was placed in the isothermal and one sample was placed in the semi-adiabatic calorimeter. The sample size is between 50-100 g of mortar in the isothermal calorimeter, and around 300-500 g in the semi-adiabatic calorimeter /Gr 1/.

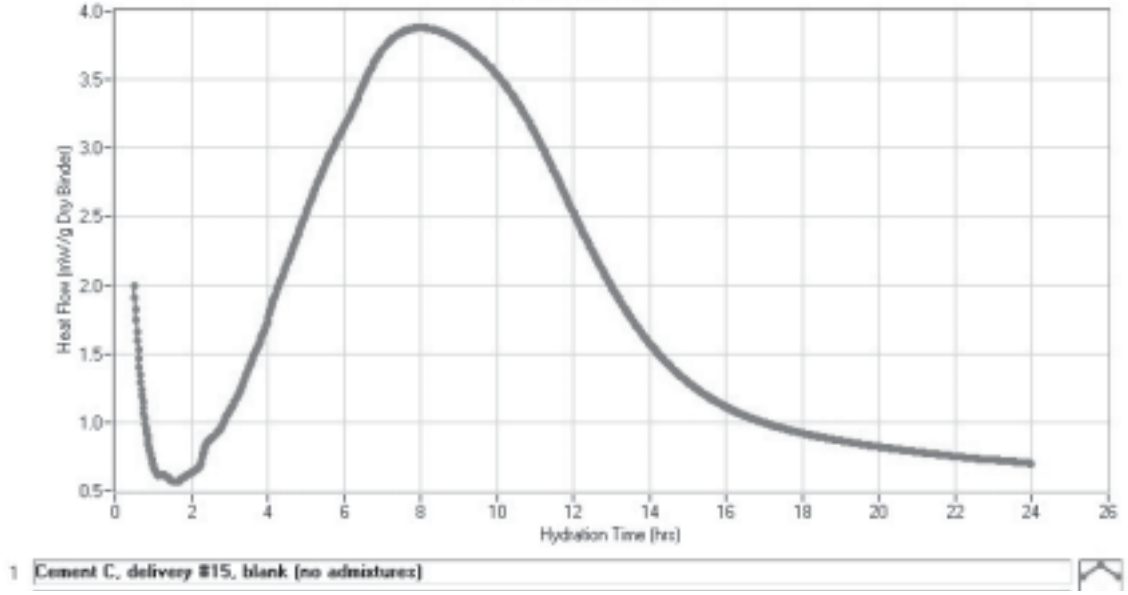

Figure 5.1.4.1: Hydration curve under isothermal conditions

The maximum of the second peak was reached slightly earlier under semi-adiabatic conditions (see Figure 5.1.4.2). The first peak cannot be detected in the semi-adiabatic calorimeter. This is natural, as the released energy is just heating up the sample. Under isothermal conditions, the released energy leaves the measuring cell much quicker. According to these results, a **ΔT** of ~2 K on the semi-adiabatic scale indicates the end of the dormant period and start of the acceleration phase.

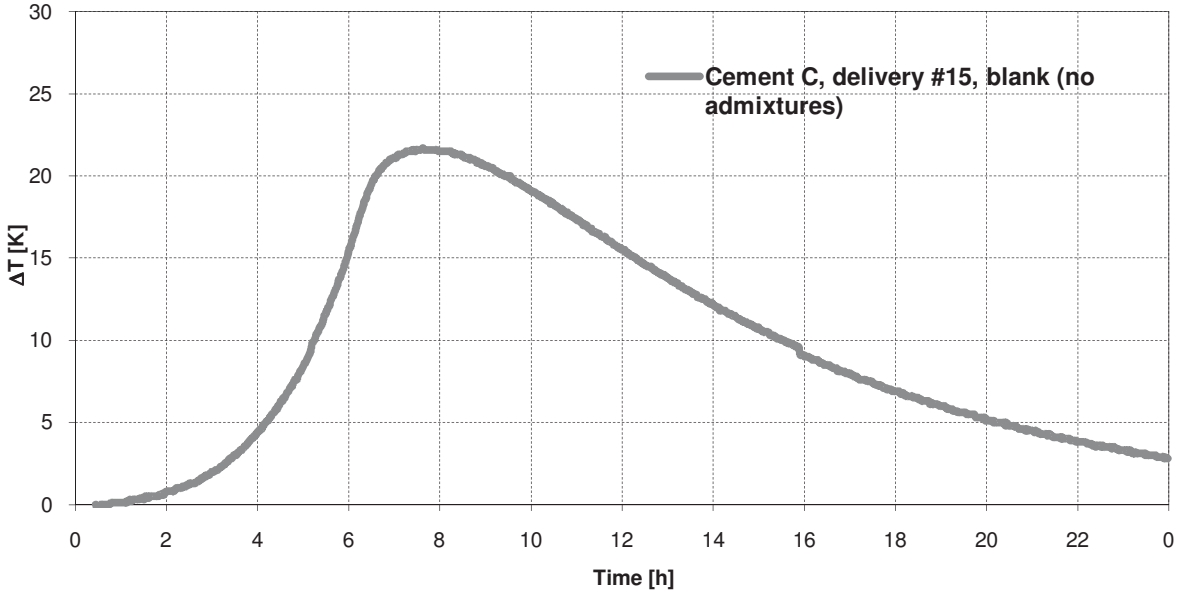

Figure 5.1.4.2: Hydration curve under semi-adiabatic conditions

5.1.5 Determination of reference system

The influence of cement production date on rheological properties was investigated on three mortar mixtures: (1) the "blank mix" without admixture, (2) the "PC mix" containing various kinds of polycarboxylate as dispersing admixture and (3) the "Mel mix" containing one kind of sulfonated melamine condensate as dispersing admixture.

The requirements for the blank mix were:
The yield stress should be in the range of 300 ±25 Pa and plastic viscosity around 4 ±2 Pa·s in mortar. These values represent a relatively plastic mix, comparable to a normally vibrated concrete or a concrete without any admixtures. One bag of EN 196 standardized sand (1350 g) should be used for one litre of mortar. Pre-tests with different sand/cement-ratios (not displayed here) showed an optimum for a sand/cement-ratio of around 2. The sand/cement-ratio in the blank mix was 2,16. Sand/cement-ratios in the range of 2,5 to 3,0 gave too coarse and thereby too stiff mixtures. For a sand/cement-ratio of 2,16 the correct water/cement-ratio was found to be 0,46. Figures 5.1.5.1 and 5.1.5.2 illustrate the effect of different water/cement ratios on rheological properties in blank mix.

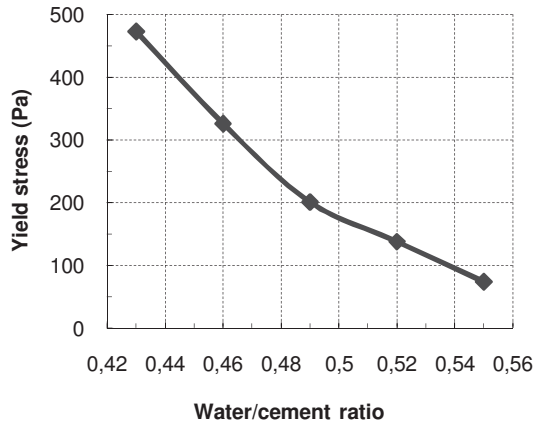

Figure 5.1.5.1: Effect of water/cement ratio on yield stress in blank mix

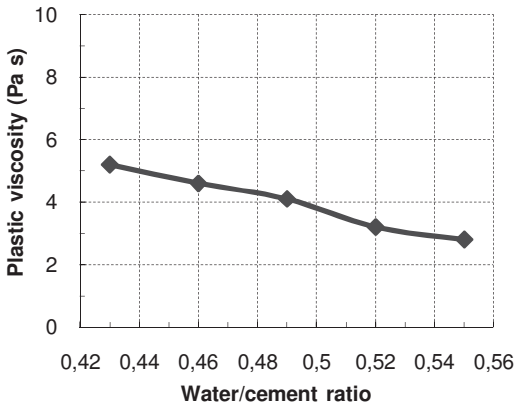

Figure 5.1.5.2: Effect of water/cement ratio on plastic viscosity in blank mix

The requirements for the polycarboxylate/PC mix were:
The yield stress should be in the range of 150 ±25 Pa and plastic viscosity around 6 ±2 Pa·s in mortar. These values represent a relatively fluid but viscous mix, comparable to a concrete with self compacting properties. One bag of EN 196 standardized sand (1350 g) should be used for one litre of mortar. The sand/cement-ratio of the PC mix should be kept as close as possible to the sand/cement-ratio of the blank mix. In the PC mix the sand/cement-ratio was 1,88. The water/cement-ratio of the PC mix was set to 0,36 which is in the range of High Performance Concrete (HPC) and Self Compacting Concrete (SCC). Another reason for this low water/cement-ratio was the admixture used, which is based on modified polycarboxylate ether. Due to their good performance, polycarboxylates are usually used for water/cement-ratios below 0,40. At a water/cement-ratio of 0,36, the optimum dosage of PC1 was found to be 0,11% by weight of cement (dry content of polymer). At a dosage of 0,05% PC1, the yield stress and plastic viscosity was far too high and at a dosage of >0,15%, the mixes started to segregate. Figures 5.1.5.3 and 5.1.5.4 depict the effect of dosage of PC1 on rheological properties. PC1 showed a good workability retention during first half hour after water addition. Thereafter, fluidity was lost quickly. Additional tests were carried out with three

more polycarboxylates. The otimum dosage for PC2 was 0,29%, for PC3 it was 0,22% and for PC4 it was 0,16%.

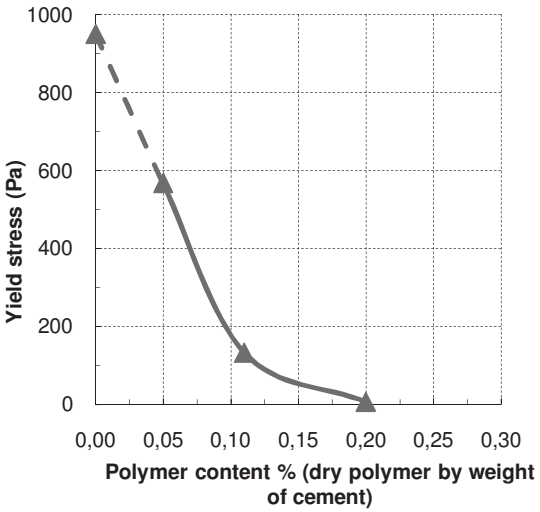

Figure 5.1.5.3: Effect of dosage of PC1 on yield stress in PC mix

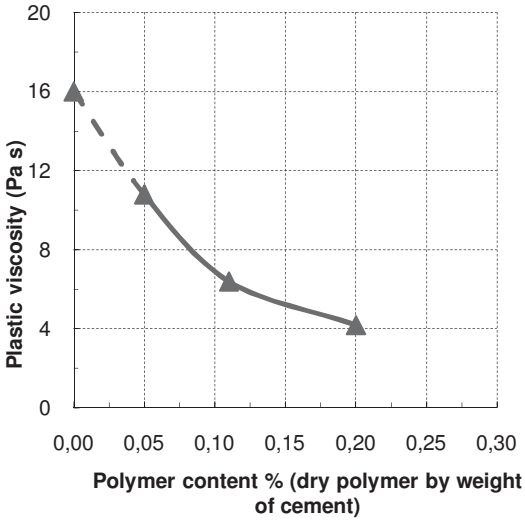

Figure 5.1.5.3: Effect of dosage of PC1 on plastic viscosity in PC mix

The requirements for the melamine/Mel mix were:
Yield stress should be in the range of 225 ±25 Pa and plastic viscosity around 4 ±2 Pa·s in mortar. This mix represents a relatively fluid mix, comparable to a flowable concrete with a low viscosity (such as concretes in the consistency class F5 to F6 according to EN 206). One bag of EN 196 standardized sand (1350 g) should be used for one litre of mortar. The sand/cement-ratio of the Mel mix should be kept as close as possible to the sand/cement-ratio of the blank mix. In the Mel mix the sand/cement-ratio was 1,97. The water/cement-ratio of the Mel mix was chosen with 0,40 which is also in the range of High Performance Concrete (HPC) and SCC. At a water/cement-ratio of 0,40, the optimum dosage of sulfonated melamine was found to be 0,60% by weight of cement (dry content of polymer). Lower dosages (<0,50%) gave too high yield stress and plastic viscosity and higher dosages (>0,80%) resulted in segregating mixes. The melamine used showed a good workability retention during 15-20 minutes after water addition. Thereafter, mixes stiffened very quickly.

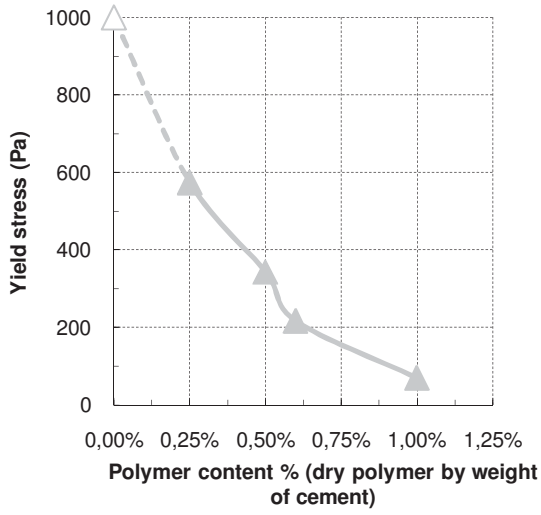

Figure 5.1.5.5: Effect of admixture dosage on yield stress in Mel mix

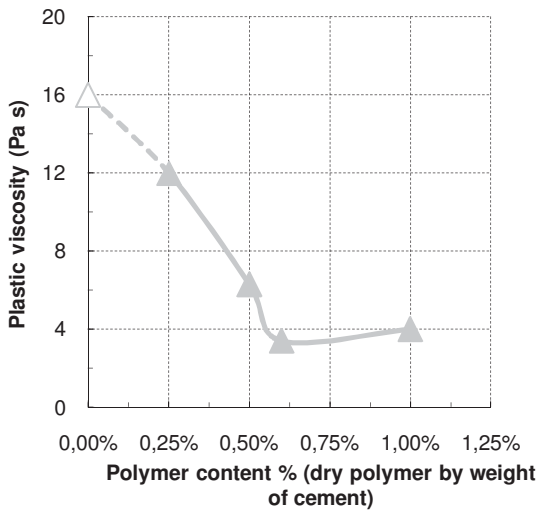

Figure 5.1.5.6: Effect of admixture dosage on plastic viscosity in Mel mix

5.1.6 Flow curves obtained by use of Rheomixer and Viscometer 6

The mortar was mixed and measured in the Rheomixer and thereafter measured again in the Viscometer 6. Both devices are described in chapters 3.3.1 to 3.3.3. Measurements differ in two things. First, the measurement geometry from Rheomixer is rather different from Viscometer 6 (impeller based system versus co-axial cylinder system). Second, the testing age of the mortar is not identical because the measurement in the viscometer was done 6 minutes after the measurement in Rheomixer. However, the results indicate an excellent correlation between both devices. Figure 5.1.6.1 a) depicts the flow curve of a one litre mortar mix without dispersing admixture measured in the ConTec Rheomixer and Figure 5.1.6.1 b) depicts the same mix measured in ConTec Viscometer 6. The shear rate and duration of the test is about the same in both devices. Each measurement takes less than a minute. Both devices, regardless of their different measuring geometries, show a Bingham-fluid like behaviour for mortar. According to the Bingham model, the matter behaves like Newtonian fluid (linear relation between rate of shear and shear stress) when it flows and is rigid when the shear stress is less than τ_0. Figures 5.1.6.1 a) and 5.1.6.1 c) depict the raw data from Rheomixer. Rheomixer measures the torque at 6 speed steps, whereas Viscometer 6 measures the torque at 7 speed steps. The raw data of Rheomixer consists of 16 data points for each speed step. Rheomixer's control box collects 4 data points per second for a duration of 4 seconds and calculates the median of these 16 data points. This median is the characteristic value for each speed step. The line connecting the data points intercepts the y-axis at a certain value. This value is the so-called G-yield, corresponding to yield stress in ConTec Viscometer 6. The slope of the line is the so-called H-viscosity, corresponding to plastic viscosity in ConTec Viscometer 6.

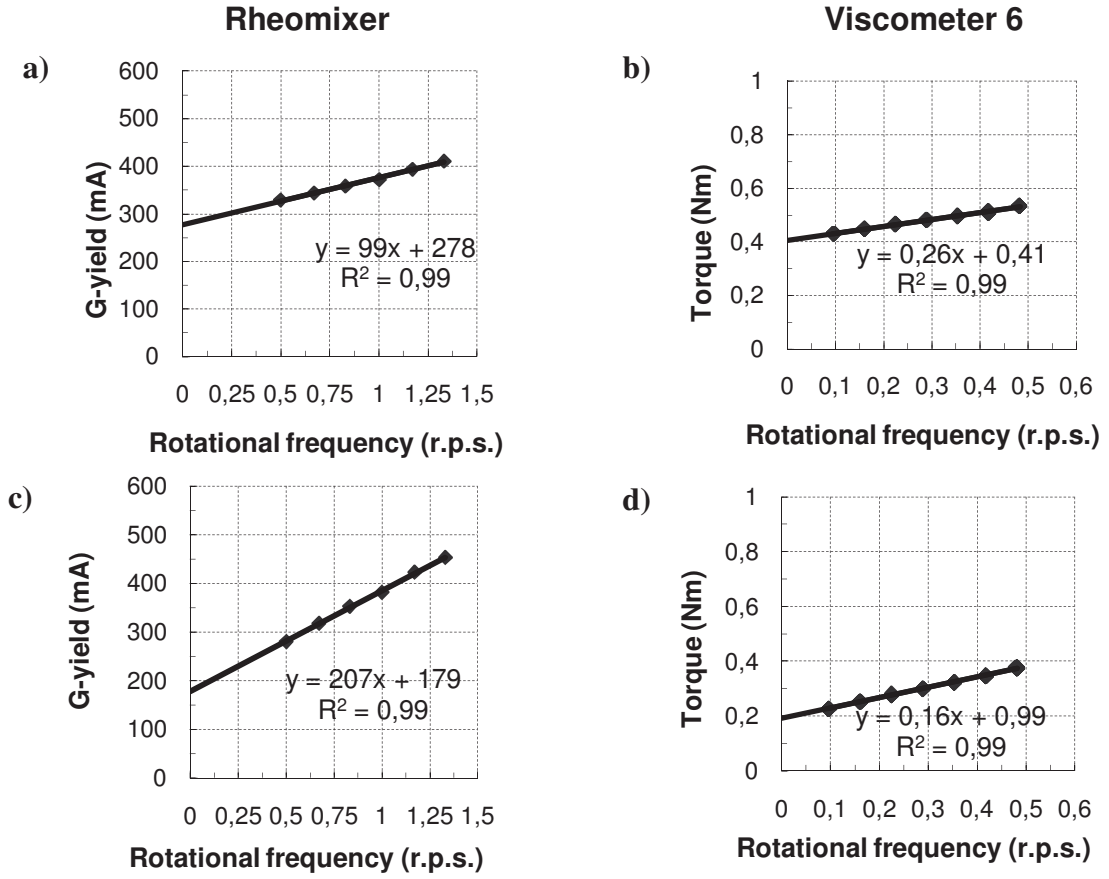

Figure 5.1.6.1: Flow curves of mortar with and without dispersing admixture (Rheomixer and Viscometer 6)

Figure 5.1.6.1 c) depicts the flow curve of a one litre mortar mix with dispersing admixture measured in the ConTec Rheomixer. Figure 5.1.6.1 d) depicts the flow curve of same mix measured in ConTec Viscometer 6. It can be seen that the incline of the mix with a dispersing admixture is higher than the incline of the blank mix. The mortar with a dispersing admixture contains less water than the blank mix. Thereby, the relative particle distance (which affects the particle friction) is larger in the mix without the dispersing admixture, leading to a lower resistance/viscosity within the fluid.

5.1.7 Performance and characteristics of admixtures used

The admixtures used within this study differ greatly in performance and initial dispersing effect. The melamine based admixture and the polycarboxylate based PC1 disperse the cement grains well for 20-30 minutes. Thereafter, mixes lost their flowability. PC2, PC3 and PC4 disperse the cement grains for a longer time. Depending upon polymer dosage the workability with PC2, PC3 and PC4 was sufficient for 60 to 90 minutes. Figure 5.1.7.1 depicts the effect of polymer dosage on yield stress and plastic viscosity in mortar. Mixes containing polycarboxylate (PC1, PC2, PC3 and PC4) had the same mix design (w/c-ratio 0,36). Mixes containing melamine had a slightly higher w/c-ratio (w/c-ratio 0,40). The rheological data displayed in the figures below is the mean of the 18 and 22 minute measurement. Within the polycarboxylates, PC1 showed the greatest initial dispersing effect. The second most effective polymer was PC4, followed by PC3, PC2 and melamine. The high effectiveness of PC1 can be explained by its quick and aggressive adsorption behaviour. The high number of charges incorporated in the backbone (see table 5.1.7.1) of PC1 leads to a much quicker adsorption on the cement surface than with PC2, PC3 and PC4 or melamine polymers. However, PC1´s high initial degree of adsorption (70-90% depending upon cement type) in the first minutes leaves only few polymers as a reservoir for a dispersion at later ages. If the adsorbed polymers are incorporated or overgrown by hydration products the mix loses its flowability as can be seen in Figure 5.1.7.2 a). On the contrary, PC2, PC3 and PC4 have a lower degree of adsorption (10-70% depending upon cement type), leaving a bigger reservoir of non adsorbed polymers in solution. These reservoir polymers provide a good flowability at later ages.

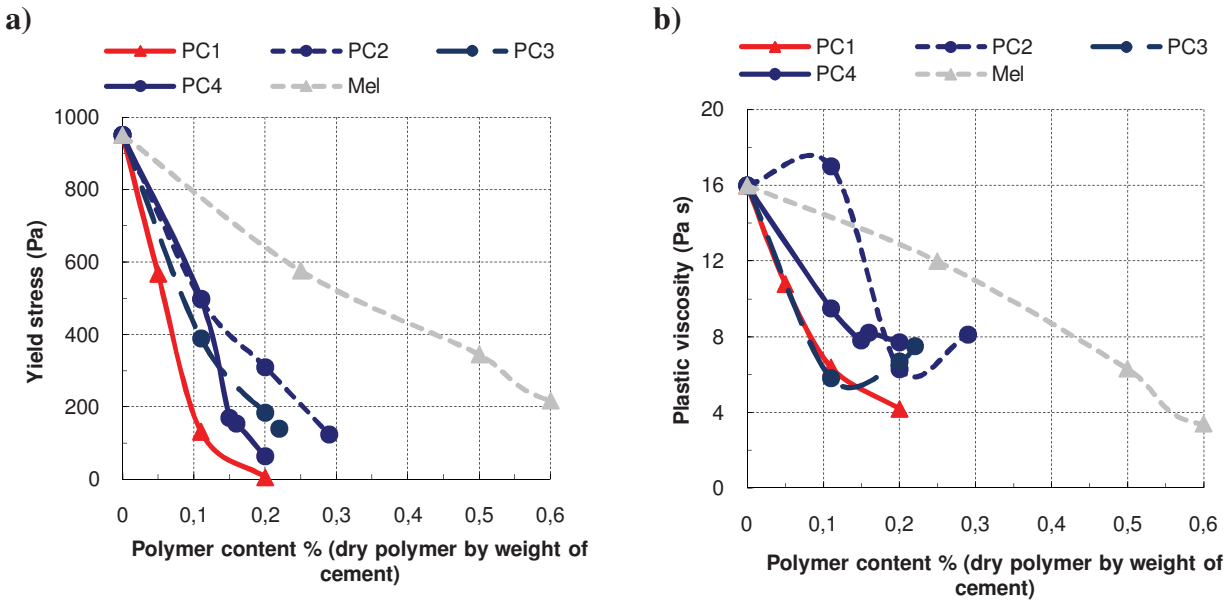

Figure 5.1.7.1: Initial dispersion, 20 minutes after water/SP-addition

Beyond the differences in performance, the polymers showed clear differences during the initial dispersion phase. The majority of polymers, such as PC1, PC3 and Mel showed a workability loss with testing age, meaning the yield stress and plastic viscosity increased with time from first measurement on (see Figure 5.1.7.2 a) and b)). As can be seen on the grey dotted line in Figure 5.1.7.2 a), the melamine based admixture had the highest workability loss. The opposite was observed with PC2 and PC4. These polymers show a contiuous reduction of yield stress in the first 15 minutes after water addition. From the 7 minute measurement to 15 minute measurement, the yield stress in mixes with PC2 and PC4 decreased by ~20 to 70% depending upon cement delivery. Thereafter, the yield stress of mixes containing PC2 and PC4 remained unchanged for some time or increased only slightly. This additional dispersing effect is since >50% of the polymers in PC2 and PC4 are slump retainers combined with high effective water reducers. The water reducers (similar to PC1 polymers) adsorb quickly on the cement surface whereas the slump retainers stay non adsorbed in solution and are available for dispersion at later ages. In contrast, PC3 contains only slump retaining polymers with a relatively high charge in the backbone but no additional water reducers. Hydration curves of mixes with PC1 to PC4 are given in Appendix M.

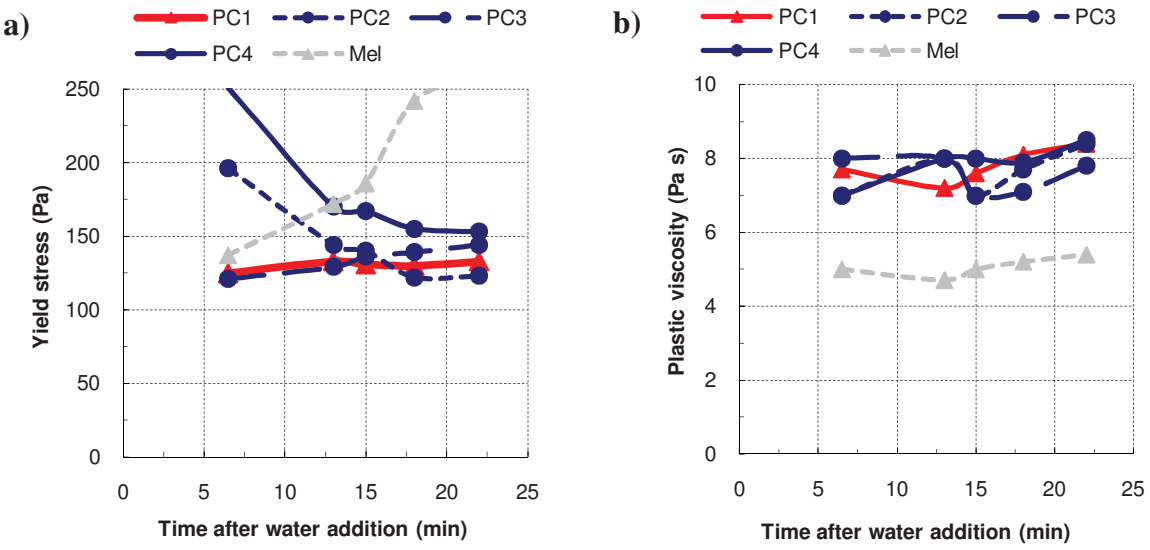

Figure 5.1.7.2: Yield stress and plastic viscosity as a function of time for the admixtures used

Table 5.1.7.1: Characteristics of admixtures used

Designation	Mel	PC1	PC2	PC3	PC4
Based on	Sulfonated melamine polymer	Modified polycarboxylate ether	Polycarboxylate ether	Polycarboxylate ether	Polycarboxylate ether
Density	1,21 kg/dm³	1,10 kg/dm³	1,07 kg/dm³	1,05 kg/dm³	1,05 kg/dm³
Polymer content	39,5%	36,9%	30,2%	23,5%	20,3%
Recommended dosage (dry polymer)	0,15 – 0,8%	0,1 – 0,7%	0,1 – 0,9%	0,1 – 0,7%	0,1 – 0,6%
Charge/100 C-atoms	16	40	27	26	35
Number of side chains	-	10	18	19	16
Length of side chains	-	100% short	93% medium-long 7% very long	100% medium-long	18% short 82% medium-long
Charge equivalent (mmol/g polymer)	3	2,22	0,85	1,5	1,0

5.1.8 Mortar mini slump versus mortar rheology

The rheology of mortar can also be determined by use of a mini slump test. The mini slump test is an empirical test method which leaves the operator with a unit less number describing the flow properties of mortar or concrete. On the contrary, measurements by use of a viscometer give real physical values which enable the operator to quantify the flow properties of mortar or concrete. The method consists of a cone which is filled with fresh mortar and lifted. The flow diameter of the mortar cake is the characteristic slump flow value. Mixes differing in admixture dosage were tested in a viscometer and by use of the mini slump flow. As a rule of thumb one can say that the mini slump flow can be correlated with the yield value while the flow time necessary to reach a certain mini slump flow can be correlated with the viscosity. The paste volume of all mixes reported here was identical. The water to cement ratio of the mixes displayed below was 0,40 and the admixture used was not as effective as PC1. With an increase in admixture dosage, the mini slump flow increased (see Figure 5.1.8.1 and Figure 5.1.8.4). Results indicate a somewhat linear relationship between the mini slump flow and the admixture dosage. The relationship between yield value and mini slump flow is displayed in Figure 5.1.8.2. However, the curve displayed in Figure 5.1.8.2 is only valid for the mortar tested here. This curve might change with the paste volume of mortar. Note that mortar with the highest mini slump flow was on the limit of segregation. Rheological results point towards a saturation level for the admixture which is around 0,4%. Above the saturation level, the decrease in yield value is only minor while the mix started to segregate. When the admixture dosage increased the plastic viscosity of the mixes decreased significantly (results not reported here).

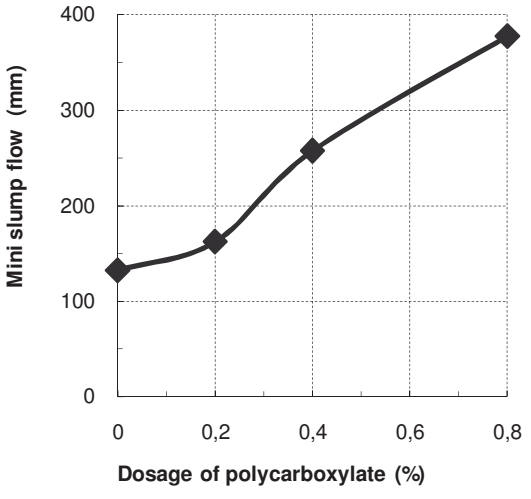

Figure 5.1.8.1: Effect of admixture dosage on mini slump flow

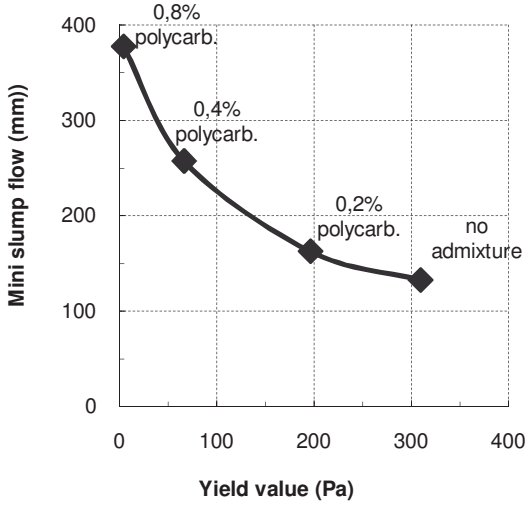

Figure 5.1.8.2: Relation between mini slump flow and yield value

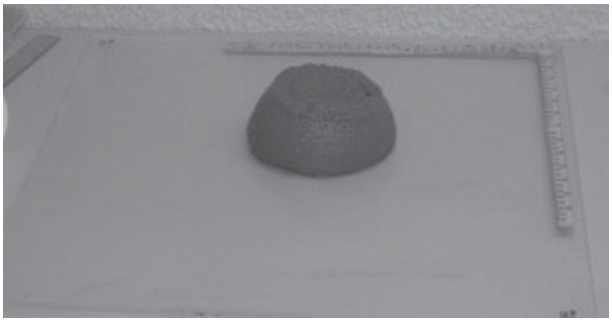

Figure 5.1.8.3: No admixture, mini slump flow 140 mm

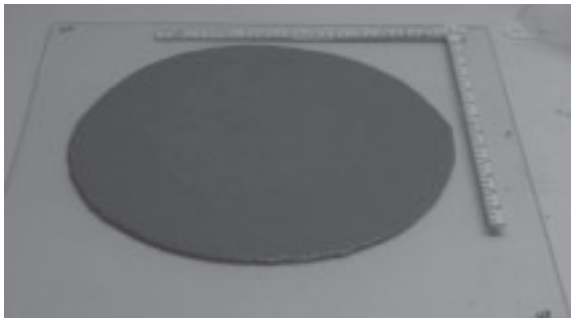

Figure 5.1.8.4: 0,8% polycarboxylate, mini slump flow 380 mm

5.2 Main objective

5.2.1 Cement production date

5.2.1.1 Effect of cement production date on rheology of mortar

While testing the rheology of mortar the following trends were observed: (1) the G-yield value was relatively stable in the mixes without a dispersing admixture, (2) whereas the G-yield value varied clearly in the mixes with a dispersing admixture, e.g. PC1 and melamine (broken and dotted line in Figure 5.2.1.1.2). Using a new cement delivery could change the G-yield by the factor 2 to 3. The fluctuations in G-yield were higher in these mixes when a dispersing admixture was present. This can be seen by comparing the coefficient of variation (c.o.v.) of the blank mixes with the c.o.v. of the mixes containing PC1 and melamine (see table 5.2.1.1.1). The c.o.v. of the blank mixes was clearly less than the c.o.v. of the PC1 and melamine mixes (see also Figure 5.2.1.1.1). This trend can be stated for all tested cements. The results obtained here are also relevant for producers of admixtures. Based on these results one could conclude that the polycarboxylate used provides a more stable production in terms of rheology (e.g. in a ready mix or pre cast plant) than the melamine based product. Rheological tests were done on the same mix in Rheomixer and Viscometer 6. The trend was observed in both devices.

Table 5.2.1.1.1: Statistical parameters of rheological results of cements used

Name	Cement type	Mix design	Number of samples	Mean G-yield (mA)	Std. dev. (mA)	G-yield c.o.v. (%)	Mean H-viscosity (mA·s)	Std. dev. (mA·s)	H-viscosity c.o.v. (%)
Cement A1	CEM I 42,5	blank	3	313	14	5	134	10	8
		polycarb. (PC1)	3	149	104	70	241	12	5
		melamine	3	130	161	124	157	22	14
Cement A2	CEM II/ B-S 32,5R	blank	3	333	39	12	138	5	4
		polycarb. (PC1)	3	206	91	44	244	15	6
		melamine	3	244	234	96	148	5	3
Cement B2	CEM I 42,5R	blank	5	404	10	3	106	21	19
		polycarb. (PC1)	5	465	87	19	203	40	20
		melamine	5	181	33	19	113	16	14
Cement C	CEM I 52,5N	blank	29	351	58	16	98	15	16
		polycarb. (PC1)	29	216	58	27	185	15	8
		melamine	29	263	108	41	114	20	17

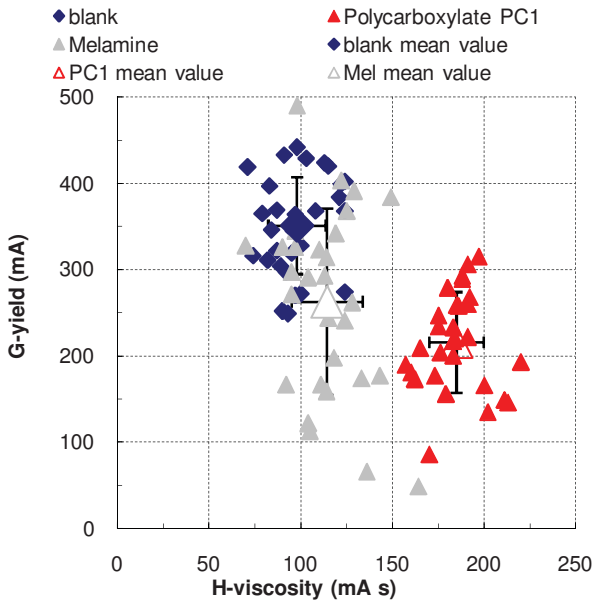

Figure 5.2.1.1.1: G-yield vs. H-viscosity for cement C (n=29)

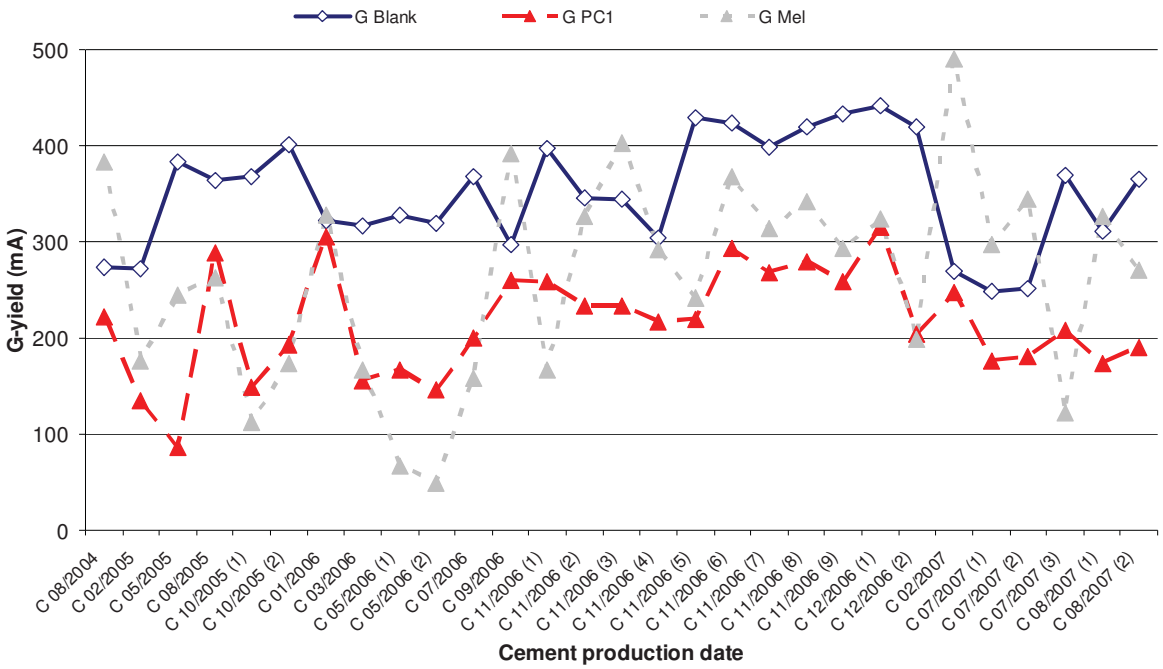

Figure 5.2.1.1.2: Effect of cement delivery/production date of cement C on G-yield (mA)

Figure 5.2.1.1.2 depicts the G-yield (mA) of 29 production dates of cement C. The fluctuations in rheology due to production date are significant. The reader should know that the effect of production date on rheology is relatively small in cement C compared to other cements. If a new cement delivery of cement C is used, the maximum variation in yield stress could be around 200 mA/180 Pa in mortar. With other cements, the maximum variation in yield stress could be around 500 mA/450 Pa in mortar. Again, it is not a must but it can happen. In other words, the cement factory producing cement C produces a relatively stable product with respect to rheology. Figure 5.2.1.1.3 is showing the H-viscosity (mA s) of cement C for the same production dates. It can be seen that the fluctuations in H-viscosity due to production date are insignificant compared to those in G-yield.

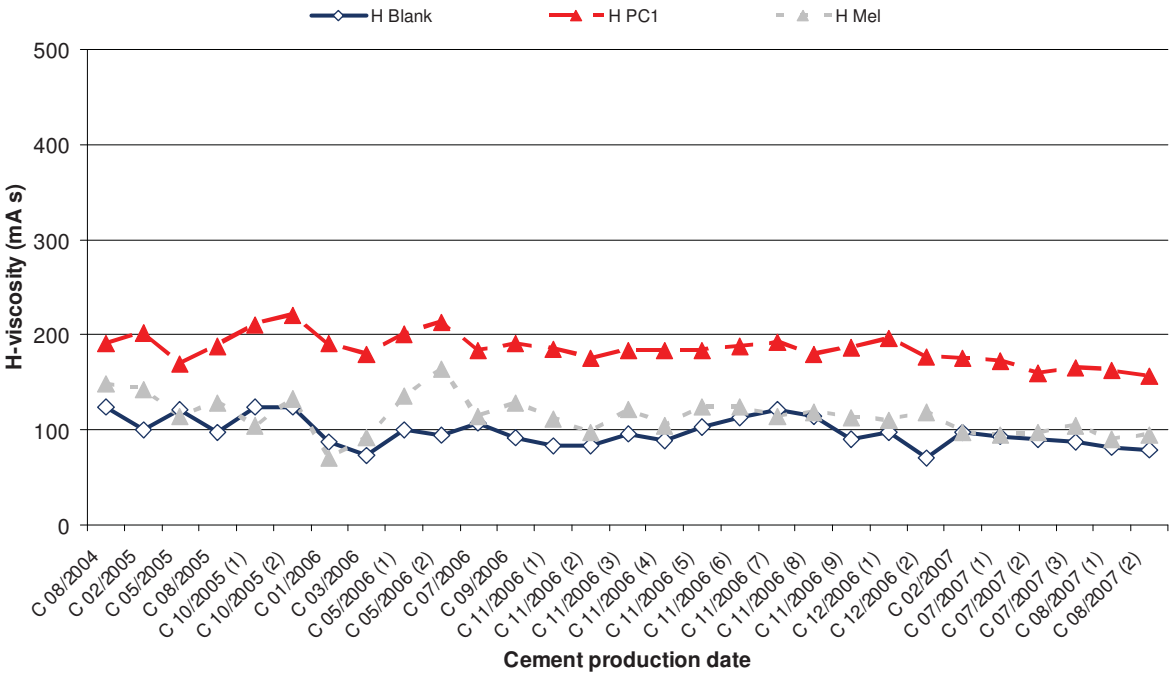

Figure 5.2.1.1.3: Effect of cement delivery/production date of cement C on H-viscosity (mA s)

Definition of low yield and high yield cement

Some cement deliveries showed significantly higher, others significantly lower yield stress than the majority of samples tested. In a series of cement deliveries (production dates) those which generate a yield stress below the mean minus one standard deviation of that series are named low yield cement deliveries. Analogously, those which generate a yield stress above the mean plus one standard deviation of that series are named high yield cement deliveries. If a concrete is produced with these cements, the utilization of low yield cement results in a relatively fluid concrete, whereas the utilization of high yield cement can result in a sticky mix with relatively fast workability loss /Ku 3/.

Figure 5.2.1.1.4 depicts the G-yield of the mixes containing polycarboxylate (PC1) and the limits for one standard deviation above and below the mean value within the test series. High yield cement deliveries (see also Figure 5.2.1.1.5) can be found above the upper broken red line. Low yield cement deliveries (see also Figure 5.2.1.1.6) can be found below the lower broken red line. Each cement delivery was tested three times in mortar. The repeatability was good (see chapter 5.2.1.3). A somewhat similar graph could be drawn for mixes containing melamine. However, the standard deviation of melamine mixes was by a factor of ~2 higher than that of polycarboxylate mixes. Another finding was that cement showing a high yield stress (respectively low yield stress) in the polycarboxylate mix did not necessarily show a high yield stress (respectively low yield stress) in the melamine mix. Sometimes, the contrary was observed.

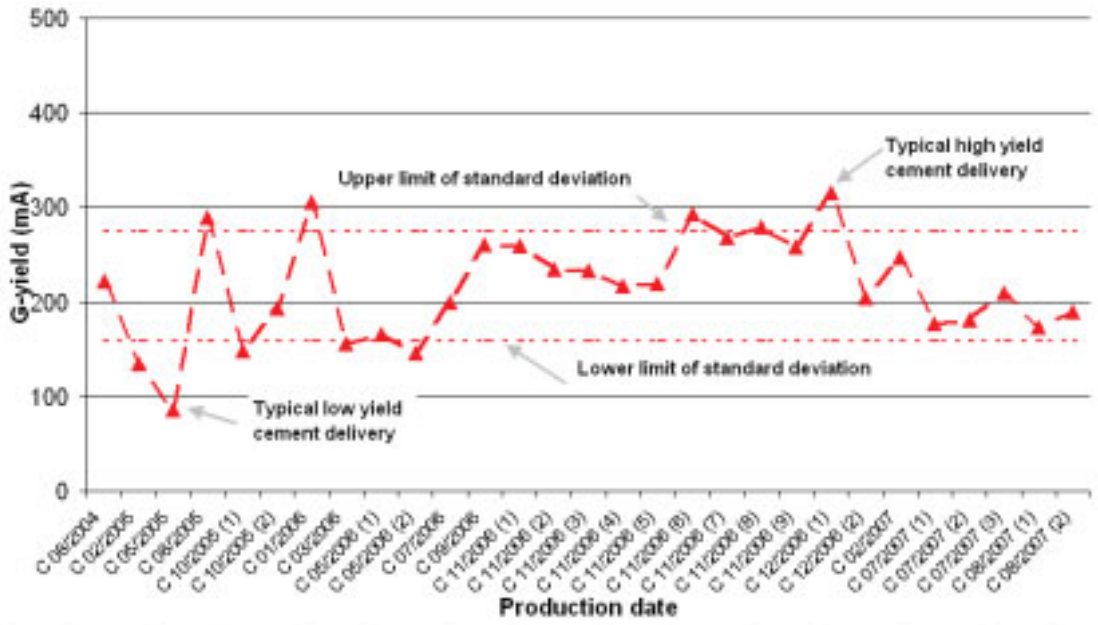

Figure 5.2.1.1.4: G-yield of mortar containing polycarboxylate, its standard deviation and remarkable cements

Figure 5.2.1.1.5: Mini slump of mortar produced with high yield cement

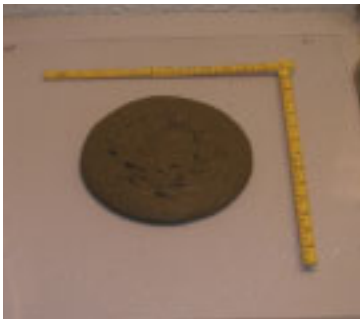

Figure 5.2.1.1.6: Mini slump of mortar produced with intermediate cement

Figure 5.2.1.1.7: Mini slump of mortar produced with low yield cement

5.2.1.2 The interval between sampling and its effect on rheology

During the project we had the opportunity to test 11 cement samples of cement C representing a 2 month production period. The comparison of the statistical parameters of the 2 month production period with the statistical parameters of the 2 year production period was quite interesting. Figure 5.2.1.2.1 is showing the effect of production date of cement on G-yield in mortar. The graph distinguishes between production period as well as type of packing (sub issue). It can be seen that the longer the interval between sampling, the higher the possible variation in G-yield. The 2 year production period showed a much higher variation in G-yield (in blank and PC mix) than the 2 month production period. This can also be seen by comparing the c.o.v. of the 2 year production period with the c.o.v. of the 2 month production period. In mixes with dispersing admixture, the 2 month production period showed less variations than the 2 year production period (see table 5.2.1.2.1). The great variations in rheology that occur when the sampling interval is increased could be explained by changes in raw material composition or different fuel types used during the burning process

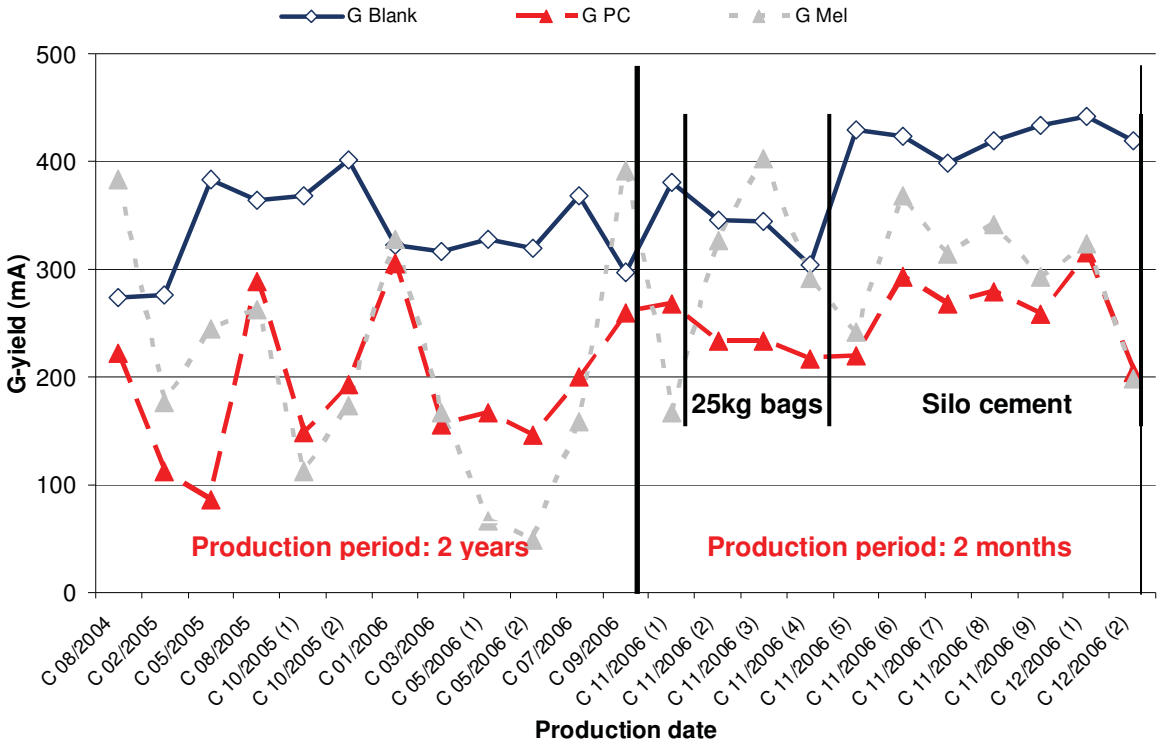

Figure 5.2.1.2.1: Effect of cement delivery/production date of cement C on G-yield (mA) and some additional information

Table 5.2.1.2.1: Statistical parameters of rheological results with regards to production period

	Cement type	Mix design	Number of samples	Mean G-yield (mA)	Standard deviation (mA)	Coefficient of variation (%)
2 year production period	CEM I 52,5N	blank	12	335	42	13
		polycarbox. (PC1)	12	190	68	36
		melamine	12	210	114	55
2 month production period		blank	11	395	45	11
		polycarbox. (PC1)	11	254	35	14
		melamine	11	297	71	24

The cements tested from November 2006 were delivered in 25 kg bags and as silo cement. As can be seen in Figure 5.2.1.2.1 the cement in the 25 kg bags seems to have a slightly lower G-yield in blank and PC mixes than the silo cement. It might be possible that the 25 kg bags and the silo cement were exposed to different storage or transport conditions. At different storage conditions the calcium sulphate carrier can change and later react differently during hydration.

5.2.1.3 Repeatability of results in mortar

The repeatability of results in mortar was determined on five cement samples of cement C. The five cement samples cover the whole territory of yield stress of cement C. The samples S1 and S2 represent low yield cement. Sample S3 represents intermediate cement. The samples S4 and S5 represent high yield cement. Each production date was tested three times in blank mix (no admixtures) and three times in PC mix (PC1). Figure 5.2.1.3.1 depicts the results for yield stress and plastic viscosity obtained by use of ConTec Rheomixer and ConTec Viscometer 6. Table 5.2.1.3.1 shows the results for G-yield of the five cement samples tested. Without admixtures the coefficient of variation (c.o.v.) was in the range of 2 to 6%. The c.o.v. of mixes containing polycarboxylate was higher. Both low yield cements and one of the high yield cements showed a c.o.v. of approximately 15%. This was observed in ConTec Rheomixer and ConTec Viscometer 6. Errors of repeatability can be caused by variation in the mixing procedure, variation in testing temperature and variation caused by test equipment and operator. All mortars were produced in the fully automatic ConTec Rheomixer. Thus, it is unlikely that the mixing procedure and the test equipment caused the errors of repeatability. Possible error sources are differing temperatures of the environment and testing equipment (impeller, cylinder, bucket) and slight differences in addition time of admixtures or a combination of both.

Table 5.2.1.3.1: Statistical parameters of repeatability measurements (G-yield)

	Cement sample	Production date	Mean G-yield (mA)	Standard deviation (mA)	Coefficient of variation (%)	Minimum (mA)	Maximum (mA)
Without admixtures	S2	24.02.2005	272	8	3	263	278
	S1	23.05.2005	384	23	6	360	405
	S4	01.11.2006	397	18	4	381	416
	S5	28.11.2006	399	22	6	374	415
	S3	04.12.2006	419	8	2	412	427
With admixtures (PC1)	S2	24.02.2005	135	20	15	112	149
	S1	23.05.2005	86	11	13	74	96
	S4	01.11.2006	259	9	4	250	268
	S5	28.11.2006	268	44	16	225	312
	S3	04.12.2006	204	12	6	194	217

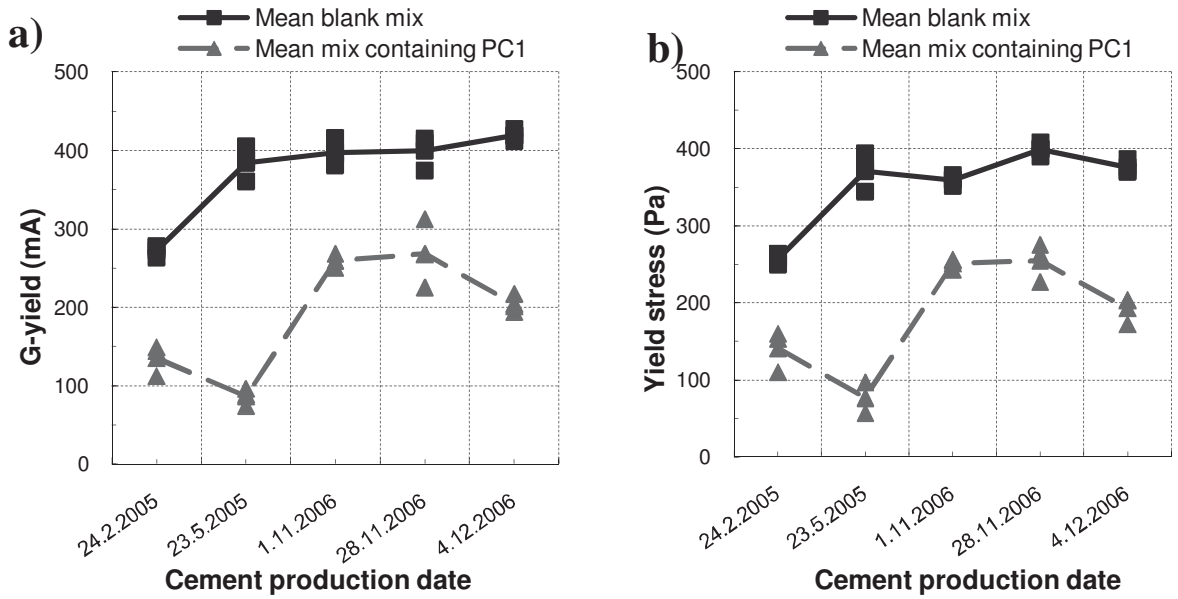

Figure 5.2.1.3.1: G-yield, yield stress and repeatability of different production dates

Table 5.2.1.3.2 shows the results for H-viscosity/plastic viscosity of the five cement samples tested. The plastic viscosity of the mixes containing polycarboxylate was higher than without

admixtures. Mixes without admixtures have a higher water to cement ratio (0,46 in blank versus 0,36 in PC1 mix), thus providing more space between the cement particles and thereby reducing the dynamic friction between them. Without admixtures the coefficient of variation (c.o.v.) was in the range of 2 to 27%. One measurement on sample S5, resulting in a c.o.v. of 27%, can be considered as an outlying data point. In the mixes with polycarboxylate the c.o.v. was in the range of 1 to 8%. The results indicate that the effect of production date on H-viscosity/plastic viscosity is insignificant, compared to the effect of production date on yield stress.

Table 5.2.1.3.2: Statistical parameters of repeatability measurements (plastic viscosity)

	Cement sample	Production date	Mean H-viscosity (mA s)	Standard deviation (mA s)	Coefficient of variation (%)	Minimum (mA s)	Maximum (mA s)
Without admixtures	S2	24.02.2005	100	14	14	84	110
	S1	23.05.2005	121	3	2	119	124
	S4	01.11.2006	83	6	7	77	89
	S5	28.11.2006	122	33	27	101	160
	S3	04.12.2006	71	12	17	57	78
With admixtures (PC1)	S2	24.02.2005	202	15	8	193	220
	S1	23.05.2005	170	2	1	168	172
	S4	01.11.2006	185	4	2	181	188
	S5	28.11.2006	192	6	3	188	199
	S3	04.12.2006	176	2	1	175	178

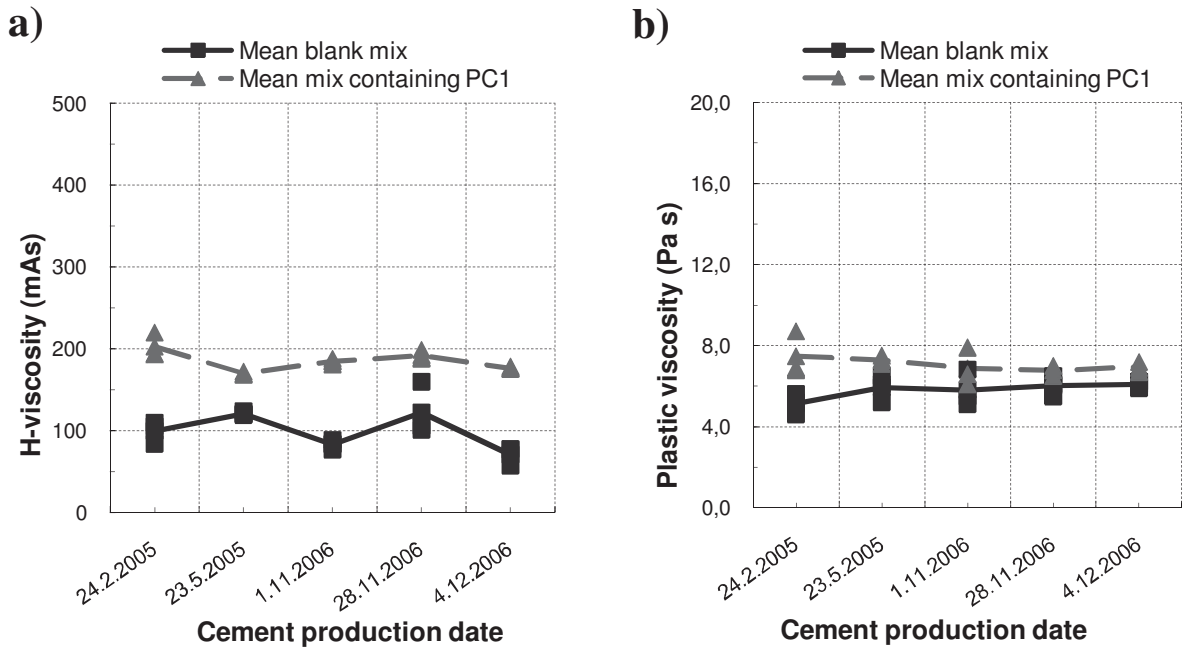

Figure 5.2.1.3.2: Effect of five cement production dates of cement C on H-viscosity and plastic viscosity of mortar and repeatability of results

Table 5.2.1.3.3: Mineralogical composition (QXRD) of five cement production dates

Cement production date	24.02.2005	23.05.2005	01.11.2006	28.11.2006	04.12.2006
C_3S (%)	n/a	51,0	57,7	60,5	58,7
C_2S (%)	n/a	22,8	19,7	17,6	19,5
C_3A (%)	n/a	3,7	4,3	4,4	4,2
$C_2(A,F)$ (%)	n/a	15,3	12,6	12,8	13,2
Calcite (%)	n/a	3,1	3,4	3,4	3,1
Hemihydrate (%)	n/a	1,3	1,5	1,4	1,4
Anhydrite (%)	n/a	0,3	0,5	---	---
Dihydrate (%)	n/a	0,4	---	---	---

---) below limit of detection

5.2.1.4 Different cement production dates in concrete

Eco-SCC

Five cement deliveries that were already tested in mortar (in previous chapter) were then used in test batches of Eco-SCC. Eco-SCC is a self compacting concrete having a relatively low binder content. The production dates from 01.11.2006 (S4) and 28.11.2006 (S5) represent high yield cement. The G-yield in mortar was in a range of ~300 mA, which is equivalent to ~255 Pa (see Figure 5.2.1.4.2). The production dates from 24.02.2005 (S1) and 23.05.2005 (S2) represent low yield cement. The G-yield of sample S1 was in a range of ~100 mA in mortar, which is equivalent to 75 Pa (see Figure 5.2.1.4.2). A G-yield of ~50 to ~100 mA in mortar indicates a very fluid mix (shortly before segregation), whereas a G-yield of ~300 mA in mortar indicates a mix which can be cut like a cake. The stiffer the concrete, the higher the measured G-yield/yield stress.

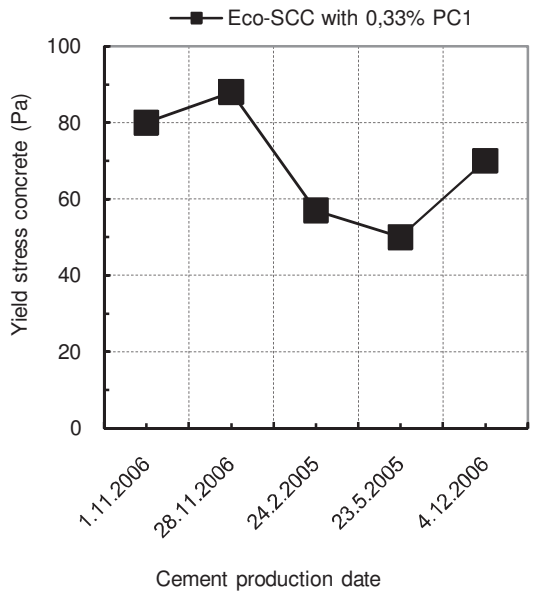

Figure 5.2.1.4.1: Effect of production date on yield stress in concrete (Eco-SCC)

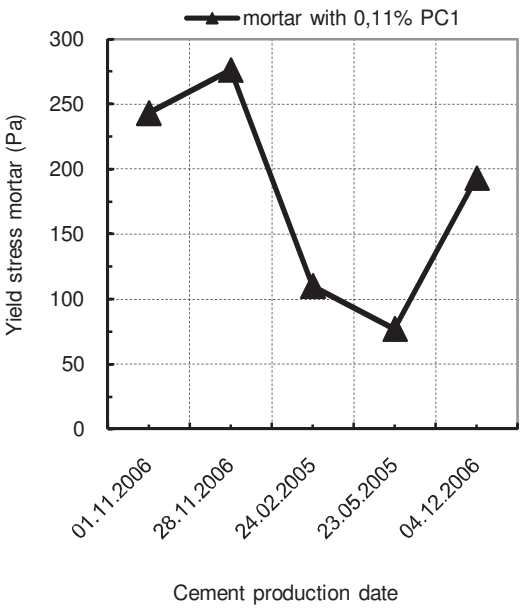

Figure 5.2.1.4.2: Effect of production date on yield stress in mortar

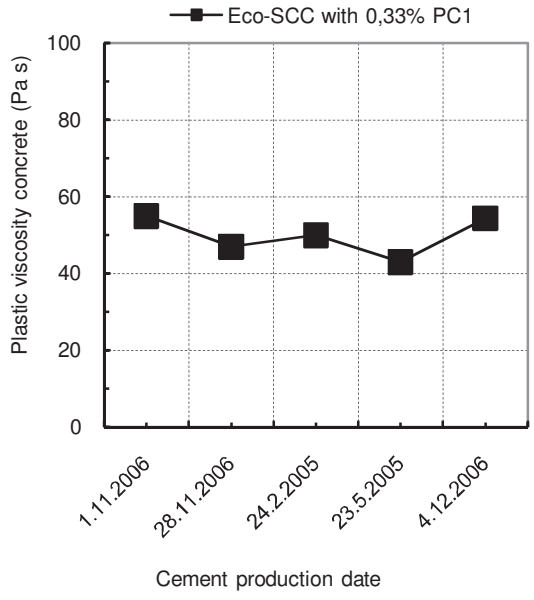

Figure 5.2.1.4.3: Effect of production date on plastic viscosity in concrete (Eco-SCC)

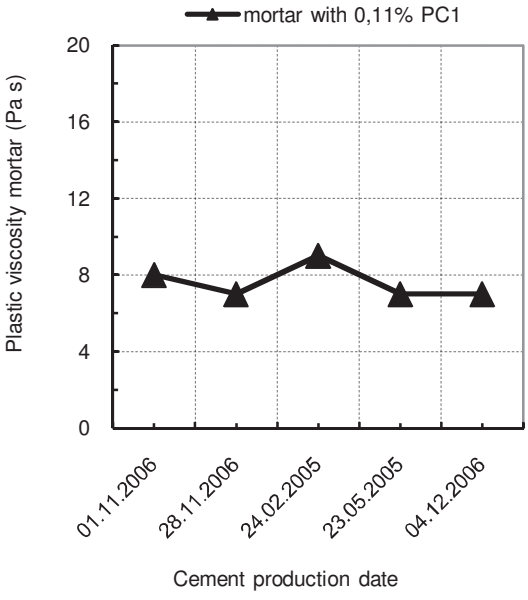

Figure 5.2.1.4.4: Effect of production date on plastic viscosity in mortar

Figures 5.2.1.4.1 and 5.2.1.4.2 depict the effect of the distinct cement deliveries in mortar and concrete. It can be seen that mortar and concrete correlate rather well. The variations in concrete (ranging from 50 Pa to 90 Pa) were not as prominent as in mortar (ranging from 77 Pa to 255 Pa). One explanation for this is the significantly higher inner shear rate of concrete /Ha 2, Wa 6/ compared to mortar. The aggregates have (during the long and more intense mixing process than for mortar) a mill-like effect on primary hydration products and coagulated cement particles. Hence, due to this inner shearing in concrete, the variations between cement production dates are less in concrete. Mixes produced with high yield cement showed high yield stress both in concrete and mortar (see Fig. 5.2.1.4.1 and 5.2.1.4.2). Figures 5.2.1.4.3 and 5.2.1.4.4 depict the effect of cement production date on plastic viscosity. The differences in plastic viscosity between high yield and low yield cement are quite low. According to these results the production date of cement seems to have a relatively small effect on plastic viscosity. The utilization of high yield cement resulted in a slump flow in the range of 550 to 580 mm. Concrete produced with high yield cement would not have been accepted for use as SCC (at least not without further addition of SP) on the construction site. The mixes produced with low yield cement showed relatively high slump flows and low G-values/yield stresses (see Fig. 5.2.1.4.5 and 5.2.1.4.6). The utilization of low yield cement resulted in a slump flow in the range of 610 to 650 mm.

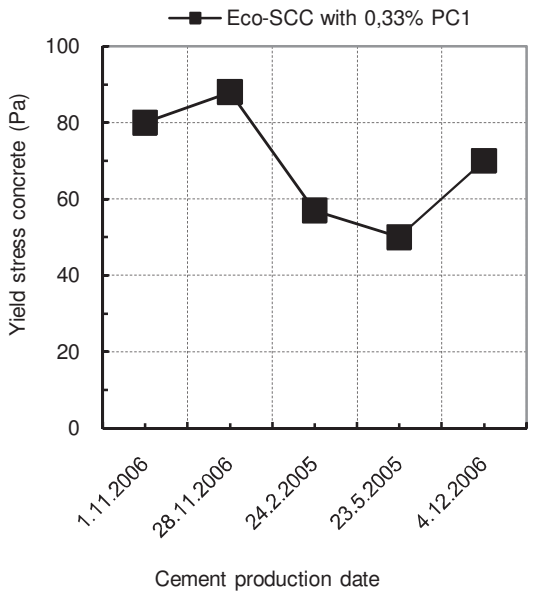

Figure 5.2.1.4.5: Effect of production date on yield stress in concrete (Eco-SCC)

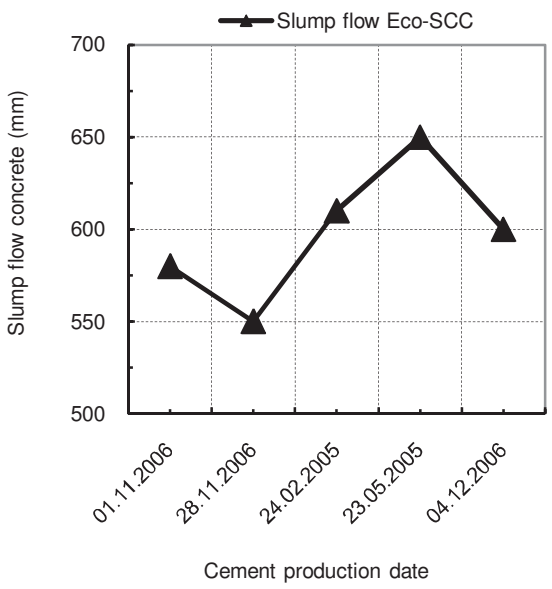

Figure 5.2.1.4.6: Effect of production date on slump flow in concrete

Figures 5.2.1.4.7 and 5.2.1.4.8 depict the relation G-value of Rheometer-4SCC versus slump flow at 13 minutes and G-yield of Rheometer-4SCC versus yield stress. Measurements were done on concrete mixes produced with high yield, low yield and intermediate cement. According to these results, the correlation between G-yield of Rheometer-4SCC and slump flow at 13 minutes is very good. The same was observed for the relation between G-yield, measured with Rheometer-4SCC and the yield stress, measured with Viscometer 5 (see Fig. 5.2.1.4.8).

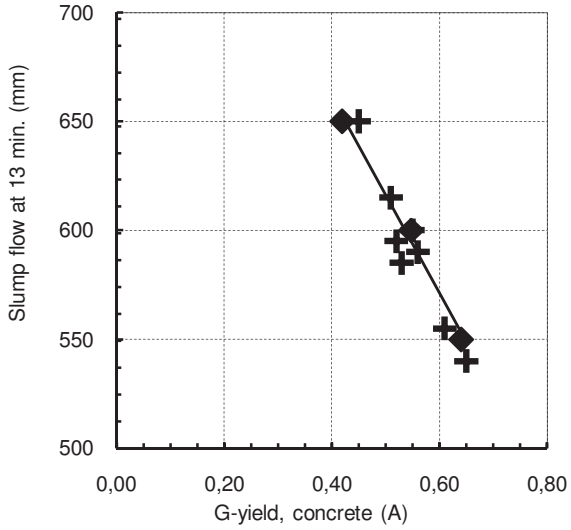

Figure 5.2.1.4.7: G-yield (A) measured in concrete versus slump flow at 13 minutes

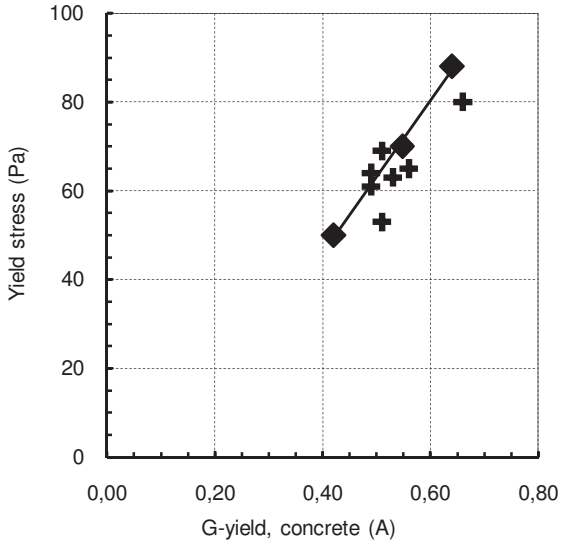

Figure 5.2.1.4.8: G-yield (A) measured in concrete versus yield stress (Pa)

Figures 5.2.1.4.9 and 5.2.1.4.10 show the slump pictures of Eco-SCC produced with high yield and low yield cement. Concrete produced with high yield cement had reduced or nearly no self compacting properties, whereas concrete produced with low yield cement had full self compacting properties. Both concretes showed no signs of segregation or bleeding on the slump table.

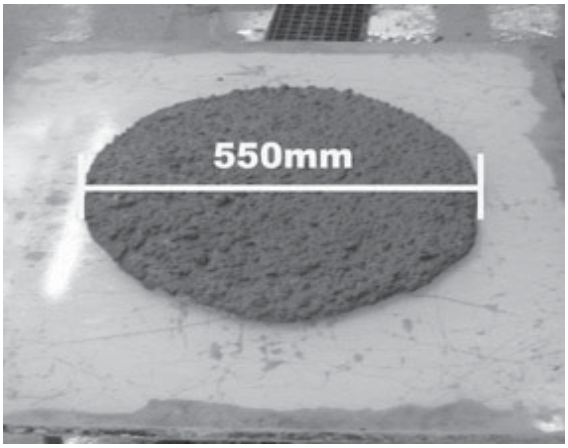

Figure 5.2.1.4.9: Slump flow of Eco-SCC produced with high yield cement

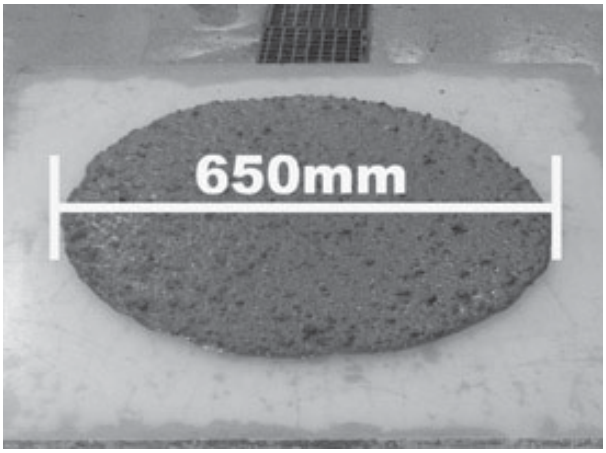

Figure 5.2.1.4.10: Slump flow of Eco-SCC produced with low yield cement

Standard SCC

Three cement deliveries of cement C were used to test batches of standard SCC. Standard SCC contains 150 kg/m³ more cement than Eco-SCC. Mixes produced with high yield cement showed low slump flow and high G-values and yield stresses (see Figure 5.2.1.4.11) for the resulting concrete. The utilization of high yield cement resulted in a slump flow in the range of 560 mm. Concrete produced with high yield cement would not have been accepted for use as SCC (at least not without further addition of dispersing admixture) on the construction site. The mixes produced with low yield cement showed relatively high slump flow and low G-values and yield stresses (see Figure 5.2.1.4.12) for the resulting concrete. The utilization of low yield cement resulted in a slump flow in the range of 650 mm. The results are in line with those obtained on Eco-SCC.

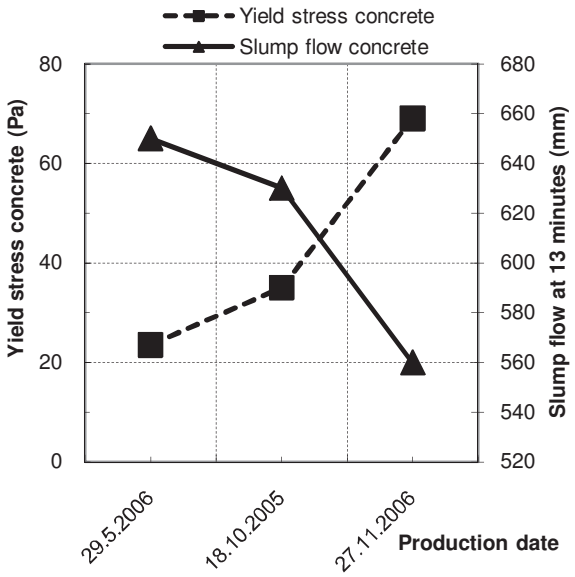

Figure 5.2.1.4.11: Effect of production date on yield stress and slump flow of concrete /Ku 2/

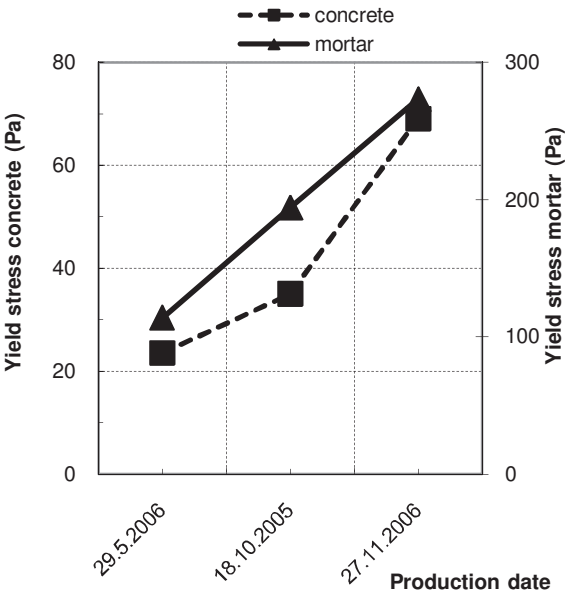

Figure 5.2.1.4.12: Effect of production date on yield stress in mortar and concrete /Ku 2/

Figure 5.2.1.4.13 depicts the yield stress versus time in SCC produced with cement having different rheological properties. When low yield cement was used, the yield stress of SCC increased only slightly (from 22 to 29 Pa) during first half hour. On the contrary, the yield stress of SCC increased clearly during first half hour (from 64 to 100 Pa) when high yield cement was used. According to these results the reactivity of the high yield cement seems to be higher than with low yield cement. The intermediate cement was somewhat in between. The cement delivery had hardly influence on plastic viscosity. As can be seen in Figure 5.2.1.4.14 the plastic viscosity increased at the same rate for the three cement deliveries.

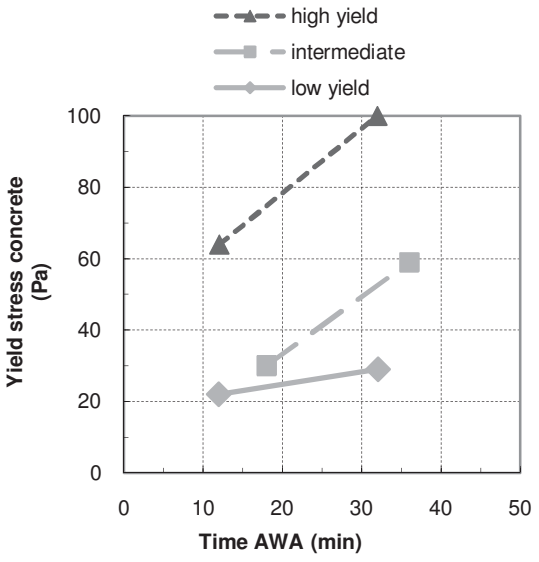

Figure 5.2.1.4.13: Yield stress versus time in concrete with high and low yield cement

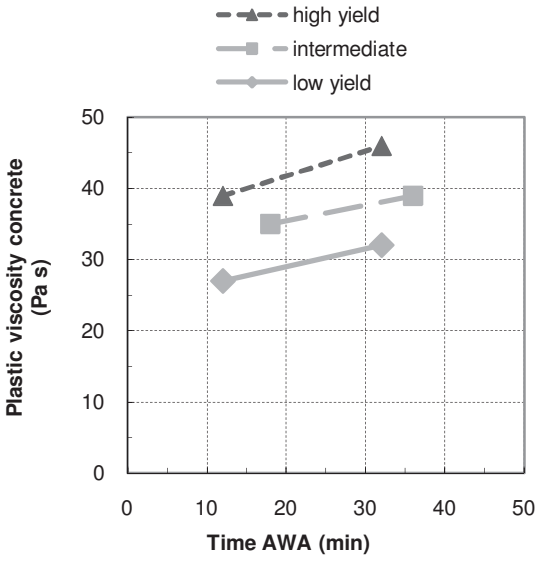

Figure 5.2.1.4.14: Plastic viscosity versus time in concrete with high and low yield cement

5.2.1.5 Effect of cement production date on hydration process

The effect of cement production date on hydration progress of mortar can be seen in Figures 5.2.1.5.1 and 5.2.1.5.2. Figure 5.2.1.5.1 depicts the hydration curves of five different mortar mixes produced with cement C. Figure 5.2.1.5.2 shows the total energy release for these five deliveries of cement C. The time between start of mixing and loading into the calorimeter was same for all mixes. The method of preparation was the same for all mixes. Figure 5.2.1.5.1 indicates that the two deliveries of cement C, produced in May 2006, hydrated clearly faster than the three other production dates. The dormant period in samples of May 2006 was noticeably shorter. Due to that, the second peak was already reached after 6 hours. The significant differences in hydration can not be correlated to the mineralogical composition of these cements (see table 4.3.2). The mineralogical composition of the last five deliveries was in a very narrow range. Both aluminate content and sulfates, which could have caused an accelerated hydration were nearly the same. One reasonable explanation might be the ratio of gypsum and hemi hydrate in the sulfates of this cement. If the content of gypsum is not high enough and the reactivity of the aluminate phase slightly higher (specific surface can also have influences), the dormant period is reduced as it can be seen in Figure 5.2.1.5.1.

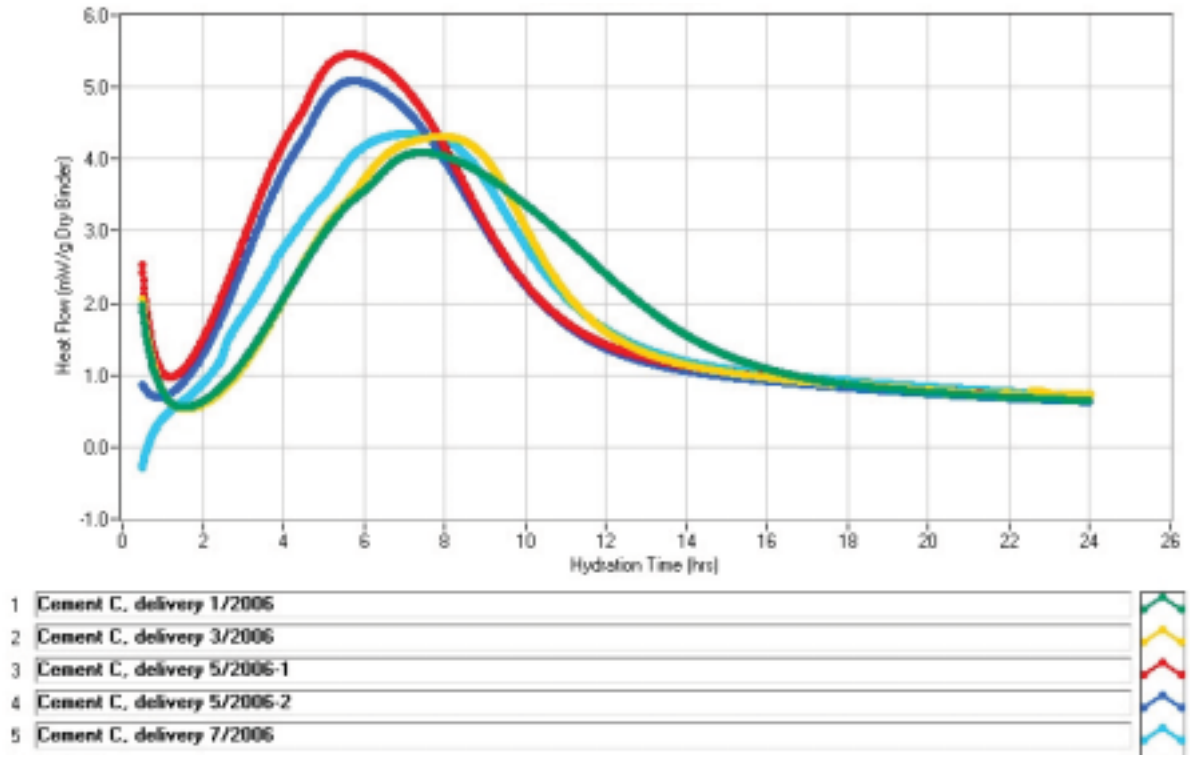

Figure 5.2.1.5.1: Effect of cement delivery on hydration progress in blank mixes (cement C)

Figure 5.2.1.5.2 shows the total energy release of five deliveries of cement C. These curves indicate that the cements with a relatively long dormant period (such as delivery 3/2006) also generate less heat in the first 24 hours. Whereas the cements from May 2006 generated the most energy in the first 24 hours. The difference in total energy release in first 24 hours between the fastest and slowest delivery was more than 20%. This can later result in fluctuations in early strength. Byfors et al. /By 1/ have shown that the degree of hydration, the heat produced and the strength are related.

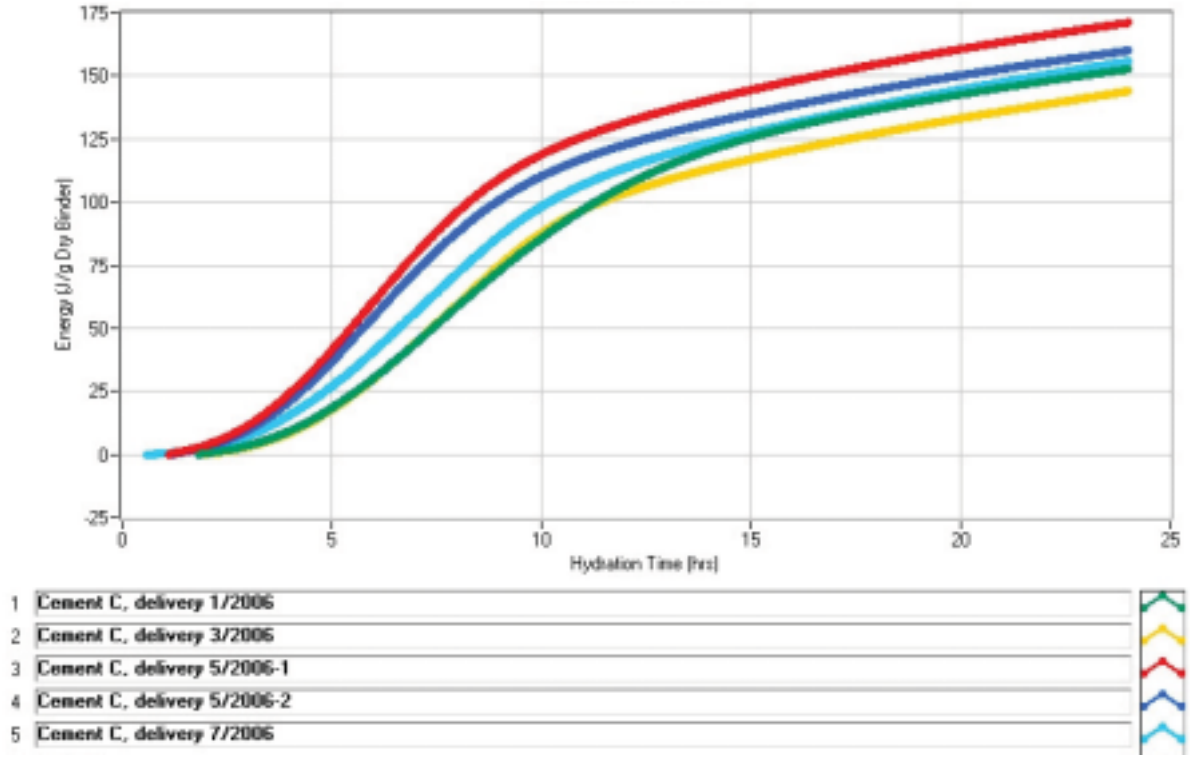

Figure 5.2.1.5.2: Effect of cement delivery on total energy release in first 24 hours in blank mixes (cement C)

Appendix D depicts the hydration curves of the last five cement production dates of cement B2. Cement B2 is a pure Portland cement of type CEM I 42,5R. The differences observed here are quite remarkable and higher than with cement C. Particularly, the sample from 10/2005 showed a different hydration reaction than the other four production dates. The dormant period was twice as long as in the other deliveries. The maximum of the second peak was reached after 16 hours. This means a delay of 8 hours. The difference in total energy release in the first 24 hours between the fastest and slowest sample was more than 25%. A slow hydration progress results in lower early strength /By 1/. Particularly, on sites or in pre fab plants which rely on consistent cement quality and constant strength level (e.g. pre-stressed concrete), a cement delivery like B2-10/2005 can cause serious problems.

5.2.1.6 Microstructural investigations on cement by use of ESEM Weimar

From chapter 5.1 it was concluded that the fluctuations in G-yield were higher in the mixes where the dispersing admixtures melamine and PC1 were present. Hence, cement pastes with and without admixtures made of cement C were choosen for a more detailed investigation under an ESEM-FEG (Environmental Scanning Electron Microscope with Field Emission Gun). The ESEM-FEG allows the imaging of wet systems with no prior specimen preparation like in a conventional Scanning Electron Microscope (SEM). The sample environment can be dynamically altered, and so hydration and dehydration processes can be followed as they happen in the sample chamber. Particularly with cementitious systems, the usage of the ESEM-FEG was a scientific breakthrough. For this investigation, the ESEM-FEG from F.A. Finger Institute at Bauhaus University Weimar was used. Two cements were investigated under the microscope in order to see if the fluctuations in G-yield could be correlated to visible differences in microstructure. The delivery C#7 from 5/2005 represents a low yield cement, showing a normal behaviour when PC1 was added. The delivery C#8 from 8/2005 represents a high yield cement, showing an abnormal jump in G-yield when PC1 was added. Cement pastes were produced with and without admixture. The w/c-ratio of the reference paste was 0,46, the w/c-ratio of the paste containing PC1 was 0,36. First investigations were done on pastes without any admixture of both cements after 15 minutes of hydration. Note that the G-yield was also measured after 15 minutes. Figure 5.2.1.6.1 a) depicts the cement particle surface of the low yield cement. Figure 5.2.1.6.1 b) shows the particle surface of the high yield cement. Several pictures indicate that the particle surface of the high yield cement is covered much more densely with ettringite as well as gypsum particles. Although the G-yield was nearly the same in blank mixes for both low yield cement and high yield cement, one could notice clear differences in microstructure of the early hydration products. These differences in microstructure had no effect on rheology in the blank mixes. Effects from microstructure are most likely neutralised by the huge amount of water available as diluting liquid in the blank mixes.

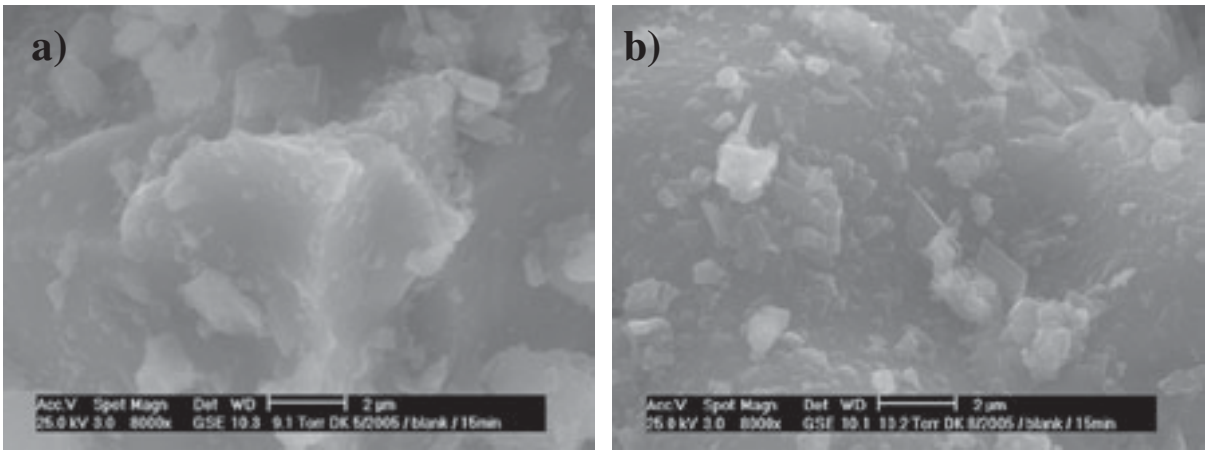

Figure 5.2.1.6.1: ESEM-FEG pictures of Cement C, clinker surface of low-yield (a) and high-yield cement (b) in blank mixes after 15 minutes, 8000x magnification

Pastes containing polycarboxylate (PC1) were also investigated under the ESEM-FEG after 15 minutes of hydration. Figure 5.2.1.6.2 a) shows primary hydration products on the cement surface of the low yield cement at a magnification of 32000x. Figure 5.2.1.6.2 b) shows the high-yield cement at the same magnification. By comparing the size of the primary hydration products one can see that the particle surface of the low yield cement was covered with larger and more massive structures than the particle surface of the high yield cement. In this context it should be noted that Chartschenko et al. /Ch 1/ showed that differences in morphology of

ettringite are due to differences in ionic strength and thereby pH value of the pore solution /Ch 1/.

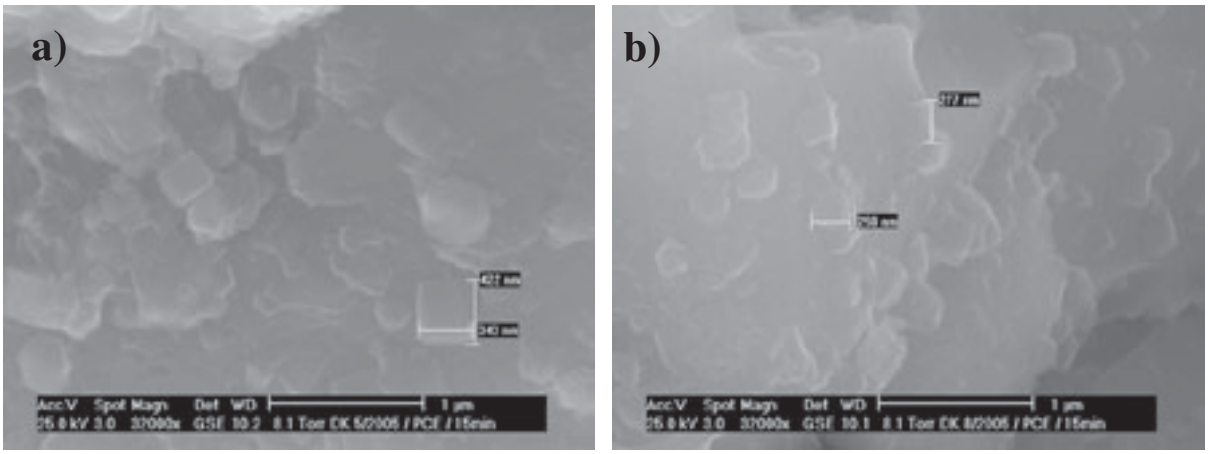

Figure 5.2.1.6.2: ESEM pictures of cement C, clinker surface of low-yield (a) and high-yield cement (b) in PC mixes after 15 minutes, 8000x magnification

Another interesting observation was made with the high-yield cement after 15 minutes of hydration. Figure 5.2.1.6.3 shows a needle shaped crystal formation (highly reasonable syngenite) at a magnification of 8000x. Syngenite can be formed from the bassanite/hemi hydrate and potassium from the clinker, occuring as needles with a length up to 10 µm. Rößler et al. /Rö 1, Rö 2/ found that the rheology of mortar or paste is influenced significantly when syngenite is formed at early stage of hydration. This observation is also correlating with the results obtained by the quantitative clinker phase composition (Rietveld refinement).

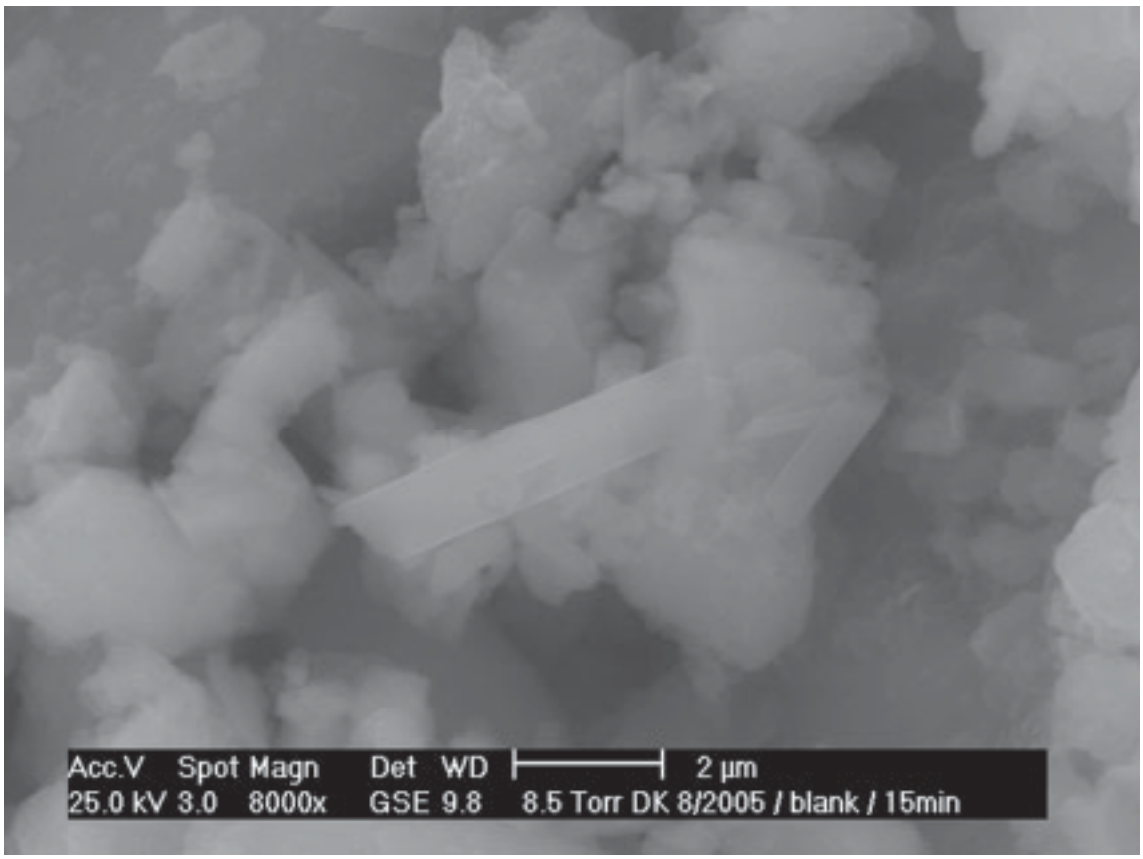

Figure 5.2.1.6.3: ESEM picture of cement C, syngenite near clinker surface after 15 minutes, 8000x magnification

5.2.1.7 Microstructural investigations on cement by use of SEM Reykjavik

During 2006, the SEM at ICI was used to investigate the microstructure of two cements which have already been investigated under an ESEM-FEG. One cement represented low yield cement, the other cement represented high yield cement. Pastes with and without admixture PC1 were produced. The main objectives of this investigation were:

- analysis of micro structure in both cements
- investigation of micro structure with respect to primary and secondary formed hydration products (e.g. gypsum, syngenite)
- determining if SEM pictures are comparable to ESEM-FEG
- resulting in the question: Do we see any differences in the SEM pictures which can be related to fluctuations in rheology?

For investigations in the vacuum chamber of a SEM it is necessary that the samples be completely dry. The method used here to stop the hydration process and dry the samples without artefacts is called freeze drying. A sample holder made of aluminium was placed into liquid nitrogen and cooled down to –198°C. Thereafter mixes with and without PC1 were prepared and placed on the sample holder after 15 and 45 minutes. The cement paste froze immediately and cooled down to the temperature of the sample holder. Then the sample holder was placed in a desiccator. The desiccator was connected to a high vacuum pump which maintained a vacuum of <20 mbar over a period of 16 hours. Freeze drying involves the removal of water or other solvent from a frozen sample with a process called sublimation. Sublimation occurs when a frozen liquid goes directly to the gaseous state without passing through the liquid phase. In contrast, drying at ambient temperatures from the liquid phase usually results in changes in the cement sample. Figure 5.2.1.7.1 shows the surface of a cement grain under the SEM. Hydration products and other particles cover the cement surface densely.

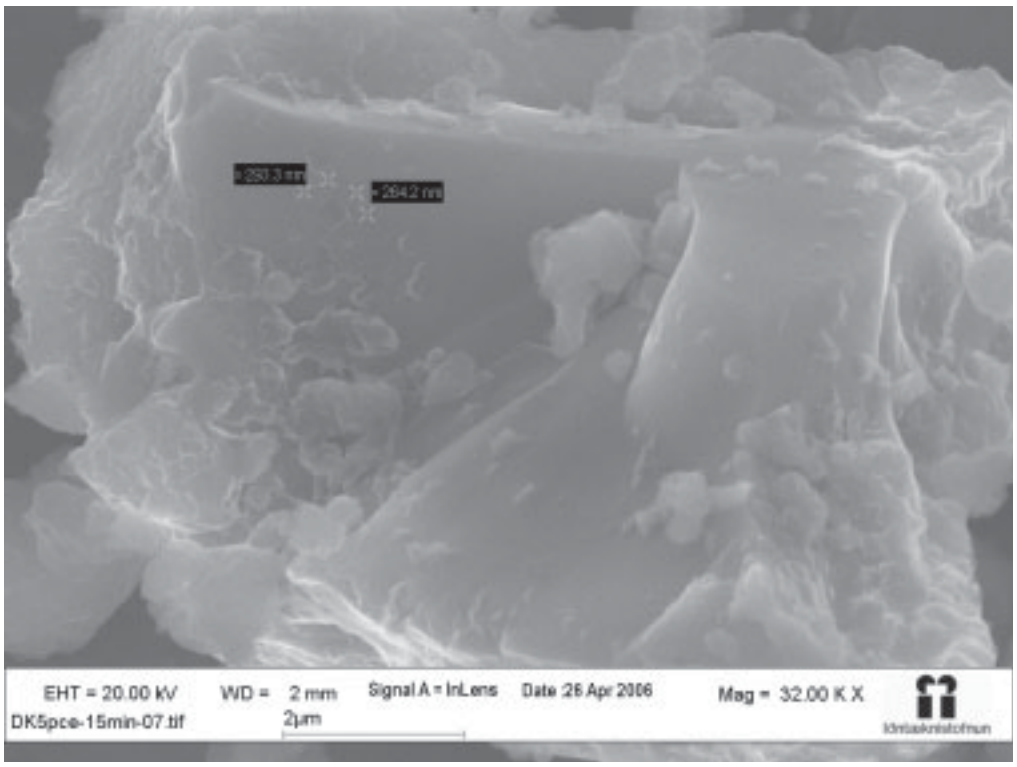

Figure 5.2.1.7.1: Low yield cement, mix with PC1 after 15 minutes, 32000x, average size of ettringite

Figure 5.2.1.7.2 gives an indication of the size of ettringite formations and how densly the cement surface is covered in the high yield cement paste.

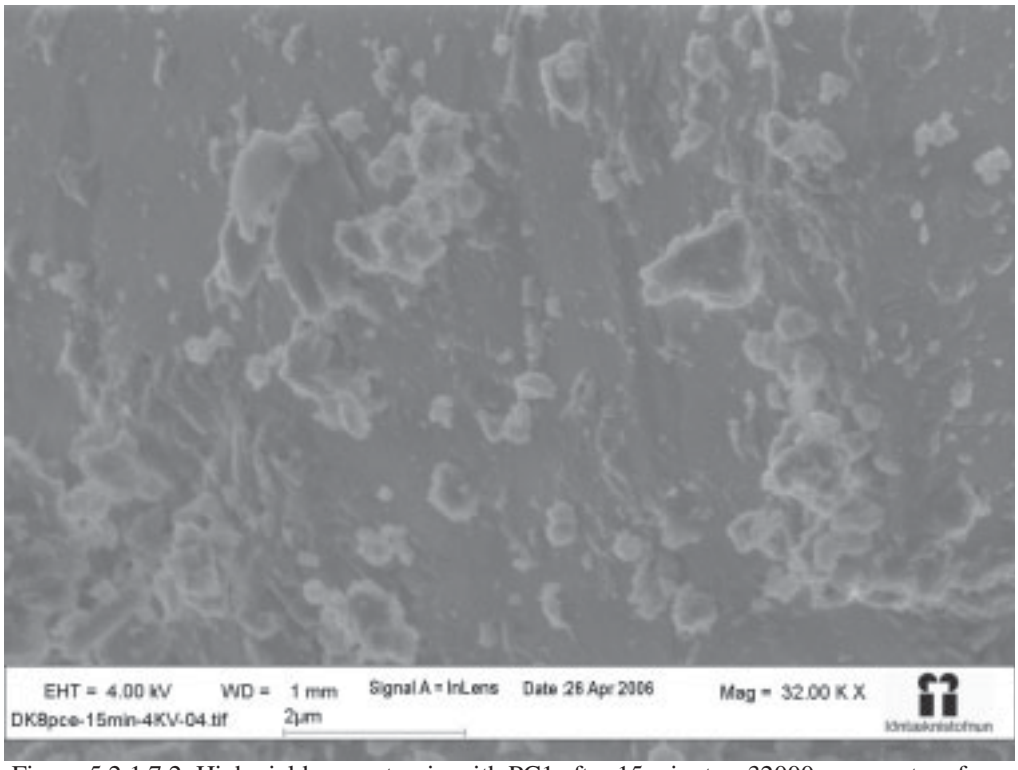

Figure 5.2.1.7.2: High yield cement, mix with PC1 after 15 minutes, 32000x, cement surface

Figure 5.2.1.7.3 depcits some interesting agglomerates of needle-shaped formations which were found in the high yield cement paste.

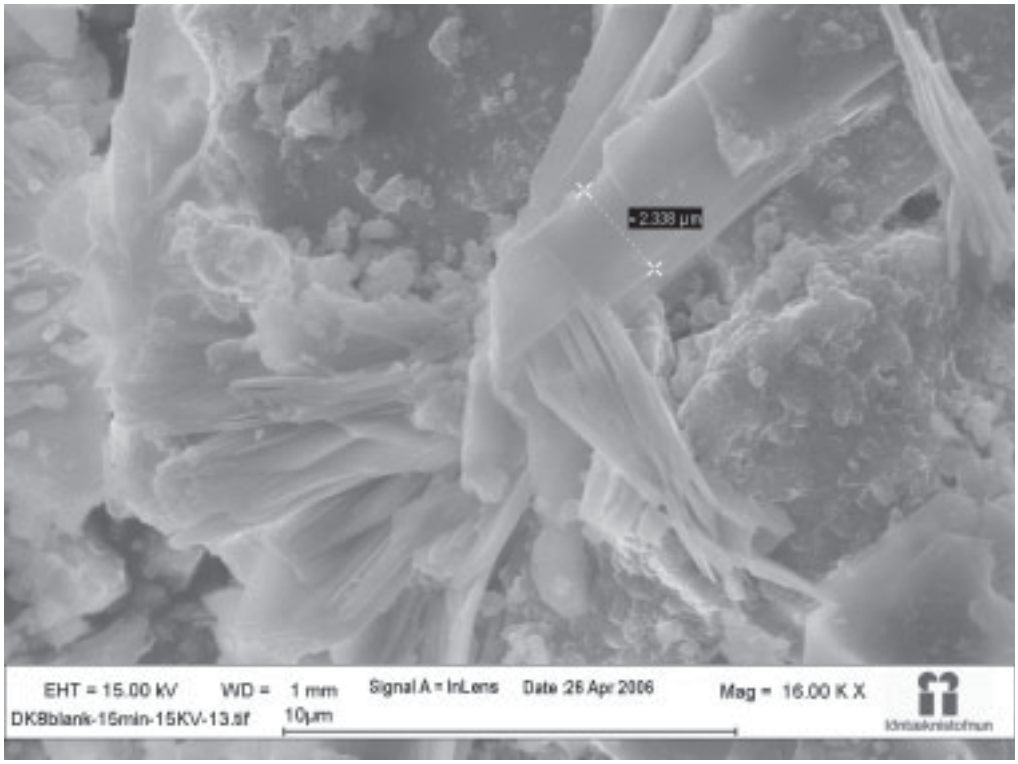

Figure 5.2.1.7.3: High yield cement, blank mix after 15 minutes, 16000x, agglomeration of needle shaped formations

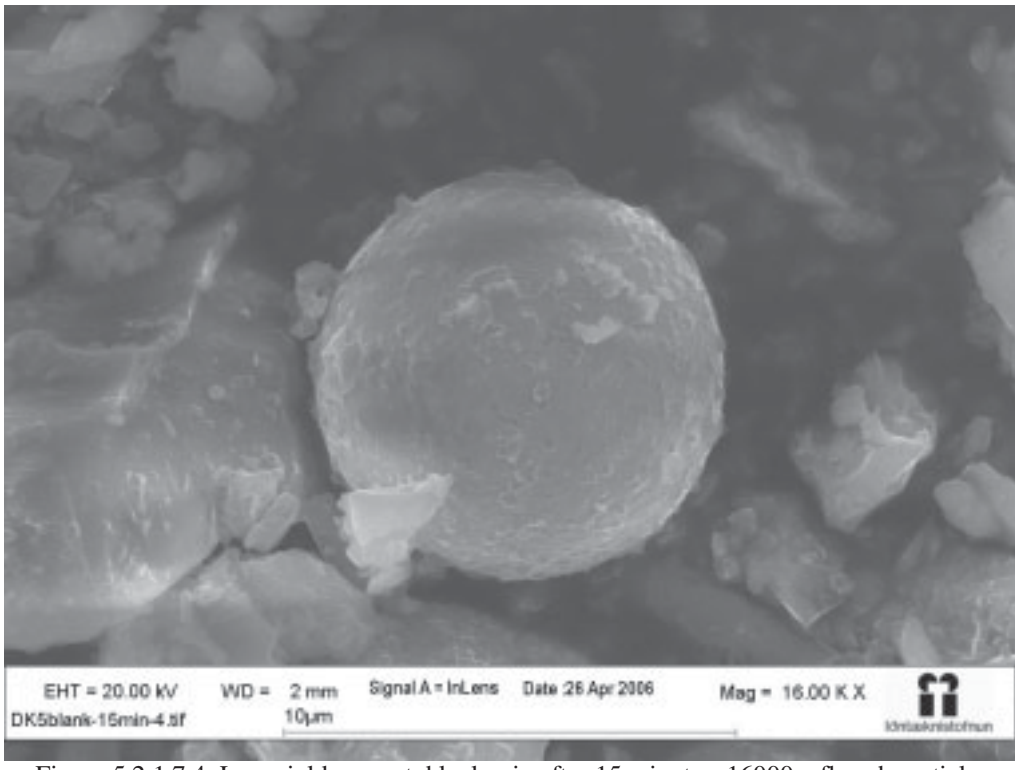

Figure 5.2.1.7.4: Low yield cement, blank mix after 15 minutes, 16000x, fly ash particle

Figure 5.2.1.7.4 depicts a fly ash particle. Fly ash was found in all investigated samples. The figure below shows a cement grain surface, covered with short prismatic ettringite <1 µm. Cavities on the cement surface and nearby agglomerates of ettringite are a sign of a hydrated aluminate phase.

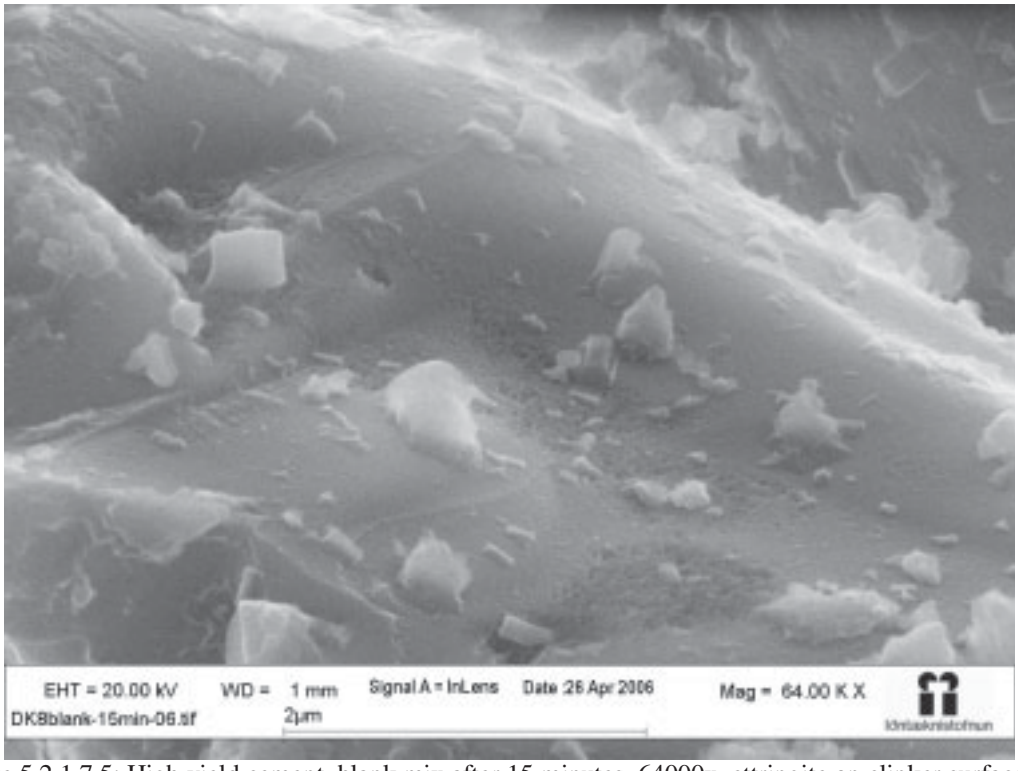

Figure 5.2.1.7.5: High yield cement, blank mix after 15 minutes, 64000x, ettringite on clinker surface and cavities in surface due to hydration of aluminate phase

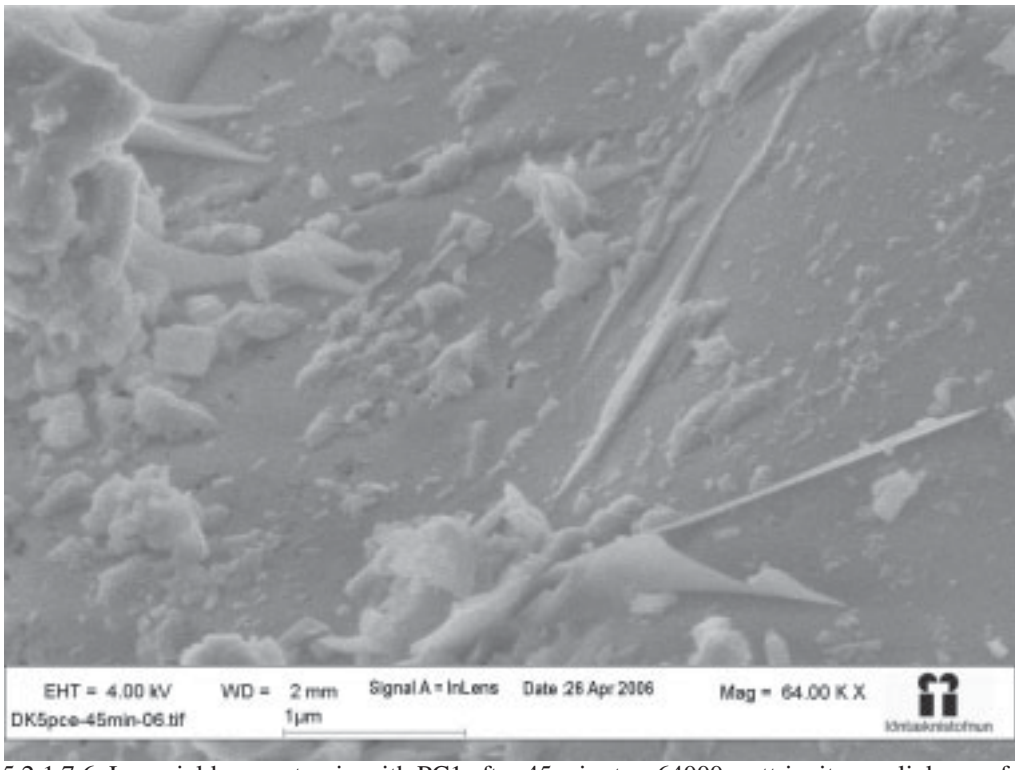

Figure 5.2.1.7.6: Low yield cement, mix with PC1 after 45 minutes, 64000x, ettringite on clinker surface and cavities in surface due to hydration of aluminate phase

After comparing the pictures from the ESEM-FEG at Weimar with the SEM at Reykjavik one could state the following remarks:

- Some clinker surfaces look rather unhydrated with only few traces of ettringite. Hydration products might be blown away during sample preparation with pressurized air. Some needle-shaped formations were found in the high yield cement (see Figure 5.2.1.7.3).
- Fly ash particles were found in both cements (see Figure 5.2.1.7.4).
- The surface of the high yield cement was covered with area shaped cavities (in samples where the hydration was stopped after 15 and 45 minutes). The cavities are a sign for a hydrated aluminate phase. When the aluminate phase comes in contact with water it hydrates, and together with sulphates and water forms ettringite (see Figure 5.2.1.7.5 and Figure 5.2.1.7.6).
- The surface of the low yield cement was covered with more pointy looking cavities. Short prismatic ettringite was observed in the vicinity of the cavities. In mixes with PC1, some interesting crystal formations were visible 45 minutes after water addition (see Figure 5.2.1.7.6).
- Samples appeared to be covered with freeze dried pore solution.

5.2.1.8 Hydration process of cements having different rheological properties

The hydration process of cement paste was logged in an isothermal calorimeter. At start of measurement the calorimeter and the materials had reached temperature equilibrium, meaning all materials were stored in the calorimeter cells overnight to ensure that water, cement, admixture and sample containers had the same temperature. Temperature logging started when water was added to the cement and pastes were handmixed for 30 seconds. Graphs are already normalized, meaning they show the heat evolution per gram of cement.

Cement C (most likely a relative reactive aluminate phase)

The initial hydration curves of two production dates of cement C (CEM I 52,5N), having different rheological properties, are displayed in Figure 5.2.1.8.1. Pastes produced with a cement having a high initial yield stress (yellow curve) reacted significantly faster than cement with a low initial yield stress (green curve).

Table 5.2.1.8.1: Mineralogical composition (QXRD/Rietveld) of two cement production dates

Cement production date	23.01.2008 (low yield)	15.04.2008 (2) (high yield)
Yield value in mortar with PC1 (Pa)	135	330
Plastic viscosity in mortar with PC1 (Pa·s)	7	8
C_3S (%)	58,6	58,6
C_2S (%)	19,8	19,4
C_3A (%)	4,1	4,0
$C_2(A,F)$ (%)	12,4	12,3
Calcite (%)	3,9	3,6
Hemihydrate (%)	1,3	1,6
Anhydrite (%)	---	0,4
Dihydrate (%)	---	---

---) below limit of detection

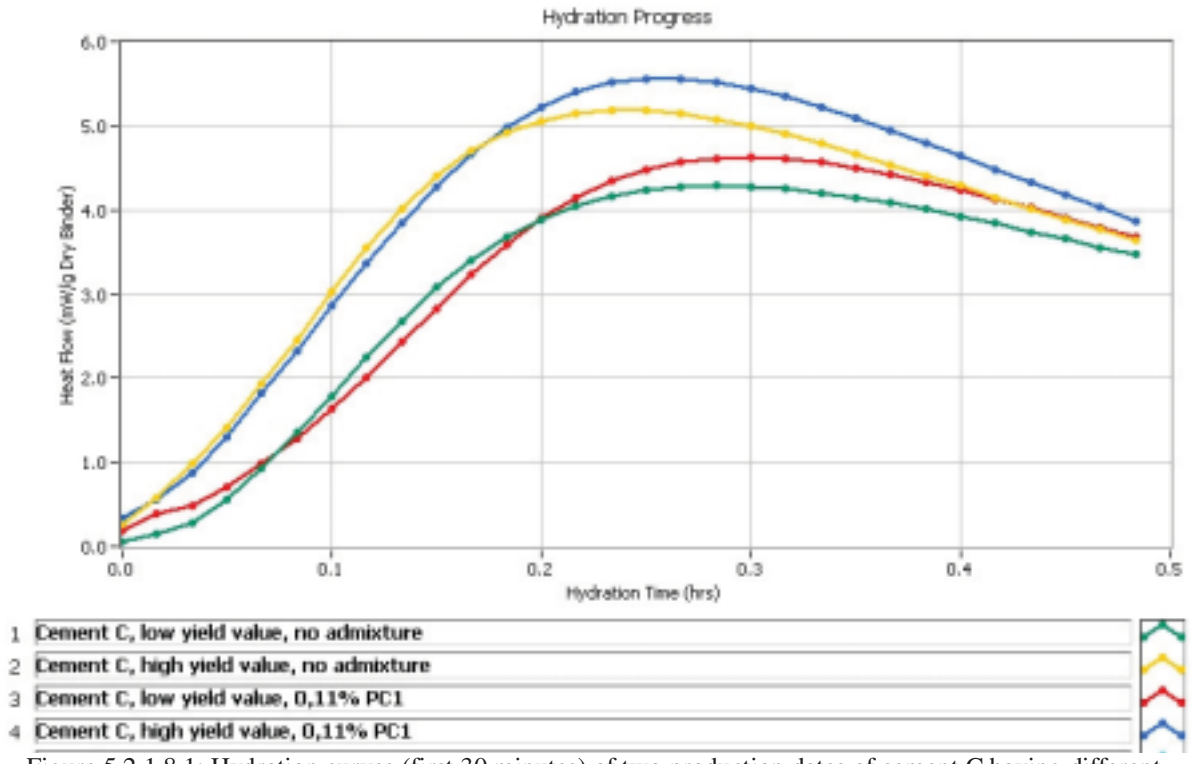

Figure 5.2.1.8.1: Hydration curves (first 30 minutes) of two production dates of cement C having different rheological properties

At rheological testing age of 15 minutes, the high yield cement released approximately 30% more energy than the low yield cement. The same was observed for pastes containing 0,11% PC1 (see blue and red curve), during first half an hour the high yield cement reacted faster than the low yield delivery. It should be noted that the difference in yield value between the red and the blue curve is around 200 Pa in mortar. Mineralogical data (QXRD Rietveld) for both, the high and low yield cement, showed identical mineralogical compositions (see table 5.2.1.8.1). The aluminate phase was around 4%, the hemihydrate content was between 1,3% and 1,6% and other calcium sulphate carriers were below the limit of detection. This indicates that either the aluminate phase in the high yield cement was more reactive than in the low

yield delivery or that some kind of accelerator was present in the high yield delivery. Figure 5.2.1.8.2 depicts the hydration curves of the pastes for 24 hours. On the yellow and green curve one can see that the dormant period of both cements was practically identical when no admixtures were present. In pastes with 0,11% PC1, the high yield cement reacted slightly faster. However, the differences in hydration behaviour displayed in Figure 5.2.1.8.2 are insignificant compared to differences in initial rheological properties between single cement deliveries. As expected, pastes containing 0,11% PC1 were retarded for two to three hours compared to blank pastes.

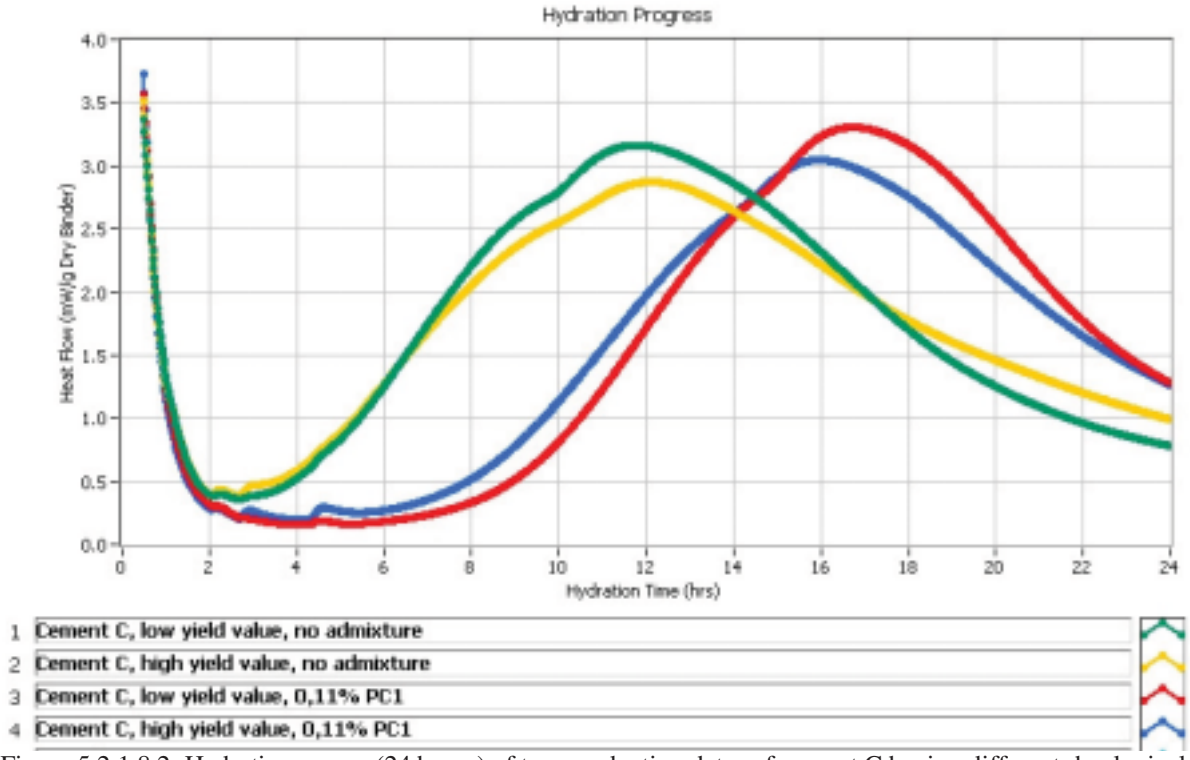

Figure 5.2.1.8.2: Hydration curves (24 hours) of two production dates of cement C having different rheological properties

Cement D (most likely a rather inactive aluminate phase)

Cement pastes produced with low yield and high yield cement of cement D (CEM II/A-M 42,5R) were placed into an isothermal calorimeter and the hydration curves were logged for 24 hours (see Figure 5.2.1.8.3). The mineralogical composition of both cement production dates is given in table 5.2.1.8.2.

Table 5.2.1.8.2: Mineralogical composition (QXRD/Rietveld) of two cement production dates

Cement production date	26.10.2007 (low yield)	17.01.2007 (high yield)
Yield value in mortar with PC1 (Pa)	100	500
Plastic viscosity in mortar with PC1 (Pa·s)	6	11
C_3S (%)	58,6	54,4
C_2S (%)	9,4	10,0
C_3A cubic (%)	1,8	1,8
C_3A orthorhombic (%)	9,7	11,0
$C_2(A,F)$ (%)	6,5	6,1
Calcite (%)	0,2	0,9
Hemihydrate (%)	1,4	1,8
Dihydrate (%)	2,4	3,4
Periclase (%)	1,9	2,3
Felspar (%)	1,6	1,4
Portlandite (%)	0,6	0,7
Amorphous (%)	6,0	6,0

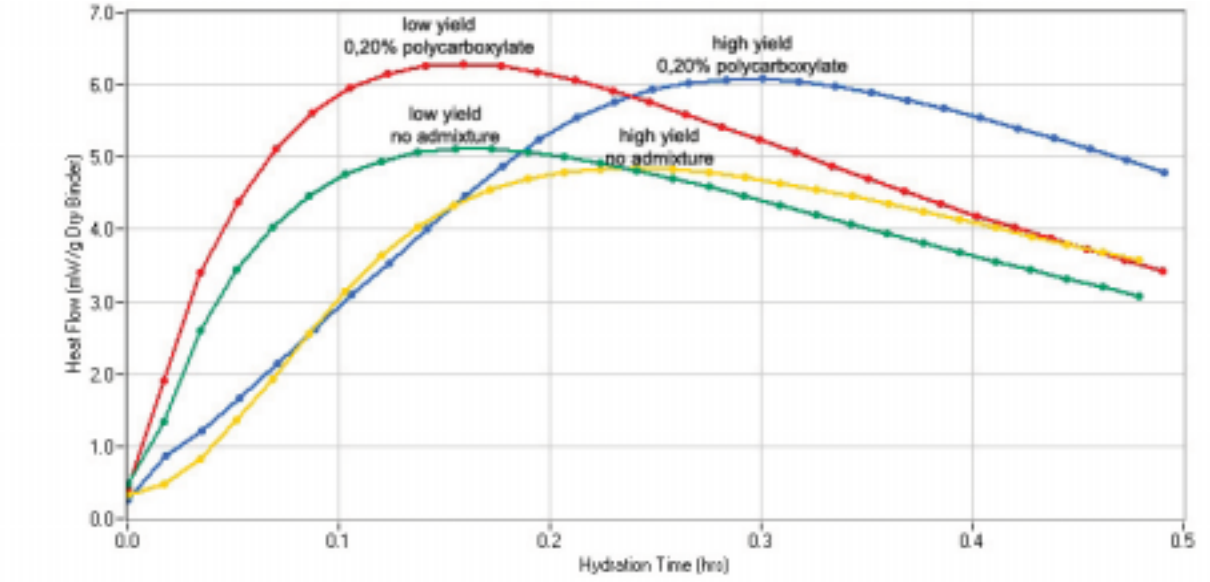

Figure 5.2.1.8.3: Hydration curves (first 30 minutes) of two production dates of cement D having different rheological properties

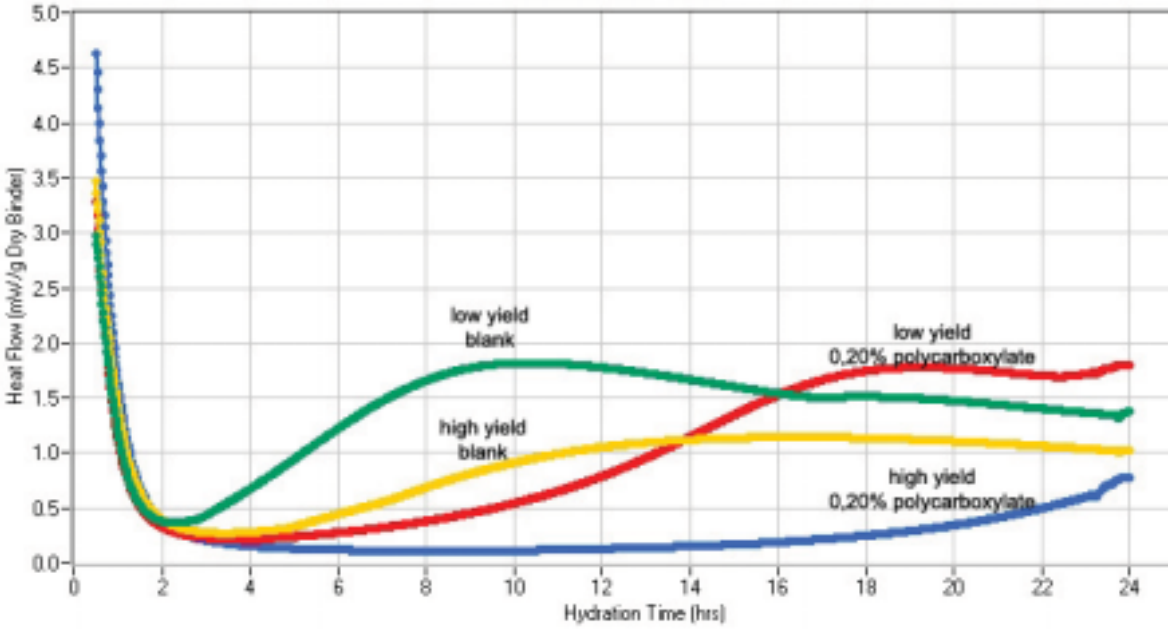

Figure 5.2.1.8.4: Hydration curves (24 hours) of two production dates of cement D having different rheological properties

Temperature logging started when calorimeter and dry materials had reached temperature equilibrium, meaning cement, water, admixture and sample container were stored overnight in the calorimeter cells to ensure that the materials and the calorimeter have exactly the same temperature. Figure 5.2.1.8.3 depicts the first 30 minutes of hydration after water addition. Unexpectedly, the cement giving the lowest yield stress showed the highest reactivity in terms of heat flow (both in paste with and without admixture). Five minutes after water addition the heat flow of the cement giving a low yield stress was twice as high as the heat flow from the cement giving a high yield stress. During the first 24 hours of hydration, the cement having a high yield stress showed a clearly lower reactivity than the cement with a low yield stress. One explanation might be an aluminate phase that was not reactive enough to consume the dissolved calcium sulphate originating from fast-dissolving hemihydrate /Sa 2/. The dissolved calcium then precipitated back to large interlocking crystals /Sa 2/ of gypsum resulting in an abnormal jump in yield stress. The hydration curves of cement C and cement D look

contradictory on the first view. However, the results can be explained. Hydration curves of cement C with a high initial yield stress look as if some kind of accelerator is present, whereas hydration curves of cement D with a high initial yield stress look as if some kind of retarder is present. Samples of cement C having a high yield stress must incorporate either an accelerator or a relatively reactive aluminate phase. On the contrary, samples of cement D having a high yield stress must contain either a strong retarder or a rather inactive aluminate phase.

5.2.1.9 Effect of polymer structure on fluctuations in rheology

Polycarboxylates differing in charge equivalent, side chain length and number of side chains were tested with six cements differing in production date and rheological properties. Tests were done on mortar. Mix designs for mortar are given in chapter 3.5. PC1 is characteristic for an admixture having a high charge equivalent, short side chains and a relatively low number of side chains. On the contrary, PC2, PC3 and PC4 feature low charge equivalent, longer side chains and larger number of side chains in compare to PC1. Figure 5.2.1.9 depicts the results for yield stress and plastic viscosity. PC1 and melamine caused relatively high fluctuations in rheology when different cement production dates (coming from same plant) are used. Depending upon the cement delivery, the fluidity of mortar containing PC1 ranged from liquid like (~100 Pa) to relatively stiff (~300 Pa) mixes. With PC2, PC3 and PC4, the influence of cement production date on rheology was clearly minor. However, this comparison has to be read carefully, as PC2, PC3 and PC4 had to be added at significantly higher dosages (150% to 300% of PC1) to achieve rheological properties comparable to PC1. Again, the major structural differences between polymers compared here are side chain length and charge equivalent. PC1, with short side chains and high charge equivalent gave the highest fluctuations when a new cement production date was used. PC2, PC3 and PC4 with long side chains and relatively low charge equivalents gave lower fluctuations when a new cement production was used.

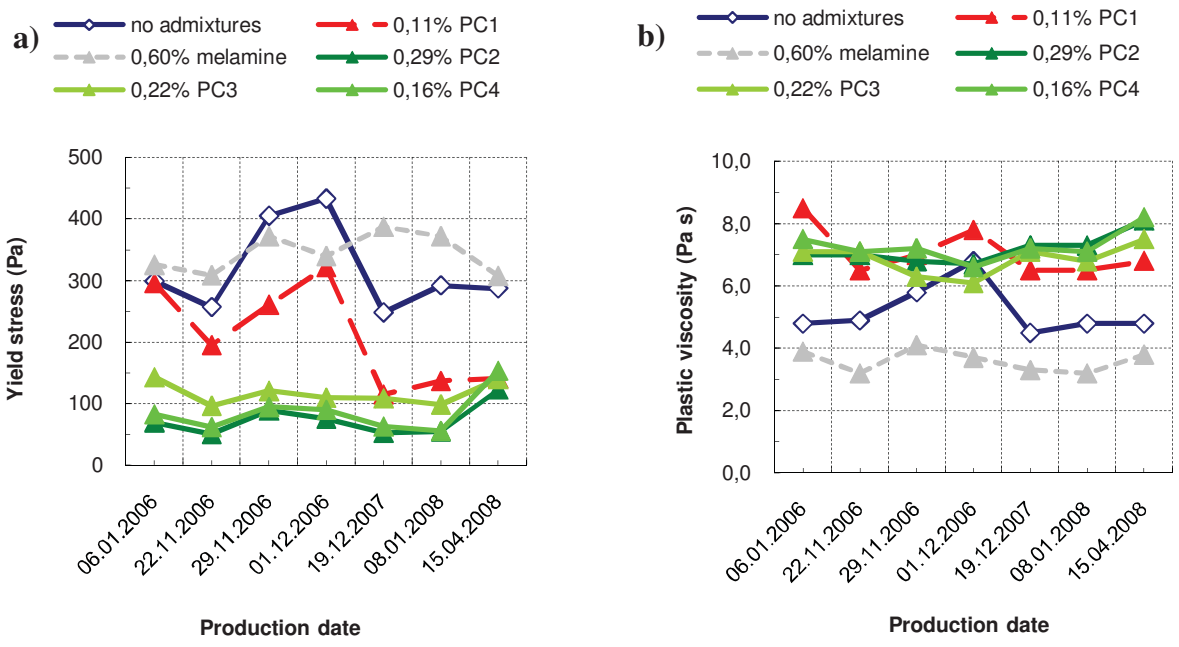

Figure 5.2.1.9.1: Effect of cement production date on rheology when different polymers are present

The differing polymer structures also resulted in differing adsorption behaviour, here given as the degree of adsorption. Note that the method used here is an indirect way to measure

adsorption. Therefore it might be better to use the term polymer consumption. During first ten minutes of hydration, 70 to 90% of PC1 was adsorbed (or consumed) by cement, whereas the polymer consumption was only 10 to 20% for PC2 and 40 to 60% for PC3 and PC4. Hence, the reservoir of free polymers in the pore solution is significantly higher with PC2, PC3 and PC4 than with PC1. It becomes clear that the polymer consumption or in other words the adsorption of polymer on cement grains and hydration products (see also /Pl 1/) controls the initial dispersion of a cementitious system. It thereby also affects possible fluctuations originating from routine cement production. Results from adsorption measurements point out that the fluctuations in rheology can be related to the initial adsorption degree of the polymer. The question which arises is if cement which generates a relatively high yield stress adsorbs (1) less of the polymers leading to lower repulsion and therefore higher yield stress or (2) adsorbs more of the polymers and consumes them more rapidly, for example by formation of an organo mineral phase /Fl 1/. Results from adsorption measurements are further discussed in chapter 5.2.7.

Figures 5.1.7.1 a) and 5.2.1.9.1 a) point out the more aggressive the adsorption behaviour of a dispersing admixture on the cement grain, the higher the fluctuations in rheology can be when a new cement production date is used.

5.2.1.10 Total organic carbon (TOC) of cement

The total organic carbon (TOC) of blank cement, differing in production date and rheological properties, was measured repeatedly. This value tells how much organically bound carbon is present in the dry cement powder. A description how the TOC was determined is given in chapter 5.2.7. The measurement of cement carbon content is part of the procedure to determine the adsorption degree, since it represents the zero value. Carbon in cement can originate from:

(1) grinding aid used during cement production,
(2) unburnt carbon coming from fly ash,
(3) other organic carbon sources such as decaying vegetation, bacterial growth, and metabolic activities of living organisms.

Source (2) is relatively unlikely for this cement, as the producer claims to use only 4% limestone filler and no fly ash. Living organisms, vegetation and bacterial growth in cement is also very unlikely. Hence, it is reasonable to assume that the carbon measured here originats from an organic compound added during cement production, i.e. grinding aid. Note that carbon coming from the limestone filler (see Appendix K) does not influence TOC results as it was eliminated beforehand. The TOC measured was in a range of 240 to 330 ppm. Results reported here are double or triple measurements showing a good repeatability. The deviation between single tests was not more than 20 ppm in the diluted solution. The carbon content (weight-%) in the molecules of grinding aid is ranging from 39% in ethylene glycole to 75% in phenole. Triethanoleamine, one of the most frequently used grinding aids, is made of 48% carbon. It was also used during the grinding process of cement C /Pr 1/. If one assumes that all measured carbon originates from grinding aid, the dosage of TEA in these cements was between 400 and 700 ppm. However, these values seem relatively high as TEA is usually added at maximum dosages of 100 to 200 ppm. TOC measurements were done on cement production dates which cover the whole territory of consistency with and without admixtures. According to these preliminary results, the TOC seems to have a clear effect on rheological properties of mixes with and without admixtures. Figure 5.2.1.10 indicates that the more carbon compound is present, the higher the measured yield stress is in mixes with PC1 and without any admixtures. These results should be read carefully and treated as preliminary results. A closer investigation is necessary.

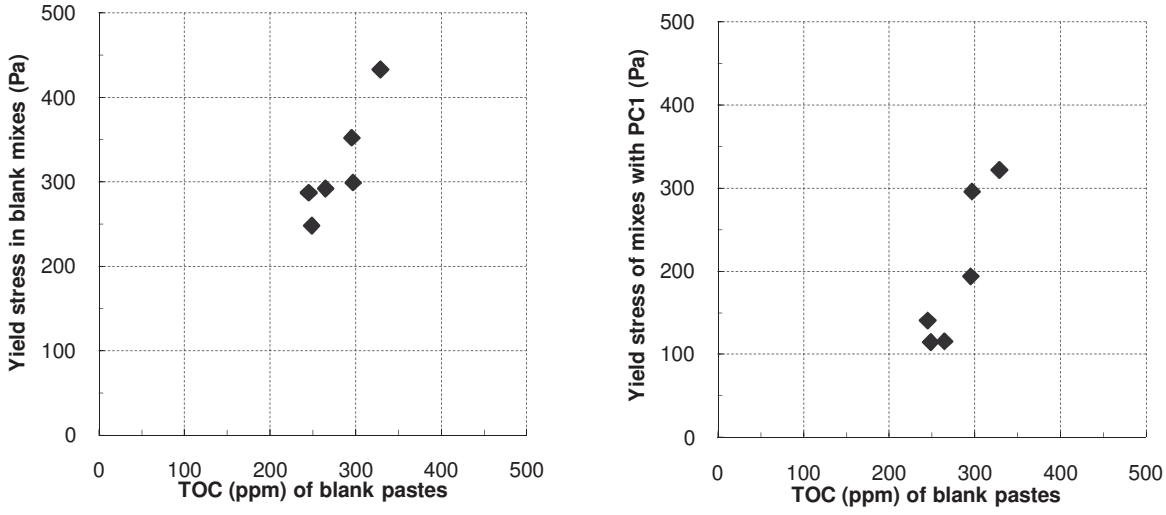

Figure 5.2.1.10: The TOC of blank cement and its influence on yield stress in blank and PC1 mixes

5.2.2 Granulometry

5.2.2.1 Effect of specific surface and particle size distribution

The effect of the specific surface on G-yield (mA) can be seen in the figures below. The graphs presented are based on 29 deliveries from cement C. At start of the project (After the first 12 deliveries) it was found that with increasing specific surface the G-yield (mA) increased. This trend did not hold. For an entity of 29 production dates no correlations were found. The more cement samples were tested on their rheology and specific surface, the greater was the scatter. In Figure 5.2.2.1.1 a) it can be seen that the latest deliveries (from 12/2006 to 8/2007) caused the high scatter in the blank mixes. Without these deliveries, the relation between specific surface and G-yield in blank mixes would be better. In the mixes where a polycarboxylate (PC1) and melamine based admixture were present, no relation between G-yield and specific surface could be established (see Figures 5.2.2.1.1 b)) and c). The specific surface is obviously not the major influencing factor on rheology when dispersing admixtures are present. It might play a role, but then most likely in connection with other parameters such as aluminate reactivity or sulphate composition /Vi 1/. As already stated the relation between the G-yield (mA) and the specific surface in the blank mixes was relatively good when less than a dozen cement production dates were tested. With increasing number of samples the correlation became worse. The outlying data points in Figure 5.2.2.1.1 a) might be caused by a fluctuating mineralogical composition, in particular the reactivity of the aluminate phase and the availability of sulfates.

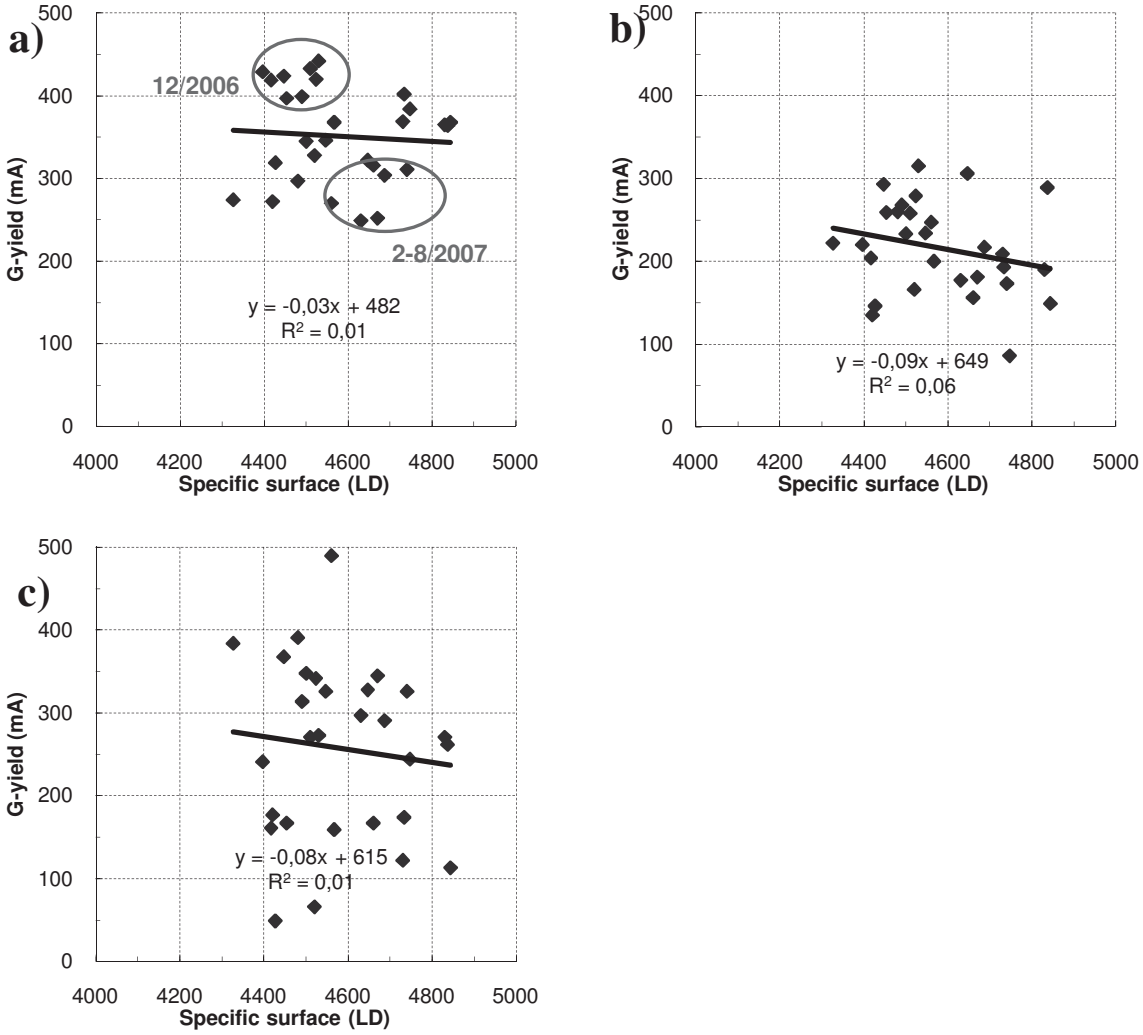

Figure 5.2.2.1.1: Effect of specific surface on G-yield in blank (a), PC1 (b) and Mel (c) mixes

Cements A1, A2, B1 and B2 showed the same trend. In mixes without admixtures the G-yield increased with increasing specific surface, whereas this trend did not hold in mixes with admixtures. Note that the relatively small number of samples (only 3-5 production dates per cement) limits the evaluation.
The effect of particles smaller than 1,8 µm on rheology can be seen in Figure 5.2.2.1.2. The testing range from 0 to 1,8 µm represents partly the colloidal particles in the cementitious system. A higher amount of colloidal particles results in a higher specific surface. Hence, the trend observed here correlates with the results from previous chapter. After the first 12 cement production dates it was found that with increasing content of colloidal particles, the G-yield (mA) in the blank mixes increased (see Figure 5.2.2.1.2 a). However, with the latest deliveries (from 12/2006 to 8/2007) this trend did not hold. It is logical that the higher the amount of colloidal particles, the higher the water demand of the cement will be, finally resulting in a higher yield stress. This trend was not observed in the mixes with dispersing admixture. The amount of colloidal particles had no clear effect on G-yield (mA) in mixes with polycarboxylate (PC1) or melamine. According to these results, the amount of colloidal particles is not a major influencing factor on rheology when dispersing admixtures are present.

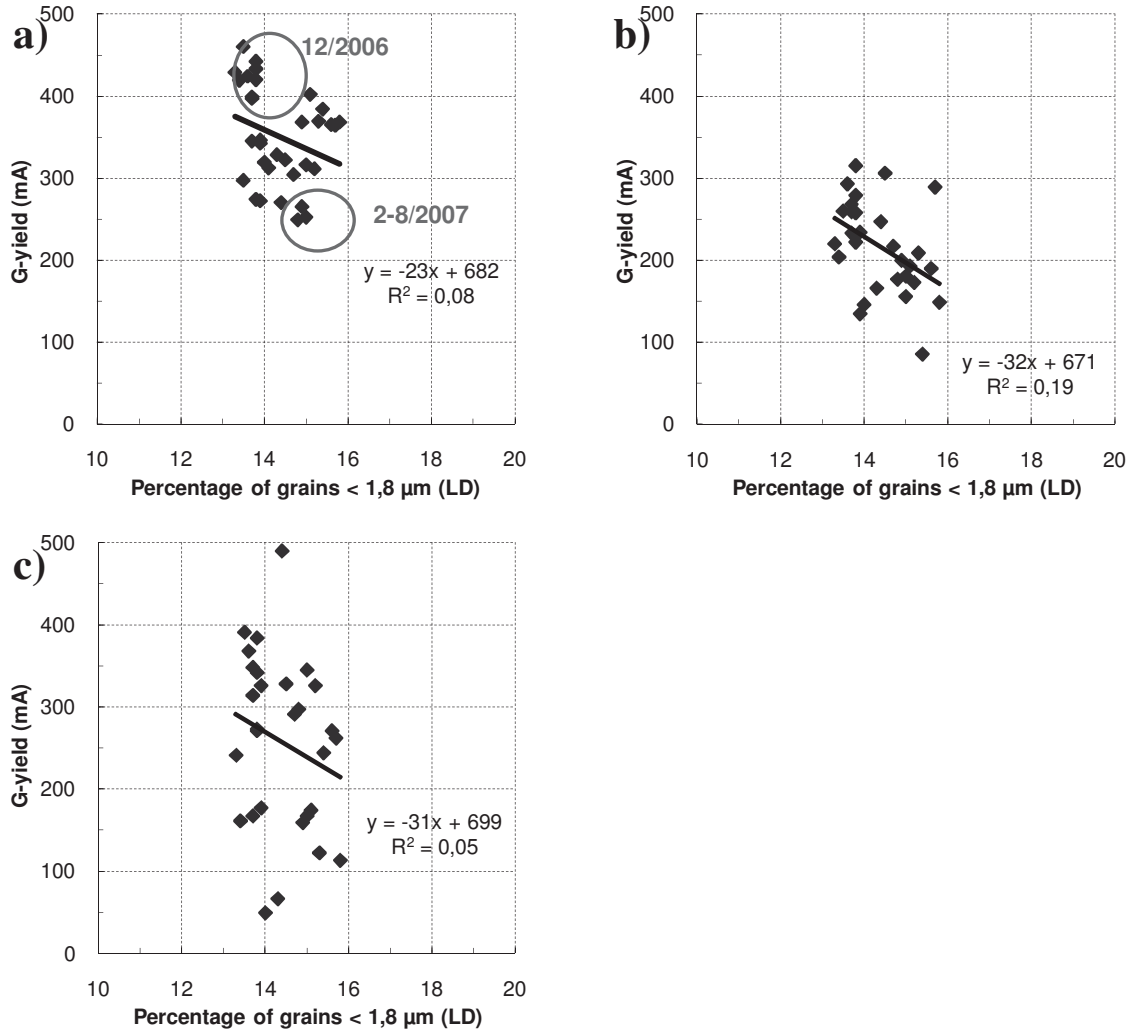

Figure 5.2.2.1.2: Effect of particle size on G-yield in blank (a), PC1 (b) and Mel (c) mixes

5.2.2.2 Dynamic particle size distribution during first hour of hydration

Cements covering the complete territory of rheological parameters were investigated on their particle size distribution after having hydrated for distinct times (dynamic PSD). Granulometric measurements were done after 1, 15, 30, 45 and 60 minutes of hydration by use of a COULTER LS 230 laser granulometer. Measurements were done on pastes with and without admixtures (PC1). The water to cement ratio of the paste without admixture was 0,46 and the w/c-ratio of the mix containing 0,11% PC1 was 0,36, identical to those of mortars investigated. The measuring range of the device is between 0,04 µm and 2000 µm. All cement samples were measured in isopropanol (water-free), which stops the cement hydration immediately. The transport medium was running in a closed loop within the device. Reference measurements were done on the unhydrated cement.

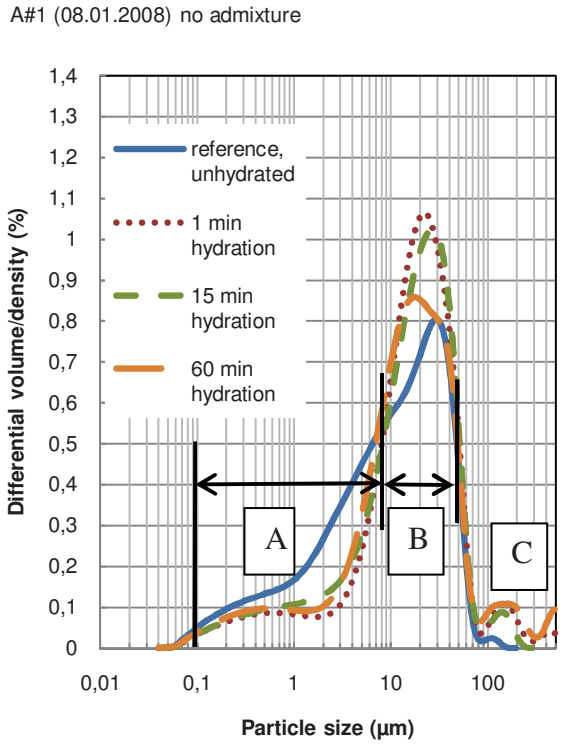

Figure 5.2.2.2.1: Particle size distribution as a function of hydration time (paste without admixture)

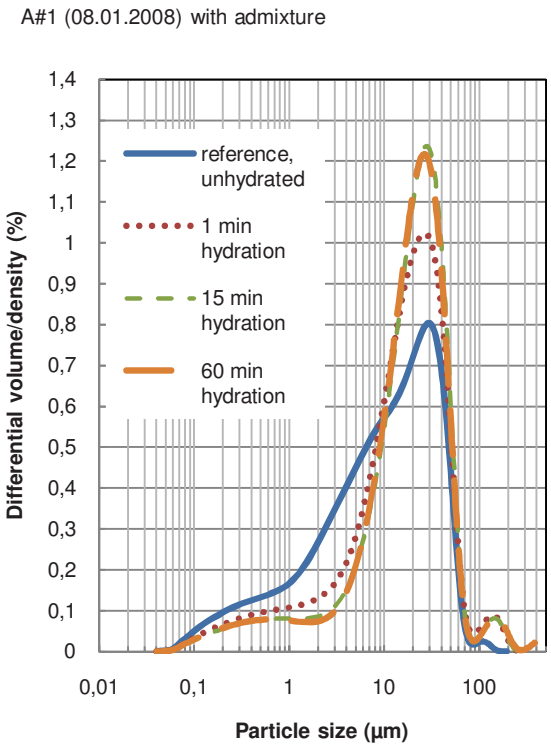

Figure 5.2.2.2.2: Particle size distribution as a function of hydration time (paste with admixture)

The observations made during this investigation are partly in line with observations reported in earlier studies /Er 1, Sta 6, Mu 1/. The following major trends were observed:

- The differential volume (amount of particles) in the range of 0,1 to 8 µm decreases significantly during the first minute of hydration (see area A in Figure 5.2.2.2.1). This can be stated for pastes with/without admixtures.
- The differential volume (amount of particles) in the range of 8 to 50 µm increases significantly during the first minute of hydration (see area B in Figure 5.2.2.2.1). This was observed in pastes with/without admixtures.
- Some cements form agglomerates >100 µm during the first minute of hydration, both in pastes with/without admixtures (see area C in Figure 5.2.2.2.1).
- The dispersing admixture (polycarboxylate) has no clear influence on the particle size distribution, meaning the system with admixture was not necessarily better dispersed than without the admixture (see Figure 5.2.2.2.3).

- During first 15 minutes of hydration, pastes with admixture contained less colloidal particles (0,1 to 8 µm) than pastes without admixture (see Figure 5.2.2.2.3 and 5.2.2.2.4). According to these results, the formation of bigger agglomerates (made of smaller particles) is more prominent when admixture is present.
- There is the likelihood that the shifting in particle size distribution influences the rheological properties. Cements with a lower yield value (good flowability) seem to form more agglomerates in area B (8 to 50 µm) than cements with a higher yield value (poor rheology). Or in other words cement with a lower yield value have fewer colloidal particles in area A (0,1 to 8 µm) after one minute hydration than cement with a higher yield value.

Table 5.2.2.2.1: Cements investigated and their rheology in mortar

Sample	Production date	Blank mortar (no admixture) Yield value (Pa)	Blank mortar (no admixture) Plastic viscosity (Pa·s)	PC1 mortar (0,11 % PC1) Yield value (Pa)	PC1 mortar (0,11 % PC1) Plastic viscosity (Pa·s)
A#1	08.01.2008	292	5	116	6
A#2	19.07.2007	352	5	194	6
A#3	01.12.2006	433	7	322	8
A#4	06.01.2006	299	5	296	9
A#5	19.12.2007	248	5	115	7

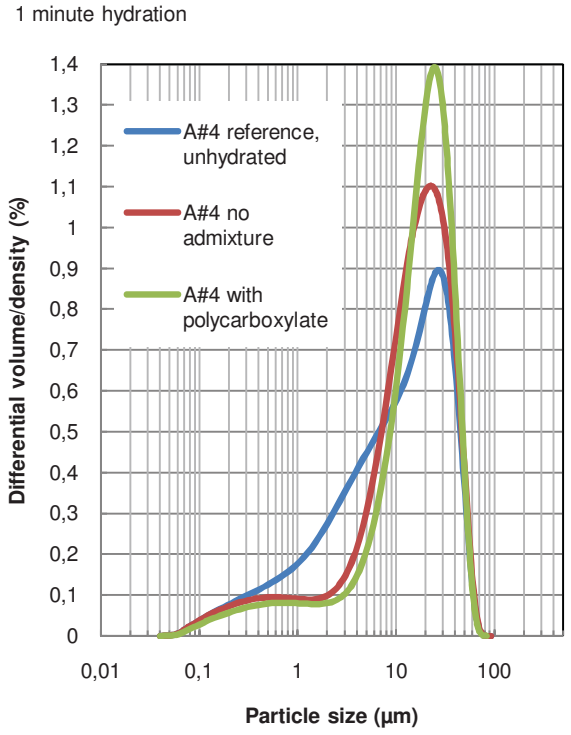

Figure 5.2.2.2.3: Particle size distribution after one minute hydration with/without admixture

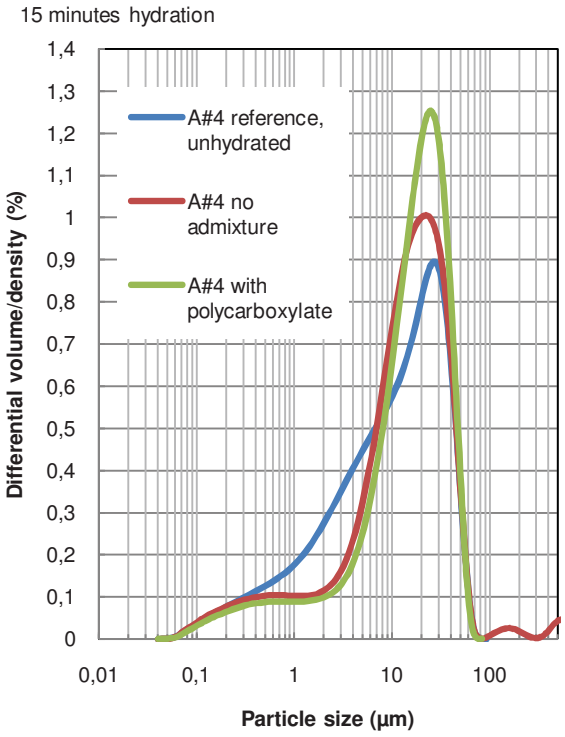

Figure 5.2.2.2.4: Particle size distribution after 15 minutes hydration with/without admixture

In the unhydrated state, the particle size distribution differed slightly between single cement production dates (see Figure 5.2.2.2.5). In pastes with polycarboxylate, the biggest difference in particle size distribution between cement production dates was observed after 1 minute of hydration (see Figure 5.2.2.2.6). At later testing ages (such as 15, 30, 45 and 60 minutes), the difference in particle size distribution between deliveries became smaller (see Figures 5.2.2.2.7 and 5.2.2.2.8). Surprisingly, the particle size distribution of pastes without admixture differed much more between single cement production dates than those with admixture. It

appears as if the dispersing admixture reduces the variations in particle size distribution due to some kind of homogenising effect (see Fig. 5.2.2.2.7 and Fig. 5.2.2.2.8).

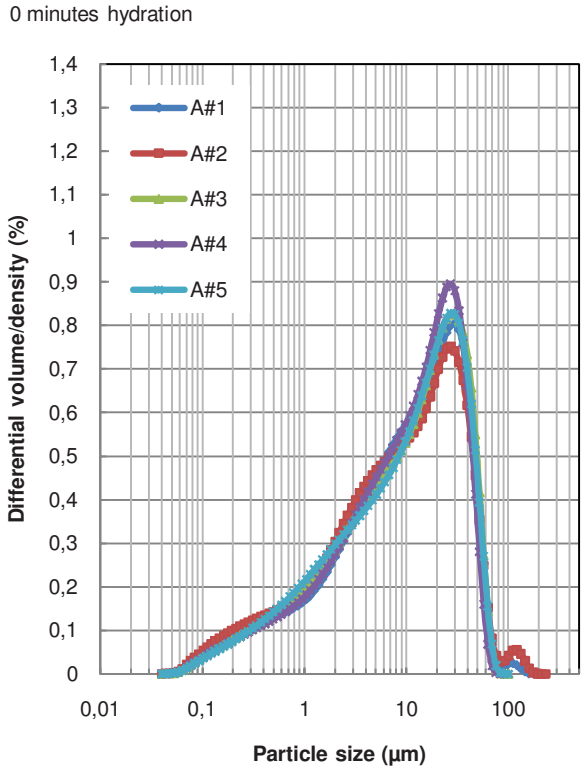

Figure 5.2.2.2.5: Particle size distribution of unhydrated cement

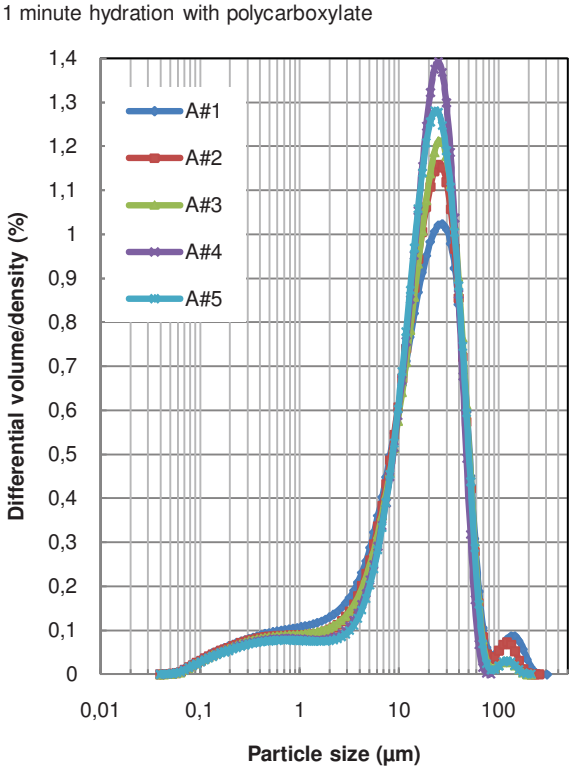

Figure 5.2.2.2.6: Particle size distribution after 1 minute hydration with admixture

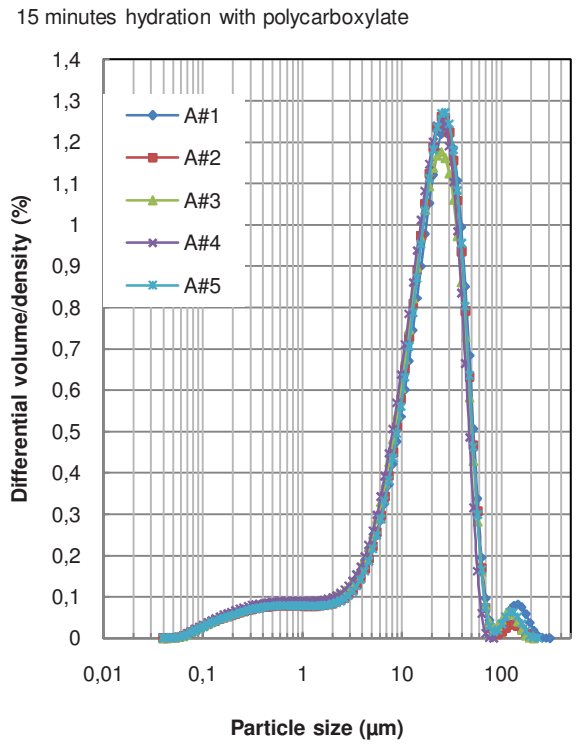

Figure 5.2.2.2.7: Particle size distribution after 15 minutes hydration with admixture

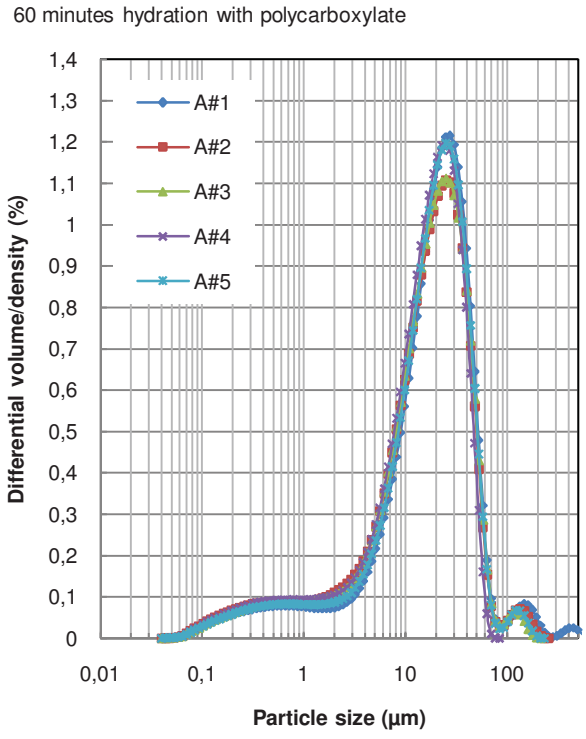

Figure 5.2.2.2.8: Particle size distribution after 60 minutes hydration with admixture

5.2.3 Aluminate phase

5.2.3.1 Effect of aluminate phase (modified Taylor-Bogue) on rheology

The aluminate phase is the most reactive constituent in cement. The hydration reaction starts directly when the aluminate phase gets in contact with water. Results from mineralogical measurements (modified Bogue and QXRD) on cement C indicate that the aluminate phase is in a narrow bandwidth. The C_3A bandwidth is very low for a correlation. However, the results indicate that the C_3A content of cement C is quite stable during routine cement production. Within 29 different production dates the C_3A content was ranging from 4,3 to 5,5%, whereas the G-yield varied between 100 mA and 400 mA. In mixes without admixtures no relationship was found between the G-yield and the C_3A content (see Figure 5.2.3.1.1 a)). This might be natural as in blank mixes the G-yield did not change too much. A linear correlation between C_3A content and water demand, which is often mentioned in literature, could not be observed. A similar picture showed up when polycarboxylate (PC1) or melamine was added to the mixes (see Figure 5.2.3.1.1 b) and c)). Though, in mixes with admixtures there seems to be a trend that with increasing C_3A content, the G-yield increases. In the beginning of the project, when the number of cement production dates was around ten, the correlation coefficients were better. It seems as if with increasing number of cement samples the established relations do not hold for all cement production dates. This is logical as cement is a multi compound system produced on a big scale where each property is changing slighty in a new cement batch. Note that the results for C_3A were determined by use of modified Taylor-Bogue equations and Rietveld refinement. The aluminate phase determined by use of modified Taylor-Bogue can differ around ±10% compared to Rietveld.

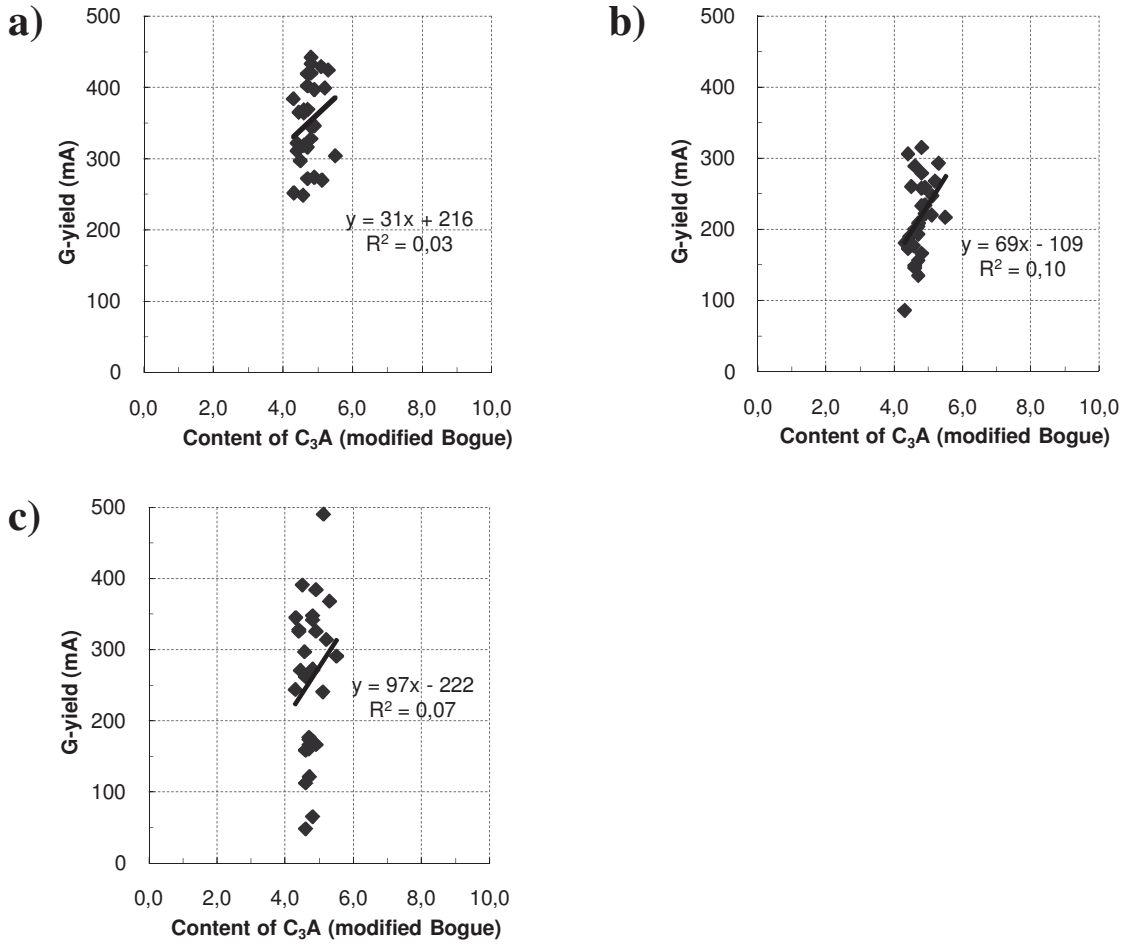

Figure 5.2.3.1.1: Effect of aluminate phase on G-yield in blank (a), PC1 (b) and Mel (c) mixes

5.2.3.2 Effect of C_3A addition on rheology

The effect of C_3A addition was investigated by using a sulfate resistant cement with a C_3A content of 3% as a reference. Scope and objective of this part of the project was to investigate the effect of increasing C_3A content on rheology in mixes with and without admixtures while the sulfate content remained unchanged. The C_3A was of orthorhombic and cubic type. According to literature sources, the orthorhombic is considered to be the more reactive type. Synthetically produced C_3A was milled by use of a ball mill to a specific surface of 4500 cm²/g, and was added in exchange for reference cement. The w/c-ratio of the mixes without admixtures was 0,50, and the w/c-ratio of the mixes containing PC1 was 0,42 (0,10% PC1 by weight of cement). Results are given in table 5.2.3.2.1.

Table 5.2.3.2.1: Results of C_3A addition in blank and PC mixes

		orthorhombic type of C_3A		cubic type of C_3A	
Mix	C_3A content (%)	G-yield (mA)	H-viscosity (mA s)	G-yield (mA)	H-viscosity (mA s)
Reference blank	**3**	145	79	145	79
blank +2%C_3A	**5**	218	46	176	73
blank +4%C_3A	**7**	232	49	231	77
Reference PC	**3**	92	102	92	102
PC +2%C_3A	**5**	177	96	251	149
PC +4%C_3A	**7**	247	97	280	125

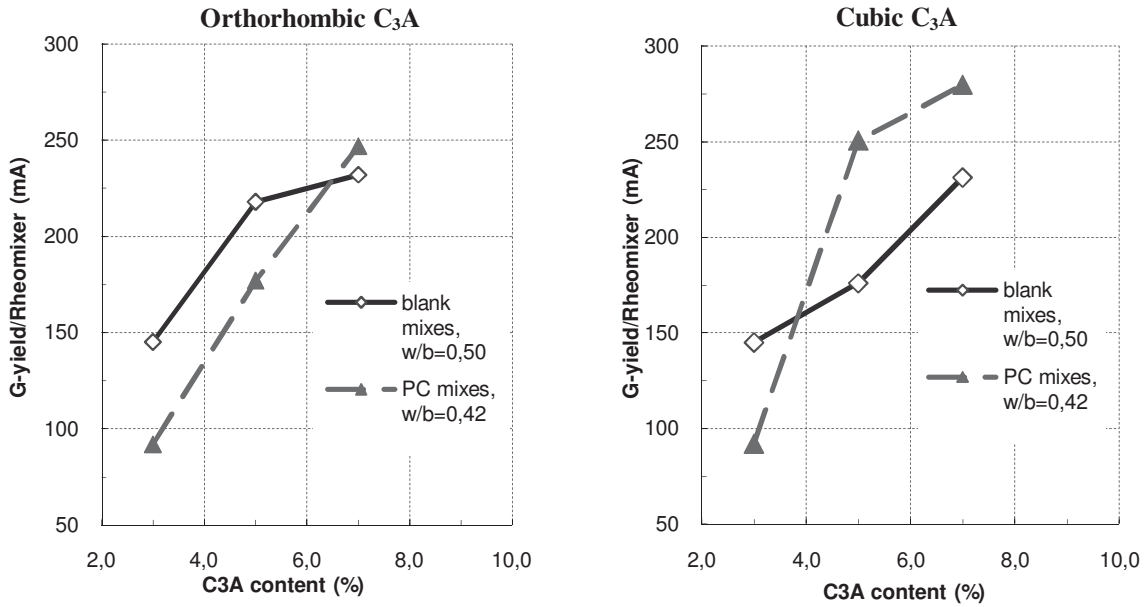

Figure 5.2.3.2.1: Effect of orthorhombic and cubic C_3A on rheology

The results in Figure 5.2.3.2.1 show that there is a linear relationship between C_3A content and G-yield in mixes with and without admixtures. For both types of C_3A it can be stated that with increasing C_3A content the G-yield increased. The G-yield of mixes containing PC1 increased more than the G-yield of mixes without any admixture. This can be explained by the higher w/c-ratio in blank mixes and therefore higher content of water as dispersing and diluting liquid. A higher reactivity of the orthorhombic type of C_3A (in terms of higher water demand) can not be concluded from these results. According to these results it might be even questionable if there are differences in reactivity between both types of C_3A. Again, the sharp increase in G-yield due to C_3A addition was generated by the lack of sulfates. The hydration process is also influenced by the C_3A addition (see Appendix G). However, these results show how important the balance between C_3A content and gypsum actually is for a well balanced cementitious suspension.

5.2.3.3 Mineralogical composition obtained by QXRD (Rietveld)

The mineralogical composition of cement C and D was measured by use of modified Taylor-Bogue and quantitative X-ray diffraction (QXRD) according to Rietveld. While modified Taylor-Bogue is based on indirectly calculated values, Rietveld is based on directly measured values. According to a NIST report /Stu 1/, the accuracy of QXRD, given careful experimental procedure, is about 2% to 5% absolute for alite and belite and 1% to 2% for aluminate and ferrite. Rietveld is considered to become state of the art for quality control in cement plants. The composition of cement C obtained by both methods is given in table 5.2.3.3.1. This was mainly done to compare and verify results from modified Taylor-Bogue. Remarkable differences in mineralogical composition for the major constituents were observed. Comparing the Rietveld results with the results obtained by modified Taylor-Bogue, Rietveld gave lower values for alite and ferrite, and higher values for belite and aluminates. Differences in the results are due to different sources, laboratories, instruments and methods. For example, small impurities in the clinker can have a great effect on the mineralogical composition. Impurities are measured by QXRD but they are not considered in modified Taylor-Bogue equations. Further cement constituents measured by Rietveld are anhydrite, bassanite/hemi hydrate, calcite, gypsum, periclase, portlandite, quartz and syngenite. Such minor constituents can no be calculated by modified Taylor-Bogue.

Table 5.2.3.3.1: Mineralogy of cement C (4 deliveries)

	C#6		C#7		C#8		C#9	
	Modified Bogue	QXRD/ Rietveld	Modified Bogue	QXRD/ Rietveld	Modified Bogue	QXRD/ Rietveld	Modified Bogue	QXRD/ Rietveld
CaO (%)	65,4		65,2		65,3		65,6	
SiO_2 (%)	19,6		19,8		19,7		19,8	
Al_2O_3 (%)	5,0		5,0		5,0		5,0	
Fe_2O_3 (%)	3,3		3,4		3,4		3,4	
SO_3 (%)	3,4		3,3		3,3		3,3	
MgO (%)	0,7		0,8		0,8		0,9	
K_2O (%)	0,5		0,4		0,5		0,4	
Na_2O (%)	0,1		0,1		0,1		0,1	
Total (%)	97,8		98,0		98,1		98,5	
CaO $_{free}$ (%)	1,3		1,2		1,5		1,4	
CaO $_{eff}$ (%)	61,7		61,7		61,4		61,9	
C_3S (%)	61,8	***54,5***	59,6	***51,0***	58,6	***49,9***	60,2	***52,6***
C_2S (%)	10,8	***20,4***	13,3	***22,8***	13,8	***21,5***	12,8	***20,2***
C_3A (%)	4,9	***4,5***	4,3	***3,7***	4,6	***3,5***	4,6	***3,4***
$C_2(A,F)$ (%)	11,8	***13,9***	12,4	***15,3***	12,4	***16,4***	12,2	***15,8***
$C_3S+C_2S+C_3A+C_2(A,F)$ (%)	89,3		89,6		89,4		89,8	
CaO $_{eff}$ $+SiO_2+Al_2O_3+Fe_2O_3$ (%)	89,3		89,6		89,4		89,8	

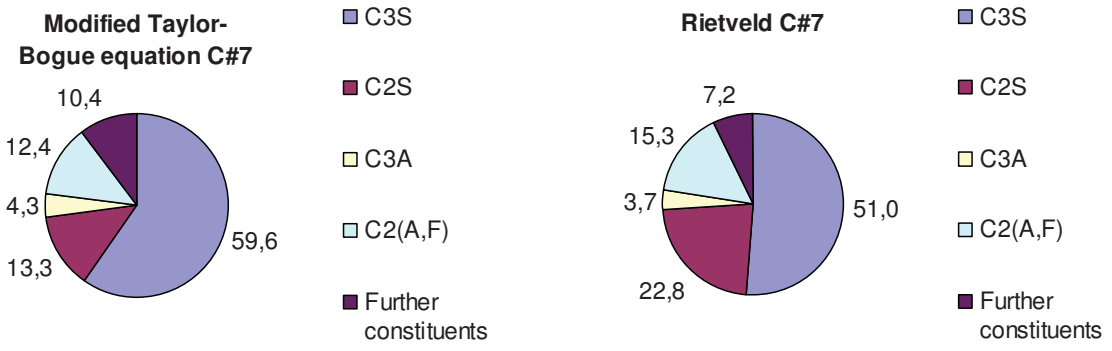

Figure 5.2.3.3.1: Comparison of clinker phase composition for cement C#7

5.2.4 Alkalies

5.2.4.1 Effect of Na_2O equivalent of reference cement on rheology

The literature survey showed that alkalies originating from cement can influence the rheological properties of mortar and concrete. Hence, rheological properties of mortar were correlated with the Na_2O equivalent of 29 cement production dates. Similar to chapter 5.2.3 the reference cement was relatively stable; it showed only little variations within the alkalies. The Na_2O equivalent of 29 cement production dates was varying from 0,29 to 0,47. This indicates a steady production process of cement C. No relationship was found between the G-yield and the Na_2O equivalent if no admixtures or melamine was present (see Figure 5.2.4.1.1 a) and c)). The relation between G-yield and Na_2O equivalent in mixes containing PC1 was slightly better but still far off from previous results (Figure 5.2.4.1.1 b)). Although the correlation is relatively weak there seems to be some influence of alkalies on yield stress when PC1 is present. It should be noted that the Na_2O equivalent is not the same as the amount of soluble alkalies. Only the readily available soluble alkalies can interact with the admixture. This could be the reason for the somewhat weak correlation between rheological data and Na_2O equivalent. With more soluable alkalies the ionic strength in the mortar is increased so that mainly electrostatic repulsion is lowered. As a result the cement grains are getting closer to form agglomerates, and the yield value increases.

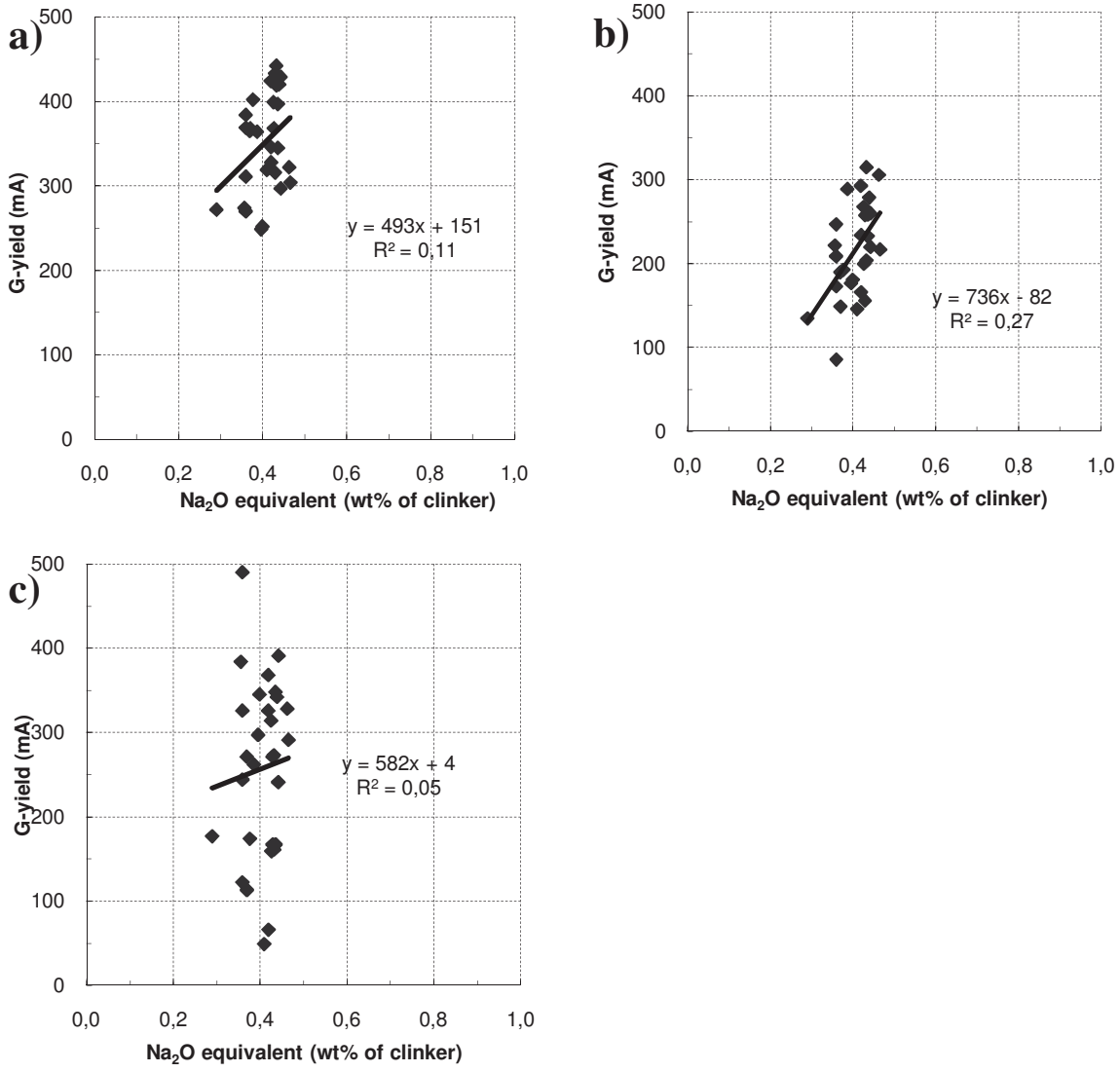

Figure 5.2.4.1.1: Effect of alkalies on G-yield in blank (a), PC1 (b) and Mel (c) mixes

5.2.4.2 Effect of sodium and potassium hydroxide on rheology

The previous chapter indicates that alkalies might have an impact on a cementitious suspension when polycarboxylate (PC1) is used for dispersing this suspension. However, the effect of alkalies in a system without admixtures or in a system with melamine is different. Hence, a study was carried out to investigate how sodium and potassium influence the rheology in mortar. Alkalies were added in form of sodium (NaOH) and potassium hydroxide (KOH). A delivery of cement C (18.04.2008) was taken as the reference. Sodium and potassium hydroxide were added to normal tap water. Note that the water was not added before all hydroxide was completely dissolved in it. When sodium (or potassium) hydroxide comes in contact with water at 20°C it dissolves in a sodium (or potassium) cation and an OH anion. In water, the cations and anions are then surrounded by water molecules due to the dipol properties of water. The dissolving process of sodium and OH ions in water is an exothermic reaction. By adding 0,5% NaOH (by weight of cement), the Na_2O equivalent increased by 0,29%. Table 5.2.4.2.1 gives the results of the rheological measurements.

Table 5.2.4.2.1: Rheological results of sodium hydroxide addition to mortar

NaOH added to mix	Blank mixes (no admixtures)				PC mixes (PC1)				Mel mixes (melamine)			
	Rheomixer		Viscometer		Rheomixer		Viscometer		Rheomixer		Viscometer	
	G (mA)	H (mAs)	τ (Pa)	μ (Pas)	G (mA)	H (mAs)	τ (Pa)	μ (Pas)	G (mA)	H (mAs)	τ (Pa)	μ (Pas)
Reference	295	111	257	4	221	213	185	7	397	117	374	4
0,5% NaOH	217	125	186	5	334	217	277	7	462	174	411	6
1,0% NaOH	203	112	175	4	540	180	490	8	374	188	322	7
1,5% NaOH	293	123	252	5	too stiff, not measureable				too stiff, not measureable			

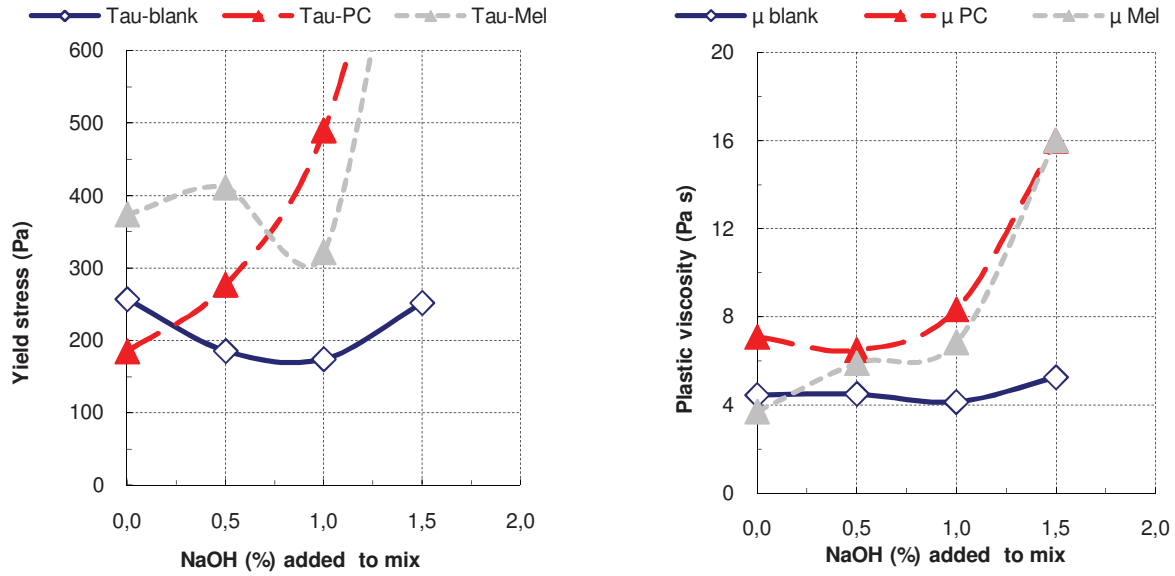

Figure 5.2.4.2.1: Effect of addition of sodium hydroxide on yield stress and plastic viscosity

Figure 5.2.4.2.1 depicts the effect of addition of sodium hydroxide on rheology in blank, PC1 and Mel mixes. The data shown here was obtained by use of the coaxial cylinder system ConTec Viscometer 6. Results with the impeller based Rheomixer show the same trend. By adding sodium hydroxide to mixes without any admixtures the yield stress decreased. A decreasing yield stress means that the mixes became more fluid. It is not clear yet if this is a result of the higher pH value and its effect on ettringite morphology. Alkalies influence the hydration process, in particular during the early hydration. An increasing alkali content leads to an increase in pH value and further on to an alteration of the shape of the primary hydration products like ettringite. With lower pH value, ettringite occurs as needle-shaped formations

with a length of 10 to 100 µm and a thickness of several µm. At higher pH values, ettringite has the shape of rod-like crystals with a length of 1 to 2 µm and a thickness of 0,1 to 0,2 µm /Me 1/. One hypothesis is that the addition of sodium hydroxide could have resulted in the formation of hydration products which generated the lower yield stress of the blank mix.
The broken red line (see Figure 5.2.4.2.1) indicates the mixes with the polycarboxylate based admixture PC1. When the sodium content and pH value increased the yield stress increased significantly. Increasing the Na_2O-equivalent from 0,6% to 1,1% (due to 1,0% NaOH addition), the yield stress dropped by a factor of 2,5, whereas the plastic viscosity remained unchanged. After adding 1,5% sodium hydroxide (by weight of cement), the mix became too stiff for a measurement in Rheomixer and Viscometer. The interesting question is of course, did the sodium ions lower the steric effect of the polycarboxylate side chains (and electrostatic repulsion) or did changes in microstructure between the cement particles result in this high yield stress? Cement pastes having the same water to cement ratio and admixture dosage as the tested mortars were investigated by use of a SEM. Note that the hydration of the cement pastes displayed here was stopped with liquid nitrogen 15 minutes after water addition. Figure 5.2.4.2.2 depicts the reference paste for this study. The reference paste had a water to cement ratio of 0,36 and contained 0,11% polycarboxylate (PC1). Its corresponding mortar had a yield stress of 200 Pa and plastic viscosity of around 7 Pa·s, indicating a mix with self levelling properties. Most surfaces of the cement grains were covered with small ettringite blocks in the size of 0,1 to 0,5 µm and gypsum prisms of various shapes and sizes. Some cement production dates contained coccolithophorids. Coccolithophorids are unicellular planktonic algae /W8, W9/. On the death of the organism, the individual coccoliths fall to the seafloor to make a major contribution to the calcareous oozes. The stratigraphical range of coccolithoporids is long, from the Triassic to Recent /W8/.

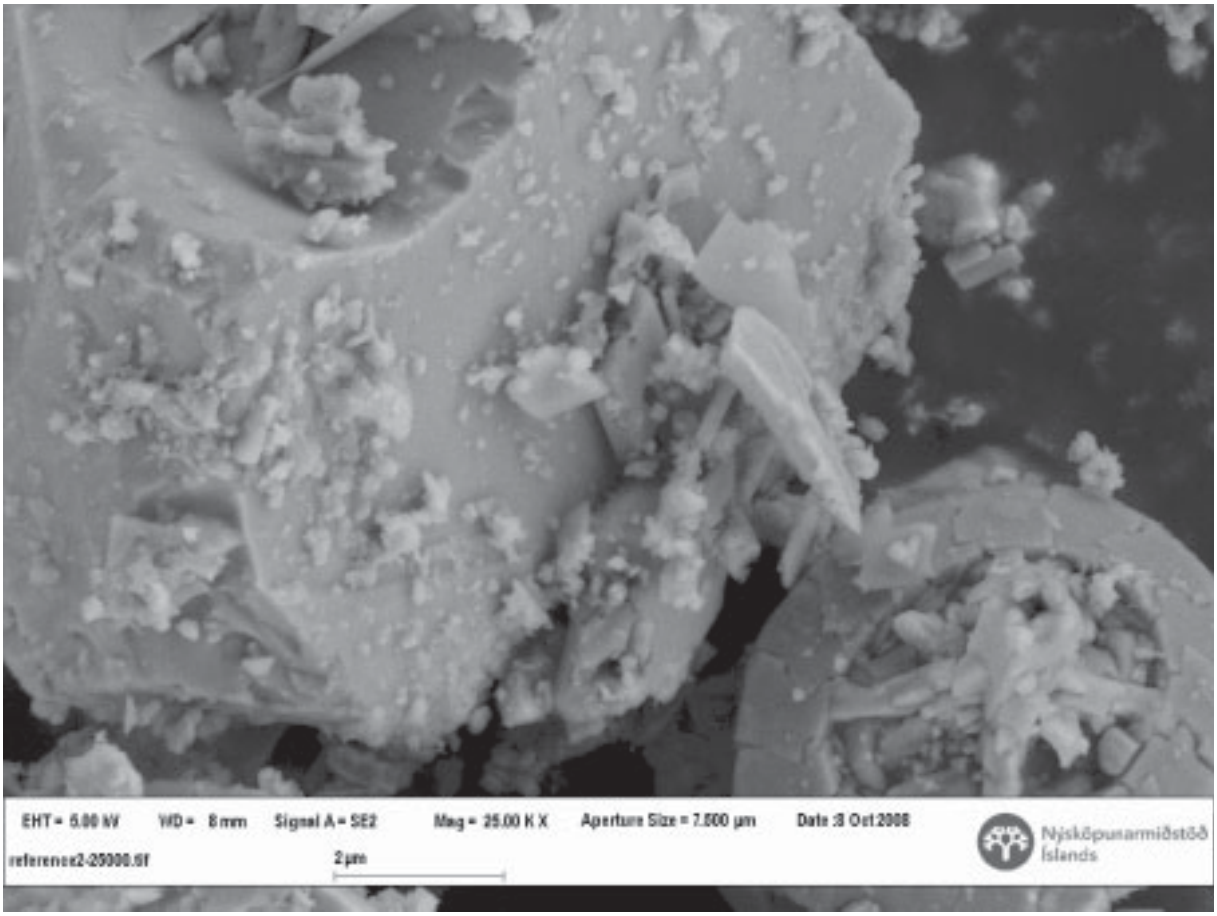

Figure 5.2.4.2.2: Reference SEM picture (magnification 25000) of Portland cement grain, 0,11% PC1 at w/c of 0,36 and coccolithophorid in right corner

The microstructure of a paste having the composition of the reference plus 1,0% of NaOH is displayed in Figure 5.2.4.2.3. The corresponding mortar mix (containing 1,0% NaOH) gave a yield stress of 500 Pa and a plastic viscosity of around 8 Pa·s, indicating a rather stiff mix which can be cut like a cake. Like in the reference mix, the surface of the cement grains was covered with ettringite, gypsum in various sizes and all kind of remains from freeze dried pore solution. The surface of single cement grains did not show significant differences between the reference paste and the paste containing 1,0% NaOH.

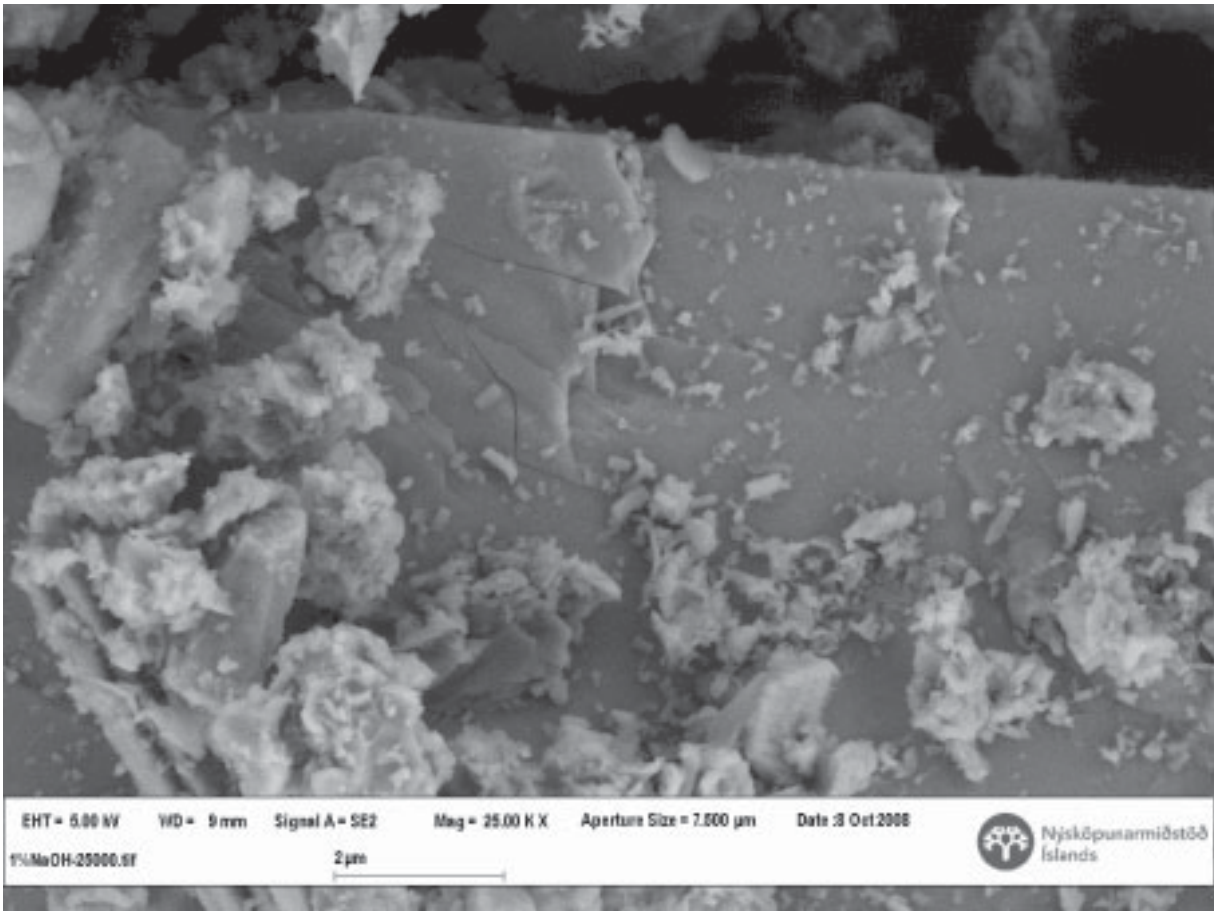

Figure 5.2.4.2.3: SEM picture (magnification 25000) of Portland cement grain, 0,11% PC1 at w/c of 0,36 containing 1,0% NaOH

An interesting observation was made with mixes containing melamine (see dotted grey line in Figure 5.2.4.2.1). When 0,5% sodium hydroxide was added, the yield stress increased slightly. This increase seems logical as the pH value increased, thus increasing the ionic strength of the pore solution. Surprisingly, when 1,0% sodium hydroxide was added, the yield stress went down significantly (from 400 Pa to 300 Pa), whereas the plastic viscosity showed a continuous increase. If 1,5% sodium hydroxide was added to the water, the mix became too stiff and not measurable. At 1,5% NaOH, the mix showed a flash set or false set-like behaviour. It was obvious that the dispersing effect of the melamine was neutralized. The sinusoidal waveform of the yield stress curve shows that there is no linear relation between the yield stress and the sodium or potassium ion concentration in mixes with melamine. This explains also why no relation was found for sodium equivalent and yield stress in Mel mixes (chapter 5.2.4.1). The addition of potassium hydroxide resulted in trends more or less identical to those of mixes with sodium hydroxide. Note that due to the higher molecular weight of potassium in comparison to sodium, the potassium hydroxide was added at slightly higher dosage (0,5% versus 0,7%) than sodium hydroxide to reach a similar ionic concentration. By comparing the rheological data it becomes obvious that potassium and

sodium, if present at same concentration, have the same effect on yield stress and plastic viscosity. However, microstructural investigations on pastes containing 0,5% or 1,0% KOH show clear differences in comparison to pastes containing NaOH. Figures 5.2.4.2.5 and 5.2.4.2.5 depict the microstructure of KOH blended pastes showing needle shaped crystal formation. The EDX spectrum of these crystal formations was close to syngenite. The needles were observed even at a dosage of 0,5% KOH. However, the amount of syngenite formed at 0,5% KOH (what can be seen in Figure 5.2.4.2.5) does not affect the rheological properties of the mortar mix (see Figure 5.2.4.2.4 left). In pastes with 1,0% KOH, significantly more syngenite was observed in the free space between the cement grains and also on the cement grain surface (see Figure 5.2.4.2.6). The rheological data of the mortar with polycarboxylate (displayed in Figures 5.2.4.2.4 left and right) shows that the addition of KOH resulted only in an increase in yield stress but not in plastic viscosity. Hence, the question arises if this increase in yield stress can be attributed only to the formation of syngenite. Below a certain threshold value, the syngenite needles influence yield stress but not plastic viscosity. The content of syngenite needles, displayed in Figure 5.2.4.2.6, is obviously not high enough to affect the plastic viscosity of the mortar. A critical threshold value for syngenite, to have an effect on rheological properties, is in the vicinity of 1%.

Table 5.2.4.2.2: Rheological results of potassium hydroxide addition to mortar

KOH added to mix	**Blank mixes (no admixtures)**				**PC mixes (Polycarboxylate)**				**Mel mixes (Melamine)**			
	Rheomixer		Viscometer		Rheomixer		Viscometer		Rheomixer		Viscometer	
	G (mA)	H (mAs)	τ (Pa)	μ (Pas)	G (mA)	H (mAs)	τ (Pa)	μ (Pas)	G (mA)	H (mAs)	τ (Pa)	μ (Pas)
Reference	295	111	257	4	246	201	225	7	351	114	360	3
0,7% KOH	234	119	214	5	275	204	231	6	609	157	553	8
1,4% KOH	316	110	282	4	540	180	452	7	421	173	394	7
2,1% KOH	373	105	319	5	too stiff, not measurable				too stiff, not measurable			

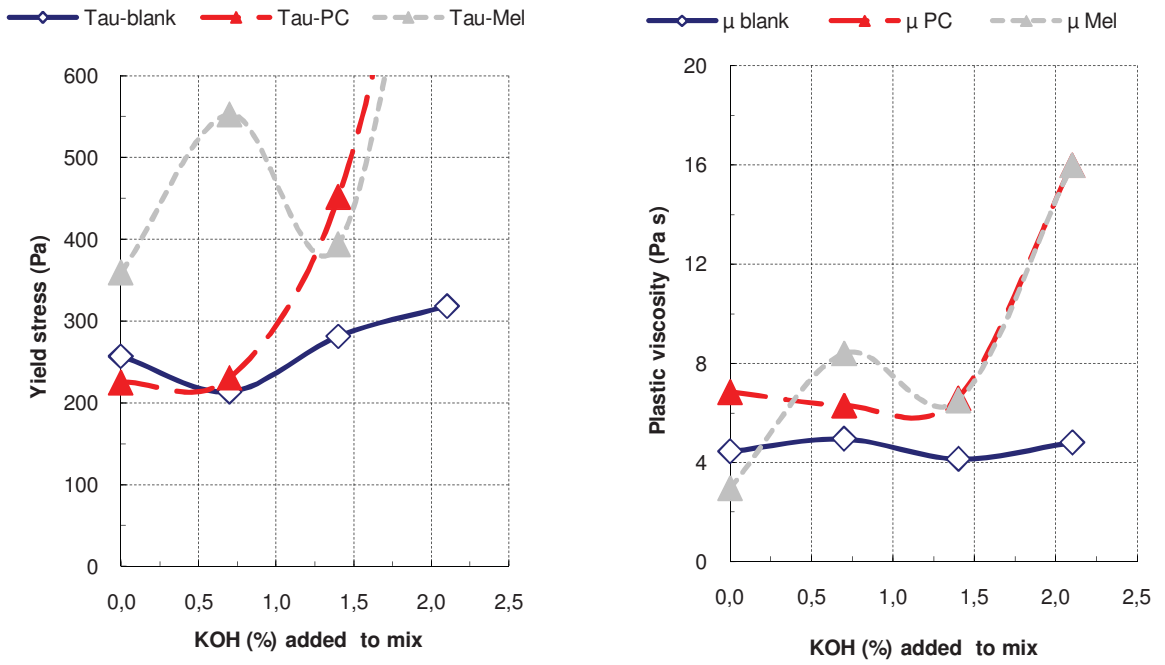

Figure 5.2.4.2.4: Effect of addition of potassium hydroxide on yield stress and plastic viscosity

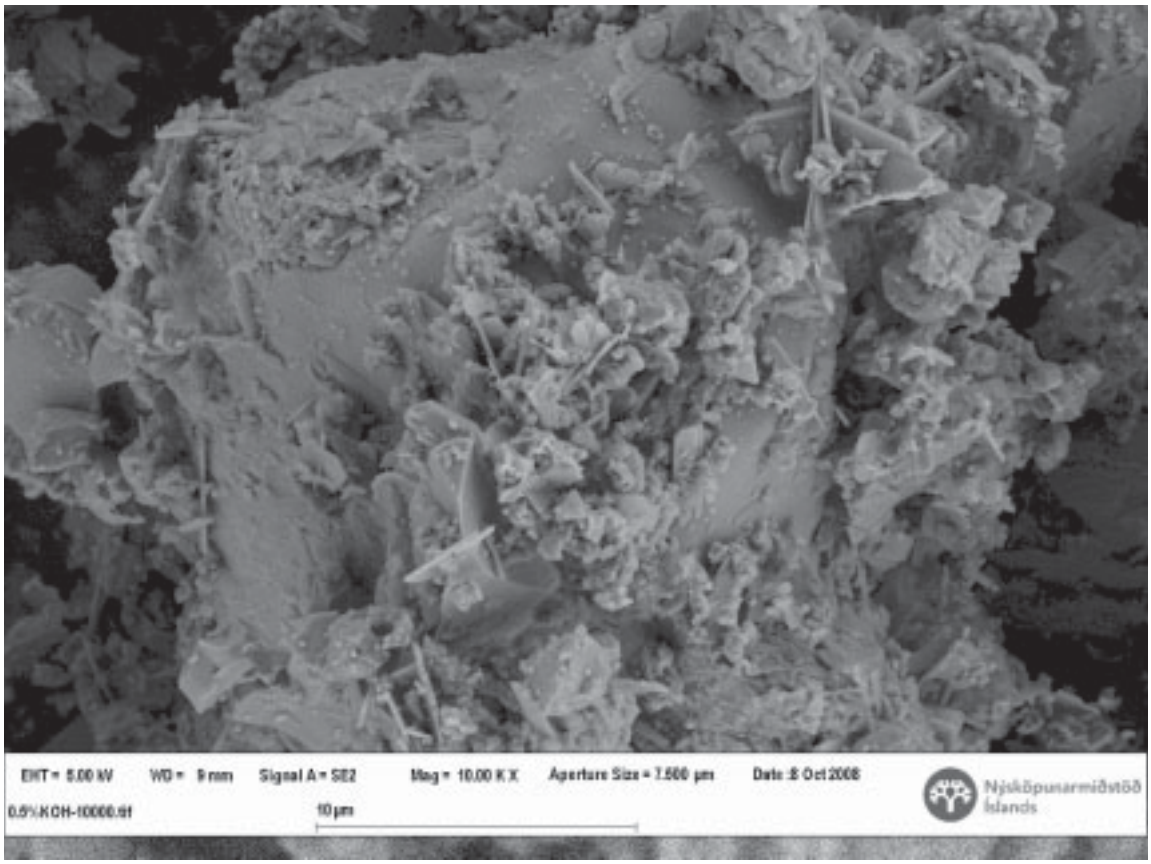

Figure 5.2.4.2.5: SEM picture (magnification 10000) of Portland cement grain, 0,11% PC1 at w/c of 0,36 containing 0,5% KOH

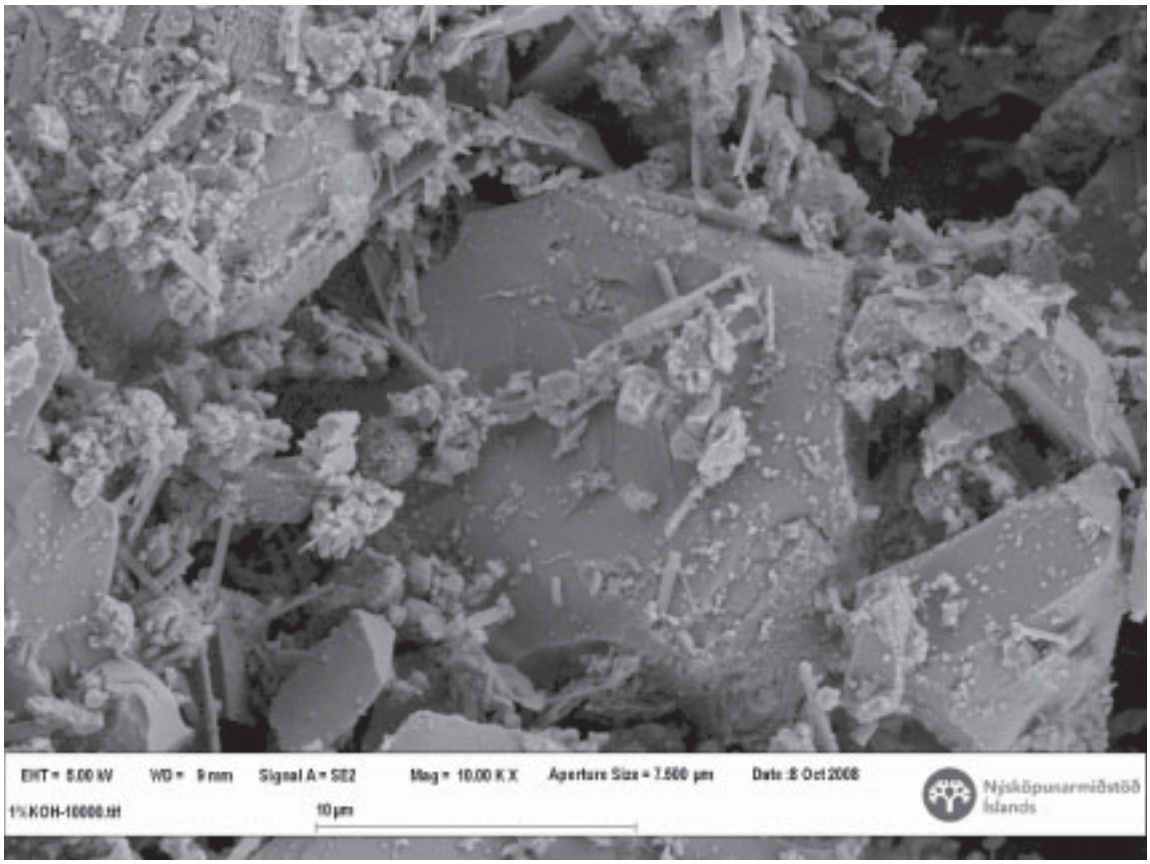

Figure 5.2.4.2.6: SEM picture (magnification 10000) of Portland cement grain, 0,11% PC1 at w/c of 0,36 containing 1,0% KOH

5.2.4.3 Effect of sodium and potassium hydroxide on hydration process

The effect of sodium hydroxide on hydration (blank mixes) can be seen in Figure 5.2.4.3.1. The addition of sodium hydroxide accelerated the hydration process considerably. From the curves it can be seen that the dormant period was reduced by up to 2 hours. The rate of hydration (incline of curves after the dormant period) was accelerated when sodium hydroxide content increased. Identical results were obtained with potassium hydroxide (see Appendix G).

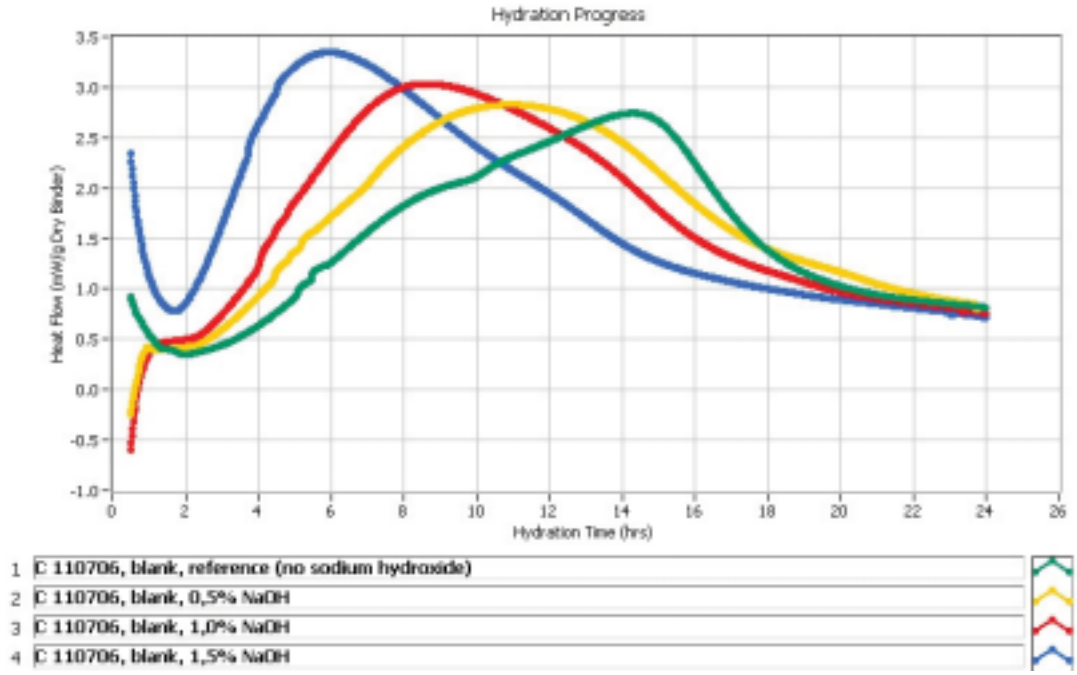

Figure 5.2.4.3.1: Effect of sodium hydroxide addition on hydration process in blank mixes

Figure 5.2.4.3.2 depicts the effect of sodium hydroxide addition on hydration process in mixes containing polycarboxylate (PC1). Like in blank mixes, sodium hydroxide accelerated the hydration process and reduced the dormant period significantly. This was also observed in mixes containing melamine (see Appendix G).

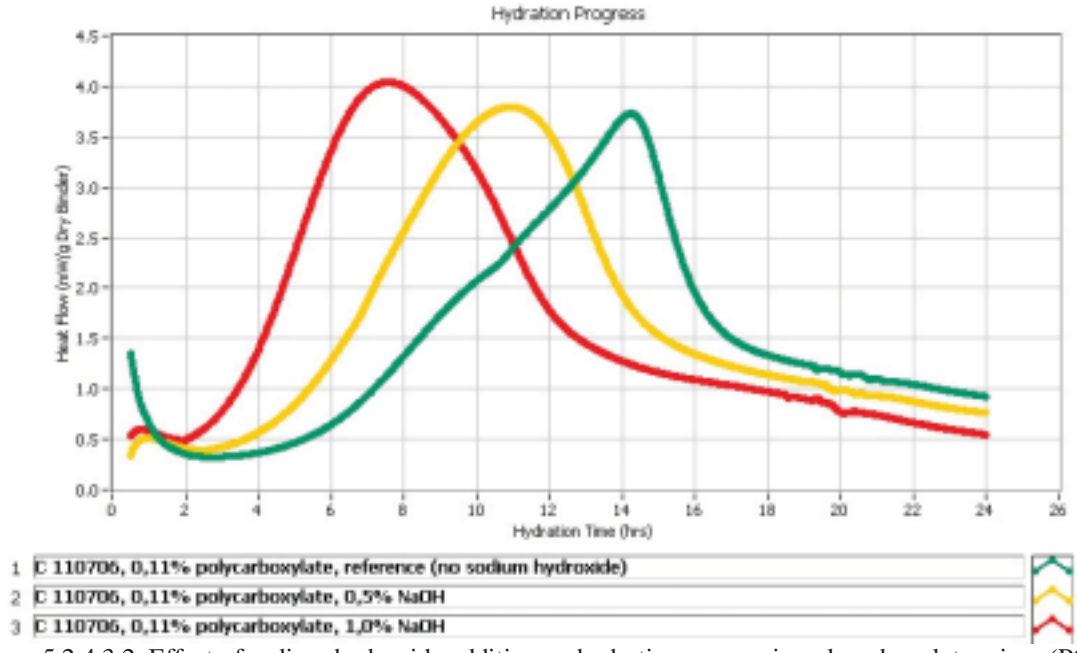

Figure 5.2.4.3.2: Effect of sodium hydroxide addition on hydration process in polycarboxylate mixes (PC1)

5.2.5 Sulphates

5.2.5.1 Sulphates and their influence on rheology

Potassium sulphate

Results from Rössler /Rö 2/ show that the needle-shaped crystal formation syngenite is formed when potassium sulphate is present in sufficient amounts. QXRD data in /Rö 2, pp.19, fig. 1-3/ also indicates that there is a linear relation between the amount of syngenite ($K_2SO_4 \cdot CaSO_4 \cdot H_2O$) formed in the cement paste and the amount of K_2SO_4 added. For example, the addition of 0,7% K_2SO_4 (by weight) resulted in ~0,8% syngenite (by weight), 1,4% of K_2SO_4 addition resulted in ~1,5% syngenite and so on. Measurements by Rössler on pastes containing K_2SO_4, done with a Schleibinger Viskomat NT, showed an increase in torque when syngenite was formed /Rö 2/. Syngenite is formed in the first 10 minutes after water addition and can be detected for at least 2 hours /Rö 2/. Hence, the formation of syngenite could be one reason why rheological parameters and the intitial dispersing effect of admixtures can change sometimes from one cement production date to another. Potassium sulphate (K_2SO_4) was added gradually to blank, PC1 and Mel mixes to evaluate the effect of syngenite formation on yield stress and plastic viscosity. It is assumed that the addition of 1,2% K_2SO_4 results in around 1,2% syngenite. Figure 5.2.5.1.1 depicts the effect of K_2SO_4 addition on rheological parameters in blank, PC1 and Mel mortar mixes. Results on blank mix (no admixture) showed that the addition of 1,2% K_2SO_4 had no effect on yield stress and plastic viscosity. However, when 2,4% and 3,6% K_2SO_4 were added to blank mortar mixes, the yield stress and plastic viscosity increased significantly. Mixes containing polycarboxylate already showed an increase in yield stress when 1,2% K_2SO_4 was added, but still no effect on plastic viscosity. This observation is in line with the results from test series with KOH. Figure 5.2.5.1.2 depicts a paste containing 1,2% K_2SO_4. The amount of syngenite in Figure 5.2.5.1.2 is assumed with ~1,2%, resulting in an increase in yield stress by a factor of 2 but no or only a minor effect on plastic viscosity. When 2,4% K_2SO_4 was added, the amount of needle-shaped formations in the free space between the cement grains increased considerably (see Figure 5.2.5.1.3). The amount of syngenite in Figure 5.2.5.1.3 is assumed with ~2,4%, resulting in an increase in yield stress by a factor of 3 and an increase in plastic viscosity by a factor of 2. The results show that mixes containing dispersing admixtures are more affected by the formation of syngenite than the mixes without an admixture. One physical explanation is that the water to cement ratio is lower in mixes with melamine and PC1 in comparison to blank mixes. The lower amount of water in PC1 and Mel mixes makes these mixes more sensitive to hydration products which could bridge the free space between cement particles. A similar tendency was observed in mixes with melamine.

Table 5.2.5.1.1: Rheological results of potassium sulphate addition to mortar

	Blank mixes (no admixtures)				**PC mixes (PC1)**				**Mel mixes (Melamine)**			
Potassium	Rheomixer		Viscometer		Rheomixer		Viscometer		Rheomixer		Viscometer	
sulphates	G	H	τ	μ	G	H	τ	μ	G	H	τ	μ
added to mix	(mA)	(mA·s)	(Pa)	(Pa·s)	(mA)	(mA·s)	(Pa)	(Pa·s)	(mA)	(mA·s)	(Pa)	(Pa·s)
Reference	251	97	239	4,5	207	194	191	6	304	96	348	3
1,2% K_2SO_4	244	106	232	4,4	384	162	352	6	496	147	423	7
2,4% K_2SO_4	579	79	446	7,4	540	180	540	11	388	174	378	7
3,6% K_2SO_4	700	200	600	12,0	1000	250	1000	16	606	122	477	8

The chemcial composition of the needle shaped formations was determined under the SEM by use of energy dispersive X-ray spectroscopy (EDX spectroscopy). Therefore, a high energy beam of charged particles, such as electrons, is focused on the material, giving a characteristic X-ray from the material investigated. This makes it possible to determine the elemental composition of the material /Mi 1/. Figure 5.2.5.1.4 displays the spectrum of the chemical elements on the investigated spot shown in Figure 5.2.5.1.5. The chemical composition of the

needle-shaped formation shown in Figure 5.2.5.1.5 contains all major components of syngenite. Major elements detected were carbon, oxygen, sulphur, calcium and potassium and small amount of silicium. The EDX spectrum of primary hydration products (such as syngenite and ettringite) contained between 5% to 10% of carbon when PC1 was present (see table 5.2.5.1.2). The carbon containing source must have been (1) incorporated in the hydration product or (2) present on the surface of hydration products.

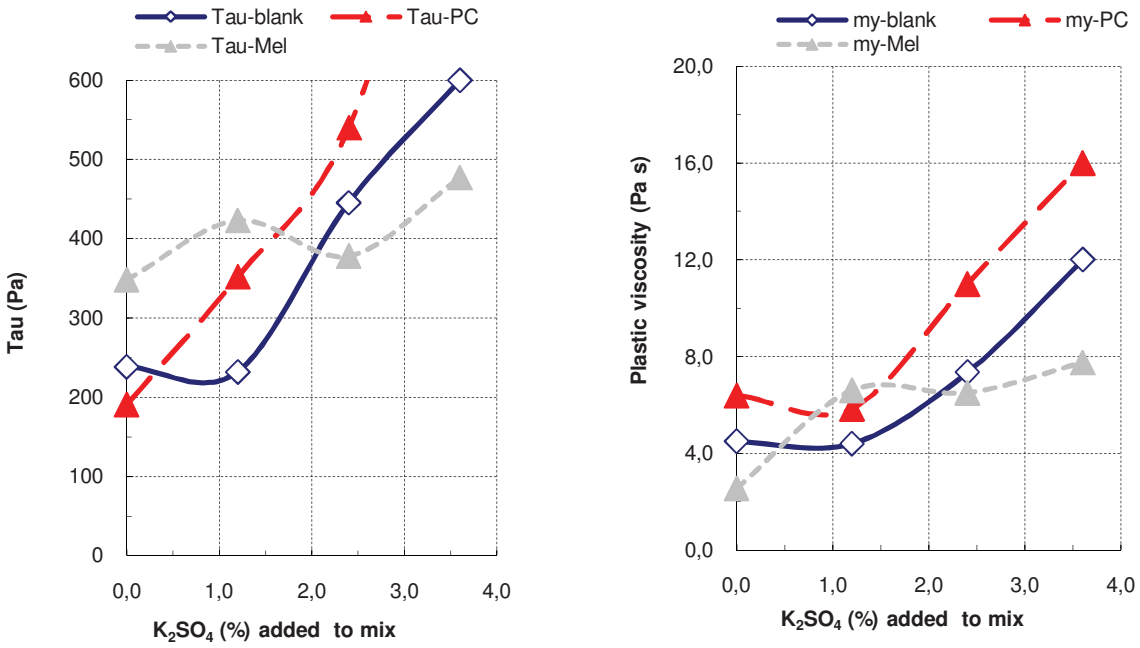

Figure 5.2.5.1.1: Effect of addition of potassium sulphate on yield stress and plastic viscosity

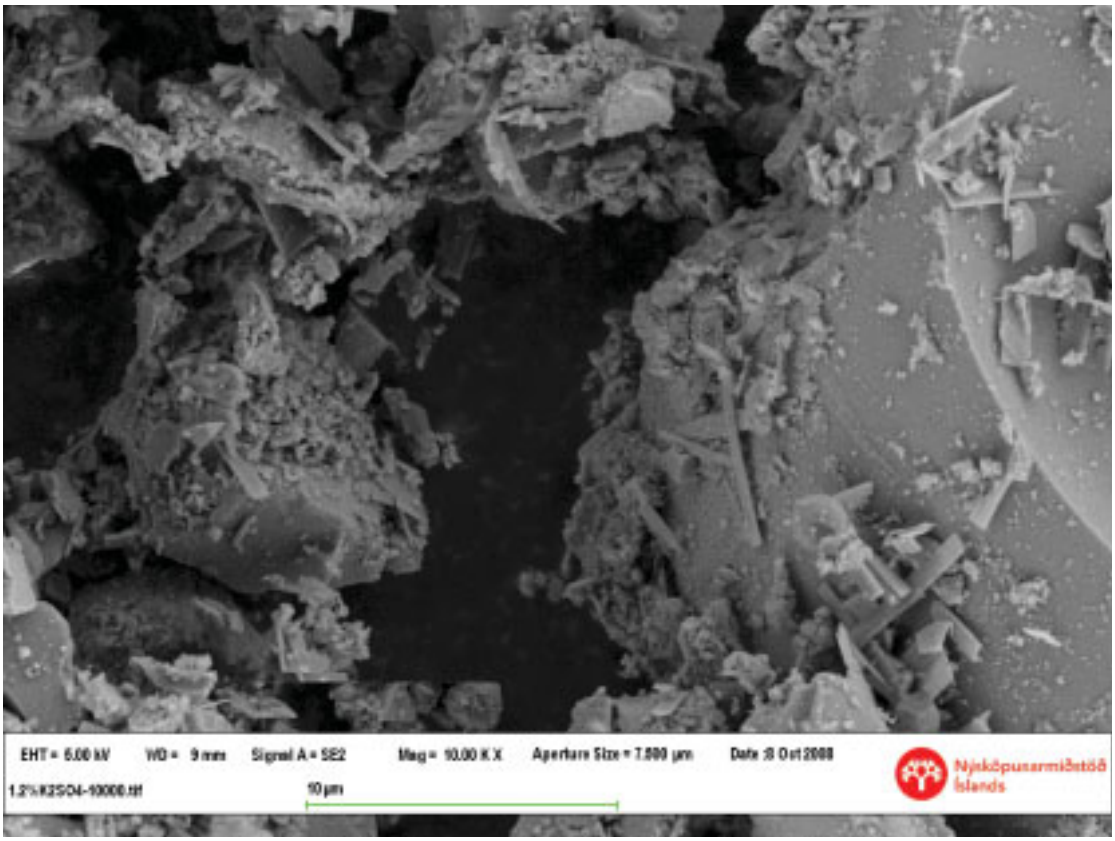

Figure 5.2.5.1.2: SEM picture (magnification 10000) of Portland cement grain, 0,11% PC1 at w/c of 0,36 containing 1,2% K_2SO_4

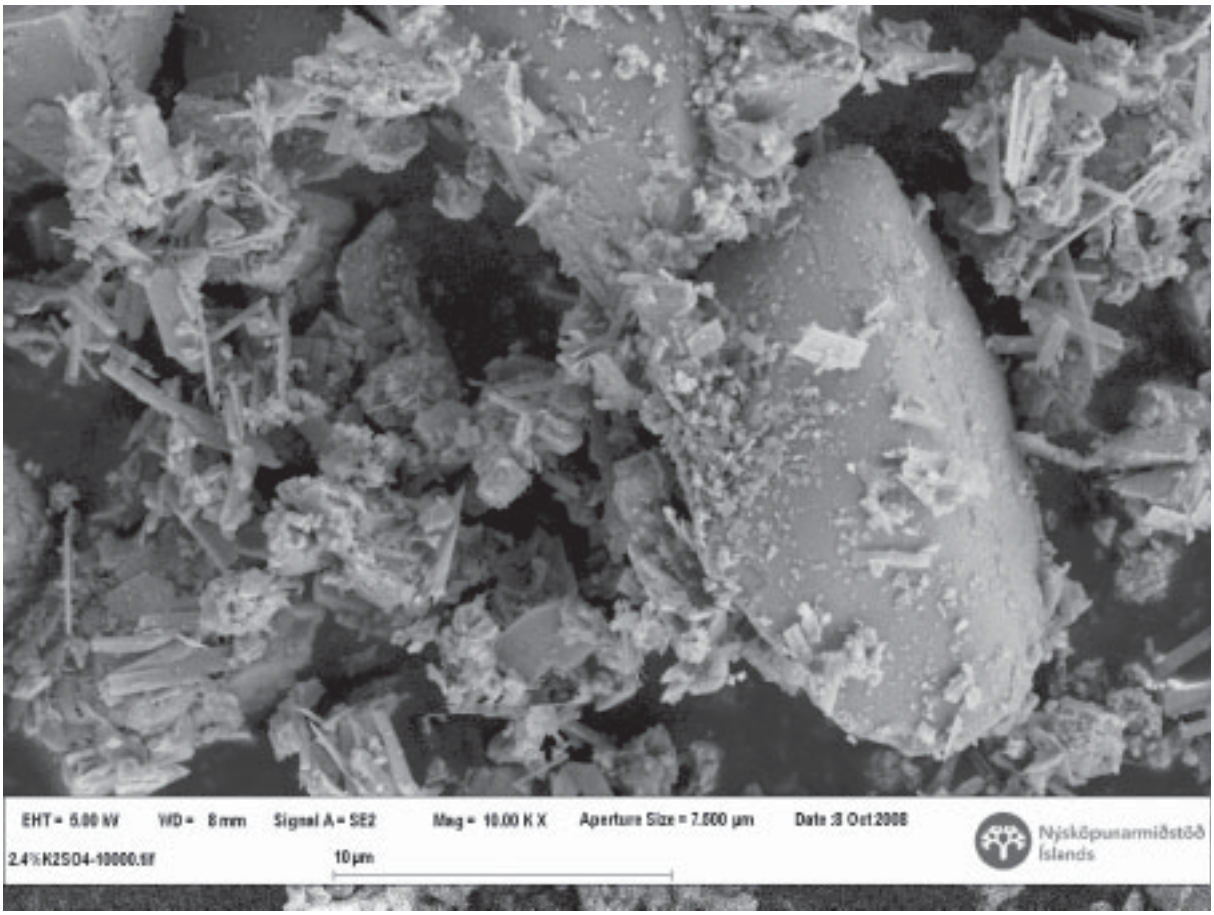

Figure 5.2.5.1.3: SEM picture (magnification 10000) of Portland cement grain, 0,11% PC1 at w/c of 0,36 containing 2,4% K_2SO_4

Table 5.2.5.1.2: Composition of EDX spectrum and syngenite

	EDX Spectrum 3			Syngenite
Element	Weight%	Atomic%		Weight%
C	7,96	13,99		-
O	44,11	58,20		43,85
Si	1,96	1,48		-
S	14,93	9,83		19,53
K	11,88	6,41		23,81
Ca	19,15	10,09		12,20

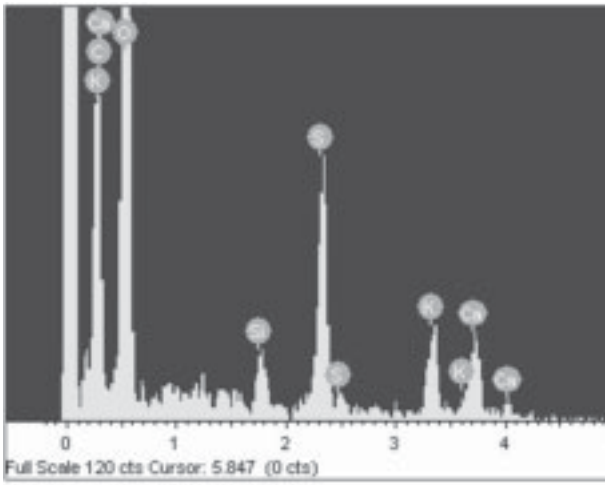

Figure 5.2.5.1.4: Chemical elements present in needle shaped formations (EDX spectrum)

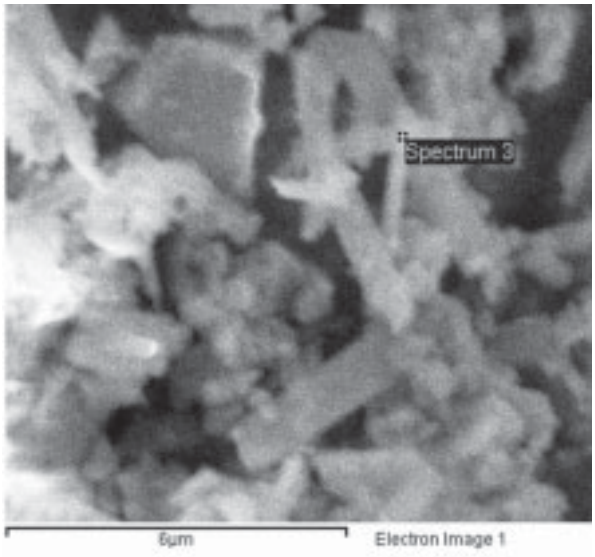

Figure 5.2.5.1.5: Location for EDX spectral analysis

5.2.5.2 How various calcium sulphate carriers affect rheology

Hemihydrate ($CaSO_4 \cdot ½H_2O$)

The previous chapter showed the influence of calcium sulphate carrier composition on the initial dispersing effect of superplasticizers. Data from Rößler on cement pastes without admixtures /Rö 2, Ku 2/ showed that the highest fluidity (in other words the lowest yield stress) was obtained when only calcium sulphate dihydrate ($CaSO_4 \cdot 2H_2O$) was present. When dihydrate was replaced by mixtures of hemihydrate and anhydrite, the pastes became less fluid (the yield stress increased) with increasing content of hemihydrate /Rö 2/. The lowest fluidity (highest yield stress) was observed when only anhydrite was added as calcium sulphate carrier /Rö 2/. Hence, the important ratio seems to be the ratio between dihydrate and hemihydrate. Therefore, hemihydrate was gradually added to mortar mixes to quantify its effect on yield stress (see Fig. 5.2.5.2.1 left) and plastic viscosity (Fig. 5.2.5.2.1 right). The yield stress increased continuously for all types of mixes when hemihydrate was added. An excess of fast dissolving hemihydrate leads to a high concentration of calcium and sulphate ions in the pore solution. If they are not consumed during the formation of ettringite, secondary formed gypsum occurs bridging the space between cement particles. Note that the yield stress increase in mixes containing PC1 was surprisingly low in comparison to mixes without admixtures and mixes with melamine. Note, that a hemihydrate content of around 5% (3% added hemihydrate plus ~2% already in cement) is very unlikely. The reference cement of this study is produced with 100% dihydrate ($CaSO_4 \cdot 2H_2O$), which dehydrates in the mill depending on the mill temperature.

Table 5.2.5.2.1: Rheological results of hemihydrate addition to mortar

Hemi hydrate added to mix	Blank mixes (no admixtures) Rheomixer G (mA)	H (mAs)	Viscometer τ (Pa)	μ (Pas)	PC mixes (PC1) Rheomixer G (mA)	H (mAs)	Viscometer τ (Pa)	μ (Pas)	Mel mixes (Melamine) Rheomixer G (mA)	H (mAs)	Viscometer τ (Pa)	μ (Pas)
Reference	274	87	268	5	190	158	178	5	338	108	352	3
1,0% HH	351	93	340	4	226	162	217	6	458	112	388	5
2,0% HH	379	85	356	5	254	167	223	7	500	113	459	5
3,0% HH	429	98	431	5	290	182	280	7	520	105	428	5

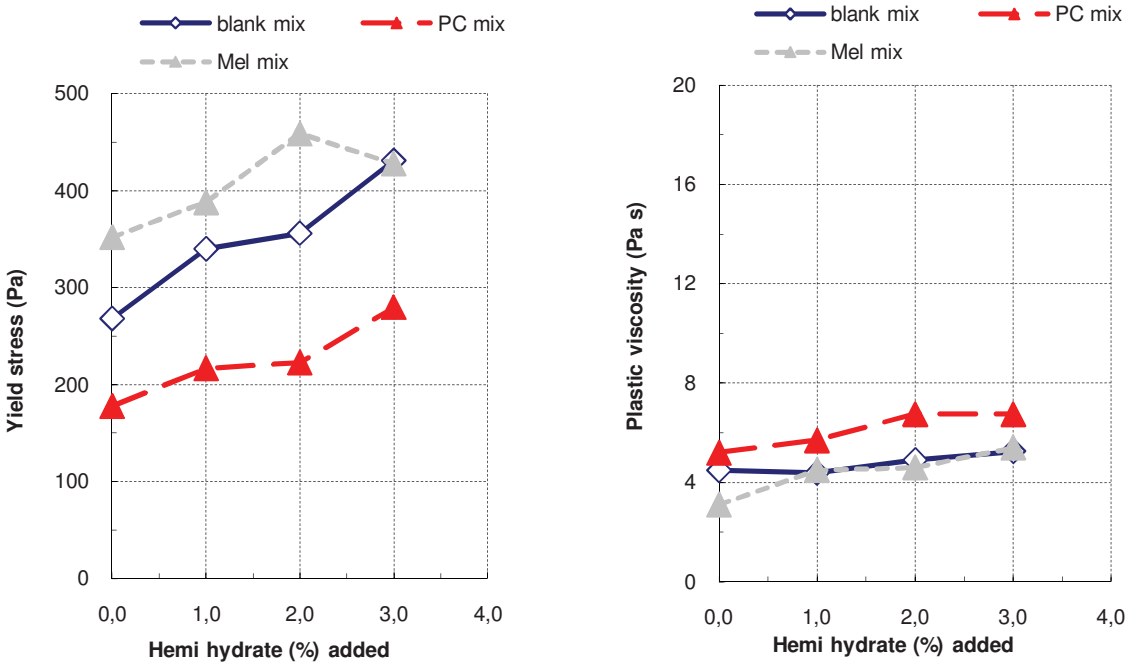

Figure 5.2.5.2.1: Effect of addition of hemi hydrate on yield stress and plastic viscosity

Although the results show a clear trend, the occurrence of high yield or low yield cement paste cannot solely be attributed to variations in calcium sulphate carrier composition. Figure 5.2.5.2.1 (right) depicts the influence of hemihydrate addition on plastic viscosity. It can be seen that the influence of hemihydrate content on plastic viscosity is rather low. Though, mixes containing a dispersing admixture showed a slightly higher increase in plastic viscosity than the mixes without admixtures. This can be explained, as the volume of available water is smaller in mixes with dispersing admixtures. Microstrutural investigations on pastes with 1,0% and 3,0% $CaSO_4 \cdot ½H_2O$ showed a mixture of secondary formed gypsum and trisulfate (ettringite) in the free space between the cement grains. Note that the hydration of the pastes was stopped 15 minutes after water addition with liquid nitrogen. The formation of secondary formed gypsum at this early age is most likely due to the excess of sulfate, coming from the fast dissolving hemihydrate. Figure 5.2.5.2.2 (1,0% $CaSO_4 \cdot ½H_2O$) depicts the surface of cement grains covered with remains of pore solution and various prismatic shaped sulfate plates attached to a cement grain surface. Figure 5.2.5.2.3 (3,0% $CaSO_4 \cdot ½H_2O$) displays the matrix between cement grains showing plates of monosulfate and trisulfate.

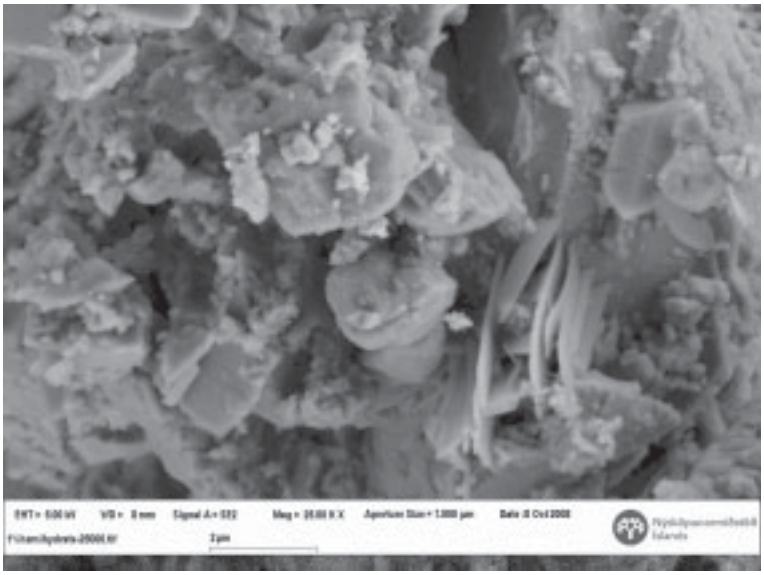

Figure 5.2.5.2.2: SEM picture (magnification 25000) of Portland cement grain, 0,11% PC1 at w/c of 0,36 containing 1,0% hemihydrate ($CaSO_4 \cdot ½H_2O$)

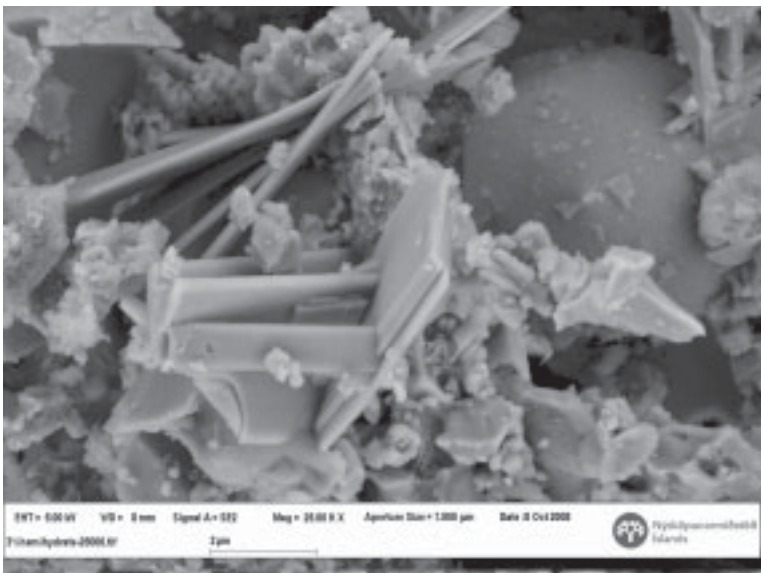

Figure 5.2.5.2.3: SEM picture (magnification 25000) of Portland cement grain, 0,11% PC1 at w/c of 0,36 containing 3,0% hemi hydrate ($CaSO_4 \cdot ½H_2O$)

Dihydrate ($CaSO_4 \cdot 2H_2O$)

In mixes without admixtures, an excess of dihydrate had no effect on yield stress and plastic viscosity. Dihydrate dissolves slower than hemihydrate so that only short prismatic ettringite and no secondary formed gypsum occurs. However, when dihydrate was added to mixes containing PC1, the yield stress and plastic viscosity increased moderately. Polymers might adsorbe on the dihydrate surface, as the specific surface of dihydrate is by an order of magnitude bigger than that of cement. Physically bound water might also be an explanation for the yield value increase as the water content in mixes with PC1 was the lowest of all here compared mixes. On the contrary, when dihydrate was added to mixes containing melamine, the yield value decreased clearly. With melamine, mixes became extraordinarily fluid (close to segregation), particularly during the first ten minutes after water addition. It seemed as if the melamine polymers had adsorbed to a great extent on the dihdyrate leading to a super dispersed system with zero yield value. However, this exceptionally low yield value can not be seen in the results below since the data displayed here is already influenced by workability loss. The results show that the speed at which the calcium sulphate carrier releases its ions has a big effect on rheological properties.

Table 5.2.5.2.2: Rheological results of dihydrate addition to mortar

	Blank mixes (no admixtures)				**PC mixes (PC1)**				**Mel mixes (Melamine)**			
	Rheomixer		Viscometer		Rheomixer		Viscometer		Rheomixer		Viscometer	
Dihydrate added to mix	G (mA)	H (mAs)	τ (Pa)	μ (Pas)	G (mA)	H (mAs)	τ (Pa)	μ (Pas)	G (mA)	H (mAs)	τ (Pa)	μ (Pas)
Reference	276	111	263	4,8	212	221	206	7	338	115	352	3
1,0% HH	276	106	259	4,7	246	236	251	8	309	120	346	3
2,0% HH	307	111	265	4,8	288	227	308	8	241	117	284	3
3,0% HH	289	101	269	4,9	282	264	291	9	217	105	247	3

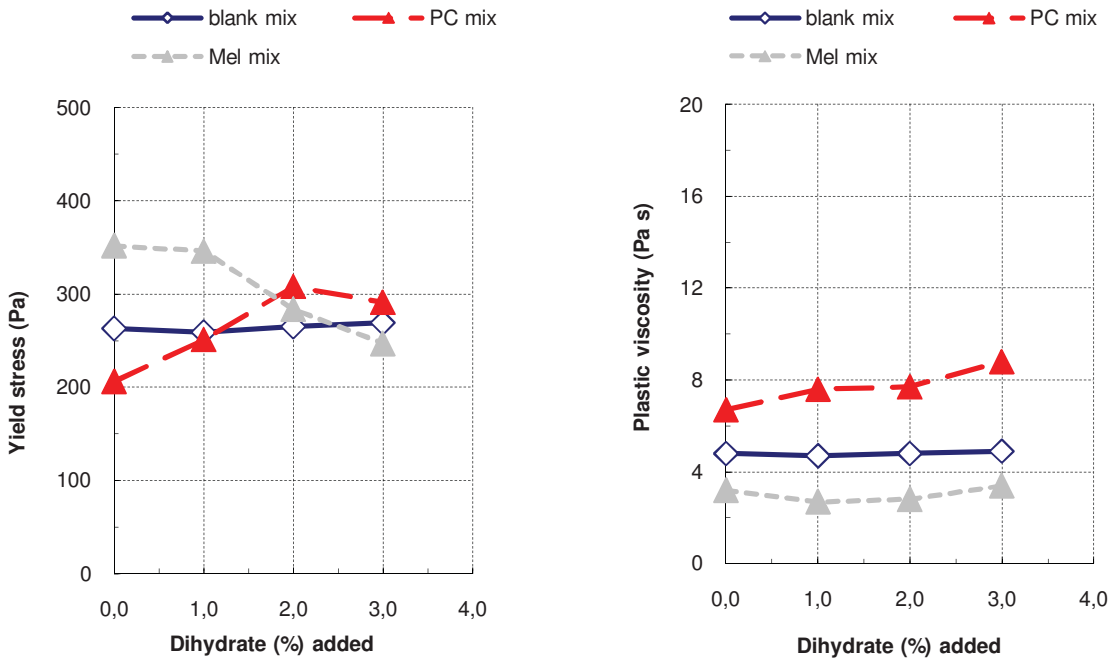

Figure 5.2.5.2.4: Effect of addition of dihydrate on yield stress and plastic viscosity

5.2.6 Pore solution analysis on cements differing in rheological properties

Cement pastes were produced with cement deliveries representing typical low yield, intermediate, and high yield cement. The cements are identical with those in chapter 5.2.1.3 and 5.2.1.4. The mineralogical composition (QXRD) of cements used for pore solution analysis is given in table 5.2.6.1.

Table 5.2.6.1: Mineralogical composition of three cement production dates

Cement production date	01.12.2006 (high yield)	22.11.2006 (intermed.)	23.05.2005 (low yield)
Yield value in mortar with PC1 (Pa)	320	195	80
Plastic viscosity in mortar with PC1 (Pa·s)	8	7	7
C_3S	61,0	57,9	51,0
C_2S	18,0	17,3	22,8
C_3A	4,2	4,9	3,7
$C_2(A,F)$	12,1	12,0	15,3
Calcite	3,4	5,7	3,1
Hemihydrate	1,3	1,2	1,3
Anhydrite	---	1,0	0,3
Dihydrate	---	---	0,4

---) below limit of detection

From each cement delivery, one blank paste without admixture at a w/c ratio of 0,46 and one paste containing 0,11% PC1 at a w/c-ratio of 0,36 were produced. 300 grams of cement were handmixed with respectively 138 g, and 108 g of deionized water. The delay in admixture addition was approximately 5 seconds. Pore solutions of pastes were obtained by vacuum extraction using a Bucher funnel and a Whatman grade 40 ashless filter paper with a pore size of 8 µm. At testing age, around 50 ml of cement paste was placed on the pre-wetted filter paper and exposed to a vacuum. Pore solutions were extracted at 5, 15, 30 and 60 minutes after water addition. Each pore solution extraction lasted 20 seconds. The concentrated pore solution was acidified right after extraction using 0,5% nitric acid solution.

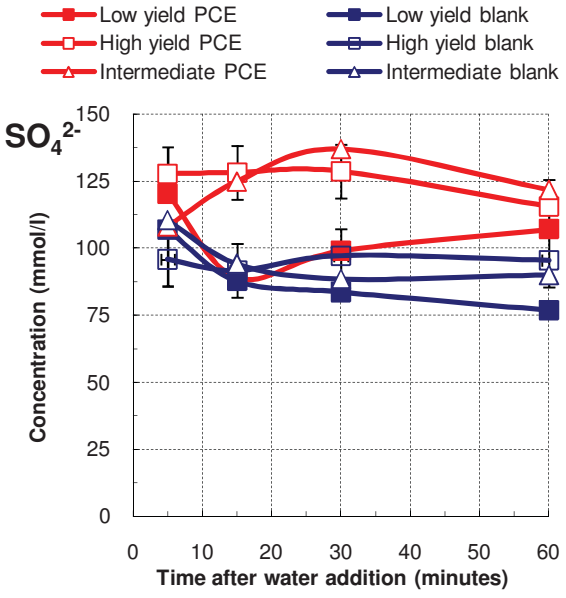

Figure 5.2.6.1: Sulphate ion (SO_4) concentration as a function of time

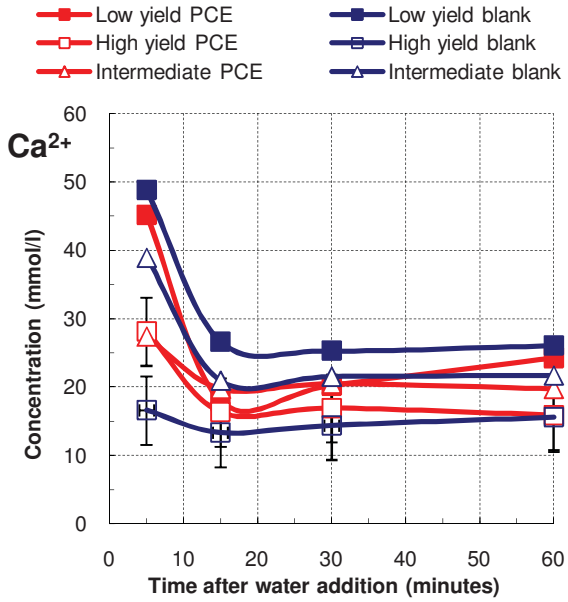

Figure 5.2.6.2: Calcium ion (Ca) concentration as a function of time

The ionic concentration was measured by use of inductively coupled plasma optical emission spectrometry (ICP-EOS) in the chemistry department of Innovation Center Iceland. All experiments were carried out at an ambient temperature of 22±2°C. Results are given in Appendix H1 to H3. Repeat measurements were done on pastes made with low yield and high yield cement showing a good repeatability.
Usually, the SO_4^{2-} concentration follows the Ca^{2+} concentration over time as they tend to follow gypsum solubilities. However, this is not the case with high yield and intermediate cement containing polycarboxylate. The relatively high initial sulphate and calcium concentration in low yield cement followed by a steady decrease indicates a fast dissolving calcium sulphate carrier that may react with the aluminates to control rheology and prevent early stiffening. This observation is supported by calorimeter data of cement C. Low yield deliveries gave a lower rate of hydration than typical high yield deliveries. Relatively low SO_4^{2-} and Ca^{2+} levels in the high yield cement suggest that aluminates might react directly with water for rapid setting or may react with calcium sulphate and water to form monosulphoaluminate resulting in poorer rheology. At later testing ages (15, 30 and 60 minutes), only minor differences in SO_4^{2-} concentration were observed in blank pastes. When polycarboxylate (PC1) was present, high yield and low yield cement showed significant differences in SO_4^{2-} concentration. In mixes with PC1, the SO_4^{2-} concentration of low yield cement after 15 minutes was significantly lower than with intermediate and high yield cement. According to QXRD measurements on cement from 01.12.2006 (high yield), the sulphate level of this delivery is very low. This is somewhat contradictory to the pore solution data. The QXRD results might be too low in this case, as the sulphates have the tendency to preferred orientation which can influence the QXRD results considerably.
Cements having different rheological properties differed greatly in their alkalinity. In mixes with PC1, the potassium and sodium concentration (see Figure 5.2.6.3 and 5.2.6.4) was clearly less in low yield cement compared to high yield and intermediate cement.

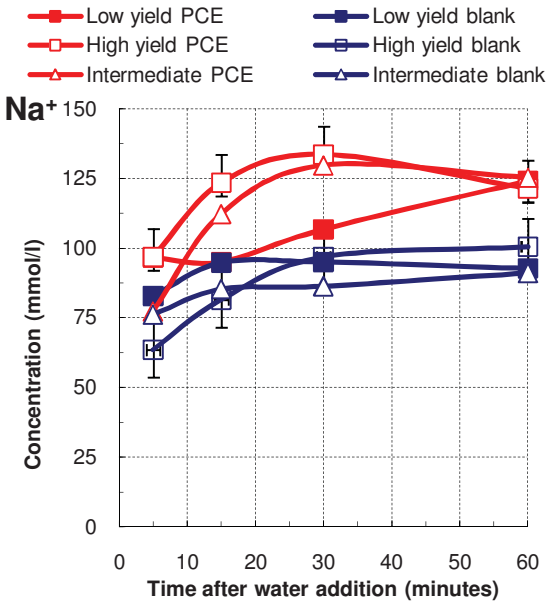

Figure 5.2.6.3: Sodium ion (Na) concentration as a function of time

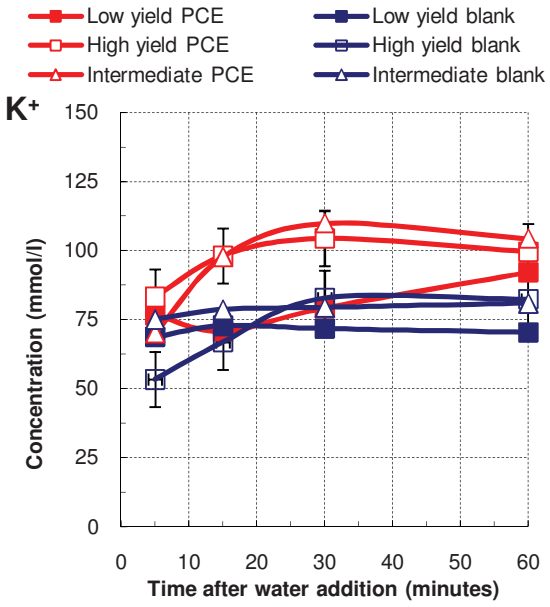

Figure 5.2.6.4: Potassium ion (K) concentration as a function of time

In mixes with polycarboxylate (PC1), the cement which gave a high yield stress (sticky mix) also showed the highest K^+ and Na^+ ion concentration and the cement having the lowest yield stress (fluid mix) showed the lowest K^+ and Na^+ ion concentration. However, this was not as clear when no admixtures were present, then the high yield cement had the lowest K^+ and Na^+

ion concentration. It seems as if the presence of polycarboxylate influenced the solubility of alkalies in pore solution.

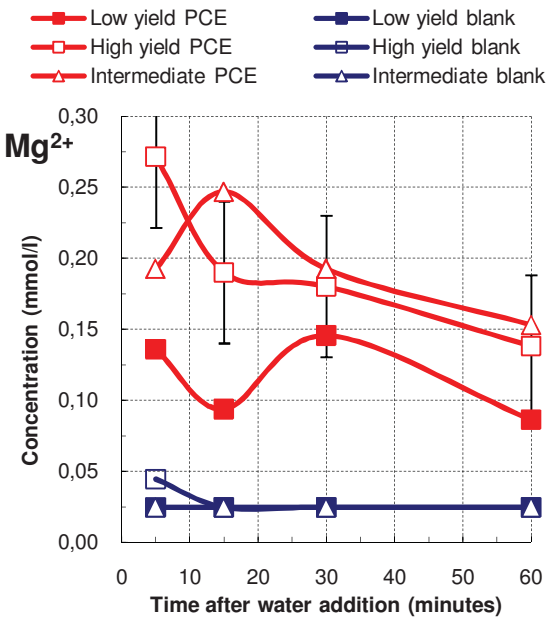

Figure 5.2.6.5: Magnesium ion (Mg) concentration as a function of time

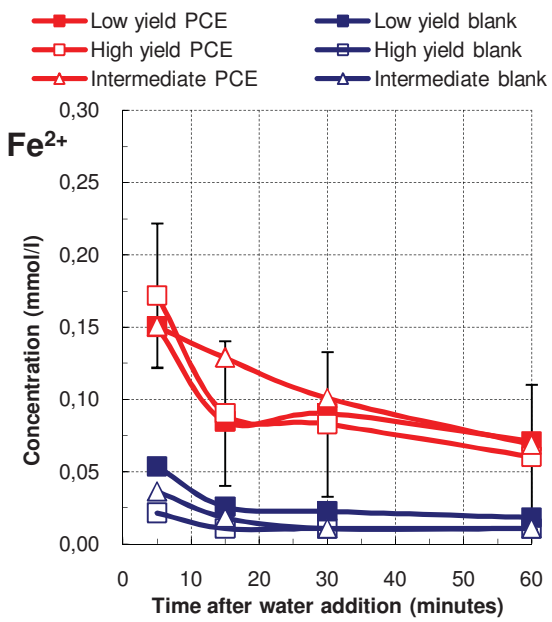

Figure 5.2.6.6: Ferrite ion (Fe) concentration as a function of time

What seems contradictionary on the first view, is actually not. This observation can explain why some cements are more problematic and less predictable than others. The determining factor might not be the water soluble alkali content of a blank cement (no admixtures present, which is what is typically measured). The major influencing factor is most likely the water soluble alkali content in presence of polycarboxylate.

Figure 5.2.6.5 and 5.2.6.6 depict the Mg^{2+} and Fe^{2+} concentration. The iron concentration is more or less the same for all three deliveries, whereas the Mg^{2+} concentration is higher in the high yield cement compared to the low yield cement. The relatively great differences in Mg^{2+} concentration between pastes with and without polycarboxylate is due to the solubilizing effect of the admixture on divalent cations like magnesium ions. However, the presence of magnesium has also been attributed to loss of fluidity due to its precipitation in the form of brucite.

5.2.7 Adsorption measurements

The total organic carbon (TOC) of cement paste was measured to calculate the adsorption degree. The TOC of pastes with and without polycarboxylate (PC1) was investigated by use of a LABTOC analyzer from PPM Ltd., Borough Green, Kent, UK. This device has a measuring range of 0 to 4000 parts per million (ppm). One should be aware that TOC measurements are an indirect way to measure polymer adsorption, so the term adsorption has to be used carefully here. Some authors /Fl 1/ prefer the term polymer consumption instead of adsorption. The cement samples tested cover the complete territory of rheological parameters within the study, from low yield to high yield cement. Three different cement pastes were made of each cement batch:

(1) paste without dispersing admixture
(2) paste containing 0,11% PC1
(3) paste containing 0,20% PC1.

The water used was Icelandic tap water, and the polycarboxylate was added with the water. 100 g of cement were mixed with the water for three minutes in a high shear mixer (2 blade rotor @800 rpm). 10 minutes after water addition, the pastes were centrifuged for 10 minutes at 4000 rpm to obtain the pore solution. Thereafter, the pore solution was filtered through a 0,45 µm nylon filter. In a next step, 2 ml of pure pore solution were acidified with 600 µl HNO_3 and further diluted 1:20 with deionized water. By adding HNO_3 the inorganic carbon content was eliminated. However, it later turned out that it was not necessary to acidify the pore solution as the TOC analyzer eliminates all inorganic carbon before the organic carbon is measured. The TOC of blank cement paste, water and water plus the admixture was measured beforehand. The TOC of blank cement tells how much carbon containing compound is actually present before any admixtures are added. An extraordinary high TOC of blank cement paste could have its supply in remains of grinding aid or other organic carbon sources. Grinding aids are briefly described in chapter 2.2.5. Inorganic carbon, originating from limestone filler/$CaCO_3$ (see Appendix K), does not influence TOC as it was eliminated before measurement.

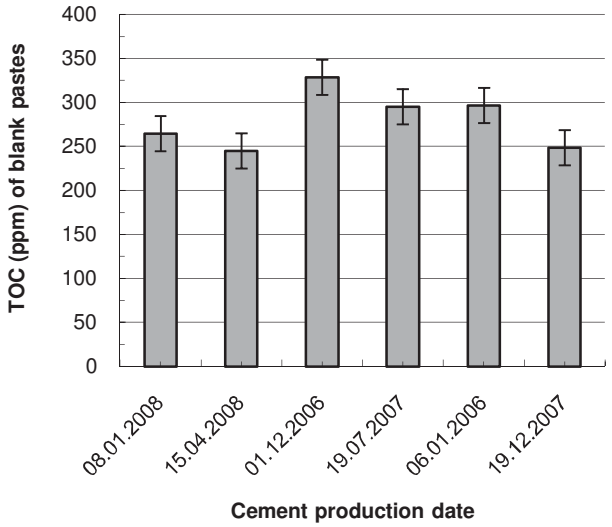

Figure 5.2.7.1: Organic carbon (ppm) in blank cement paste

The TOC of blank cement paste was measured repeatedly. Figure 5.2.7.1 depicts the results of blank pastes, showing significant differences in TOC between single cement production dates. Pastes made with cement from 01.12.2006 and 19.07.2007 smelled distinct from the four other deliveries. After 3 minutes of mixing with a high shear mixer, pastes produced with cement from 01.12.2006 had a fruity citrus-like odor and cement from 19.07.2007 had an

odor like cough medicine. Pastes with the same water to cement ratio and polymer content as mortar mixes were measured on their TOC. Figure 5.2.7.2 depicts the degree of adsorption of PC1 on six cements differing in production date and rheology. Cement giving a high yield stress in mortar adsorbed (or consumed) significantly more polymer within ten minutes of hydration than cement giving a low yield stress. Or in other words, the pore solution of cement giving a lower yield stress had a bigger reservoir of free polymers available for dispersion than the pore solution of high yield cement. However, the degree of polymer adsorption had only a minor effect on plastic viscosity (see Figure 5.2.7.2 right). When the admixture dosage was increased from 0,11% to 0,20%, the adsorption degree shifted to lower values. This is logical as more polymer was available for adsorption. However, even at an overdosage of polycarboxylate the trend was the same. Cement having a high yield value consumed more polymers than cement having a low yield value. One has to be aware that the polymer adsorption/consumption could be the effect of something else and not the cause for the variations in rheology.

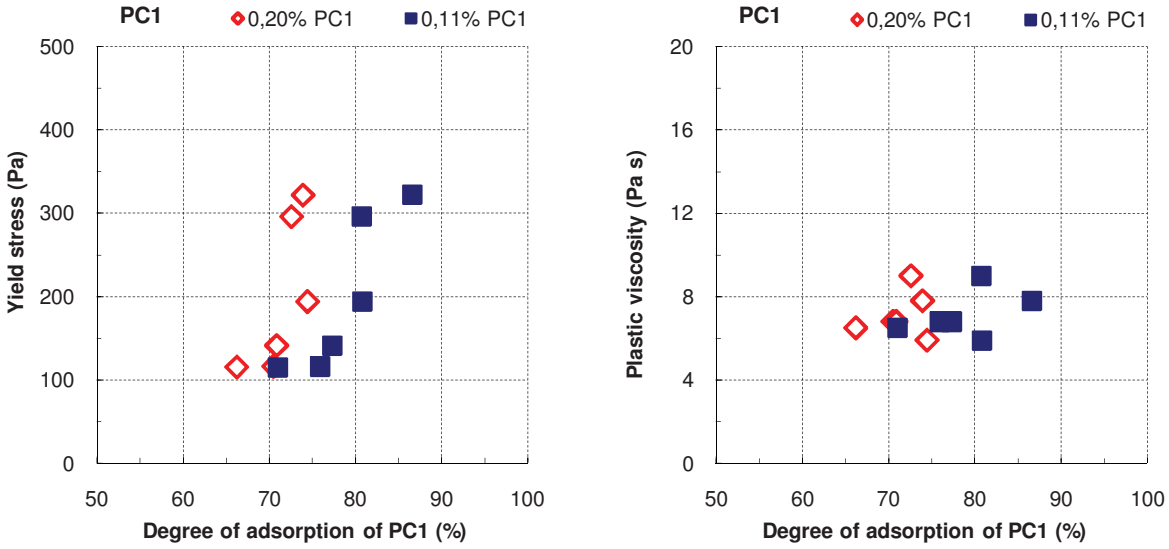

Figure 5.2.7.2: Degree of adsorption of PC1 (%) and rheological parameters of six different cement production dates

5.2.8 Grinding aid

The effect of four grinding aids on rheology and hydration was tested in mortar mixes. The grinding aids used were ethylene glycol (EG), tetraethylenepentamine (TEPA) and two different kinds of triethanolamine (TEA). Chemical compounds were provided by Sigma Aldrich and a cement producer. Tests were done on mixes with and without PC1. According to technical data sheets, the recommended dosage for grinding aid is between 100 and 1000 ppm (0,01 to 0,1%) by weight of clinker. Starting from a reference mix (0,0%), the chemicals were added at dosages of 0,1%, 0,5% and 1,0% by weight of cement. All tests were done on the same cement production date having a low TOC. By using a cement with a low TOC it is assumed that the initial level of grinding aid is low in the reference.

5.2.8.1 Various grinding aids and their influence on rheology

The chemical compounds were all present in liquid form. They were added to the dry material (sand and cement) and dry mixed in the Rheomixer for 30 seconds. Figure 5.2.8.1 depicts the effect of various grinding aids on the rheological parameter yield stress. The various grinding

aids had the greatest effect in mixes with PC1. In mixes without admixtures their influence on rheology was relatively low. With EG, TEPA and TEA 1, the yield stress of blank mixes was slightly reduced or remained unaffected. When TEA 2 was added to blank mixes the yield stress increased considerably. TEA 2 is a pure triethanolamine compound whereas TEA 1 is a triethanolamine cocktail. TEA 2 has a great effect on rheological properties and it acts like a relatively strong accelerator. Results from next chapter support this observation.
In mixes with polycarboxylates, EG and TEA 2 increased the yield stress, while TEA 1 and TEPA reduced the yield stress or had no effect. It is not clear yet if the influence on rheology is due to the interaction of cement and grinding aid or due to the interaction of polycarboxylate and grinding aid. This question might be answered by use of an inert model powder such as limestone or magnesium powder. However, results from next chapter point towards a grinding aid - clinker phase interaction and not a grinding aid – admixture interaction. Nevertheless, the results show that the effect of grinding aid on rheology can not be generalized. Some chemical compounds have hardly any influence on rheological properties while others have a great effect on workability. From a rheological perspective, TEA 1 is the most favourable compound as it causes the fewest variations. TEA 1 is a triethanolamine cocktail developed by a cement producer.

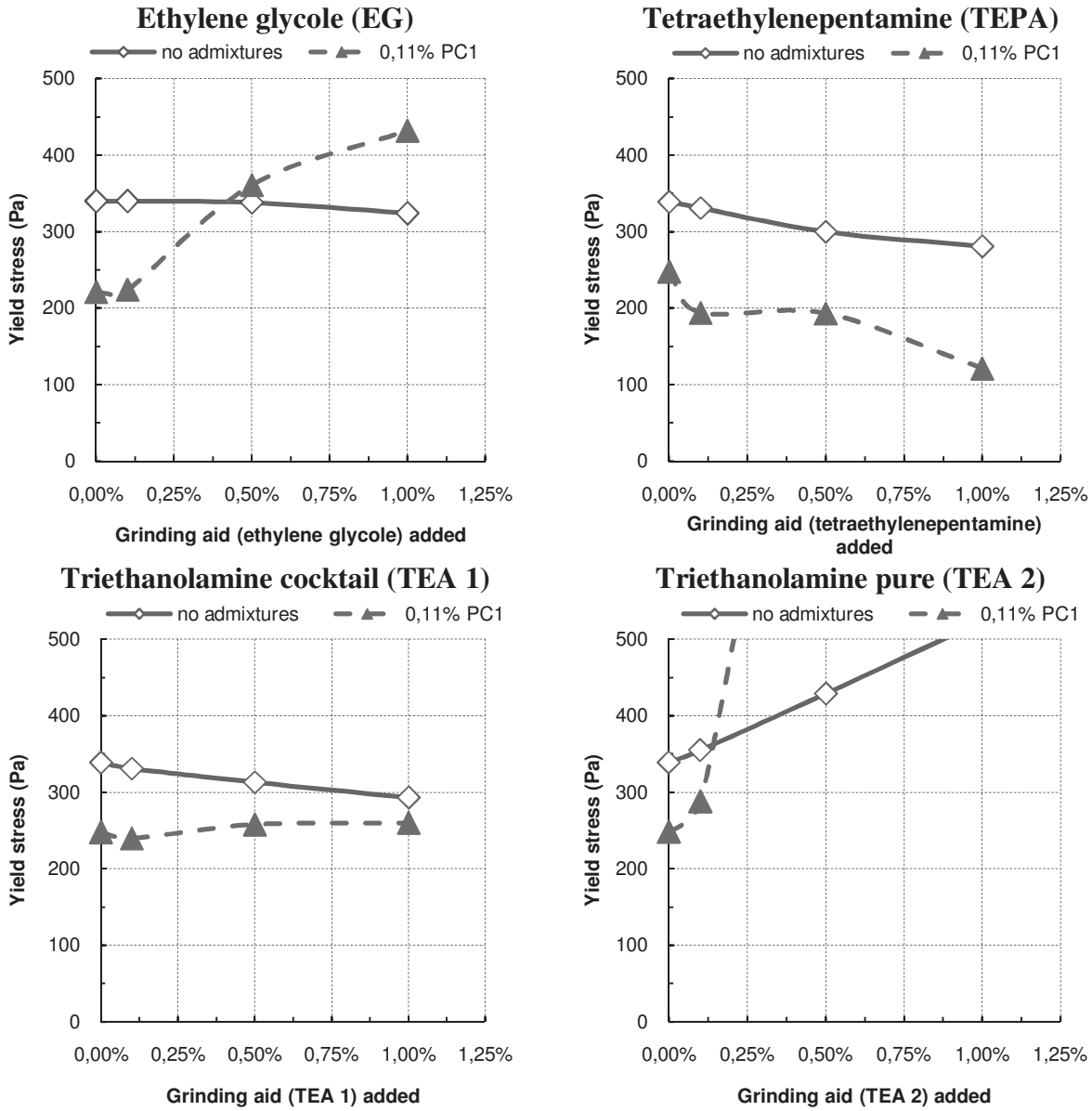

Figure 5.2.8.1: Four different grinding aids and theior effect on yield stress

5.2.8.2 Effect of various grinding aids on hydration process

Ethylene glycole acts like a mild retarder in blank mixes and like a slight accelerator in mixes with PC1 (see Appendix O-1). Tetraethylenepentamine has a retarding effect both on blank and PC1 mixes. The higher the TEPA content the greater the retarding effect (see Appendix O-2). The triethanolamine cocktail TEA 1 has a slightly accelerating effect in blank and PC1 mixes. However, TEA 1 acts like a mild set retarder during the first three hours of hydration and thereafter it acts like an accelerator. This effect increases with increasing content of TEA 1 (see Appendix O-3). Note that TEA 1 had nearly no effect on rheological properties. The pure triethanolamine (TEA 2) acts like a severe accelerator in mixes with and without PC1. Figure 5.2.8.2.1 depicts the hydration curves of blank mixes with TEA 2. Mortar mixes which contained 0,5% (5000 ppm) and 1,0% (10000 ppm) of TEA 2 stiffened already five to ten minutes after water addition. After the high initial peak the hydration stopped completely (see blue and red line in figure below). According to this data, the threshold for pure triethanolamine in cement is around 1000 ppm. If this threshold is exceeded the hydration is accelerated to an extent that rheological properties become uncontrollable. The effect of grinding aid on hydration was more pronounced in pastes than in mortar. This is probably because of the bigger amount of cementitious materials in pastes than in mortar.

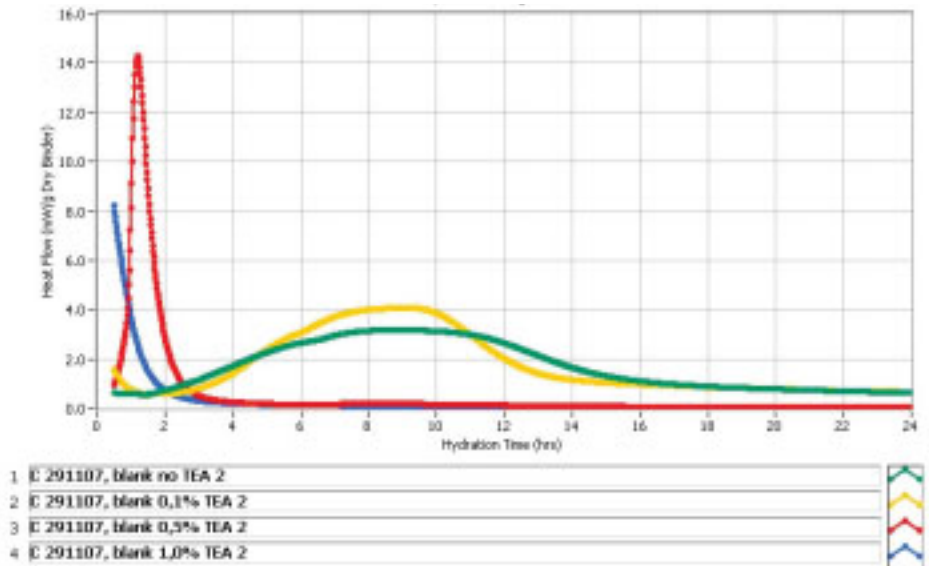

Figure 5.2.8.2.1: Hydration curves of blank mortar with TEA 2

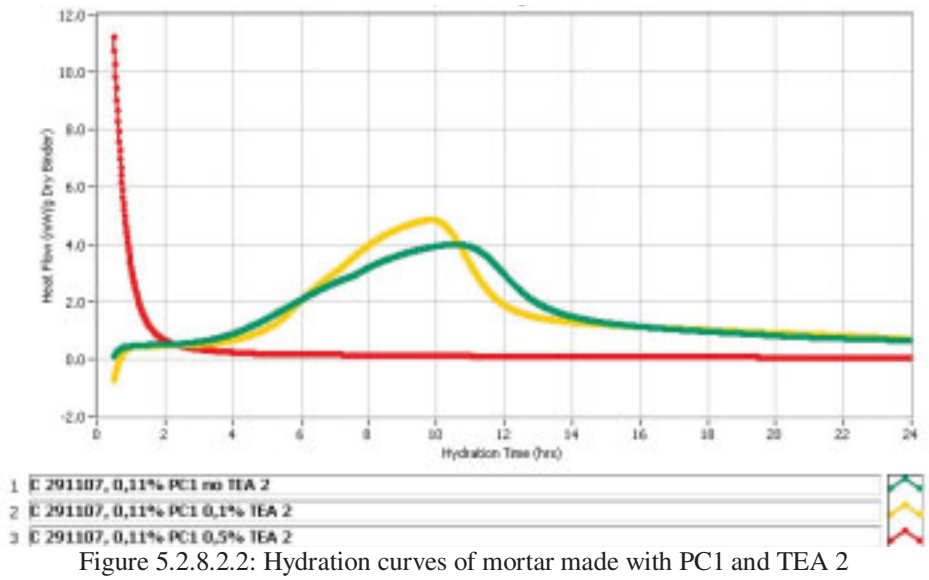

Figure 5.2.8.2.2: Hydration curves of mortar made with PC1 and TEA 2

5.2.8.3 Microstructure of pastes blended with grinding aid

All pastes for this study were made with a water to cement ratio of 0,36 and contained 0,11% PC1 plus the grinding aid. The grinding aid was added at a dosage of 5000 ppm. Note that this is far above the 1000 ppm normally used for cement grinding. The aim was to magnify the effect of gringing aid on microstructure. Cement, water, admixture and grinding aid were handmixed for one minute. Ten minutes after water addition, the hydration was stopped with liquid nitrogen. Thereafter, samples were stored in vacuum until investigation under the SEM.

Reference paste (no grinding aid)

Cement particles of the reference paste were partly covered with hydration products. However, some areas of cement grains were more covered with ettringite than others (see figure 5.2.8.3.2). The more covered areas of cement grains are most likely more aluminate rich than the surfaces which looked less hydrated (see Figure 5.2.8.3.1). From Figure 5.2.8.3.4 it can be seen that the formed ettringite was of short prismatic shape. Short prismatic ettringite has a length-thickness ratio (l/d) between one and three /Rö 2/ while long prismatic ettringite is defined by a l/d of >four. Short prismatic ettringite occurs when the saturation index for ettringite is relatively high (SI >10) while long prismatic ettringite occurs when the saturation index is rather low (SI 6-8) /Rö 2/. An excess of calcium and sulphate ions due to highly soluble calcium sulphate carrier results in short prismatic ettringite, whereas a high aluminate content available for hydration or a less soluble calcium sulphate carrier results in long prismatic ettringite. The formation in Figure 5.2.8.3.2 (left of the cement grain) is a coccolithophorid (planktonic algae), presumably originating from the limestone filler.

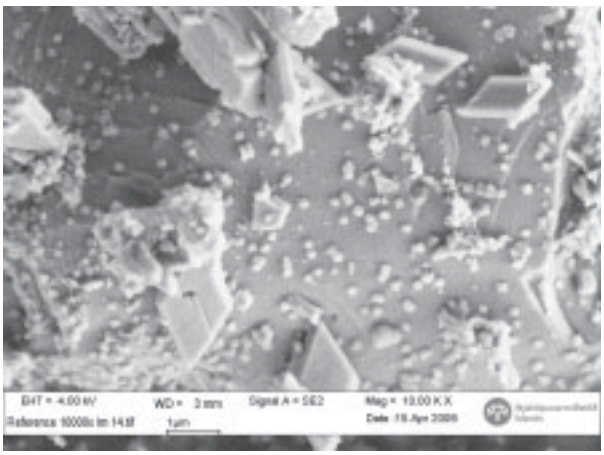

Figure 5.2.8.3.1: Cement surface of reference paste less covered with ettringite

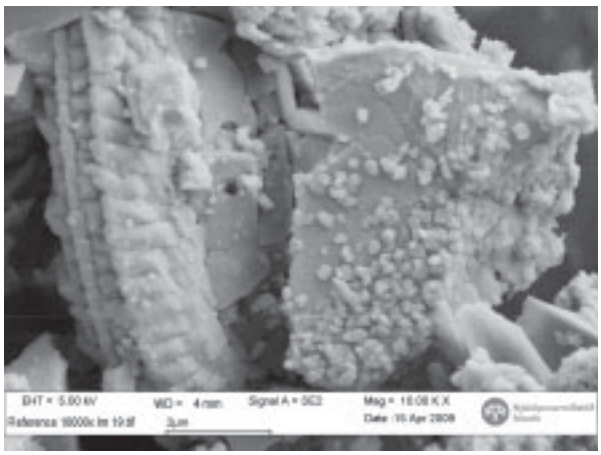

Figure 5.2.8.3.2: Cement surface of reference paste more densely covered with ettringite

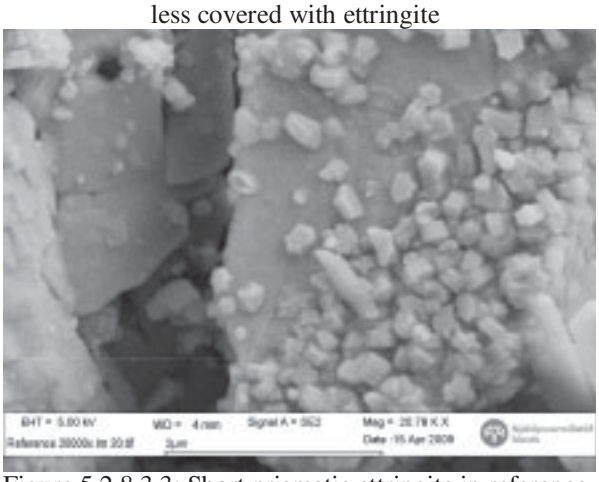

Figure 5.2.8.3.3: Short prismatic ettringite in reference paste

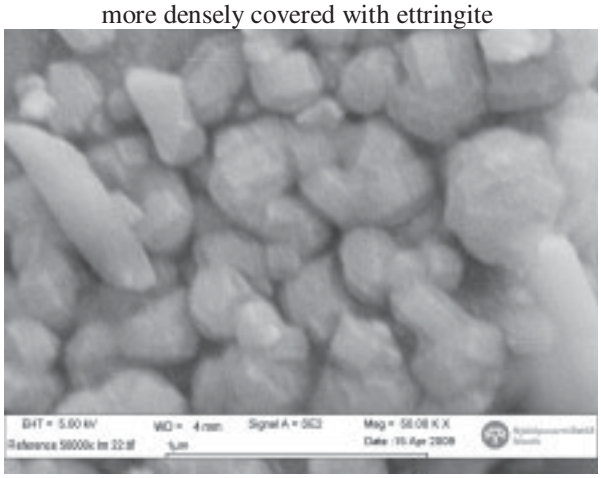

Figure 5.2.8.3.4: Short prismatic ettringite in reference paste

Paste containing 5000 ppm EG and TEPA

Some cement particles of paste containing 5000 ppm ethylene glycole were covered greatly with ettringite (see Figure 5.2.8.3.6) while others looked rather unhydrated (see Figure 5.2.8.3.5). The ettringite found was of short prismatic type. As can be seen from Figure 5.2.8.3.8 the ettringite in pastes made with EG is longer than in the reference paste. The same was observed for pastes made with tetraethylenepentamine (see Figures 5.2.8.3.9 and 5.2.8.3.10).

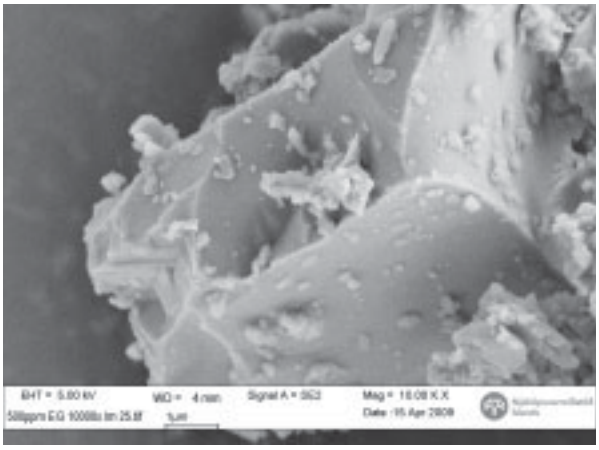

Figure 5.2.8.3.5: Cement surface of paste containing 5000 ppm ethylene glycole covered with few ettringite crystals

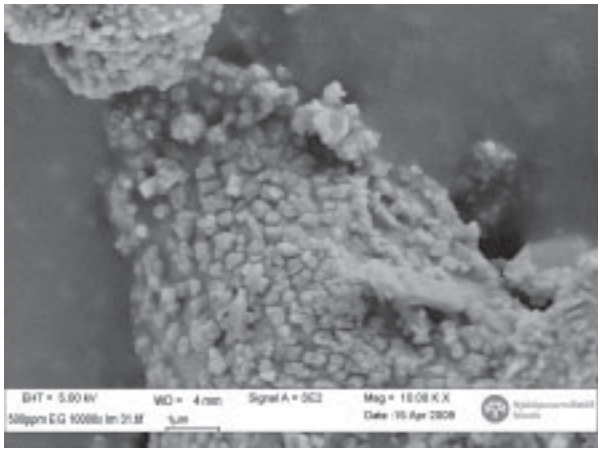

Figure 5.2.8.3.6: Cement surface of paste containing 5000 ppm ethylene glycole densly covered with ettringite crystals

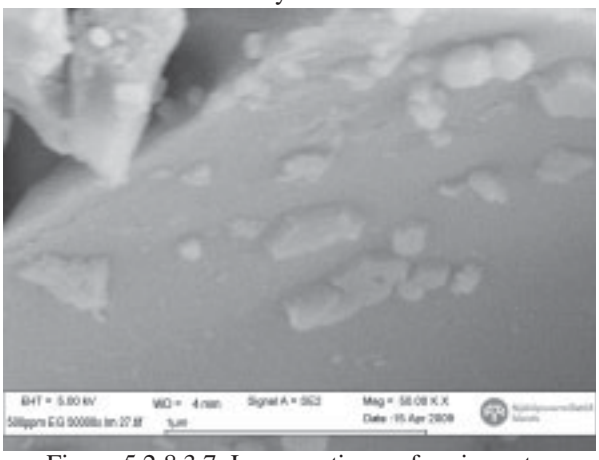

Figure 5.2.8.3.7: Less reactive surface in paste containing 5000 ppm ethylene glycole

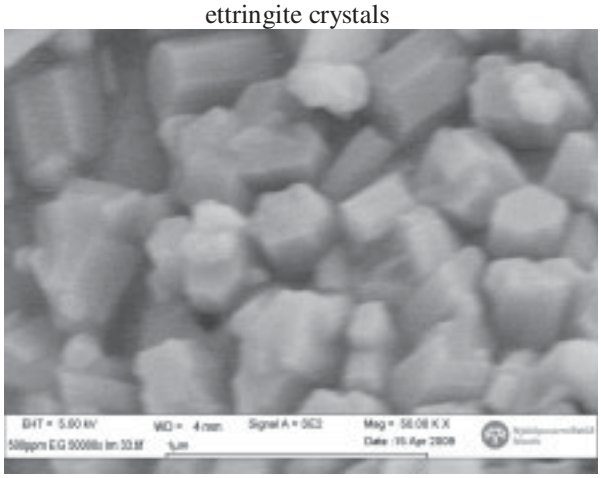

Figure 5.2.8.3.8: Short prismatic ettringite in paste with 5000 ppm ethylene glycole, slightly longer than in reference paste

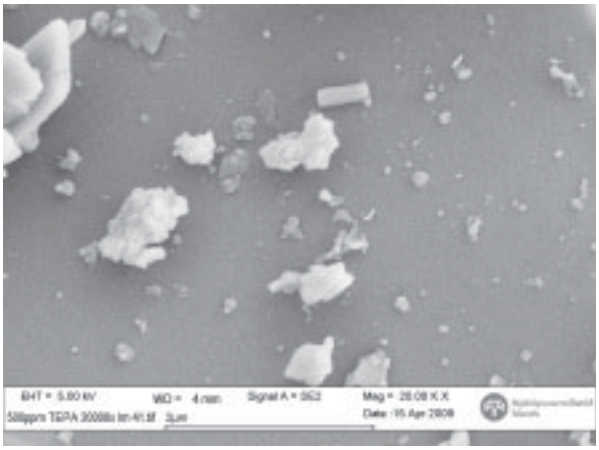

Figure 5.2.8.3.9: Less reactive surface in paste containing 5000 ppm tetraethylenepentamine

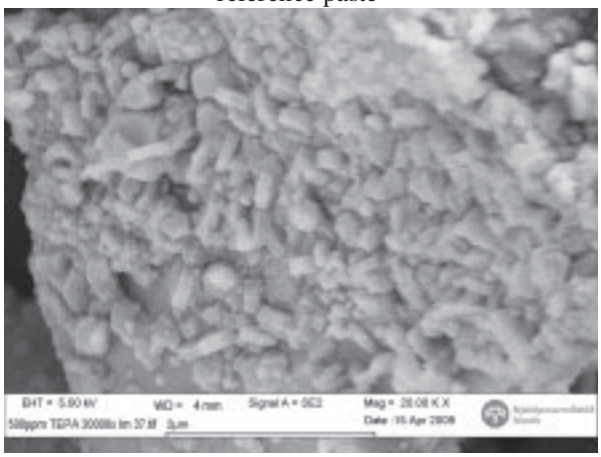

Figure 5.2.8.3.10: Relatively reactive surface in paste containing 5000 ppm tetraethylenepentamine

Paste containing 5000 ppm TEA1 and TEA2

The paste made with TEA 1 contained calcium aluminate hydrate plates (CAH). CAH was observed both in pastes made with TEA 1 and TEA 2. However, TEA 1 had no effect on yield value of mortar mixes (even not at dosages of 1% TEA 1). This is a somewhat contradictory observation to literature in which poor rheology is often attributed to platy calcium aluminate hydrate phases. CAH occurs when the aluminate phase reacts directly with water due to the absence of calcium and sulphate ions.

When 5000 ppm TEA 2 was present, the surfaces of cement grains were completely covered with relatively long ettringite. The length to thickness ratio of most ettringite found in pastes made with TEA 2 was in the range of three to four or above four, meaning the saturation index for ettringite was lower than in previous pastes. One reason for a low saturation level of ettringite could be a high amount of aluminates available for hydration. Figures 5.2.8.3.13 and 5.2.8.3.14 depict the surfaces of densely covered cement grains. Cement surfaces looked as if some kind of leaching process had happened because some parts of cement grains were missing while others looked unhydrated (see also Appendix P-1). Figure 5.2.8.3.15 illustrates the growth of the ettringite on a cement surface covered with cavities. The cavities indicate the spot where the aluminate phase was present. Based on these observations it appears that TEA 2 accelerated the hydration of the aluminate phase considerably. The relatively high amount of ettringite found in paste with TEA 2 could be due to an accelerated or activated ferrite phase. Note that pastes made with TEA 2 stiffened already after seven minutes of hydration.

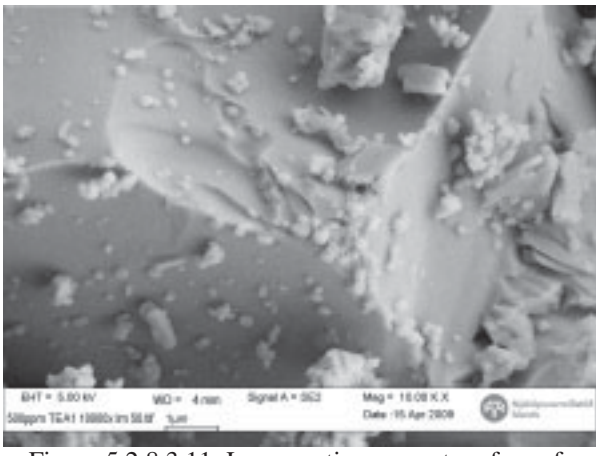

Figure 5.2.8.3.11: Less reactive cement surface of paste containing 5000 ppm TEA 1

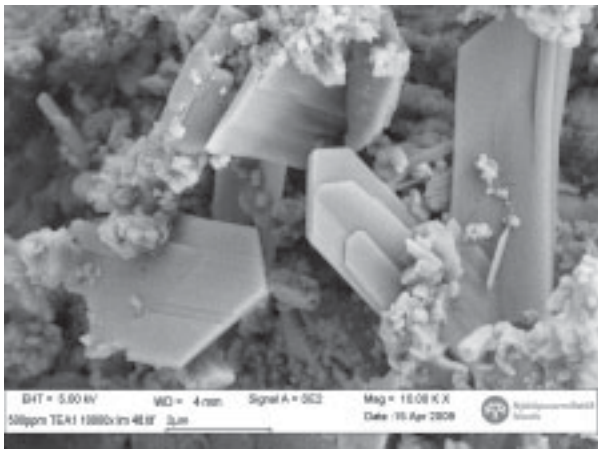

Figure 5.2.8.3.12: Platy calcium aluminate hydrate in paste containing 5000 ppm TEA 1

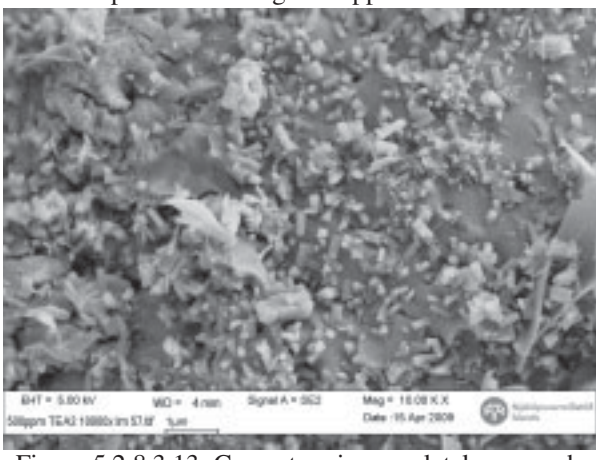

Figure 5.2.8.3.13: Cement grain completely covered with ettringite in paste containing 5000 ppm TEA 2

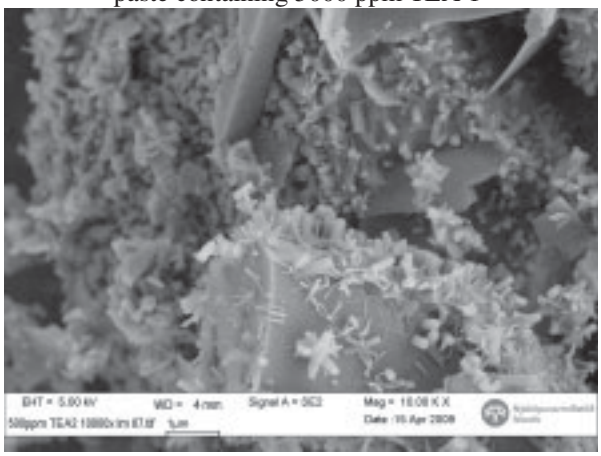

Figure 5.2.8.3.14: Ettringite in paste with 5000 ppm TEA 2

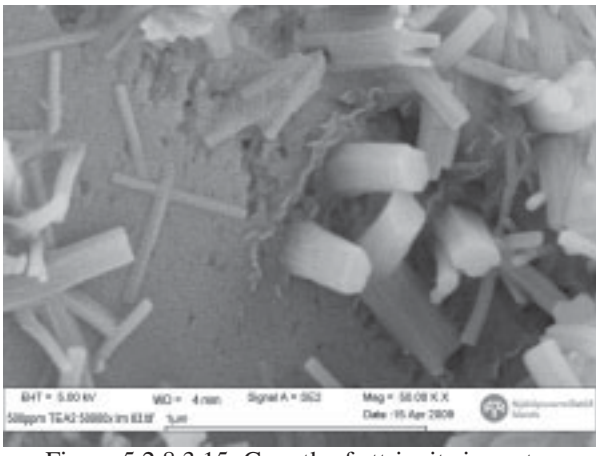

Figure 5.2.8.3.15: Growth of ettringite in paste containing 5000 ppm TEA 2

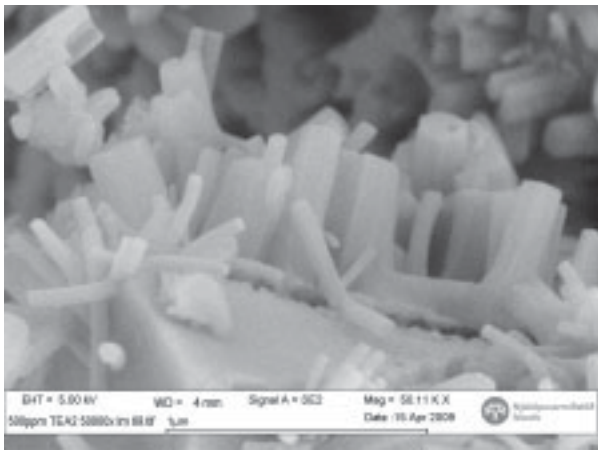

Figure 5.2.8.3.16: Growth of ettringite in paste containing 5000 ppm TEA 2

The paste made with TEA 2 showed a great amount of calcium aluminate hydrate folies bridging the free space between cement grains. Most likely the CAH folies formed when all available calcium sulphate had been consumed so that the remaining aluminates (and maybe even the ferrite phase) reacted directly with water.

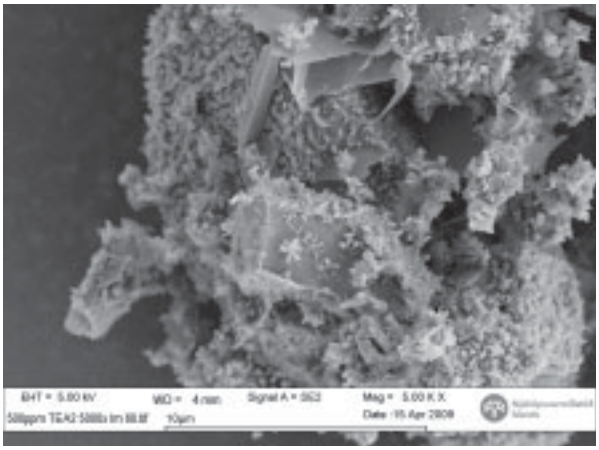

Figure 5.2.8.3.17: CAH folies bridging the free space between particles in paste with 5000 ppm TEA 2

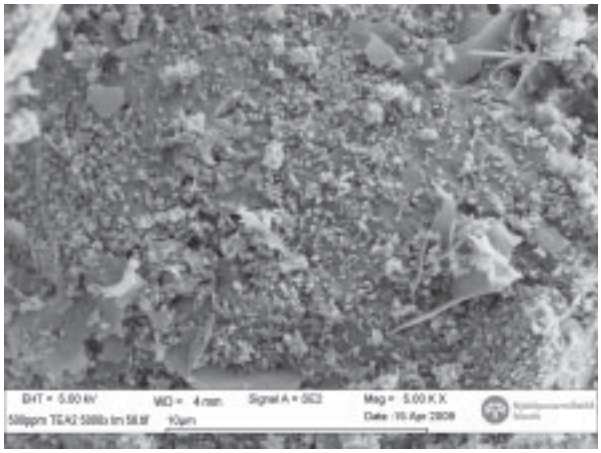

Figure 5.2.8.3.18: Calcium aluminate hydrate folies in paste containing 5000 ppm TEA 2

According to EDX analysis, the ettringite from Figure 5.2.8.3.15 contained around 10% carbon (see table 5.2.8.3.1) This is in line with results from chapter 5.2.5.1, where various EDX spectra of hydration products (such as syngenite and ettringite) contained 5% to 10% carbon when PC1 was present (see table 5.2.5.1.2). This means that a carbon containing compound (such as PC1) was either present on the suface or incorporated in the hydration products. The detected gold (element Au) is due to gold coating of samples.

Table 5.2.8.3.1: EDX spectrum ettringite

	EDX			Ettringite
Element	Weight%	Atomic%		Weight%
C	5.72	10.85		-
O	42.26	60.23		65,1
Si	10.70	8.69		-
S	0.42	0.30		7,4
Al	2.17	1.83		4,1
Ca	30.07	17.11		18,5
Au	8.67	1.00		-

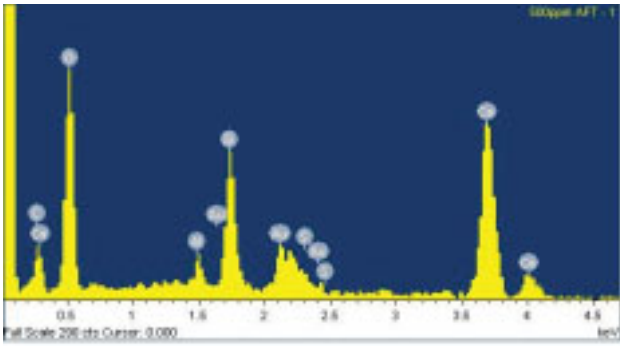

Figure 5.2.8.3.19: Chemical elements present in ettringite (EDX spectrum)

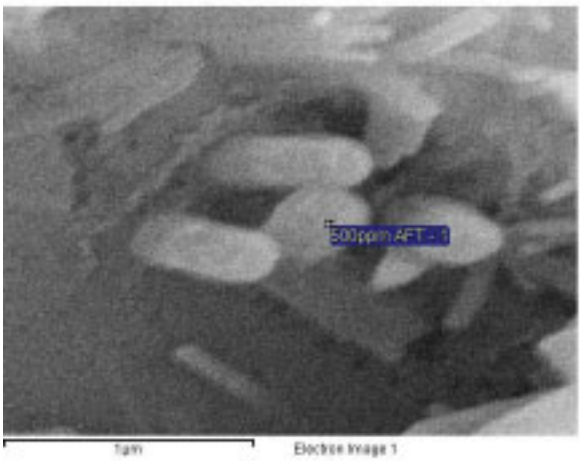

Figure 5.2.8.3.20: Location for EDX spectral analysis

The initial hydration curves of pastes blended with TEA 2 and microstructural observations on same pastes after ten minutes hydration indicate that the high reactivity of paste with 500 ppm TEA 2 is related to the formation of relatively much ettringite (see Figure 5.2.8.3.21). Next to ettringite the paste with 5000 ppm TEA 2 contained plates and folies of calcium aluminate hydrate. The reference paste showed only a moderate formation of short prismatic ettringite.

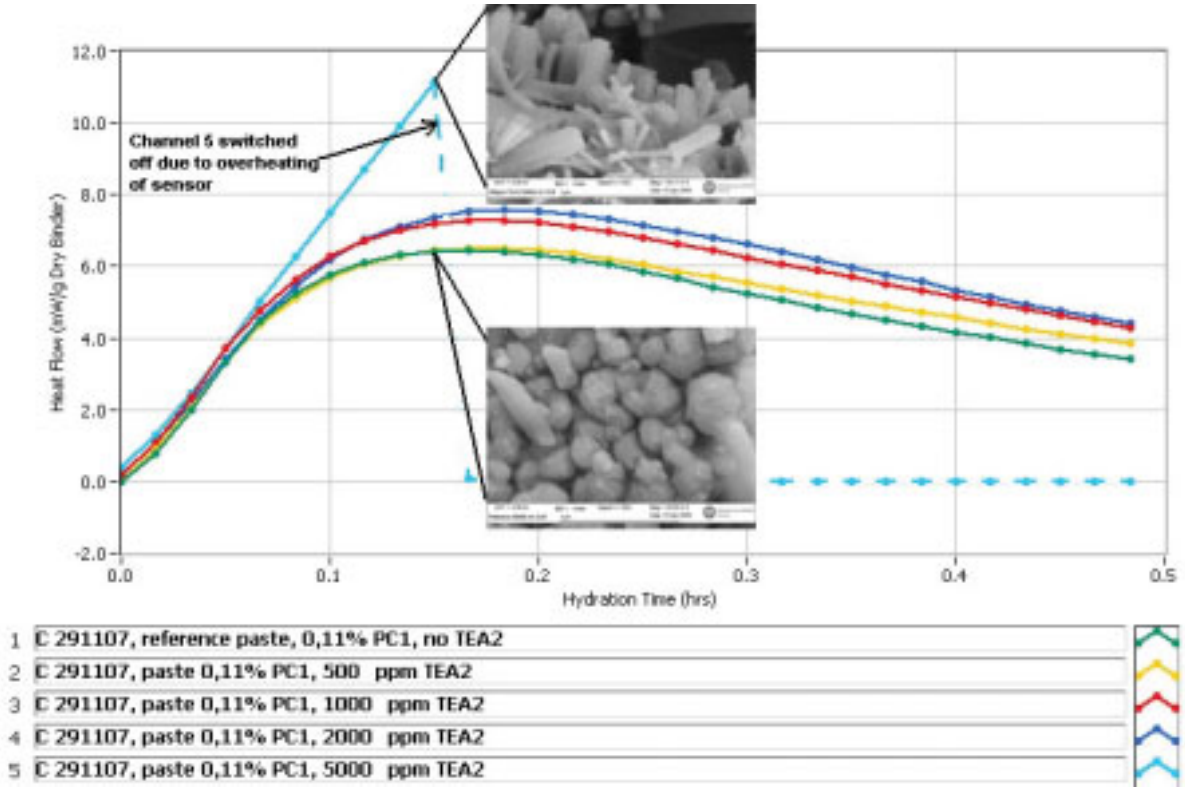

Figure 5.2.8.3.21: Hydration of pastes containing different dosages of TEA 2

5.2.9 Brief summary of parameters investigated and how they influence yield stress

Figure 5.2.9.1 illustrates how the yield value of mortar changes when various chemical compounds were added to mixes without admixtures. Chemicals were added at dosages up to 0,5% by weight of cement. A column and a fluctuation number indicate the influence on yield value. The fluctuation number is simply the difference between the reference mix and the maximum fluctuation. An increase in alkalinity and pH value resulted in a decreasing yield value or more or less stable yield value. One possibility is that at higher pH values the ettringite shifted to short prismatic type, resulting in a lower yield value than in the reference. Variations in alkalie sulphates had only minor influence on rheology. When the content of hemihydrate increased, the yield value went up due to secondary formed gypsum. On the other hand, when the slower dissolving dihydrate is present the yield value did not change. In mixes without admixtures, an excess of hemihydrate made mixes less fluid while a higher alkalinity made mixes more fluid.

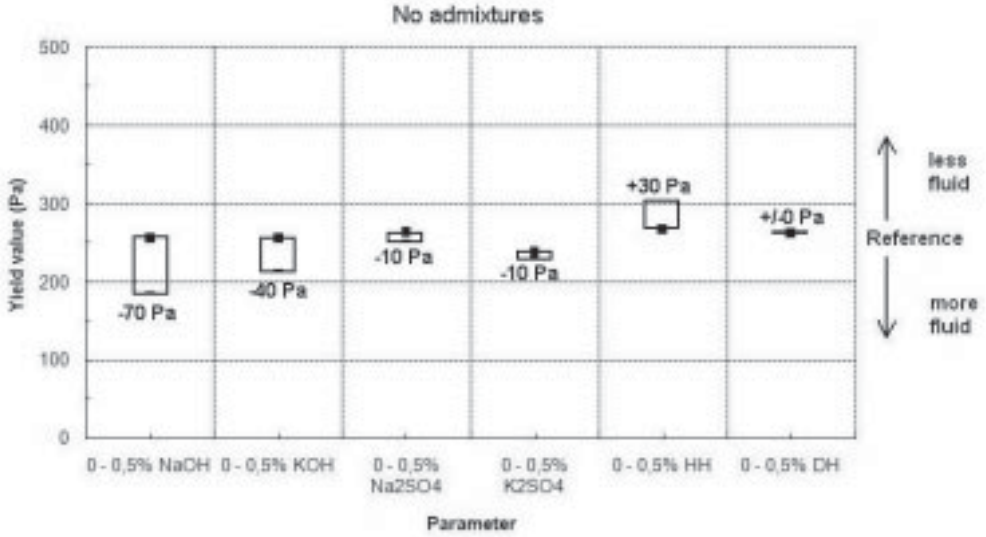

Figure 5.2.9.1: Various parameters and their effect on yield value in blank mixes

Figure 5.2.9.2 illustrates how the yield value changed when various chemicals were added to mixes containing PC1. PC1 is a typical fast adsorbing polymer with a high charge in the backbone and short side chains. Alkalie sulphates followed by sodium hydroxide had the greatest influence on the dispersing effect of PC1. In contrast, variations of the calcium sulphate carrier had nearly no effect on the dispersing effect of PC1. By comparing Figure 5.2.9.1 with Figure 5.2.9.2 it can be seen that parameters having an influence on blank mixes have only minor or even opposite effect on mixes with PC1.
Similar results were obtained with mixes containing melamine. Alkalie hydroxides and sodium sulphate had greater effect on yield value than variations in the calcium sulphate source.
In mixes with PC2, alkalie hydroxides and alkalie sulphates had the highest impact on yield value. Fluctuations in yield value due to an excess of hemihydrates or dihydrate are insignificant.

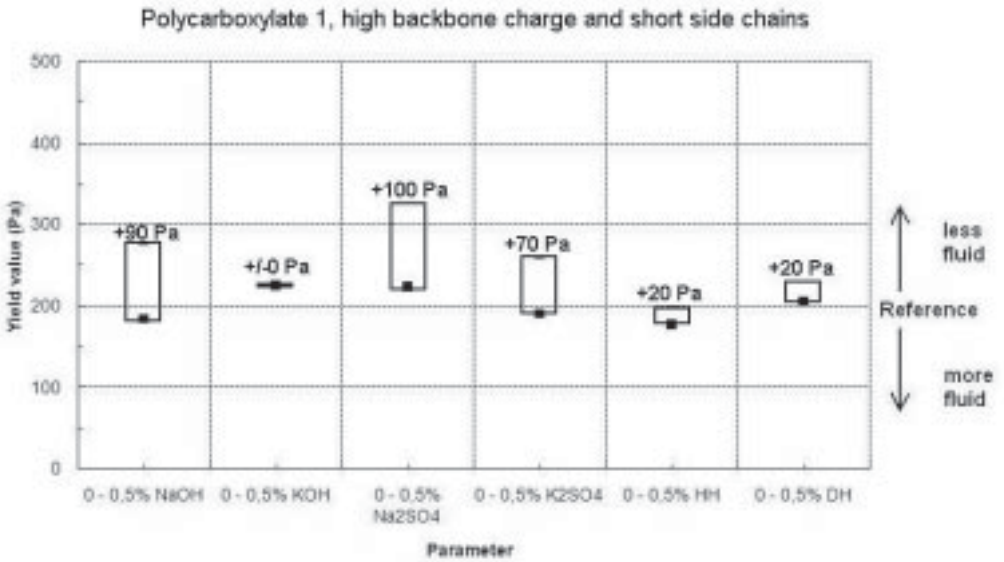

Figure 5.2.9.2: Various parameters and their effect on yield value in mixes with PC1

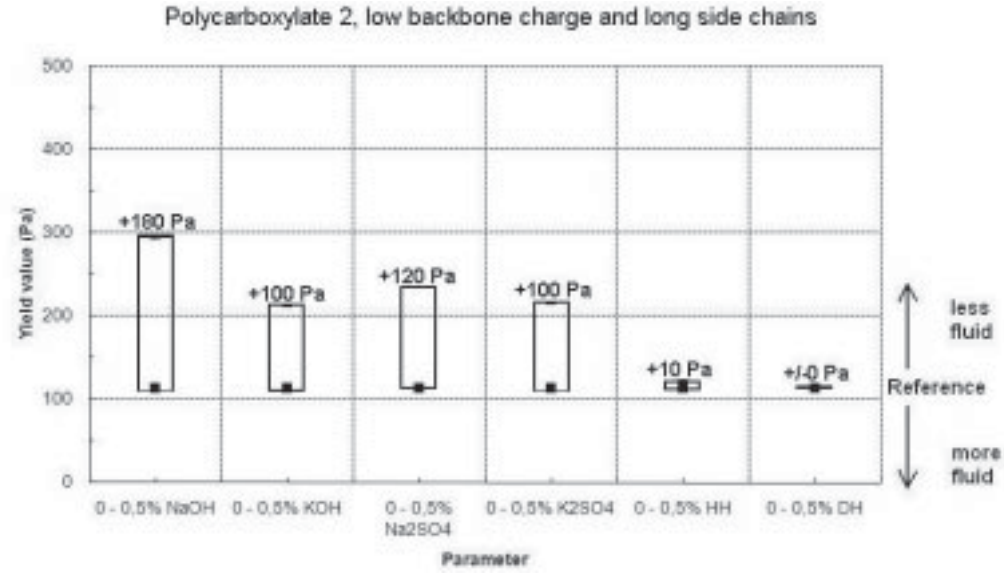

Figure 5.2.9.3: Various parameters and their effect on yield value in mixes with PC2

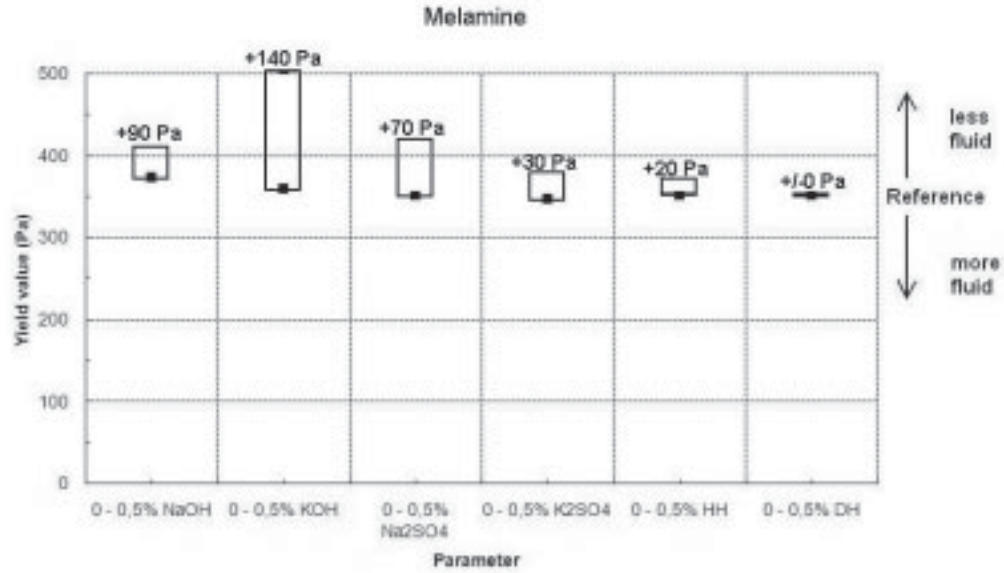

Figure 5.2.9.4: Various parameters and their effect on yield value in mixes with melamine

5.2.10 Some hypothesis

Rheological properties of mortar and concrete can change with cement production date. As a result mortar and concrete mixes can become more sticky or more liquid than expected. A major reason for such a cement-admixture interaction problem seems to be the shape, size and number of early hydration products. Several parameters influencing the formation of hydration products were identified during this study. It was found that an interaction problem affects more the rheological parameter yield value than the plastic viscosity. Hydration products which can lead to an increase in yield value are syngenite, folies or plates of calcium aluminate hydrate, a high amount of ettringite and secondary formed gypsum. It is assumed that a higher amount of ettringite is related to a more reactive aluminate or ferrite phase. Two independent mechanisms could generate the rheological fluctuations. Firstly, needle shaped syngenite, plates and folies of calcium aluminate hydrate and secondary formed gypsum increase the yield value by creating mechanical entanglements between cement particles. Figure 5.2.10.1 depicts this schematically. The free movement of cement particles is hindered by hydration products such as syngenite or secondary formed gypsum.

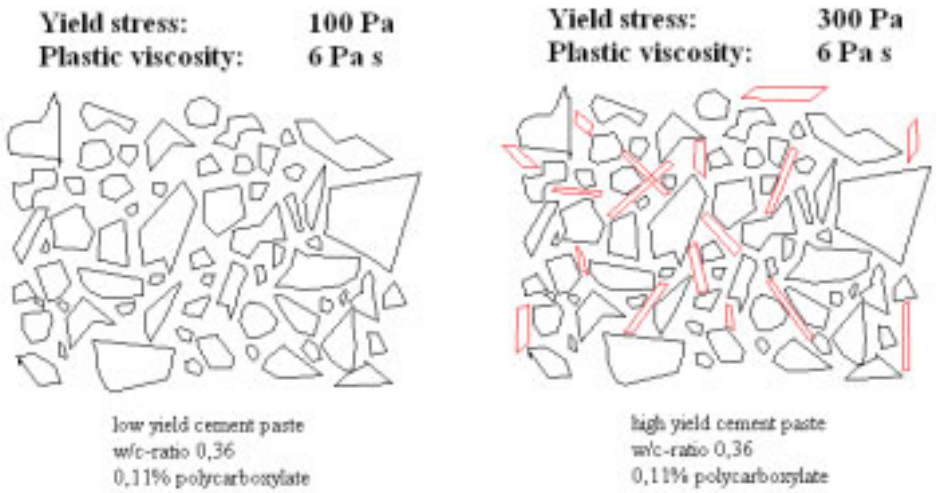

Figure 5.2.10.1: Schematic draft showing mechanical entanglements

The second mechanism can be due to an accelerated aluminate or ferrite phase resulting in a big number of ettringite crystals. They can increase the yield value by consuming the dispersing polymers. The polymers are then incorporated in the growing ettringite or simply adsorbed on the surface of the numerous ettringite particles (see Figure 5.2.10.2).

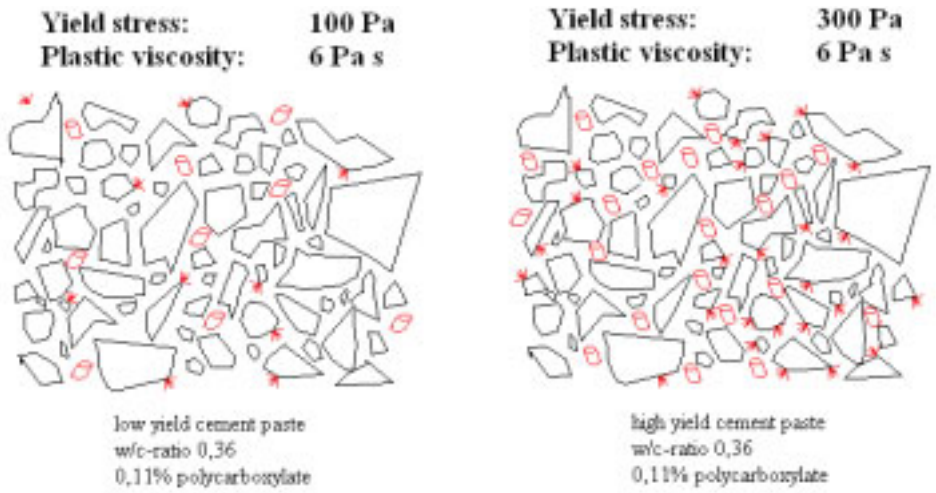

Figure 5.2.10.2: Schematic draft showing an accelerated or activated aluminate and ferrite phase

6. Final remarks

Cement samples from several countries and producers were examined on their rheological properties. The first aim of the study was to see if fluctuations due to different cement production dates can be seen in mortar mixes. The focus was on mixes in particular where dispersing admixtures were used. The admixtures used were based on melamine and polycarboxylate.

- A clear impact of different cement production dates on rheological properties was observed. The effect is moderate (c.o.v. ~15%) in mixes without any dispersing admixtures but far more prominent (c.o.v. ~40%) in mixes containing dispersing admixtures.
- The melamine-based admixture caused the highest fluctuations (c.o.v.~41%), whereas the fluctuations with the polycarboxylate based admixture were less (c.o.v.~27%).

The second aim of the study was to identify the constituents in cement which lead to the fluctuations in the mortar mixes.

- The ingredients which seemingly exert the largest influence on yield value are not the same for blank mixes as for those containing dispersing admixtures.
- In blank mixes there is an indication that the increase in yield value is seen to go together with increasing surface area of the cement used, whereas this effect is not observed if dispersing admixtures are present.
- From the received cement production dates, no influence of C_3A on yield value was observed in blank mixes and mixes containing melamine. In mixes containing polycarboxylate (PC1) there is an indication that an increase in C_3A resulted in increase in yield value. It should be noted that the fluctuations in C_3A content were very low. Thereby it is rather difficult to establish any relation between C_3A content and rheological data.
- When synthetic C_3A was added to blank mixes, a clear influence of C_3A content on rheology was observed.
- For alkali content (Na_2O equivalent), a similar tendency was observed; no clear trend in blank mixes or those containing melamine, but an increase in yield value of PC1 mixes with increasing Na_2O equivalent.
- When alkalie sulphates and hydroxides ($NaSO_4$, K_2SO_4, NaOH and KOH) were added to blank mixes the yield value decreased, whereas it increased when alkalie sulphates and hydroxides were added to PC1 and Mel mixes.
- Syngenite was observed in mixes with KOH and K_2SO_4

The third aim of the study was to investigate and quantify the effect of cement delivery on production properties of Eco and standard SCC. Cement samples of the same type of cement, differing only in production date were now used for production of SCC. Typical high and low yield cements were incorporated.

- The utilization of high yield cement in Eco and standard SCC resulted in low slump flows and high yield stresses, whereas the utilization of low yield cement resulted in high slump flows and low yield stresses.
- The variations in concrete due to production date were in the range of one consistency class (~10 to 12 cm).

- The variations in concrete were less prominent as in mortar. This might be explained by: (1) the lower cement content in Eco-SCC and (2) the higher inner shear rate in concrete.
- The devices used for rheological measurements in mortar showed a good ability to predict the rheological properties in concrete.

Additional tests were carried out with respect to,

- Adsorption measurements indicate that cements differing in rheological properties also differ greatly in polymer consumption. Cement giving a low initial yield stress had a bigger reservoir of available polymers after ten minutes of hydration than cement giving a high initial yield stress. Or in other words, the cement giving high initial yield stress consumed the polymers much faster than cement giving low initial yield stress.
- Pore solution analysis on cement with differing rheological properties showed clear differences in ion concentration. Particularly in mixes with PC1, the alkalie concentration (Na, K) was much higher in cement giving high initial yield stress than in cement giving low initial yield stress.
- The addition of silica fume resulted in an improvement of rheological properties, meaning the effect of cement production date was considerably reduced when silica fume of high purity was added to the mixes.
- Grinding aids tested showed different results. While some grinding aids such as TEA1 and TEPA had no influence on rheology or even improved flow properties, compounds such TEA2 and EG had a big influence on rheology and caused sticky mixes.

More work is necessary in the following fields.

- The interaction between grinding aid and different types of dispersing admixtures should be evaluated more detailed.
- The effect of supplementary cementitious materials (SCM), such as fly ash, lime stone filler and slag on rheological properties and their interaction with admixtures should be more in focus. SCMs will play a major role in achieving the goals of the Kyoto agreement.
- A microstructural study on different types of polycarboxylates focusing on their form and orientation on the cement surface should be carried out. One possibility to observe the adsorbed polymers on cement or ettringite surface might be the chryo-technique. It might also be worth a try to use tensides for polymer dispersion to prevent the film formation.

Literature

/Ab 1/ Abrams, D.A., Design of concrete mixes, Structural Materials Research Laboratory, Levis Institute, May 1925, pp. 1-20, Reprints from Minutes of the Annual Meeting of the Portland Cement Association, N.Y., Dec. 1918.

/Ai 1/ Aitcin, P. C., Jiang, S., Kim, B. G., Nkinamubanzi P. C., Petrov, N.: Cement/superplasticizer interaction - The case of polysulfonates. Bulletin des Laboratoires des ponts et chaussées –233- 7-8/2001, pp.89-99.

/Ba 1/ Private communication and discussion on conferences and meetings with representatives from BASF

/Be 1/ Bedard, C., Mailvaganam, N., P.: The Use of Chemical Admixtures in Concrete. Part I: admixture-cement compatibility. Journal of Performance of constructed facilities. Volume 19, No. 4, November 2005, pp. 263-266.

/Be 2/ Bellmann, F.: Zur Bildung des Minerals Thaumasit beim Sulfatangriff auf Beton. Dissertation an der Fakultät Bauingenieurwesen der Bauhaus-Universität Weimar (F.A. Finger-Institut für Baustoffkunde). FIB 2005.

/Be 3/ Bensted, J.: Gypsum in cements. In: Bensted, J., Barnes, P.J. (editor): Structure and performance of cements- 2nd edition. London: Spon Press, 2002.

/Bo 1/ Bonen, D., Sarkar, S.L.: The Superplasticizer Adsorption Capacity of Cement Pastes, Pore Solution Composition, and Parameters Affecting Flow Loss. Cement and Concrete Research, Vol. 25, No. 7, 1995, pp. 1423-1434.

/Br 1/ Brown, P.,W.: Kinetics of tricalcium aluminate and tetracalcium aluminoferrite hydration in the presence of calcium sulfate. Journal of American Ceramic Society 76 (1993) pp. 2971-2976.

/By 1/ Byfors, J.: Plain concrete at early ages. Publication series Cement- och Betonginstitutet. Stockholm, Sweden. 1980.

/Ce 1/ Cerulli, T., Clemente, P., Decio, M., Ferrari, G., Gamba, M., Salvioni, D., Surico, F.: A New Superplasticizer for Early High-Strength Development in Cold Climates. 7. CANMET/ACI Conference 2003, V.M. Malhotra, pp.113-126.

/Ch 1/ Chartschenko, I., Volke, K., Stark, J.: Untersuchungen über den Einfluss des pH-Wertes auf die Ettringitbildung. Wissenschaftliche Zeitschrift der Hochschule für Architektur und Bauwesen Weimar 39 (1993) Nr.3, S. 171-176.

/Ch 2/ Chandra, S., Björnström, J.: Influence of cement and superplasticizers type and dosage on the fluidity of cement mortars - Part 1. Cement and Concrete Research, Vol. 32, 2002, pp. 1605-1611.

/Ch 3/ Chandra, S., Björnström, J.: Influence of cement and superplasticizers type and dosage on the slump loss of Portland cement mortars - Part 2. Cement and Concrete Research, Vol. 32, 2002, pp. 1613-1619.

/Co 1/ www.contec.is Information about Viscometers. Status 8/2006.

/DIN1/ DIN EN 12350: Prüfung von Frischbeton, Teil 2 Setzmaß und Teil 5 Ausbreitmaß.

/Do 1/ Dodson, V.H.: Concrete admixtures. New York: Van Nostrand Reinhold, 1990, p.211.

/Er 1/ Erfurt, S., Mueller, A.: Particle size growth of early hydrating cement – Influence of water content and admixtures. Proceedings of the 3rd Rilem International Symposium on Rheology of Cement Suspensions such as Fresh Concrete. Reykjavik 19.-21.08.2009.

/Fe 1/ Ferraris, C.F., Brower, L.E., Comparison of Concrete Rheometers, Concrete International, Vol.25, No.8, pp.41-47, August 2003.

/Fl 1/ Flatt, R.J., Houst, Y.F.: A simplified view on chemical effects perturbing the action of superplasticizers. Cement and Concrete Research 31 (2001), pp. 1169-1176.

/Fl 2/ Flatt, R.J., Bowen, R., Siebold, A., Houst, Y.F.: Cement Model Powder for Superplasticizer Properties Studies. Proc. 11th ICCC, Durban, Techbook International, New Delhi, India, May 2003, pp. 676–685.

/Gr 1/ Grace Construction Services: Materials Compatibility, Using calorimetry to understand various material effects on concrete. Indiana Ready Mixed Concrete Association, Indianapolis, Indiana, December 2007.

Gl 1/ Glasser, F.P., Kindness, A., Stronach, S.A: Stability and solubility relationships in AFm phases. Part 1: Chloride, sulphate and hydroxide. Cement and Concrete Research. Vol. 29 (1999), pp.861-866.

/Fl 3/ Flatt, R.,J., Martys, N., Bergström, L.: The Rheology of Cementitious Materials. MRS Bulletin, Materials Research Society, Vol. 29, No. 5, pp.314-318, May 2004.

/Ha 1/ Hanehara, S., Yamada, K.: Interaction between cement and chemical admixture from the point of cement hydration, absorption behaviour of admixture, and paste rheology. Cement and Concrete Research 29 (1999), pp.1159-1165.

/Ha 2/ Hammer, T.A., Wallevik, J.E.: On the correlation between rheology of paste, mortar and concrete. in "Self Compacting Concrete SCC 2005 - Proceedings of The Second North American Conference on the Design and Use of Self-Consolidating Concrete", Chicago, 2005.

/He 1/ Heren, Z., Ölmez, H.: The influence of ethanolamines on the hydration and mechanical properties of Portland cement. Cement and Concrete Research. Vol. 26, No. 5, 1996, pp. 701-705.

/Ho 1/ Houst, Y.F., Bowen, P., Siebold, A.: Some basic aspects of the interaction cement-superplasticizers. Swiss Federal Institute of Technology, Institute of Materials Science, Powder Technology Laboratory, MXD, Lausanne, Switzerland, 2002.

/Ho 2/ Houst, Y.F., Bowen, P., Perche, F., Kauppi, A., Borget, P., Galmiche, L., Le Meins, J.-F., Lafuma, F., Flatt, R.J., Schobefr, I., Banfill, P.F.G., Swift, D.S., Myrvold, B.O., Petersen, B.G., Reknes, K.: Design and function of novel superplasticizers for more durable high performance concrete (superplast project). Cement and Concrete Research 38 (2008), pp. 1-13.

/Ho 3/ Hong, S.Y., Glasser, F.P.: Alkali binding in cement pastes. Part 1: The C-S-H-phase. Cement and Concrete Research. Vol. 29 (1999), pp. 1893-1903.

/Hj 1/ Hjartarson, B.: Rheometer-4SCC – Development of a portable rheometer for self compacting concrete. M.Sc. Thesis. 2006. Háskola Íslands (University of Iceland), Reykjavik, Iceland.

/ICI 1/ Innovation Center Iceland: Brochure 2008.

/IB 2/ Icelandic Building Research Institute: Innovation in concrete production by use of rheology. Progress Report 2. July 2005. (confidential)

/IB 3/ Icelandic Building Research Institute: Innovation in concrete production by use of rheology. Progress Report 3. December 2005. (confidential)

/IB 4/ Icelandic Building Research Institute: Innovation in concrete production by use of rheology. Progress Report 4. August 2006. (confidential)

/IR 1/ Irgens F.: Rheology and non-newtonian fluids. Lecture notes from Department of Structural Engineering, Norwegian University of Science and Technology, Trondheim, 2003.

/Ja 1/ Jawed, I., Skalny, J.: Alkalies in cement: a review I. Effects of alkalies and their effect on clinker formation. Cement and Concrete Research. Vol. 7, 1977, pp. 719-730.

/Ja 2/ Jawed, I., Skalny, J.: Alkalies in cement: a review II. Effects of alkalies on hydration and performance of Portland cement. Cement and Concrete Research. Vol. 8, 1978, pp. 37-52.

/Je 1/ Jeknavorian, A.A., Barry, E.F., Serafin, F.: Determination of grinding aids in Portland cement by pyrolysis gas chromatography-mass spectrometry. Cement and Concrete Research, Vol. 28, No. 9, 1998, pp. 1335-1345.

/Ji 1/ Jiang, S., Kim, B.G., Aitcin, P.C.: Importance of adequate soluble alkali content to ensure cement/superplasticizer compatibility. Cement and Concrete Research. Vol. 29, 1999, pp. 71-78.

/Jo 1/ Jolicoeur, C., Simard, M., A.: Chemical Admixture-Cement Interactions: Phenomenology and Physio-chemical Concepts. Cement and Concrete Composites, Vol. 20, 1998, pp. 87-101.

/Ju 1/ Jugovic, Z., T., Gillam, J., L.: Early hydration of abnormal setting Portland cement. Journal of Materials, Vol. 3, pp. 517-537, 1968

/Ka 1/ Kauppi, A., Banfill, P.F.G., Bowen, P., Galmiche, L., Houst, Y.F., Lafuma, F., Mäder, U., Perche, F., Petersen, B.G., Reknes, K., Schober, I., Siebold, A., Swift, D.: Improved superplasticizers for high performance concrete, Proc. 11th ICCC, Durban, Techbook International, New Delhi, India, May 2003, pp. 528–537.

/Kh 1/ Khalil, S.M., Ward, M.A.: Effect of sulphate content of cement upon heat evolution and slump loss of concretes containing high-range water-reducers (superplasticizers). Magazine of Concrete Research, Vol. 32, No. 110, March 1980, pp. 28-38.

/Ko 1/ Kong, H.J., Bike, S.G., Li, V.C.: Effects of a strong polyelectrolyte on the rheological properties of concentrated cementitious suspensions. Cement and Concrete Research, Vol. 36, 2006, pp. 851-857.

/Ku 1/ Kubens, S., Wallevik, O.: Interaction of cement and admixtures – the influence of cement deliveries on rheological properties. 16.ibausil Weimar (20.09.2006-22.09.2006 Weimar). Proceedings ibausil, Inorganic binders, article P 1.39B.

/Ku 2/ H. Kucerova, Ch. Rößler, The influence of alkali sulphates on the fluididty of superplasticizer containing cement pastes. In: Proceedings of the international symposium on Non-Traditional Cement & Concrete, Brno, Checz Republic, Ed.: V. Bilek, pp. 295-306, 2005.

/Ku 3/ Kubens, S., Wallevik, O.H.: Cement-admixture interaction – the effect of different cement deliveries on rheology and hydration of mortar and Self Compacting Concrete. in "Self Compacting Concrete SCC 2008 - Proceedings of The Third North American Conference on the Design and Use of Self-Consolidating Concrete", Chicago, 2008.

/Ku 4/ Kubens, S., Peng, H., Oesterheld, S., Wallevik, O., H.: Some effects of silica fume on variations in rheology of mortar due to production date of cement. Annual Transactions of the Nordic Rheology Society, Volume 16 (2008) Papers presented at the Nordic Rheology Conference, Copenhagen, Denmark, August 27-29, 2008.

/La 1/ Langenfeld M., Stark, J.: Frühe Hydratation von Portlandzement unter Zusatzmitteleinfluß – dargestellt im ESEM-FEG. Manuskript zum Vortrag auf der EDO-Tagung Saarbrücken 1998.

/Li 1/ Li, C.Z., Feng, N.Q., Li, Y.D., Chen, R.J.: Effects of polyethlene oxide chains on the performance of polycarboxylate-type water reducers. Cement and Concrete Research 35 (2005), pp.867-873.

/Lo 1/ Locher, F.W., Richartz, W., Sprung, S.: Erstarren von Zement Teil 2: Einfluß des Calciumsulfatzusatzes. Zement-Kalk-Gips 33 (1980), Heft 6, pp. 271-277.

/Lo 2/ Locher, F.W., Richartz, W., Sprung, S.: Erstarren von Zement *) Teil I: Reaktion und Gefügeentwicklung. Zement-Kalk-Gips 29 (1976), Heft 10, pp. 435-442.

/MB 1/SKW-MBT: Glenium – The new generation superplasticiser for High Performance Concrete. Brochure provided by BASF 09/2008.

/Me 1/ Mehta, P. K., Wang, S.: Expansion of ettringite by water adsorption. Cement and Concrete Research. Vol. 12, 1982, pp. 121-122.

/Me 2/ Mezger T.: Das Rheologie-Handbuch: Für Anwender von Rotations- und Oszillations-Rheometern. Curt R. Vincentz Verlag, Hannover, 2000.

/Mi 1/ www.mikroanalytik.de. Online Portal – General information about microanalysis, 2008.

/Mo 1/ Mollah, M.Y.A., Adams, W. J., Schennach, R., Cocke, D.L.: A Review of Cement – Superplasticizer Interactions and Their Models.

/Mö 1/ Möser, B.: Der Einsatz eines ESEM-FEG für hochauflösende und mikroanalytische Untersuchungen originalbelassener Baustoffproben. In: Tagungsbericht der 14. Internationalen Baustofftagung-ibausil. Weimar, 20.-23.09.2000, pp. 1/089-1/114.

/Mö 2/ Möser, B., Stark, J.: ESEM-FEG: A new scanning electron microscope for the building materials research. In: Zement Kalk Gips, Volume 52 (1999), pp. 212-221.

/MP 1/ MPA Stuttgart, Otto-Graf-Institut: Untersuchungsbericht 11-9010010/St06/Sche, Statistische Auswertung der Prüfergebnisse der Korngrößenverteilung von CEN-Normsand EN 196-1 im Rahmen der werkseigenen Produktionskontrolle, 19.09.2005

/Mu 1/ Mueller, A., Stark, U., Erfurt, S.: The Early Stage of Cement Hydration: Measurement of the Particle Size Distribution at Different Times. Proc. 12th ICCC, Montreal, Canada, 2007.

/Od 1/ Odler, I., Wonnemann, R.: Effect of alkalies on Portland cement hydration II. Alkalies present in form of sulphates. Cement and Concrete Research. Vol. 13, 1983, pp. 771-777.

/Oh 1/ Ohta, A., Sugiyama, T., Yanaka, Y.: Fluidizing Mechanism and Application of Polycarboxylate-Based Superplasticizers. Proceedings Fifth CANMET/ACI, Superplasticizers and Other Chemical Admixtures in Concrete. SP 173-19, pp. 359-378.

/Oh 2/ Ohta, A., Sugiyama, T., Uomoto, T.: Study of Dispersing Effects of Polycarboxylate-Based Dispersant on Fine Particles. Proceedings Sixth CANMET/ACI, Superplasticizers and Other Chemical Admixtures in Concrete. SP 195-14, pp. 211-228.

/Os 1/ Osbaeck, B., Jons, E.S.: The influence of the content and distribution of alkalies on the hydration properties of portland cement. 7th ICCC, Paris, 1980, Vol. 2, pp. 135-140.

/Po 1/ Pollitt, H.W., Brown, A.: Proceedings of the 5th International Symposium on chemistry of cement. Tokyo 1968, Vol. I, p.322

/Pa 1/ State of the art report 2.1: Key parameters influencing the alkali aggregate reaction, PARTNER-project-GRD1-CT-2001-40103.

/Pl 1/ Plank, J., Hirsch, C.: Impact of zeta potential of early cement hydration phases on superplasticizer adsorption. Cement and Concrete Research. Vol. 37, 2007, pp. 537-542.

/Pl 2/ Plank, J., Dai, Z., Zouaoui, N., Vlad, D.: Intercalation of Polycarboxylate Superplasticizers into C3A Hydrate Phases, in: V.M. Malhotra (Editor), Eighth CANMET/ACI Conference on Superplasticizers in Concrete, ACI, Sorrento, SP-239-14, 2006, pp. 201-214.

/Ra 1/ Ramachandran, V., S., Malhotra, V., M., Jolicoeur, C., Spiratos, N.: Superplasticizers: Properties and applications in concrete. Materials Technology Laboratory, CANMET, Ottawa, Ontario, Canada, March 1998.

/Ra 2/ Ramachandran, V.S.: Action of Triethanolamine on the Hydration of Tricalcium Aluminate. Cement and Concrete Research. Vol. 3, 1973, pp. 41–54.

/Ro 1/ Rothstein, D., Thomas, J.J., Christensen, B.J., Jennings, H.M.: Solubility behavior of Ca-, S-, Al-, and Si-bearing solid phases in Portland cement pore solutions as a function of hydration time. Cement and Concrete Research. Vol. 32, 2002, pp. 1663-1671.

/Rö 1/ Rößler, C., Kettrup, C.: Wirkung von Melamin- und Naphthalinharz-basierten Fliessmitteln auf die Phasenneubildung bei der Zementhydratation. Thesis, Wissenschaftliche Zeitschrift der Bauhaus-Universität Weimar, (2001) Heft 5/6 2001.

/Rö 2/ Rößler, C.: Hydratation, Fließfähigkeit und Festigkeitsentwicklung von Portlandzement - Einfluss von Fließmitteln, Alkalisulfaten und des Abbindereglers. Dissertation am F.A. Finger-Institut der Bauhaus-Universität Weimar, 2006.

/Rö 3/ Rößler, C., Stark, J.: The influence of superplasticizers on the hydration of normal Portland cement. In: Tagungsbericht der 15. Internationalen Baustofftagung-ibausil. Weimar, 24.-27.09.2003, pp. 1/509-1/522.

/Sa 1/ Sakai, E., Daimon M.: Mechanisms of superplastification, in Skalny, J., Mindess, S. (Editors): Materials Science of Concrete IV, American Ceramic Society, Westerville, OH, 1995, pp. 91-111.

/Sa 2/ Sandberg, P.: Manual for isothermal calorimetry on cement paste, mortar or concrete.

/Sa 3/ Sakai, E., Yamada, K., Ohta, A.: Molecular Structure and Dispersion-Adsorption Mechanisms of Comb-Type Superplasticizers Used in Japan. Journal of Advanced Concrete Technology, Vol. 1, No. 1, 16-25, 2003.

/Sa 4/ Sandberg, P.J., Roberts, L.R.: Cement-Admixture Interactions Related to Aluminate Control. Journal of ASTM International, June 2005, Vol. 2, No. 6.

/Se 1/ Seebach, M.V., Schneider, L,: Update on finish grinding with improved energy efficiency. World Cement 1986; 17 (8), pp. 336-346.

/Sh 1/ Shaw, D.J.: Introduction to Colloid and Surface Chemistry. 4th. ed. Butterworth-Heinemann. Boston, 1992, pp. 1-20.

/Si 1/ Simard, M., A., Nkinamubanzi, P., C., Jolicoeur, C.: Calorimetry, rheology and compressive strength of superplasticized cement pastes. Cement and Concrete Research. Vol. 23, 1993, pp. 939-950.

/Sp 1/ Sprung, S.: Einfluß der Mühlenatmosphäre auf das Erstarren und die Festigkeit von Zement. Zement-Kalk-Gips 27 (1974), Heft 5, pp. 259-267.

/Sp 2/ Spiering, G.A.C.M., Stein, H.N.: The influence of Na_2O on the hydration of C_3A. Part I: Paste hydration. Cement and Concrete Research. Vol. 6, 1976, pp. 265-272.

/Sp 3/ Spiratos, N., Pagé, M., Mailvaganam, N., Malhotra, V., M., Jolicoeur, C.: Superplasticizers for Concrete: Fundamentals, Technology, and Practice. Marquis, Quebec, Canada, 2006.

/Sta1/ Stark, J., Wicht, B.: Zur Geschichte der Zusatzmittel. Thesis, Wissenschaftliche Zeitschrift der Bauhaus-Universität Weimar, (1998) Heft 1/2 1998, pp.210-221.

/Sta2/ Stark, J., Möser, B., Bellmann, F.: Hydratation von Portlandzement. Lehrbrief des F.A. Finger-Institutes für Baustoffkunde, Bauhaus-Universität Weimar, Stand: Sommersemester 2004.

/Sta3/ Stark, J., Wicht, B.: Zement und Kalk: Der Baustoff als Werkstoff. Hrsg. F.A. Finger-Institut für Baustoffkunde der Bauhaus-Universität Weimar. Birkhäuser 2000.

/Sta 4/ Stark, J., Möser, B., Eckart, A.: New approaches to cement hydration. Part 1, ZKG Int. 54 (1) 2001, pp.52-60.

/Sta 5/ Stark, J., Möser, B., Eckart, A.: New approaches to cement hydration. Part 2, ZKG Int. 54 (2) 2001, pp.114-119.

/Sta 6/ Stark, U., Brückner, R., Müller, A.: In-situ-Messungen der Korngrößenveränderungen bei der Hydratation von Portlandzementen, ZKG Int 58 (2005) No. 1, S. 67 – 77

/Stu 1/ Stutzman, P.E., Leigh, S.: Compositional Analysis of NIST Reference Material Clinker 8486. Proceedings from the 22nd International Conference on Cement Microscopy, April 30 - May 2, 2000, Montreal, Quebec, Canada.

/Sy 1/ Sympatec: Sympatec HELOS-system. Operating Instructions. Sympatec GmbH, System-Partikel-Technik, 38678 Clausthal-Zellerfeld, Germany, 2000.

/Ta 1/ Tattersall, G.H., Banfill, P.F.G., The Rheology of Fresh Concrete, Pitman Books Limited, 1983.

/Ta 2/ Tanaka, Y., Ohta, A.: Chemical Structure and Dispersion Mechanism of Air Entraining High-Range Water Reducing Agents. NMB Research Transaction, No.9, 5-11, 1992.

/Ta 3/ Tang, F.J., Gartner, E.M.: Influence of Sulphate Source on Portland Cement hydration. Advances in Cement Research, Vol. 1, No. 2, 1988, pp. 67-74.

/Tay1/ Taylor, H.F.W.: Cement chemistry 2nd edition. Thomas Telford Publishing, Thomas Telford Services 1997.

/Tag 1/Tagnit-Hamou, A., Aitcin, P.-C.: Cement and superplasticizer compatibility. World Cement, pp. 38-42, 1993.

/Th 1/ Thomas, N.L., Double, D.D.: Calcium and silicon concentrations in solution during the early hydration of Portland cement and tri calcium silicate. Cement and Concrete Research, Vol. 11, No. 4, pp.675-687, 1981.

/Ts 1/ Tsakiridis, P.E., Katsioti, M, Giannatos, P., Tsibouki, Z., Marinos, J.: Characterization of various cement grinding aids and their impact on grindability and cement performance. Construction and Building Materials, Vol. 23, 2009, pp. 1954-1959.

/Uc 1/ Uchikawa, H., Sawaki, D., Hanehara, S.: Influence of kind and added timing of organic admixture on the composition, structure and property of fresh cement paste. Cement and Concrete Research, Vol. 25, No. 2, pp.353-364, 1995.

/Uc 2/ Uchikawa, H., Hanehara, S., Shirasaka, T., Sawaki, D.: Effect of admixture on hydration of cement, adsorptive behavior of admixture and fluidity and setting of fresh cement paste. Cement and Concrete Research, Vol. 22, No. 6, 1992, pp. 1115-1129.

/Uc 3/ Uchikawa, H., Hanehara, S., Sawaki, D.: The role of steric repulsive force in the dispersion of cement particles in fresh paste prepared with organic admixture. Cement and Concrete Research, Vol. 27, No. 1, 1997, pp. 37-50.

/VD 1/ VDZ-Onlinearchiv: Working mechanisms of super-plasticicers based on polycarboxylate ether. 7/2006.

/Vi 1/ Vikan, H., Justnes, H., Winnefeld, F., Figi, R.: Correlating cement characteristics with rheology of paste. Cement and Concrete Research, Vol. 37, 2007, pp. 1502-1511.

/Vi 2/ Vikan, H.: Rheology and reactivity of cementitious binders with plasticizers. Doctoral Thesis at NTNU 2005:189, also available at http://www.diva-portal.org/ntnu/theses/abstract.xsql?dbid=689.

/Vo 1/ Vogel, R.: Konzept für die Kalibrierung von Quasi-Koaxialzylinderrheometern und Rührwerken. Protokoll 96/1. Weimar 23.03.1996.

/Vo 2/ Vogel, R.: Fließen von Selbstverdichtendem Beton –Das Fließgesetz- Mitteilung 04/7. Weimar 28.12.2004.

/Vo 3/ Volynskii, A.L., Bazhenov, S.: Can deformation of a polymer film with a rigid coating model geophysical processes? The European Physical Journal, Edition 24, 2007, pp. 317-324.

/Wa 1/ Wallevik, O.H.: “IBRI at Your Service – The Rheology of Fresh Concrete”, The Icelandic Building Research Institute (IBRI), 1999.

/Wa 2/ Wallevik, O.H., ”Den ferske betongens reologi og anvendelse på betong med og uten tilsetning av Silicastøv”- Dr.-Ing.avhandling 1990:45 NTH (NTNU) Trondheim, Norwegen, 1990 (in Norwegian).

/Wa 3/ Wallevik, O.H., Rheology- A scientific approach to develop self-compacting concrete; 3rd International RILEM Symposium on SCC, 2003, 33Pro, pp 23-31.

/Wa 4/ Wallevik O.H., Kubens S., Müller F.: Influence of cement-admixture interaction on the stability of production properties of SCC. in “Self Compacting Concrete SCC 2007 - Proceedings of the Fifth International RILEM Symposium” Volume 1, Ghent, pp.211-216.

/Wa 5/ Wallevik O.H., Kubens S., Kjellsen K.: Effect of cement temperature and aging of cement on rheology of mortar. Norcem Report Brevik plant.

/Wa 6/ Wallevik, J.E.: Rheology of Particle Suspensions - Fresh Concrete, Mortar and Cement Paste with Various Types of Lignosulfonates (Ph.D.-thesis); Department of Structural Engineering, The Norwegian University of Science and Technology, ISBN 82-471-5566-4, ISSN 0809-103X, 2003.

/Wa 7/ Wallevik, O.H., Hjartarson, B., Palsson, O.P.: Rheometer-4SCC, a portable rheometer for self compacting concrete”, NordDesign Conference, Reykjavik, 2006, p.7.

/W 8/ http://www.mnhn.fr/mnhn/geo/Collection_Marine/themes_recherche/PagecoccolithesEng.htm

/W 9/ http://www.greenelectron-images.co.uk/sem/coccoliths/chalk-2.html

/Wo 1/ Wolther, H.: Einfluß der Calciumsulfatformen und der Mischdauer auf das Ansteifen und Erstarren des Zementes. Zement-Kalk-Gips 42 (1989), Heft 7, pp. 373-375.

/Xu 1/ Xu Q.: Chemische Wirkung von Erstarrungsbeschleunigern auf die frühe Hydratation des Portlandzementes. Dissertation an der Fakultät Bauingenieurwesen der Bauhaus-Universität Weimar (F.A. Finger-Institut für Baustoffkunde). Cuvillier Verlag. Göttingen 2005.

/Ya 1/ Yamada, K., Takahashi, T., Hanehara, S., Matsuhisa, M.: Effects of the chemical structure on the properties of polycarboxylate-type superplasticizer. Cement and Concrete Research 30 (2000), pp. 197-207.

/Ya 2/ Yang, M., Neubauer, C.M., Jennings, H.M.: Interparticle potential and sedimentation behaviour of cement suspensions. Advanced Cement Based Materials, Vol. 5 (1997) pp. 1–7.

/Yo 1/ Yoshioka, K, Sakai, E, Daimon, M., Kitahara, A.: Role of steric hindrance in the performance of water-reducers for concrete. Journal of Amercian Ceramic Society 80 (10) 1997, pp.2667-2672.

/Yo 2/ Yoshioka, K., Tazawa, E., Kawai, K., Enohata, T.: Adsorption characteristics of superplasticizers on cement component minerals. Cement and Concrete Research, Vol. 32, 2002, pp. 1507-1513.

/Ze 1/ Zellhuber, E., Kubens, S.: Strahlenschutzbeton- Erfahrungen aus der Baustellenpraxis. 16.ibausil Weimar (20.09.2006-22.09.2006 Weimar). Proceedings ibausil, Concrete and durability, article P 2.01B.

/Zh 1/ Zhang, T., Shang, S., Yin, F., Aishah, A., Salmiah, A., Ooi, T.L.: Adsorptive behavior of surfactants on surface of Portland cement. Cement and Concrete Research, Vol. 31, 2001, pp. 1009-1015.

/Zi 1/ Zing, A.: Cement-superplasticizer interaction: link between macroscopic phenomena and microstructural data of the early cement hydration. Dissertation submitted to the Swiss Federal Institute of Technology Zürich (ETH Zürich), 2008.

Appendix

Appendix A-1 Characteristic particle size distribution of cements used

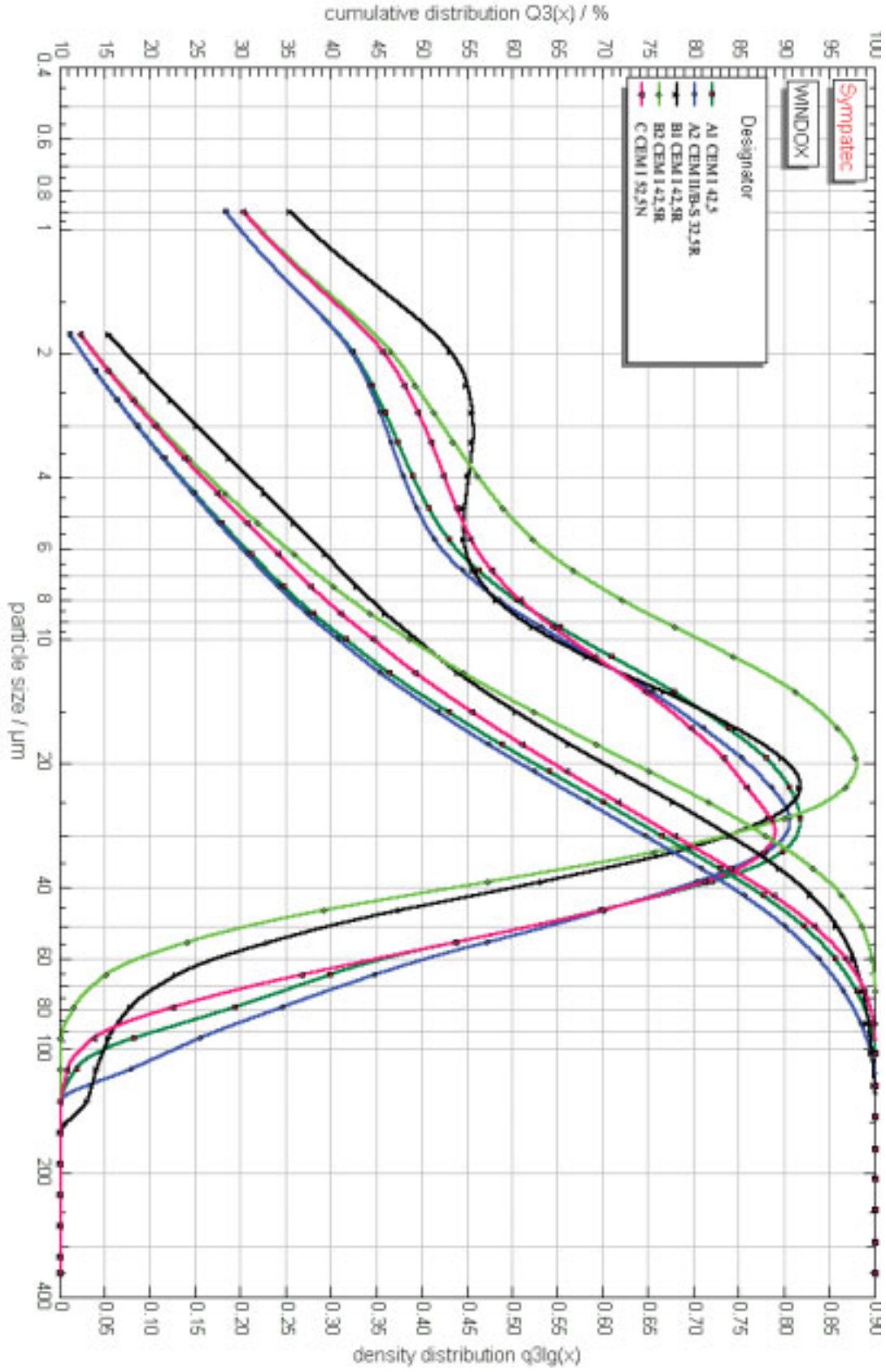

Appendix A-2 Dynamic particle size distribution (blank pastes)

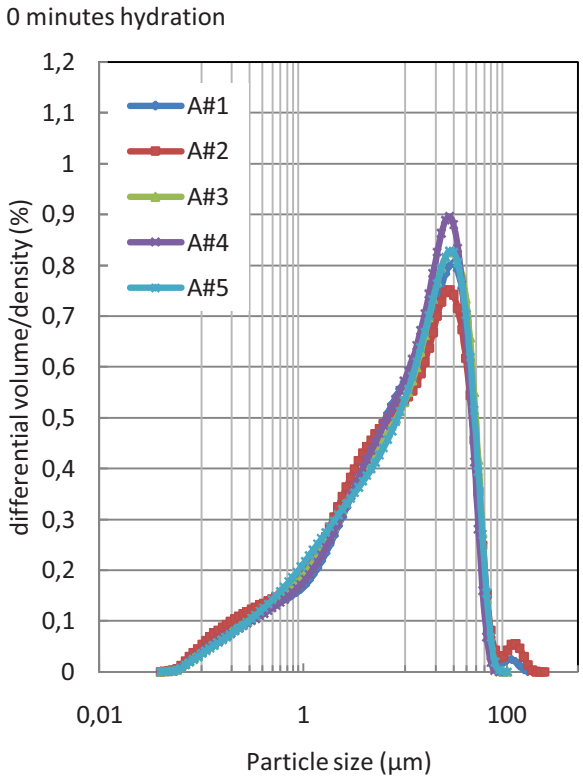

Figure A-2.1: Particle size distribution of unhydrated cement

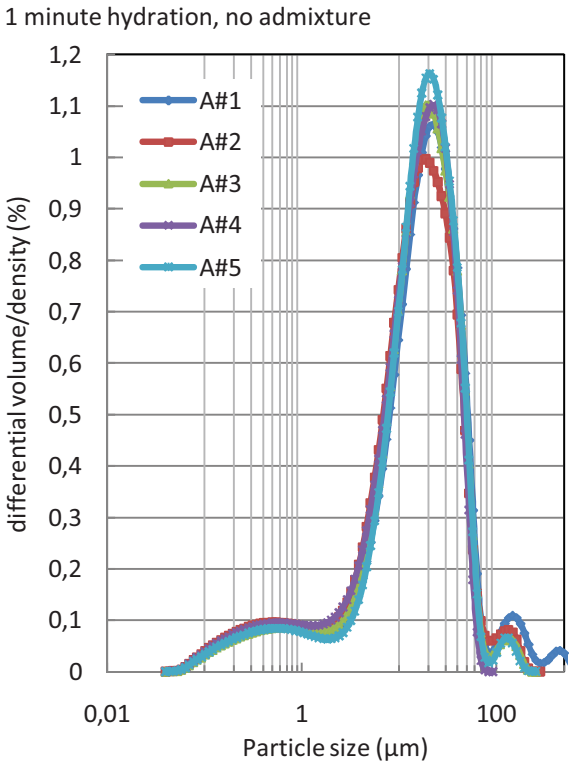

Figure A-2.2: Particle size distribution after 1 minute hydration no admixture

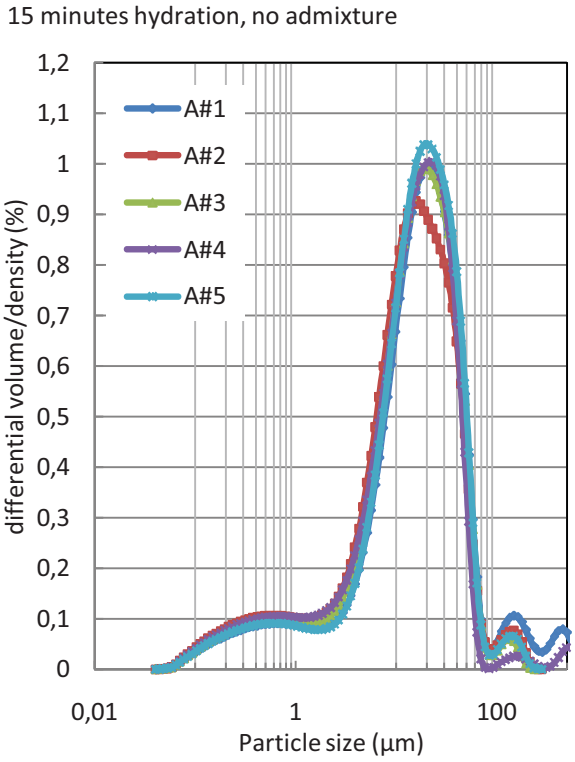

Figure A-2.3: Particle size distribution after 15 minutes hydration no admixture

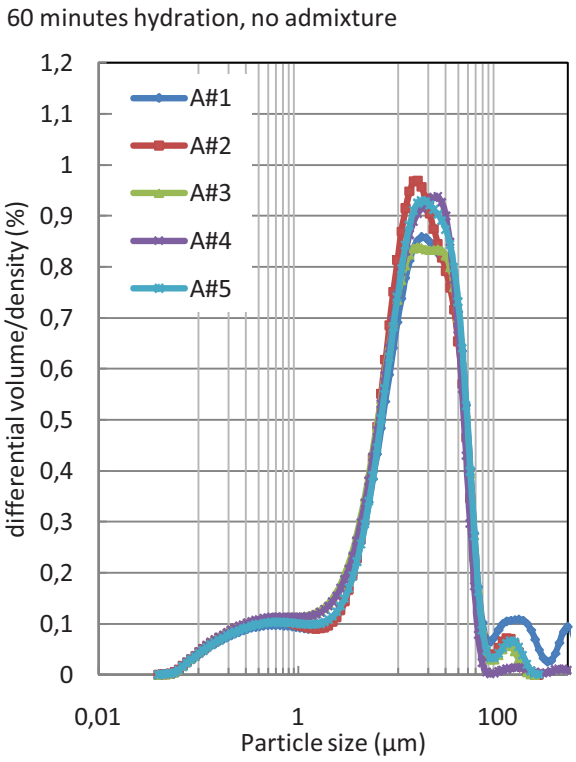

Figure A-2.4: Particle size distribution after 60 minutes hydration no admixture

Appendix B Case study with isothermal calorimeter

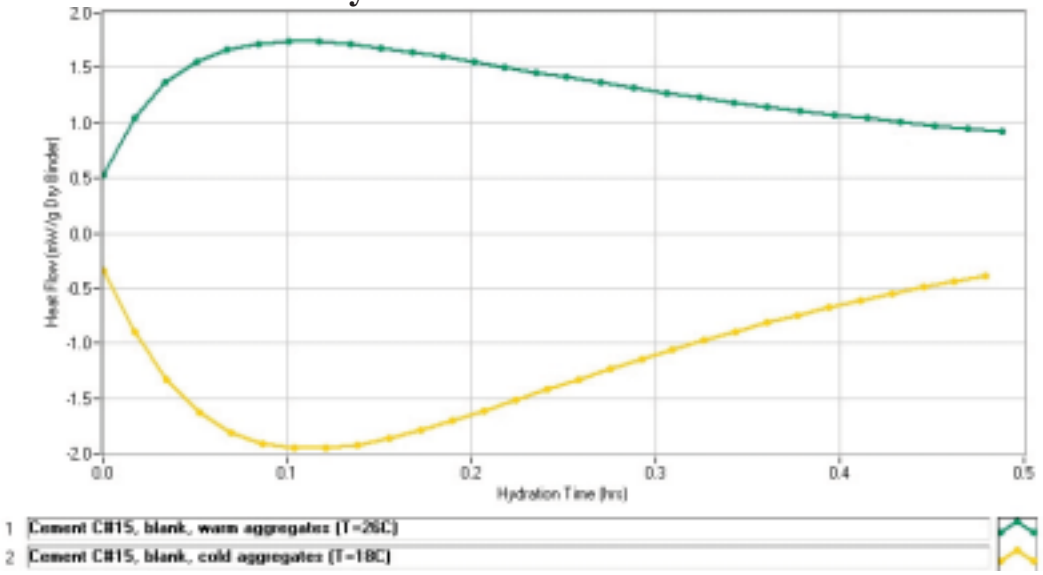

Figure B1: Effect of aggregate temperature on first peak

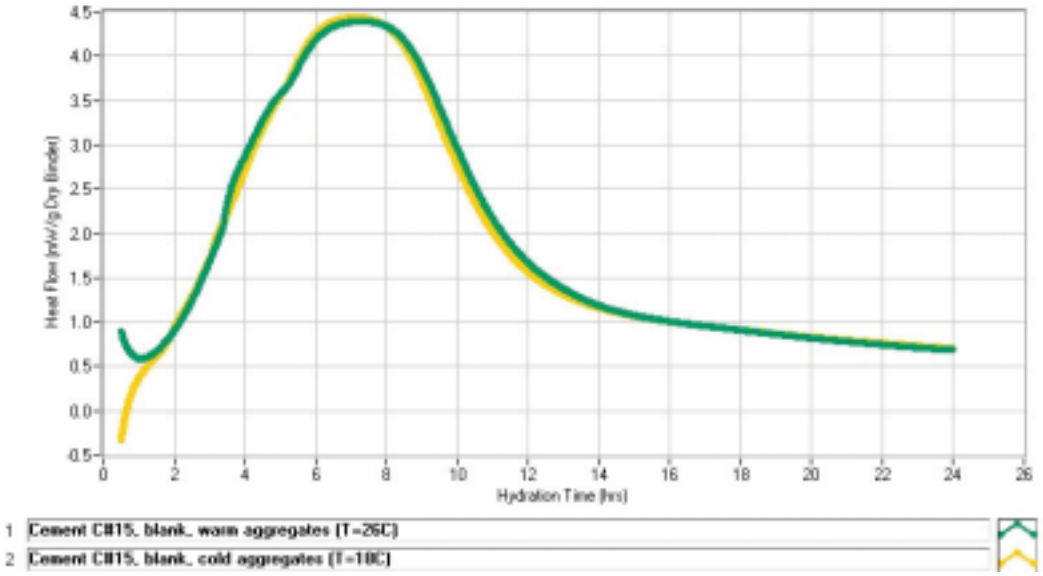

Figure B2: Effect of aggregate temperature on further hydration

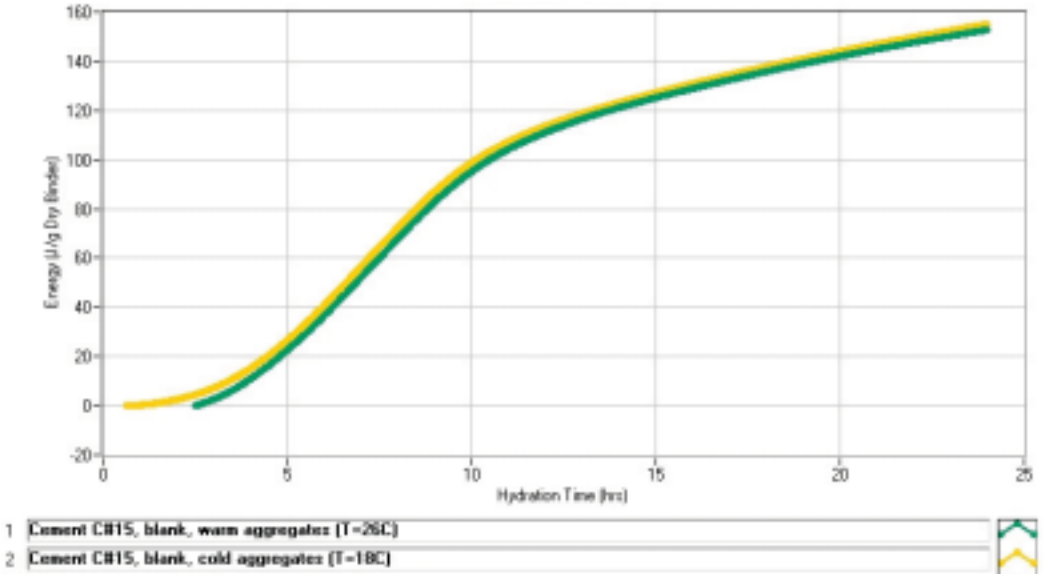

Figure B3: Effect of aggregate temperature on total energy release during first 24 hours of hydration

Appendix C Rheomixer versus Viscometer

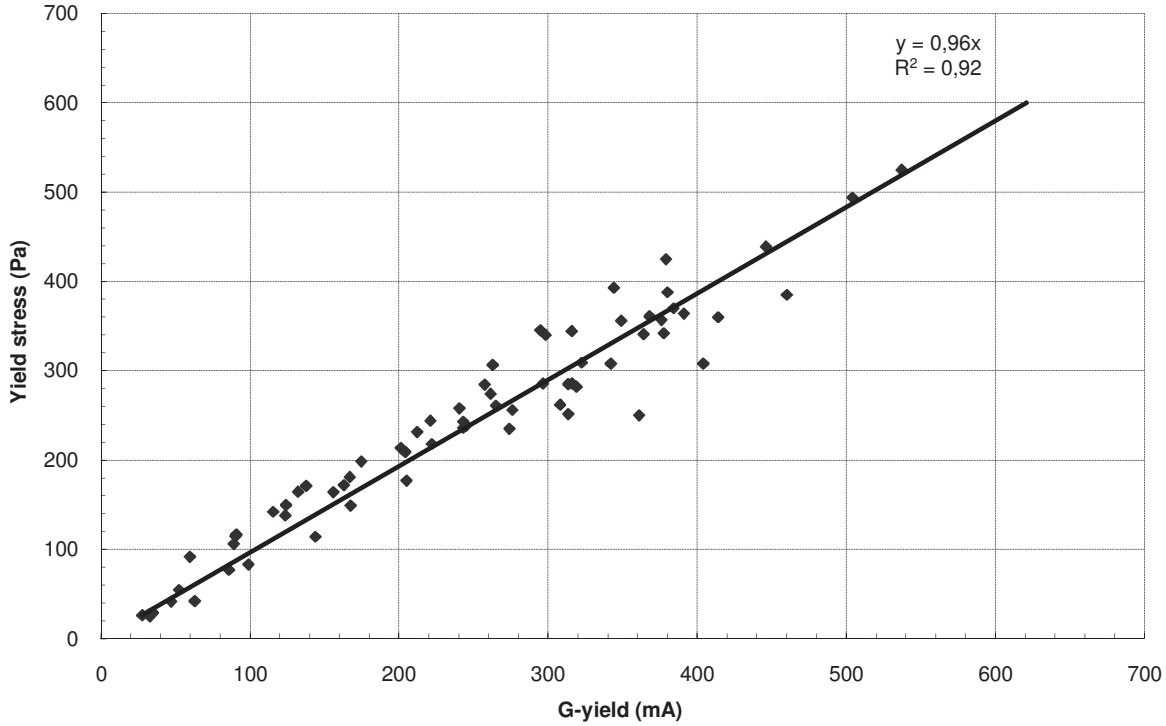

Figure C1: Relation between G-yield (Rheomixer) and yield stress (Viscometer 6)

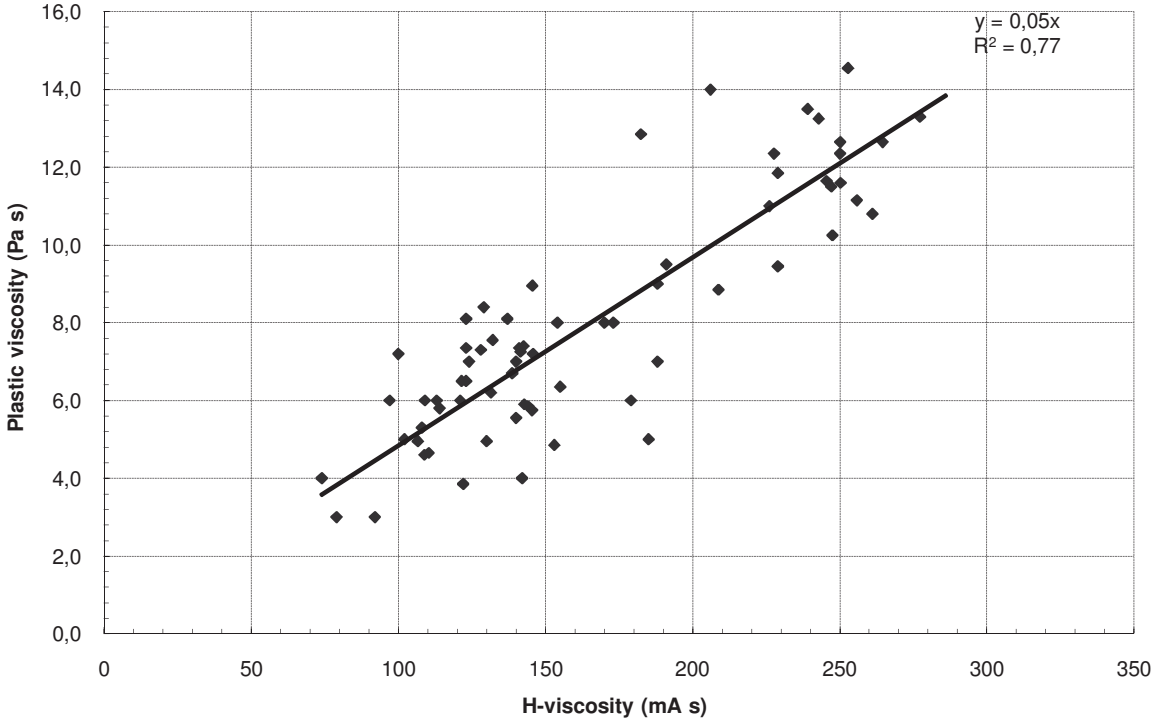

Figure C2: Relation between H-viscosity (Rheomixer) and plastic viscosity (Viscometer 6)

Appendix D Hydration curves cement B2

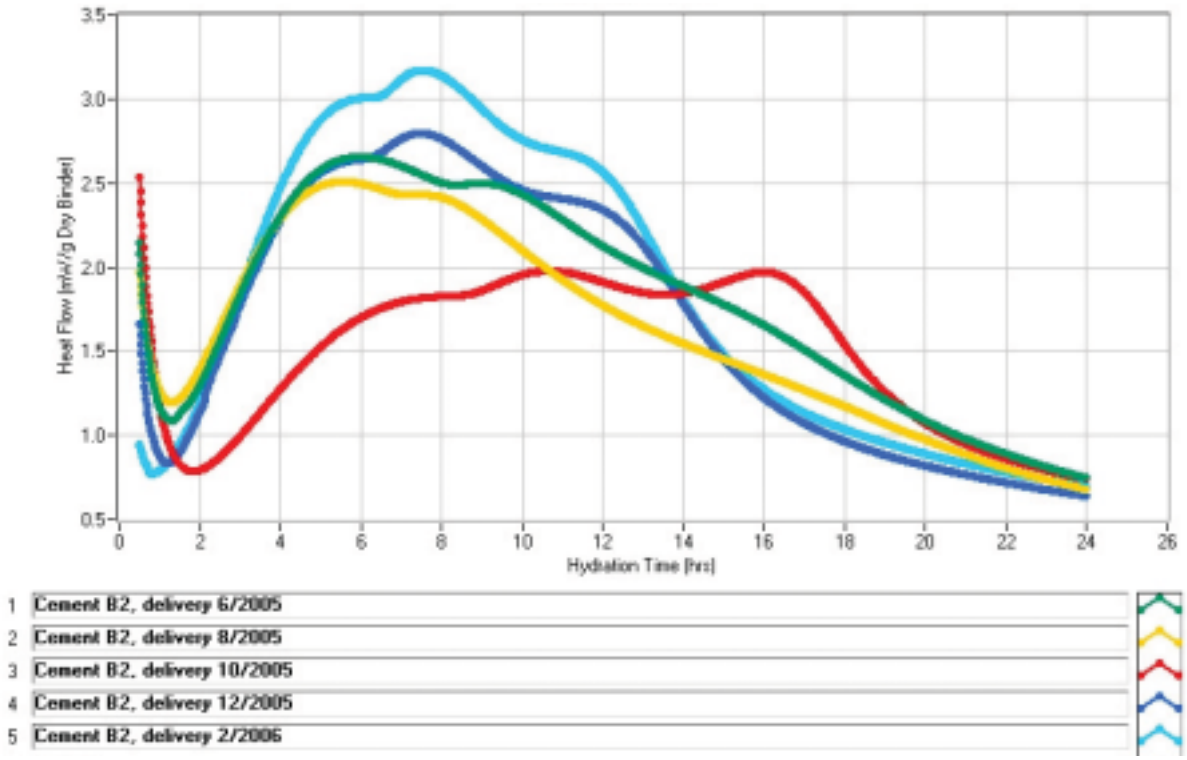

Figure D1: Effect of cement delivery on hydration progress in blank mixes (cement B2)

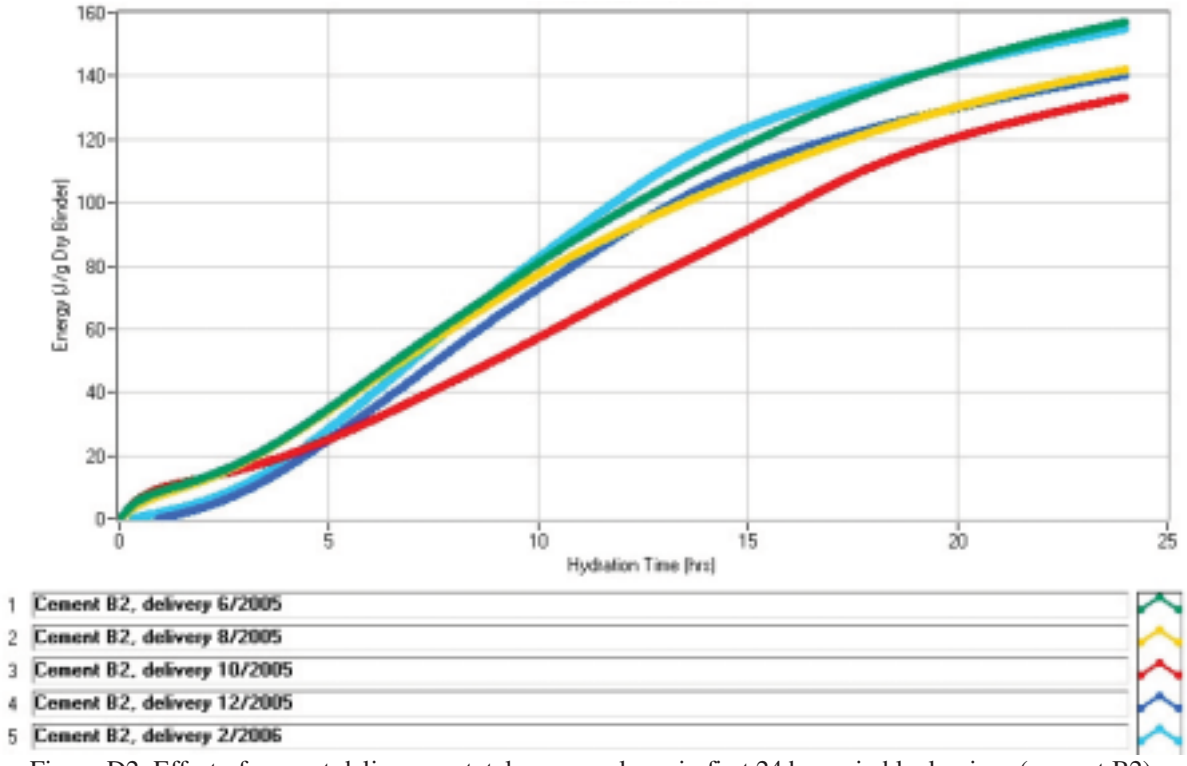

Figure D2: Effect of cement delivery on total energy release in first 24 hours in blank mixes (cement B2)

Appendix E Effect of type of admixture on hydration progress

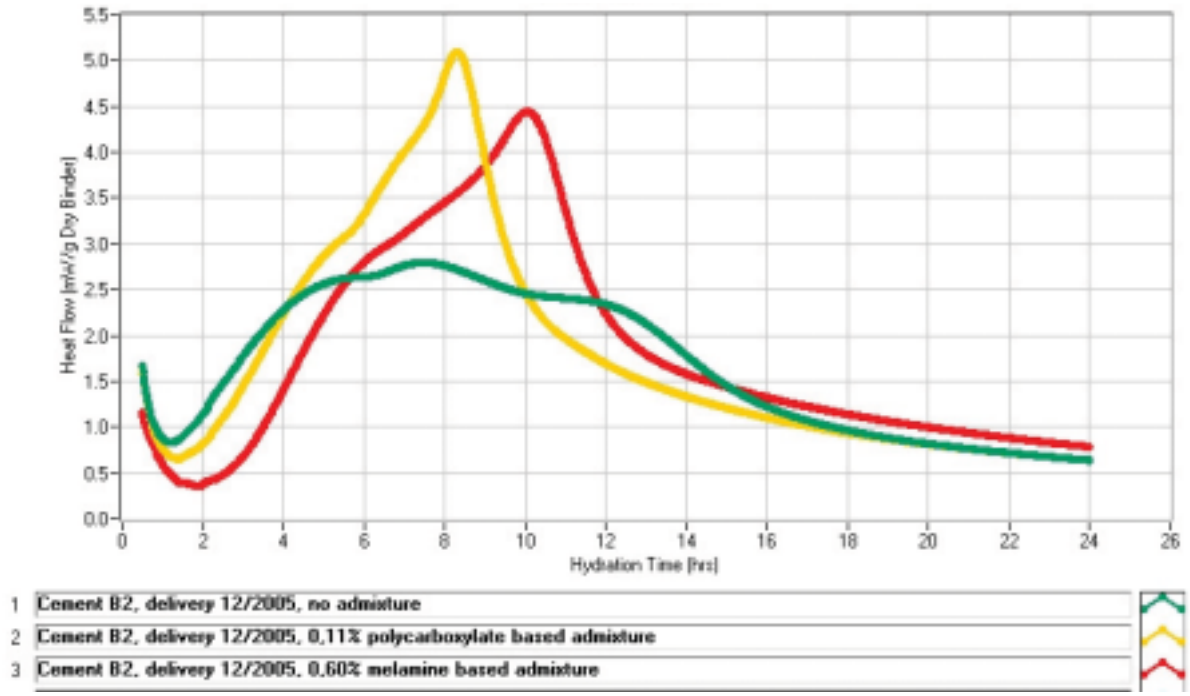

Figure E1: Effect of type of admixture on hydration (cement B2, 12/2005)

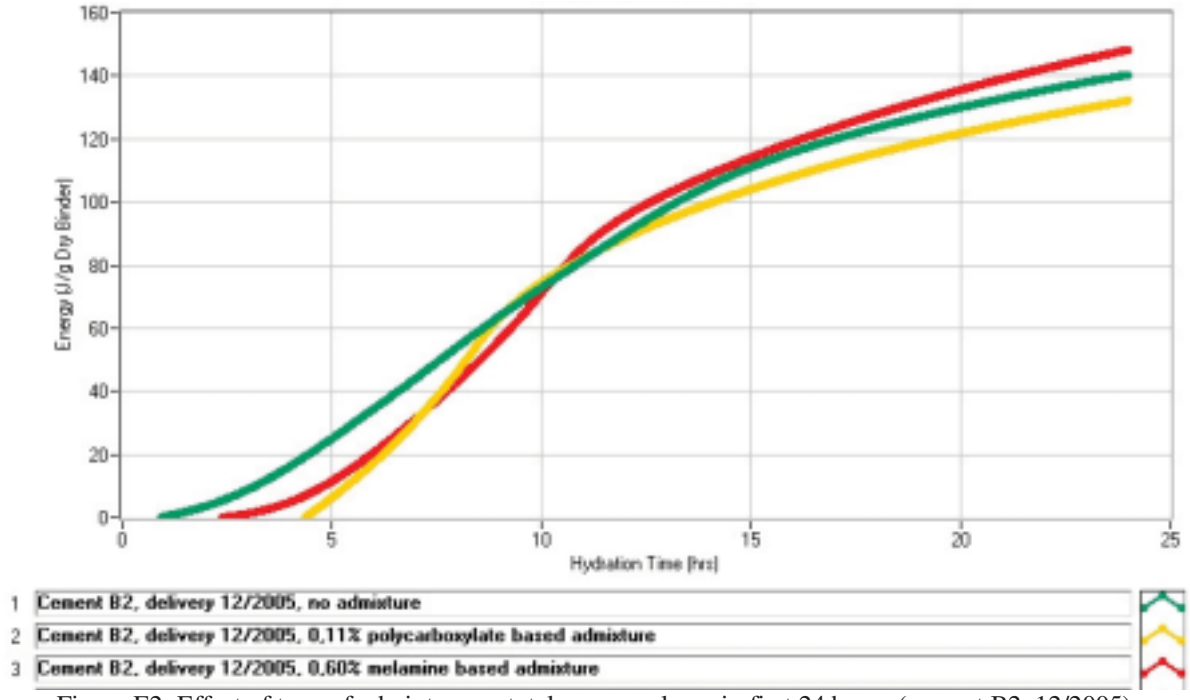

Figure E2: Effect of type of admixture on total energy release in first 24 hours (cement B2, 12/2005)

Appendix F Effect of C_3A addition on hydration progress

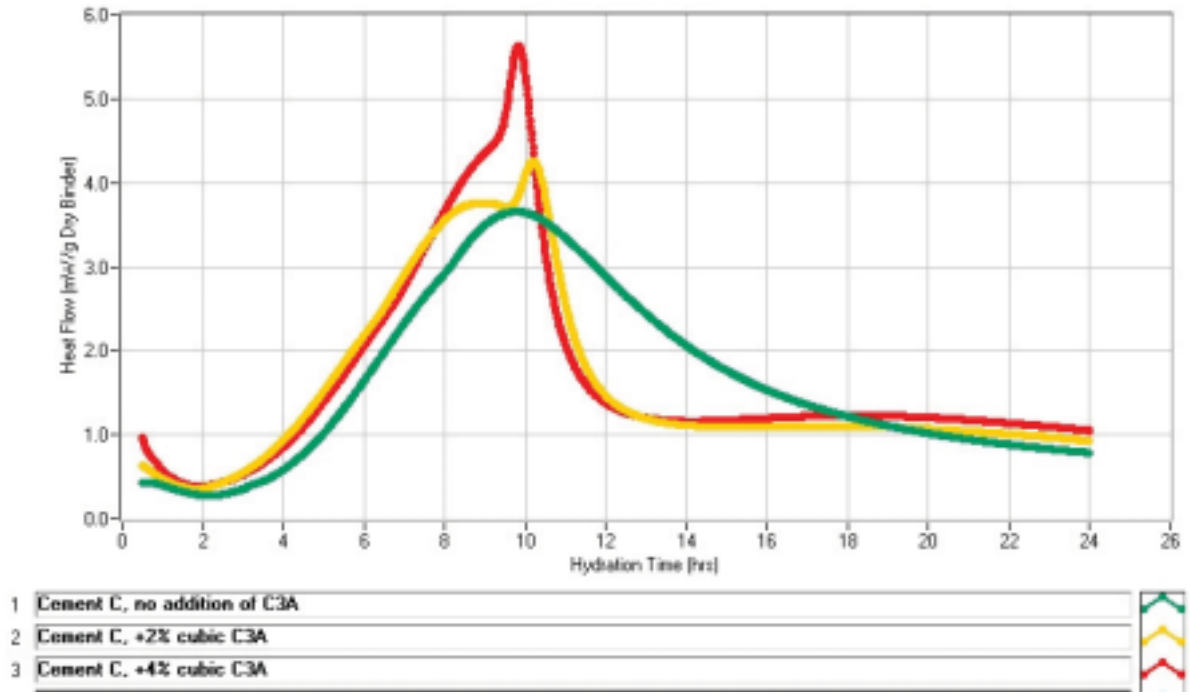

Figure F1: Effect of C_3A addition on hydration progress

Appendix G-1 Effect of sodium hydroxide and potassium hydroxide on hydration progress

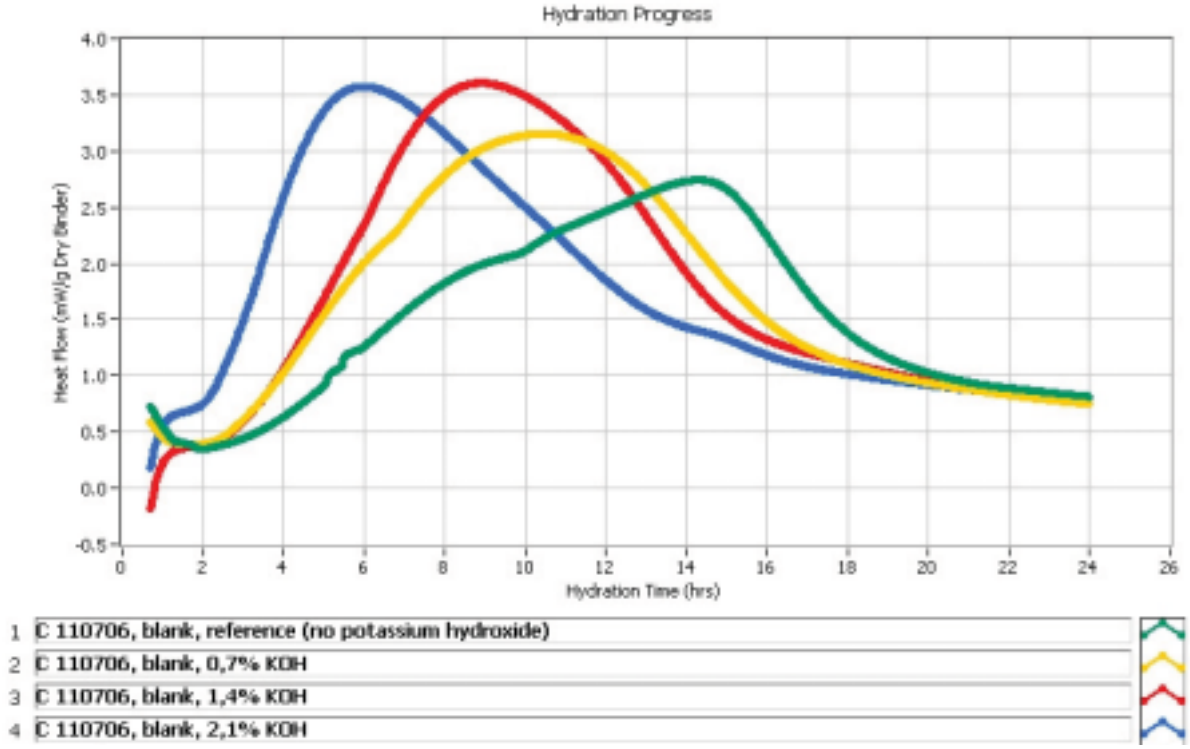

Figure G1: Effect of potassium hydroxide on hydration process in blank mixes

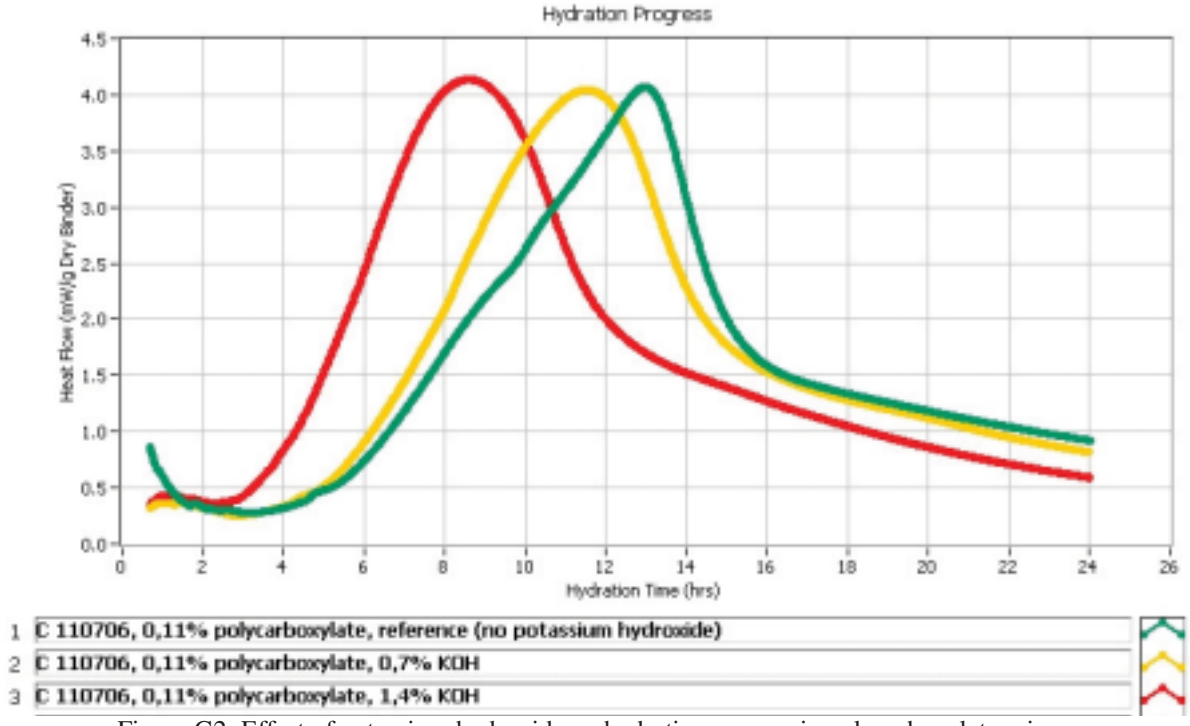

Figure G2: Effect of potassium hydroxide on hydration process in polycarboxylate mixes

Appendix G-2 Effect of sodium hydroxide and potassium hydroxide on hydration progress

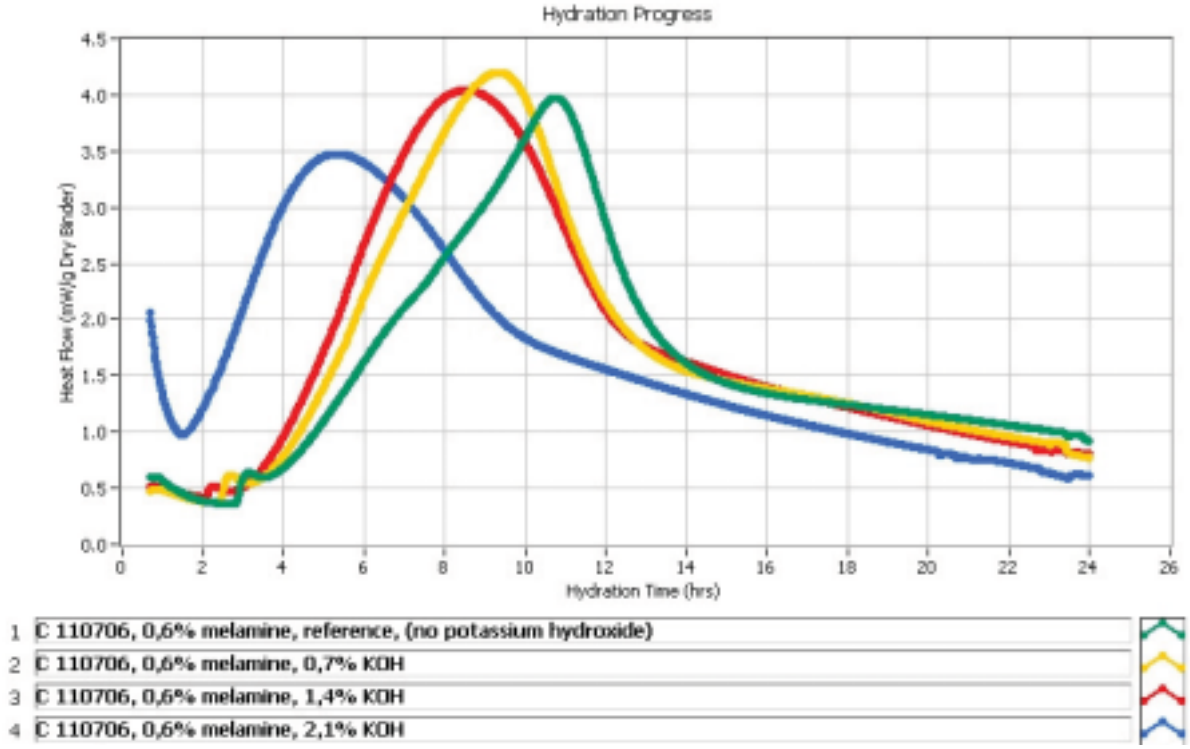

Figure G3: Effect of potassium hydroxide on hydration process in melamine mixes

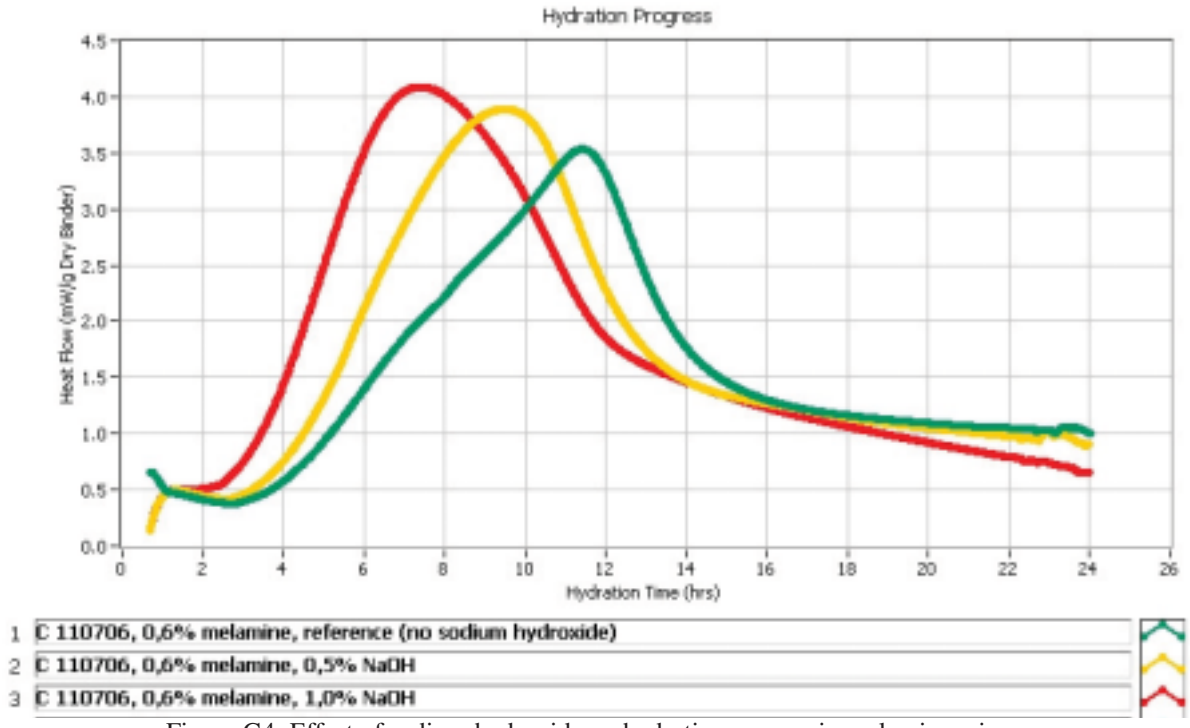

Figure G4: Effect of sodium hydroxide on hydration process in melamine mixes

Appendix H-1 Ion concentration in pore solution (cement C from 01.12.2006)

Table H-1.1: Ion concentration of pore solution (blank mix), cement C 01.12.2006

blank		5	15	30	60
SO_4^{2-}	[mmol/l]	95,81	91,69	97,12	95,44
Ca^{2+}	[mmol/l]	16,62	13,32	14,37	15,57
Mg^{2+}	[mmol/l]	0,02	0,02	0,02	0,02
K^{+}	[mmol/l]	118,8	150,7	170,3	174,5
Na^{+}	[mmol/l]	73,08	92,65	104,92	108,05
OH^{-}	[mmol/l]	n/a	n/a	n/a	n/a
Fe^{2+}	[mmol/l]	0,02	0,01 *	0,01 *	0,01 *
$Al(OH)^{4-}$	[mmol/l]	0,18 *	0,18 *	0,18 *	0,18 *

*) below limit of quantification

Table H-1.2: Ion concentration of pore solution (polycarboxylate mix), cement C 01.12.2006

PCE		5	15	30	60
SO_4^{2-}	[mmol/l]	127,62	128,18	128,56	115,46
Ca^{2+}	[mmol/l]	28,14	16,32	16,92	15,87
Mg^{2+}	[mmol/l]	0,27	0,19	0,18	0,14
K^{+}	[mmol/l]	83,2	98,1	104,3	99,6
Na^{+}	[mmol/l]	96,83	123,45	133,63	121,36
OH^{-}	[mmol/l]	n/a	n/a	n/a	n/a
Fe^{2+}	[mmol/l]	0,17	0,09	0,08	0,06
$Al(OH)^{4-}$	[mmol/l]	0,20	0,18 *	0,19	0,18 *

*) below limit of quantification

Appendix H-2 Ion concentration in pore solution (cement C from 22.11.2006)

Table H-2.1: Ion concentration of pore solution (blank mix), cement C 22.11.2006

blank		5	15	30	60
SO_4^{2-}	[mmol/l]	110,41	94,13	88,51	90,01
Ca^{2+}	[mmol/l]	38,92	20,96	21,56	21,71
Mg^{2+}	[mmol/l]	0,02 *	0,02 *	0,02 *	0,02 *
K^{+}	[mmol/l]	75,0	78,6	79,3	80,9
Na^{+}	[mmol/l]	76,21	85,34	86,39	91,08
OH^{-}	[mmol/l]	n/a	n/a	n/a	n/a
Fe^{2+}	[mmol/l]	0,04	0,02	0,01 *	0,01 *
$Al(OH)^{4-}$	[mmol/l]	0,18 *	0,18 *	0,18 *	0,18 *

*) below limit of quantification

Table H-2.2: Ion concentration of pore solution (polycarboxylate mix), cement C 22.11.2006

PCE		5	15	30	60
SO_4^{2-}	[mmol/l]	108,16	124,81	136,98	121,82
Ca^{2+}	[mmol/l]	27,40	19,76	20,51	19,76
Mg^{2+}	[mmol/l]	0,19	0,25	0,19	0,15
K^{+}	[mmol/l]	70,1	97,7	109,9	104,3
Na^{+}	[mmol/l]	77,25	112,22	129,71	125,27
OH^{-}	[mmol/l]	n/a	n/a	n/a	n/a
Fe^{2+}	[mmol/l]	0,15	0,13	0,10	0,07
$Al(OH)^{4-}$	[mmol/l]	0,18	0,18	0,18	0,18

*) below limit of quantification

Appendix H-3 Ion concentration in pore solution (cement C from 23.05.2005)

Table H-3.1: Ion concentration of pore solution (blank mix), cement C 23.05.2005

blank		5	15	30	60
SO_4^{2-}	[mmol/l]	106,85	87,76	83,65	76,91
Ca^{2+}	[mmol/l]	48,80	26,65	25,30	26,05
Mg^{2+}	[mmol/l]	0,02 *	0,02 *	0,02 *	0,02 *
K^+	[mmol/l]	68,6	72,7	71,7	70,3
Na^+	[mmol/l]	82,73	94,74	95,00	92,65
OH^-	[mmol/l]	n/a	n/a	n/a	n/a
Fe^{2+}	[mmol/l]	0,05	0,03	0,01 *	0,01 *
$Al(OH)^{4-}$	[mmol/l]	0,18 *	0,18 *	0,18 *	0,18 *

*) below limit of quantification

Table H-3.2: Ion concentration of pore solution (polycarboxylate mix), cement C 23.05.2005

PCE		5	15	30	60
SO_4^{2-}	[mmol/l]	120,32	89,07	98,99	107,04
Ca^{2+}	[mmol/l]	45,21	17,96	20,21	24,25
Mg^{2+}	[mmol/l]	0,14	0,09	0,15	0,09
K^+	[mmol/l]	76,6	70,7	79,2	92,1
Na^+	[mmol/l]	96,57	95,00	106,74	124,23
OH^-	[mmol/l]	n/a	n/a	n/a	n/a
Fe^{2+}	[mmol/l]	0,15	0,08	0,09	0,07
$Al(OH)^{4-}$	[mmol/l]	0,20	0,18 *	0,18 *	0,18 *

*) below limit of quantification

Appendix I Calibration of ConTec Rheomixer

Date of calibration: 09.08.2008
Device: Rheomixer WO7002
Procedure: The speed converter reads the torque signal 4 times per second. The motor is run for 5 seconds at 1 rps before the measurement starts. The measurement is performed for 30 seconds at 1 rps. Motor is run for 1 second at 0,5 rps after measurement. The torque value is calculated from the measuring points by using median.

Table I 1: Calibration data

Motor	Load cell Force [N]	Filename	Rotation direction	Rheomixer Torque [mA]	Stdev
3phase	2,9	1	Clockwise	255	11
3phase	5,2	2	Clockwise	421	13
3phase	7,3	3	Clockwise	576	14
3phase	10,1	4	Clockwise	773	17
3phase	15,1	5	Clockwise	1137	21
3phase	20,1	6	Clockwise	1495	22
3phase	25,4	7	Clockwise	1878	23

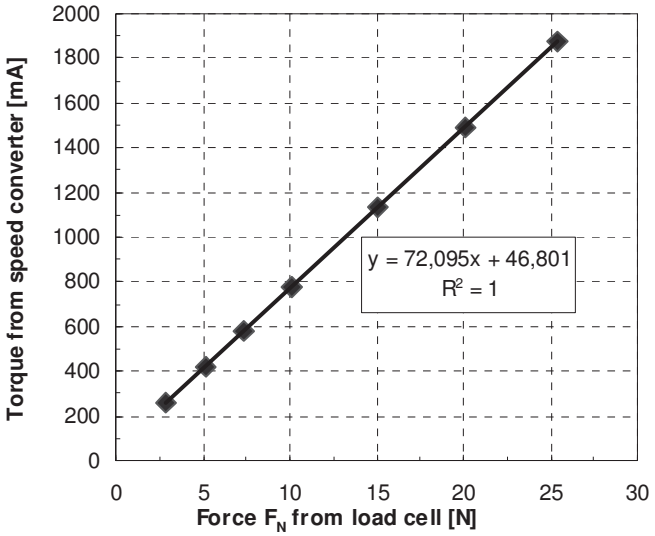

Figure I 1: Force from load [N] cell vs. torque from speed converter [mA]

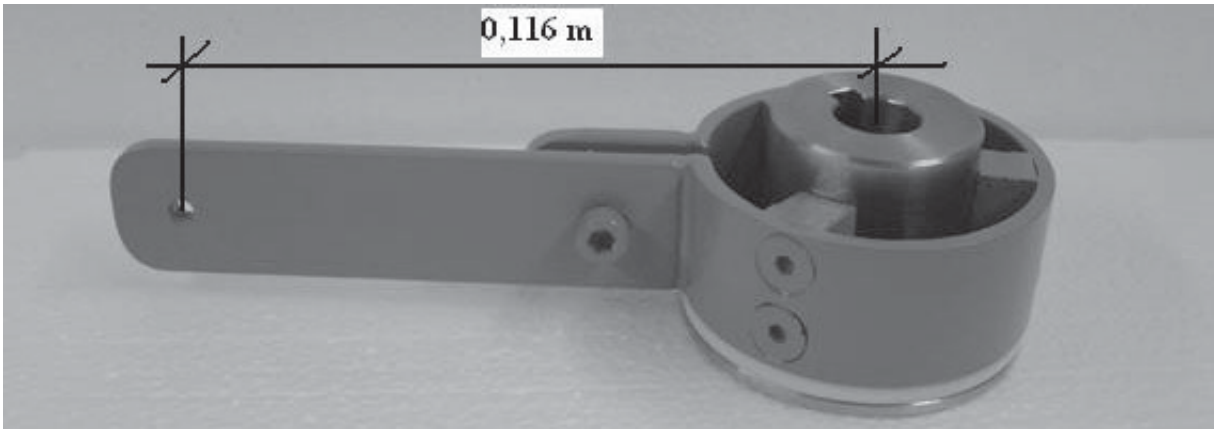

Figure I 2: Arm of force for calibration measurements

Appendix K-1 Microstructural observations

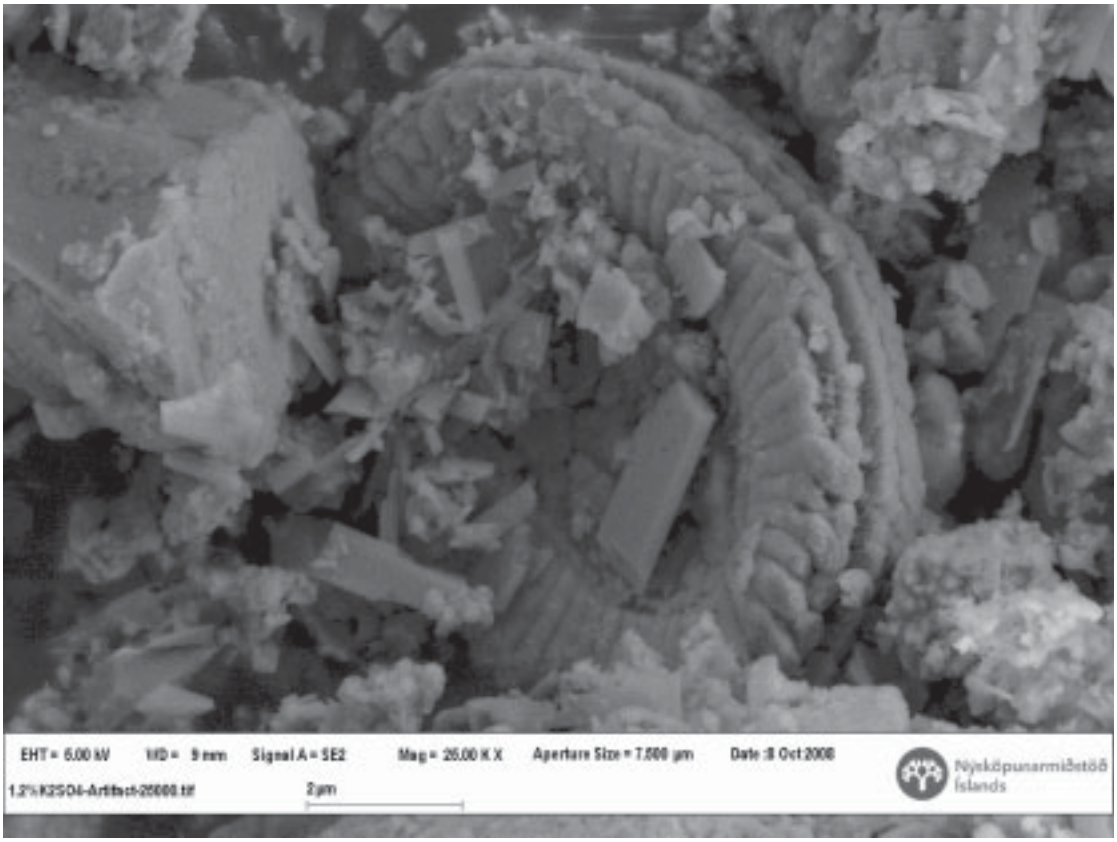

Figure K 1: Coccolithophorid found in a cement delivery

Figure K 2: Coccolithophorid found in a cement delivery

Appendix K-2 Microstructural observations

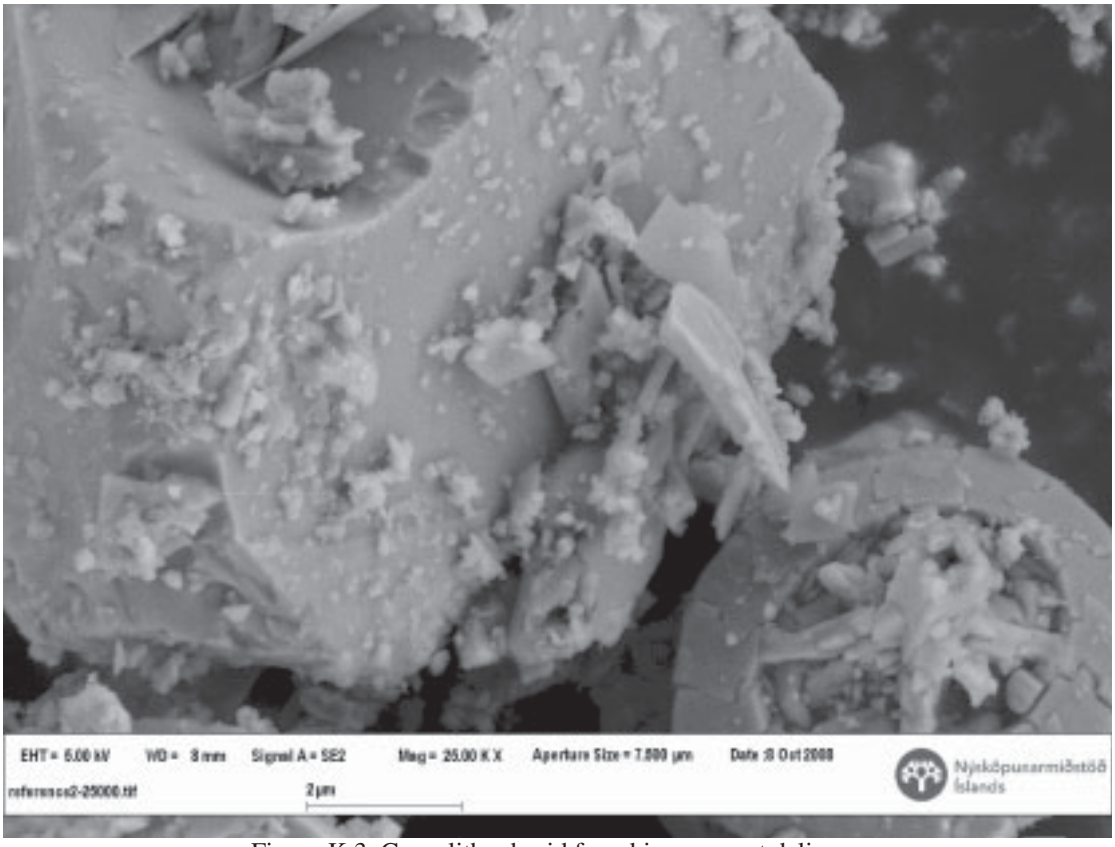

Figure K 3: Coccolithophorid found in a cement delivery

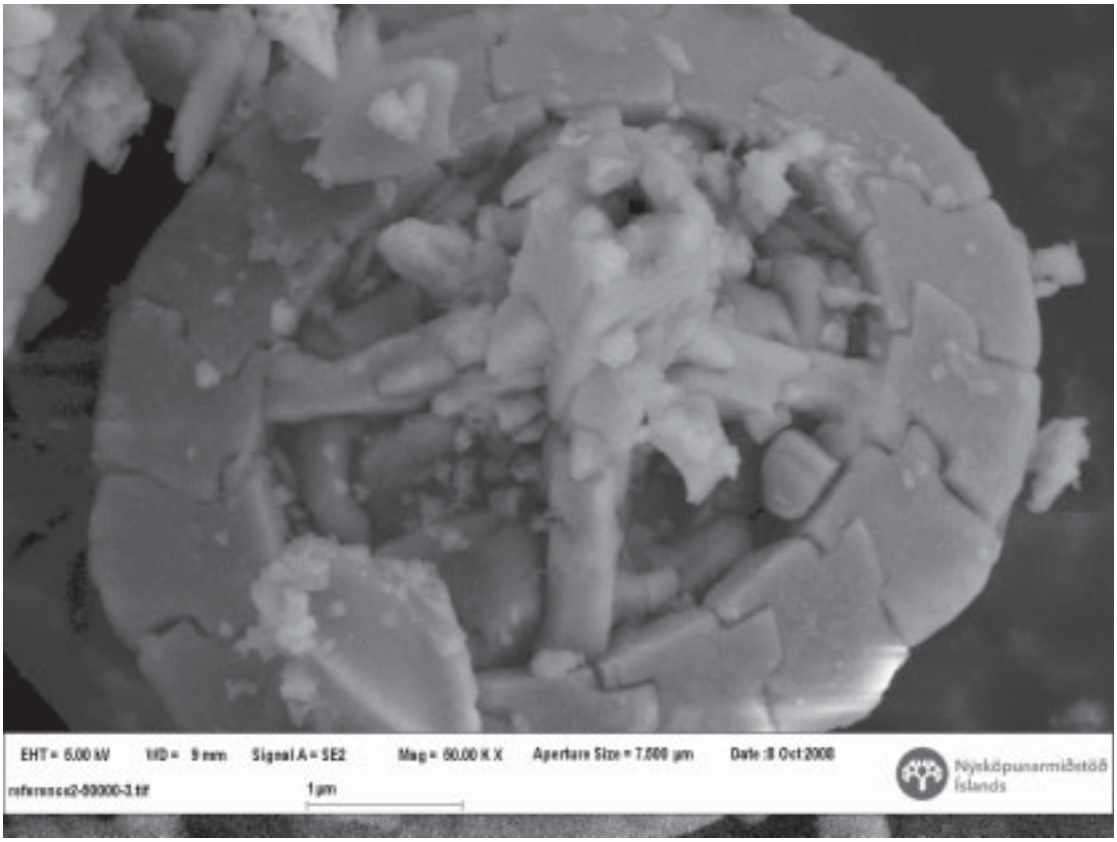

Figure K 4: Coccolithophorid found in a cement delivery

Appendix L-1 Rheological data from several countries

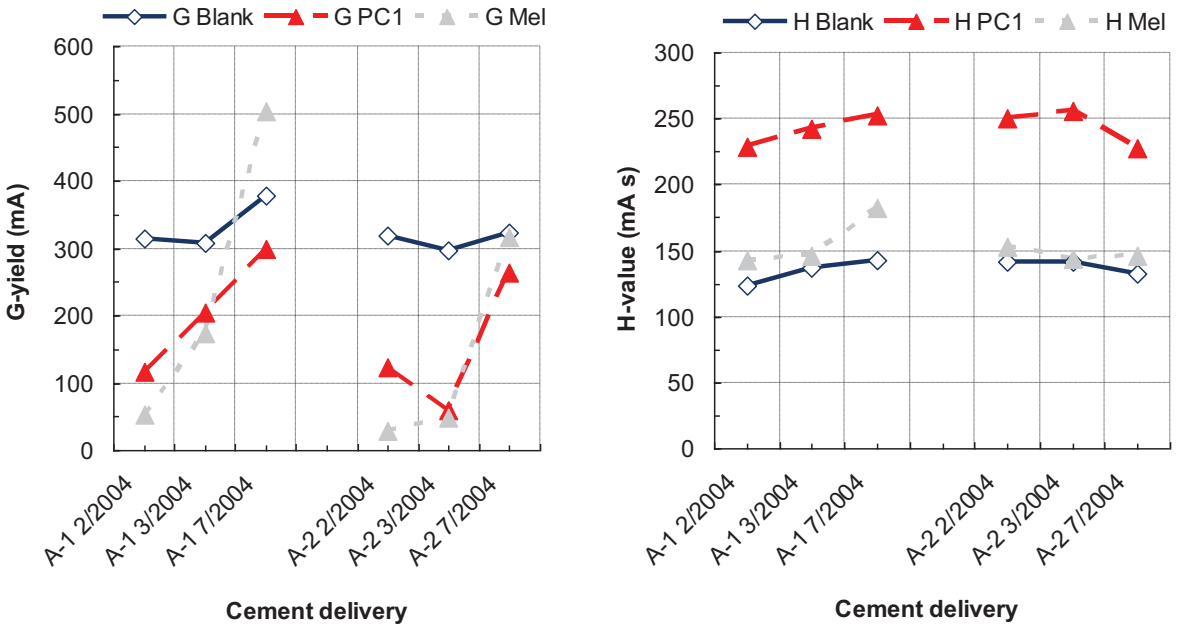

Figure L-1.1: G-yield and H-viscosity of cements A-1 (CEM I 42,5N) and A-2 (CEM II/B-S 32,5R) from country A

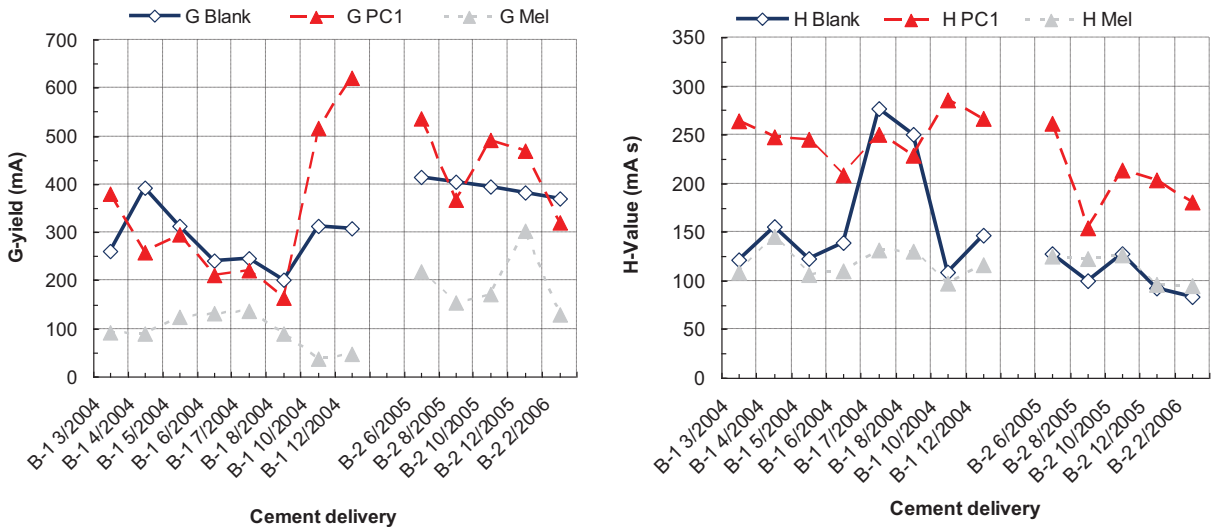

Figure L-1.2: G-yield and H-viscosity of cements B-1 (CEM I 42,5R) and B-2 (CEM I 42,5R) from country B

Appendix L-2 Rheological data from several countries

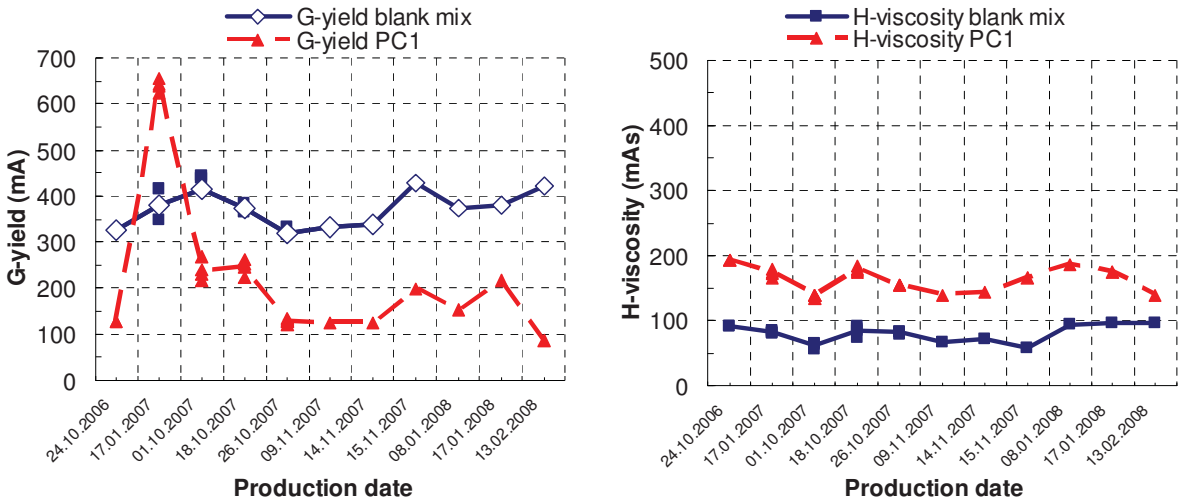

Figure L-2.1: G-yield and H-viscosity of cement D (CEM II/A-V 42,5R) from country D

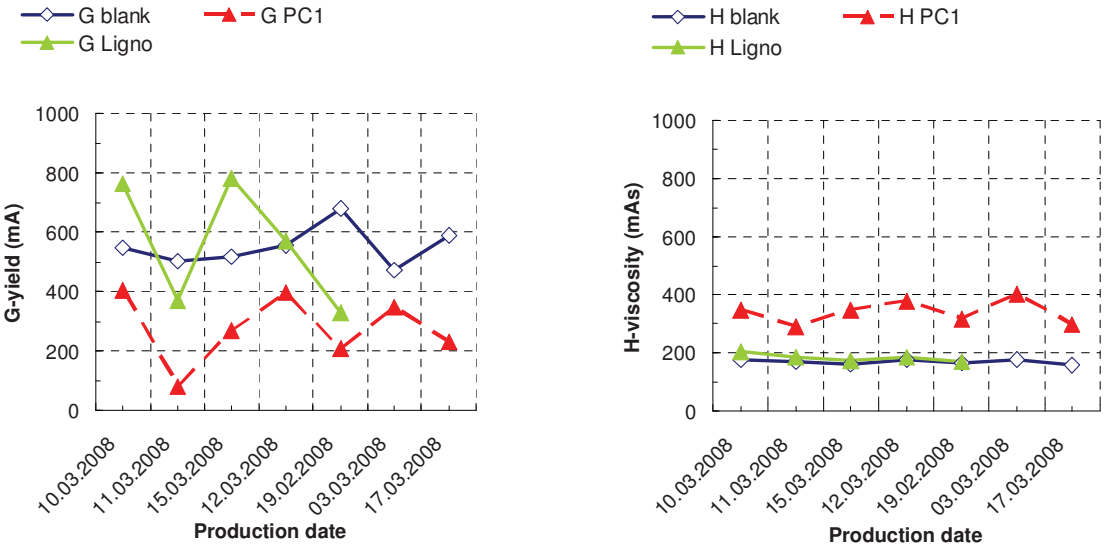

Figure L-2.2: G-yield and H-viscosity of cement E (CEM I 42,5N) from country E

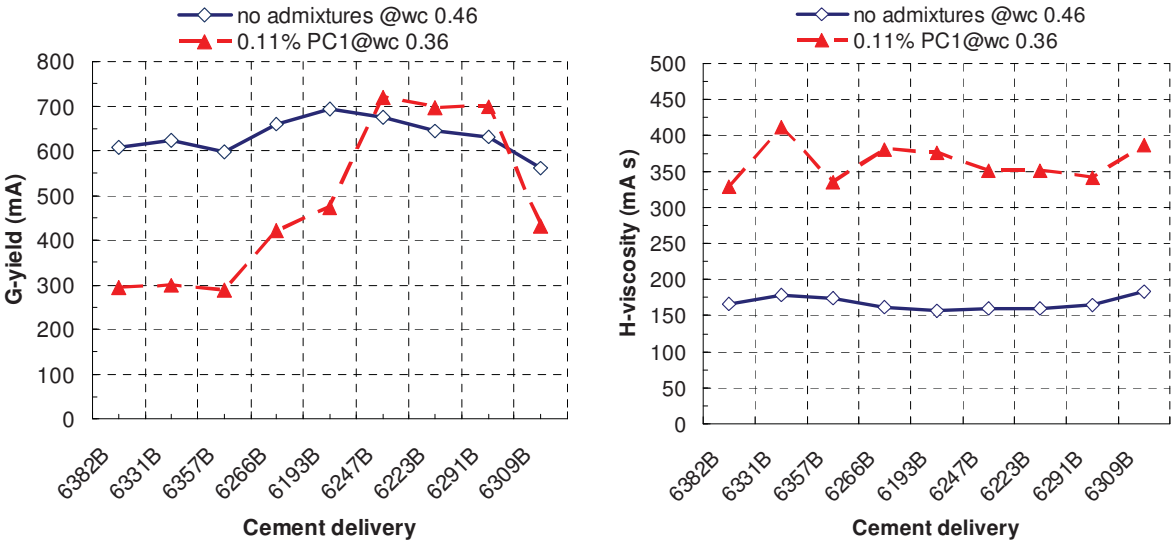

Figure L-2.3: G-yield and H-viscosity of cement F (CEM II/A-M 42,5R) from country F

Appendix M Hydration curves with four different polycarboxylates

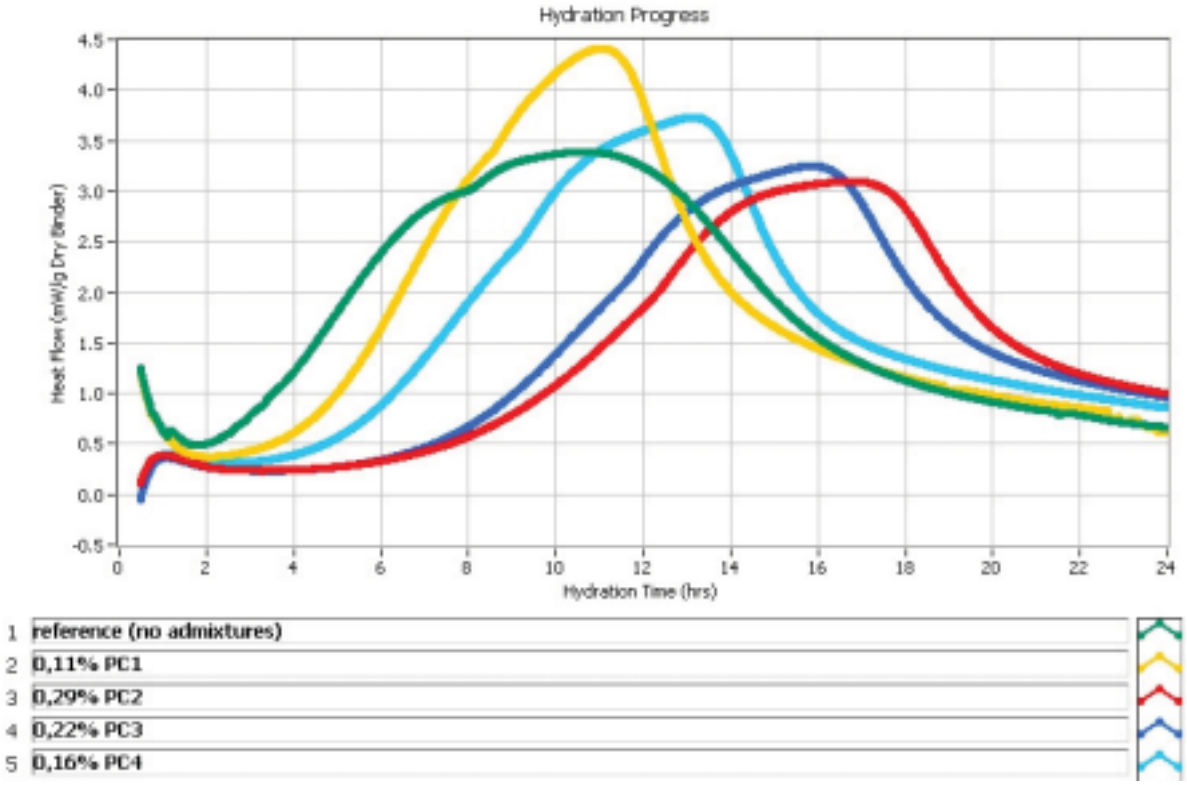

Figure M1: Effect of various polycarboxylates on hydration

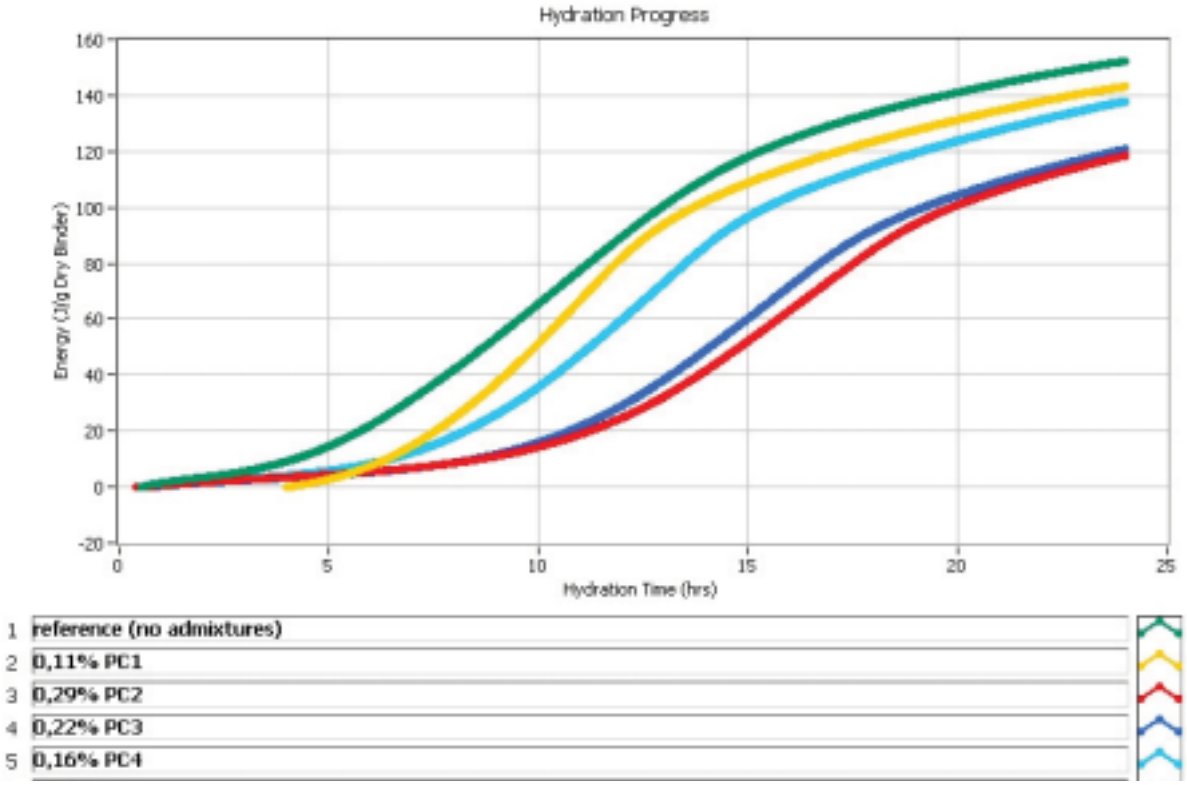

Figure M2: Effect of various polycarboxylates on total energy release in first 24 hours

Appendix N-1 QXRD (Rietveld) results of cement C

Cement production date	05.09.2003	23.03.2004	10.06.2004	09.07.2004	12.08.2004	23.02.2005
C_3S	51,7	53,6	53,8	53,2	54,5	n/a
C_2S	22,7	21,3	19,3	20,3	20,4	n/a
C_3A	3,9	4,0	3,2	4,8	4,5	n/a
$C_2(A,F)$	14,7	14,8	16,7	13,7	13,9	n/a
Calcite	3,3	2,2	3,1	3,9	2,6	n/a
Hemihydrate	1,1	1,4	1,3	1,3	1,4	n/a
Anhydrite	0,4	0,3	0,3	0,4	---	n/a
Dihydrate	0,3	0,4	0,4	0,3	0,5	n/a

Cement production date	23.05.2005	10.08.2005	04.10.2005	18.10.2005	06.01.2006	01.03.2006
C_3S	51,0	49,9	52,6	n/a	51,4	57,5
C_2S	22,8	21,5	20,2	n/a	21,5	20,0
C_3A	3,7	3,5	3,4	n/a	4,0	4,3
$C_2(A,F)$	15,3	16,4	15,8	n/a	17,1	12,3
Calcite	3,1	3,7	3,3	n/a	2,6	4,2
Hemihydrate	1,3	1,3	1,4	n/a	1,3	1,1
Anhydrite	0,3	---	0,3	n/a	---	0,6
Dihydrate	0,4	0,4	0,3	n/a	---	---

Cement production date	16.05.2006	29.05.2006	11.07.2006	13.09.2006	01.11.2006	09.11.2006
C_3S	60,3	n/a	59,4	58,2	57,7	58,8
C_2S	19,4	n/a	18,9	20,4	19,7	19,0
C_3A	4,1	n/a	4,4	4,5	4,3	4,5
$C_2(A,F)$	12,1	n/a	12,1	12,4	12,6	12,2
Calcite	2,9	n/a	3,8	3,4	3,4	3,7
Hemihydrate	1,3	n/a	1,2	1,5	1,5	1,4
Anhydrite	---	n/a	0,3	---	0,5	0,4
Dihydrate	---	n/a	---	---	---	---

Cement production date	15.11.2006	22.11.2006	24.11.2006	27.11.2006	28.11.2006	29.11.2006
C_3S	57,7	57,9	59,0	n/a	60,5	61,1
C_2S	20,1	17,3	18,6	n/a	17,6	17,5
C_3A	4,7	4,9	4,7	n/a	4,4	4,4
$C_2(A,F)$	12,3	12,0	12,8	n/a	12,8	12,5
Calcite	3,8	5,7	3,5	n/a	3,4	3,2
Hemihydrate	1,4	1,2	1,4	n/a	1,4	1,3
Anhydrite	---	1,0	---	n/a	---	---
Dihydrate	---	---	---	n/a	---	---

--- measured values were <0,3% and thereby below the limit of detection

Appendix N-2 QXRD (Rietveld) results of cement C

Cement production date	30.11.2006	01.12.2006	04.12.2006	26.02.2007	05.07.2007	10.07.2007
C_3S	61,4	61,0	58,7	59,1	55,2	55,0
C_2S	17,6	18,0	19,5	18,7	23,1	22,6
C_3A	4,3	4,2	4,2	4,9	4,0	4,2
$C_2(A,F)$	12,4	12,1	13,2	12,3	12,0	12,2
Calcite	2,9	3,4	3,1	3,6	3,9	4,1
Hemihydrate	1,4	1,3	1,4	1,5	1,4	1,4
Anhydrite	---	---	---	---	0,4	---
Dihydrate	---	---	---	---	---	---

Cement production date	19.07.2007	01.08.2007	13.08.2007	29.11.2007	05.12.2007	19.12.2007
C_3S	55,6	55,2	54,7	55,3	59,5	59,0
C_2S	22,1	23,9	23,6	24,2	17,5	19,1
C_3A	4,6	4,3	4,5	3,6	4,6	4,5
$C_2(A,F)$	12,0	11,7	11,5	11,9	12,0	12,2
Calcite	4,3	3,6	3,5	3,6	5,1	4,1
Hemihydrate	1,3	1,3	1,2	1,1	1,2	1,3
Anhydrite	---	---	---	---	0,3	---
Dihydrate	---	---	1,1	0,3	---	---

Cement production date	08.01.2008	23.01.2008	15.04.2008 (1)	15.04.2008 (2)
C_3S	59,0	58,6	59,6	58,6
C_2S	18,1	19,8	18,8	19,4
C_3A	4,5	4,1	4,1	4,0
$C_2(A,F)$	12,5	12,4	12,3	12,3
Calcite	4,4	3,9	3,9	3,6
Hemihydrate	1,4	1,3	1,3	1,6
Anhydrite	0,3	---	---	0,4
Dihydrate	---	---	---	---

--- measured values were <0,3% and thereby below the limit of detection

Appendix N-3 QXRD (Rietveld) results of cement D

Cement production date	24.10.2006	17.01.2007	01.10.2007	18.10.2007	26.10.2007	09.11.2007
C_3S (%)	56,6	54,4	57,0	59,2	58,6	56,1
C_2S (%)	10,5	10,0	10,5	7,9	9,4	10,5
C_3Ac (%)	1,6	1,8	1,9	1,8	1,8	2,0
C_3Ao (%)	10,3	11,0	9,4	9,9	9,7	10,3
$C_2(A,F)$ (%)	6,1	6,1	6,9	6,2	6,5	6,3
Calcite (%)	0,8	0,9	0,3	0,5	0,2	0,4
Hemihydrate (%)	3,0	1,8	1,0	0,8	1,4	0,6
Dihydrate (%)	0,7	3,4	2,6	3,2	2,4	3,3
Periclase (%)	2,4	2,3	2,0	2,1	1,9	2,3
Felspar (%)	1,2	1,4	1,5	1,7	1,6	1,7
Portlandite (%)	0,8	0,7	0,8	0,7	0,6	0,6

Cement production date	14.11.2007	15.11.2007	08.01.2008	17.01.2008	13.02.2008
C_3S (%)	58,6	59,4	56,1	56,4	56,9
C_2S (%)	8,6	7,7	10,5	11,3	10,4
C_3Ac (%)	2,2	2,0	1,7	2,1	1,9
C_3Ao (%)	10,3	10,4	10,1	9,6	10,2
$C_2(A,F)$ (%)	5,8	5,8	7,1	6,7	6,2
Calcite (%)	0,2	0,4	0,4	0,3	0,3
Hemihydrate (%)	0,5	0,4	2,6	2,3	1,1
Dihydrate (%)	3,3	3,6	1,2	1,1	2,6
Periclase (%)	2,4	2,3	2,0	2,0	2,4
Felspar (%)	1,5	1,5	1,4	1,3	1,5
Portlandite (%)	0,6	0,5	0,9	1,0	0,6

Appendix O-1 Hydration curves mortar with ethylene glycole

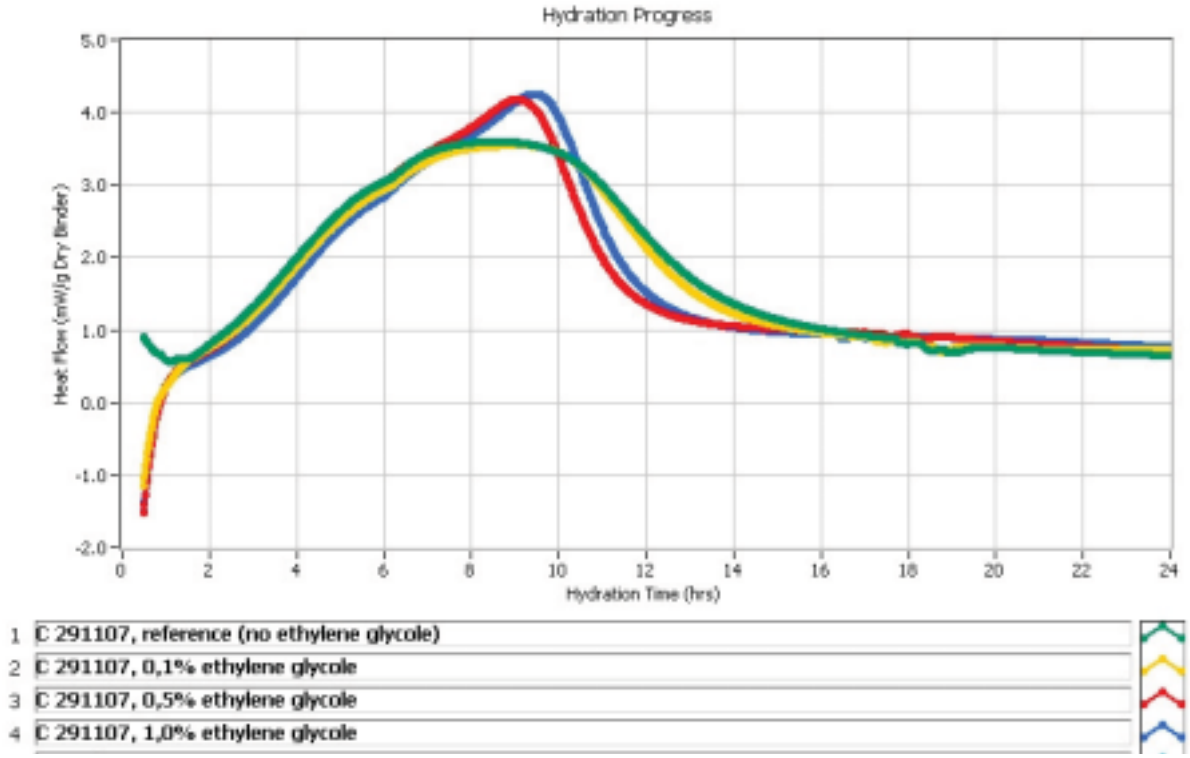

Figure O-1.1: Effect of ethylene glycole on hydration of blank mixes

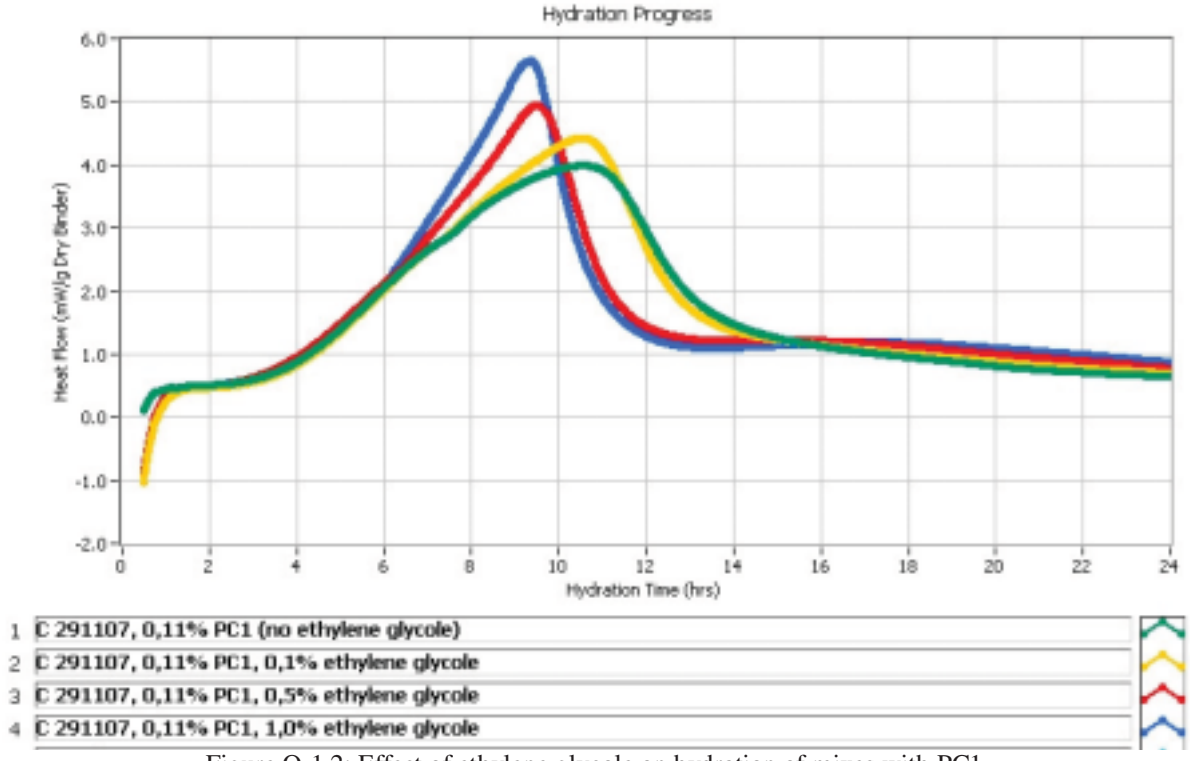

Figure O-1.2: Effect of ethylene glycole on hydration of mixes with PC1

Appendix O-2 Hydration curves mortar with tetraethylenepentamine

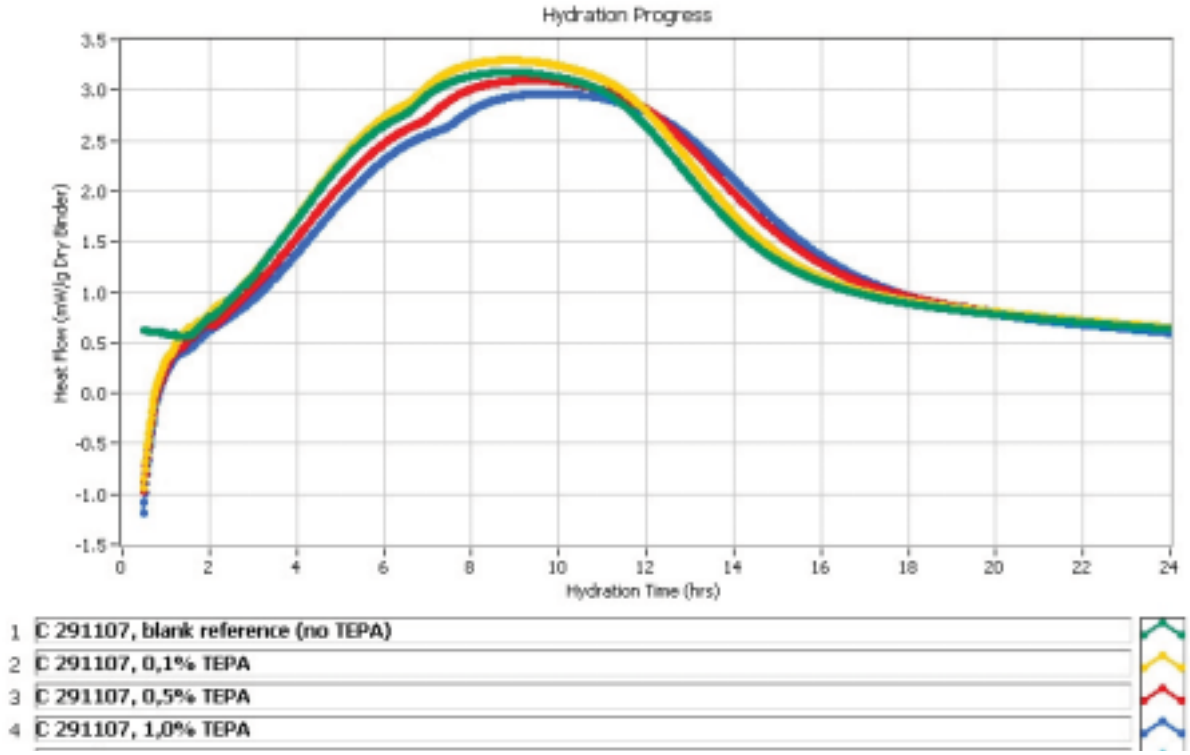

Figure O-2.1: Effect of tetraethylenepentamine on hydration of blank mixes

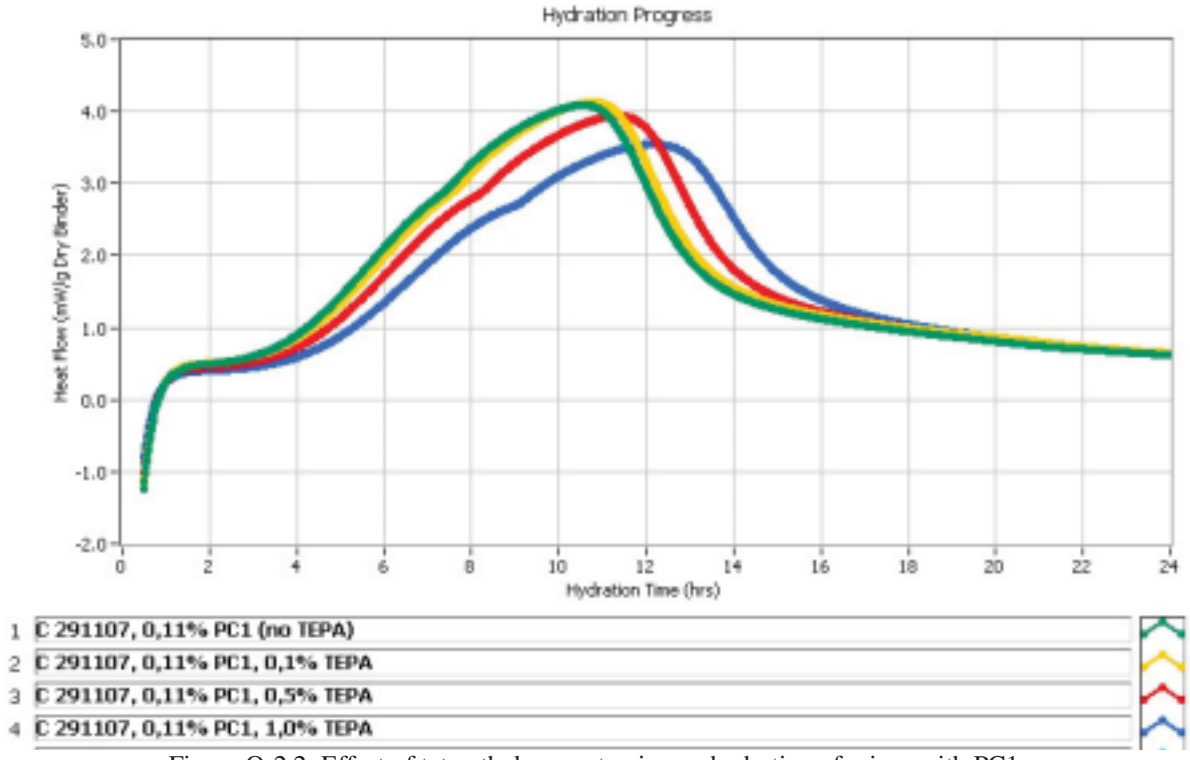

Figure O-2.2: Effect of tetraethylenepentamine on hydration of mixes with PC1

Appendix O-3 Hydration curves mortar with triethanolamine 1

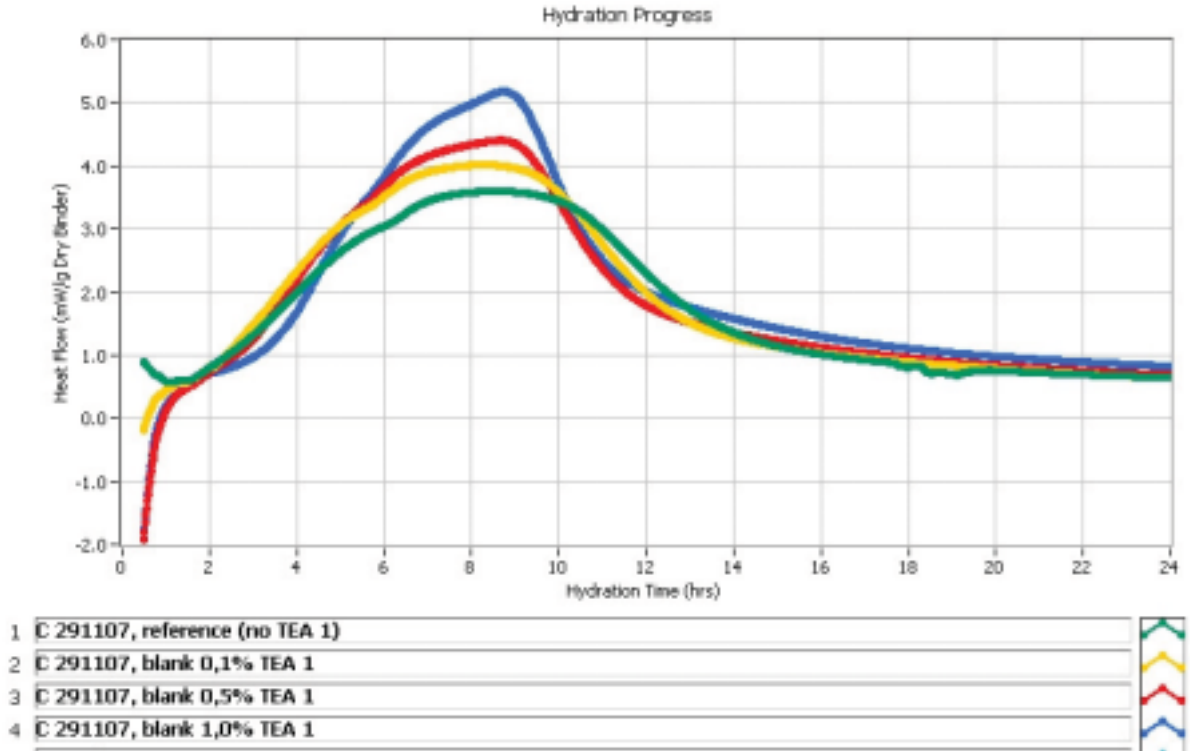

Figure O-3.1: Effect of triethanolamine 1 on hydration of blank mixes

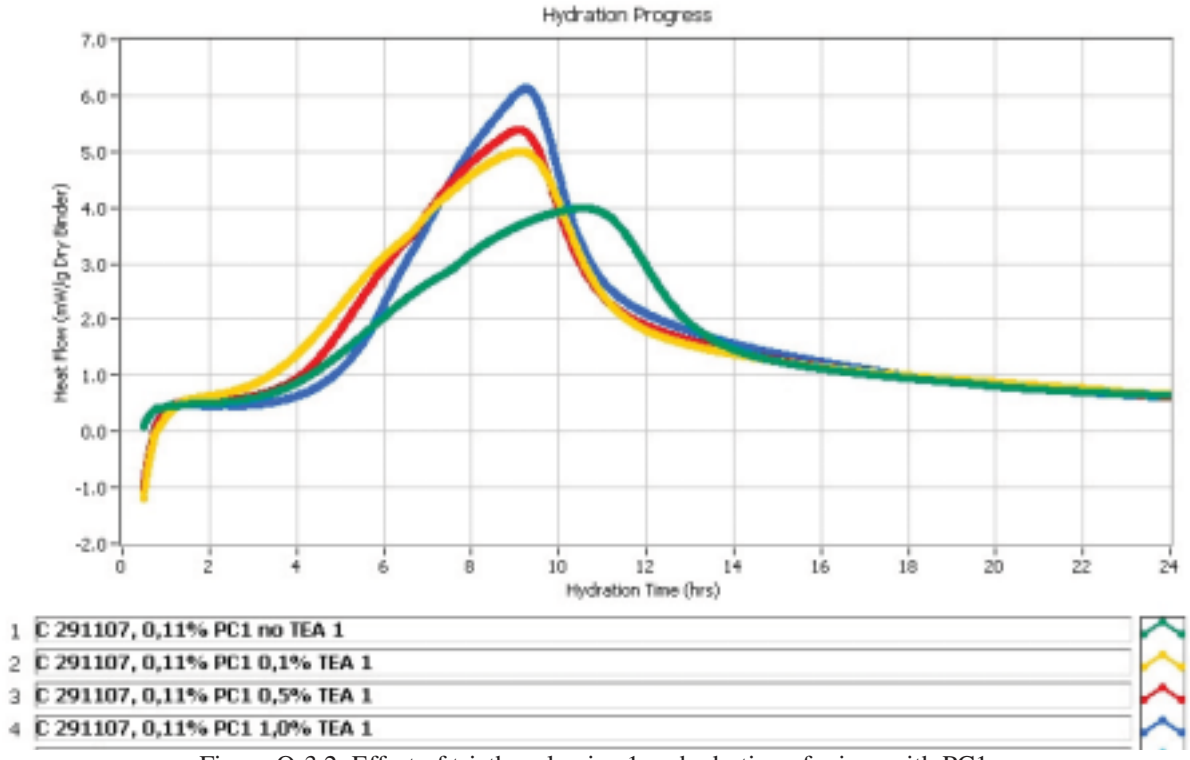

Figure O-3.2: Effect of triethanolamine 1 on hydration of mixes with PC1

Appendix O-4 Hydration curves mortar with triethanolamine 2

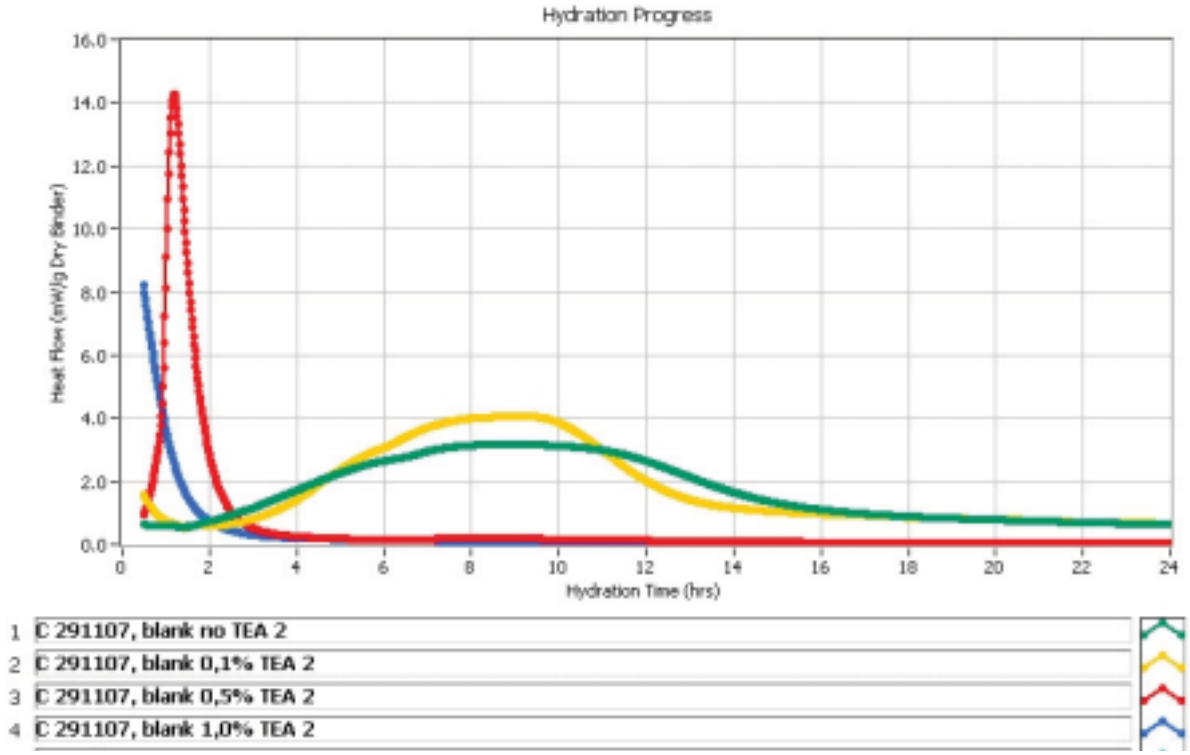

Figure O-4.1: Effect of triethanolamine 2 on hydration of blank mixes

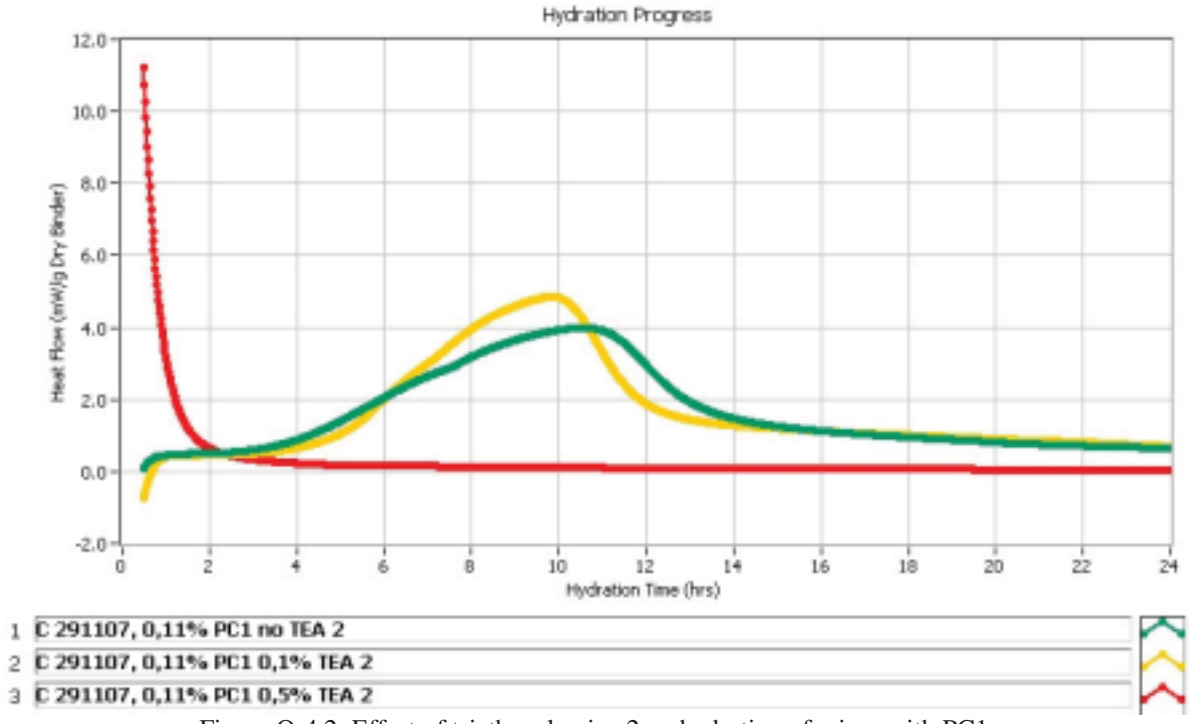

Figure O-4.2: Effect of triethanolamine 2 on hydration of mixes with PC1

Appendix P-1 Microstructural investigations on pastes

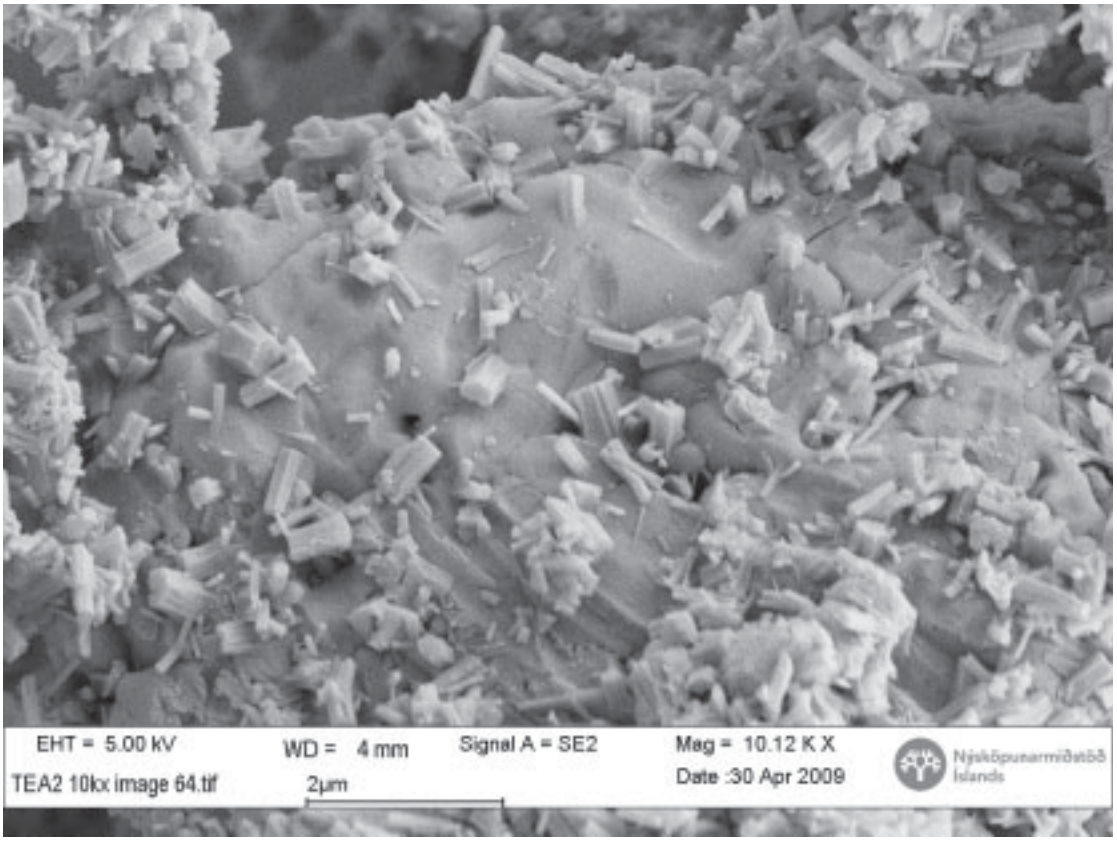

Figure P-1.1: Leached out cement surface when 5000 ppm triethanolamine 2 is present

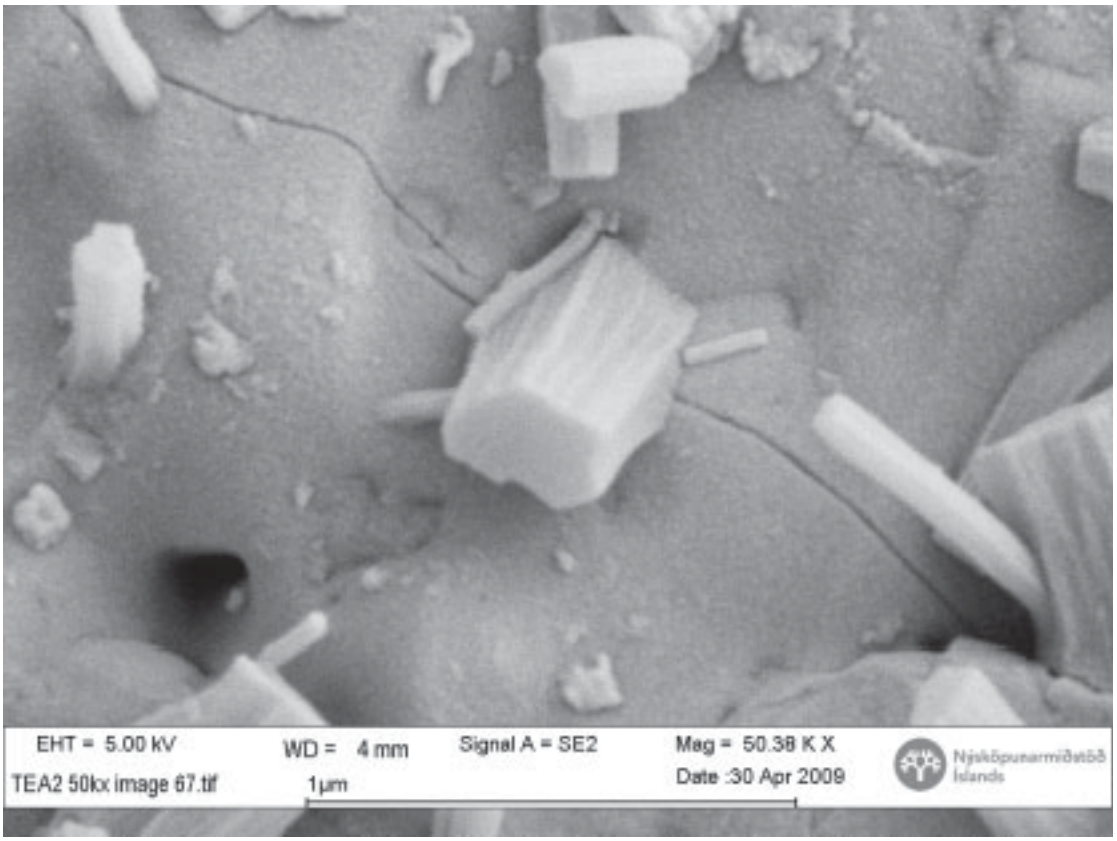

Figure P-1.2: Leached out cement surface when 5000 ppm triethanolamine 2 is present

Appendix P-5 Microstructural investigations on paste

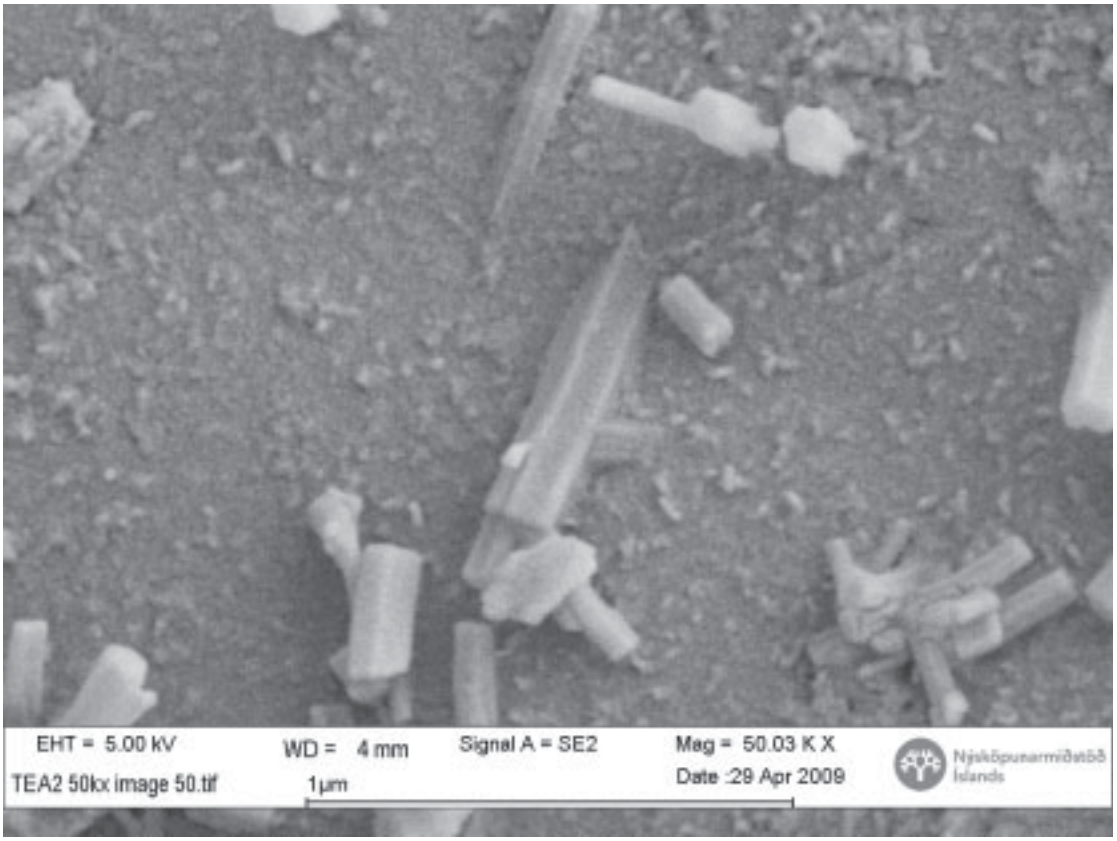

Figure P-5.1: Worm shaped formations covering the cement surface